Phytochemical and Antibacterial Studies on *Arctium lappa*, *Tussilago farfara* and *Verbascum thapsus*

Thesis submitted by

JINLIAN ZHAO

For the degree of Doctor of Philosophy

Narural Products Research Laboratories

Strathclyde Institute of Pharmacy and Biomedical Sciences

University of Strathclyde

161 Cathedral Street

Glasgow G4 0RE

UK

‘This thesis is the result of the author’s original research. It has been composed by the author and has not been previously submitted for examination which has lead to the award of a degree.’

Signed:

Date:

PRAISE THE LORD

Acknowledgements

I would like to offer my special thanks to my supervisor **Dr. V. Seidel** for her kind supervision. Her methodological approach and constructive criticism helped me greatly to improve my research ability. I also thank my second supervisor **Prof. A. I. Gray** whose expertise in NMR gave me the true essence of this technique. His support, generosity and kindness were invaluable attributes to my overall PhD experience and had a positive effect on my living in Glasgow.

I am very thankful to **Dr. Sanjib Bhakta** and **Dr. Dimitrios Evangelopoulos** of University of London, and **Pr. S. G. Franzblau** and **Ms. Baojie Wan** of the Institute for Tuberculosis Research for carrying out the anti-TB assays. I am also indebted to **Dr. Jun Yu** and **Mr. Simon Mylrea** for running anti-MRSA testing.

I will never forget the help from **Dr. Craig Irving** in running NMR experiments. I also acknowledge **Dr. Tong Zhang** and **Dr. Gavin Blackburn** for their kind assistance in MS experiments.

I would also like to express my thanks to **Dr. John Igoli**, **Ms. Hazniza Adnan**, **Ms. Hazar Mouad**, **Ms. Ngozi Igoli**, **Ms. Dima Semaan** and **Ms. Naliba Saleem** for their support and friendship which helped me to finish my work smoothly and made my life easy and comfortable in Glasgow.

Finally, my deepest gratitude goes to my parents, parents-in-low, husband, brothers, sisters and friends whose unconditional love and support make everything possible.

Table of Contents

List of Abbreviations

ADV	Adenoviruses
AIDS	Acquried Immune Deficiency Syndrome
ATCC	American Type Cell Culture
CAP	Capreomycin
CC	Open Column Chromatography
COSY	Correlation Spectroscopy
DBE	Double Bond Equivalence
DEPT	Distortionless Enhancement by Polarisation Transfer
DEPTQ	Distortionless Enhancement by Polarisation Transfer including the detection of Quaternary nuclei
DMSO	Dimethyl Sulfoxide
FU	Fluorescence Unit
GF	Gel Filtration
HIV	Human Immunodeficiency Virus
HMBC	Heteronuclear Multiple Bond Correlation
HO-1	Heme Oxygenase-1
HREI-MS	High-resolution Electron Ionization Mass Spectrometry
HRESI-MS	High-resolution Electrospray Ionization Mass Spectrometry
HSQC	Heteronuclear Single Quantum Correlation
HSV	Herpes Simplex Viruses
INH	Isoniazid
INT	*p*-Iodonitrotetrazolium Chloride
JEV	Japanese Encephalitis Virus
MABA	Microplate Alamar Blue assay

MDR-TB	Multidrug-resistant Tuberculosis
MFC	Minimum Fungicidal Concentration
MIC	Minimum Inhibitory Concentration
MRSA	Methicillin-resistant *Staphylococcus aureus*
MSSA	Methicillin-sensitive *Staphylococcus aureus*
MTT	3-[4,5-Dimethylthiazol-2-yl]-2,5 diphenyl tetrazolium bromide
NMR	Nuclear Magnetic Resonance
NOESY	Nuclear Overhauser Enhancement Spectroscopy
PFA	Platelet Activating Factor
PIV	Parainfluenza Virus
PTLC	Preparative Thin Layer Chromatography
RIF	Rifampicin
RSV	Respiratory Syncytial Virus
SM	Streptomycin
SPOTi	Spot Culture Growth Inhibition
TB	Tuberculosis
TLC	Thin layer chromatography
TOCSY	Total Correlation Spectroscopy
TSA	Tryptic Soy Agar
TSB	Tryptic Soy Broth
UV	Ultraviolet Light
VLC	Vacuum Liquid Chromatography
VRE	Vancomycin-resistant *Enterococcus*
VSE	Vancomycin-sensitive *Enterococcus*
XDR-TB	Extensively Drug-resistant Tuberculosis
XRMA	XTT Reduction Menadione Assay

List of Figures

List of Tables

List of Protocols

Abstract

This thesis described the isolation and structure elucidation of secondary metabolites from three medicinal plants selected on the basis of their traditional use in the treatment of infectious diseases. The work also focused on the evaluation of the plant extracts and some of the isolated compounds for activity in *vitro* against *Mycobacterium tuberculosis*. Compounds obtained in suffient yield were further tested for activity in *vitro* against Methicillin-resistant *Staphylococcus aureus*.

A total of 27 pure compounds and two mixtures were isolated from the three plants investigated: *Arctium lappa*, *Tussilago farfara* and *Verbascum thapsus*.

Phytochemical investigation of the aerial parts of *A. lappa* led to the isolation of four terpenoids (taraxasterol, taraxasterol acetate, isololiolide and melitensin), two steroids (sitosterol/stigmasterol mixture and daucosterol), three flavonoids (quercetin, kaempferol and kaempferol-3-*O*-glucoside), two phenolic acids or derivatives (caffeic acid and 1, 3-dicaffeoylquinic acid) and one alkane (*n*-nonacosane). Isololiolide, melitensin, kaempferol-3-*O*-glucoside and *n*-nonacosane are reported for the first time from this species, and daucosterol and kaempferol are first reported from the aerial parts of this plant.

Phytochemical investigation of *T. farfara* aerial parts led to the isolation of a monoterpene lactone (loliolide), two steroids (sitosterol/stigmasterol mixture and daucosterol), three flavonoids (quercetin, kaempferol and kaempferol-3-*O*-glucoside), and six phenolic acids or derivatives (*p*-coumaric acid, *p*-coumaric acid/4-hydroxybenzoic acid mixture, caffeic acid, 3, 4-dicaffeoylquinic acid, 4, 5-dicaffeoylquinic acid and methylcaffeate). Among them, loliolide is reported for

the first time from this species.

The aerial parts of *V. thapsus* afforded two pheophorbides (pheophorbide A and pheophorbide A ethyl ester), two pheophytins (pheophytin A and pheophytin B), one steroid (α-spinasterol), one known flavonoid (luteolin), one phenylethanoid glycoside (verbascoside), three simple pheonolic acids (*trans*-cinnamic acid, 4-hydroxybenzoic acid and 4-hydroxy-3-methoxybenzoic acid) and one fatty acid (1-monoacylglycerol). All compounds, except for α-spinasterol, luteolin and verbascoside, are reported for the first time from this species. α-Spinasterol is first reported from the aerial parts of this plant.

When screened for activity against *M. tuberculosis* in the SPOTi assay, *A. lappa* *n*-hexane extract and dichloromethane phase of methanol extact, and *T. farfara* *n*-hexane and ethyl actate extracts were active at MICs of 62.5 μg/mL; *A. lappa* ethyl acetate extract and *T. farfara* methanol extract were active at MICs of 125 μg/mL; *V. thapsus* ethyl acetate extract was active at the concentration of 250 μg/mL. Among the tested compounds isolated from active extracts, *p*-coumaric acid displayed the highest activity (MIC=31.3 μg/mL, 190.7 μM); *p*-coumaric acid/4-hydroxybenzoic acid mixture showed good activity (MIC=62.5 μg/mL); sitosterol/stigmasterol mixture exhibited moderate activity (MIC=125 μg/mL); loliolide, caffeic acid and *trans*-cinnamic acid revealed weak activity (MICs=250 μg/mL, or 1273.9, 1387.6 and 1687.4 μM, respectively). This is the first time that the antitubercular acitivity of *A. lappa*, *T. farfara* and *V. thapsus* has been investigated. The anti-TB activity of all tested compounds is also first reported in the SPOTi assay.

When initially screened for activity against *M. tuberculosis* in the MABA assay at the highest concentrations of 25 or 50 μg/mL, all plant extracts and tested compounds

were identified as inactive at such concentrations. This is the first report of the screening of *A. lappa*, *T. farfara* and *V. thapsus* extracts and of all tested compounds in the MABA assay.

Among the compounds screened for activity against Methicillin-resistant *S. aureus*, luteolin exhibited good activity with an MIC value of 62.5 μg/mL (218.3 μM), and α-spinasterol had an MIC of 500 μg/mL. No other compound was active at the highest concentration (500 μg/mL) used in this assay. This is the first report of the investigation of the anti-MRSA activity of kaempferol, α-spinasterol, 1, 3-dicaffeoylquinic acid, 3, 4-dicaffeoylquinic acid, 4, 5-dicaffeoylquinic acid, 1-monoacylglycerol, pheophorbide A ethyl ester, pheophytin A, pheophytin B and verbascoside.

CHAPTER 1

INTRODUCTION

1 Introduction

1.1 Infectious diseases

Infections remain a great threat to global public health despite improvements in sanitation and developments in methods of preventing, detecting and decreasing disease transmission (Rothman *et al*., 2006). It has been estimated that infectious diseases cause 9 million deaths annually worldwide (WHO, 2012a).

Diseases caused by antibiotic-resistant bacteria, such as methicillin-resistant *Staphylococcus aureus*, vancomycin-resistant *Enterococci*, fluoroquinolone-resistant *Pseudomonas aeruginosa* and multiple drug-resistant *Mycobacterium tuberculosis* continue to increase in frequency and cause significant morbidity and mortality (Boucher *et al*., 2009; Magiorakos *et al*., 2012; Boucher *et al*., 2013).

1.1.1 Tuberculosis

Tuberculosis (TB) is the leading bacterial killer worldwide (WHO, 2013a). About 3.7% of new TB cases worldwide are multidrug-resistant TB (MDR-TB), about 9% of which are now extensively drug-resistant (XDR-TB) (WHO, 2013b).

Tuberculosis is caused by *Mycobacterium tuberculosis*, a rod-shape acid-fast microorganism. The latter typically attacks the lungs but can also affect other parts of the body. The disease is spread when people who have active TB expel small droplets containing bacteria by coughing, sneezing or simply speaking. Generally, the proportion of people infected with *M. tuberculosis* and developing TB disease is small, but the probability becomes much higher among people infected with the human immunodeficiency virus (HIV). TB patients suffer from chronic cough with

blood-tinged sputum, fever, fatigue, night sweats and weight loss, and mortality rates are high without treatment (WHO, 2012b).

In Europe, the biggest TB outbreak happened in the 19th century when 25% of the population was estimated to have been killed by the disease (Bloom, 1994). Even if good progress towards reducing global TB cases and deaths has been achieved with a falling rate of new case incidence at 2.2% between 2010 and 2011 (WHO, 2012b), the global burden of TB remains enormous. As the first bacterial killer, it still causes ill-health among millions of people each year. This high incidence is partly due to the HIV/AIDS pandemic. According to the latest report, there were 8.7 million new cases (13% co-infected with HIV) in 2011 and 1.4 million TB deaths (990 000 deaths among HIV-negative individuals and 430 000 HIV-positive TB deaths) (WHO, 2012b).

The current recommended treatment for new cases of drug-susceptible TB is a 6-month regimen of four first-line drugs (isoniazid, rifampicin, ethambutol and pyrazinamide). The patient receives fixed doses of isoniazid and rifampicin daily for six months and during the first two months the patient is also given pyrazinamide and ethambutol (National Institute for Health and Clinical Excellence, 2011; British National Formulary, 2013).

Because TB treatments are long, they are met with poor patient compliance, which has resulted in the spread of drug-resistant *M. tuberculosis* strains. Drug-resistant TB is threatening global TB control and has become an increasing concern in several countries (WHO, 2012b). There were an estimated 310 000 multidrug-resistant tuberculosis (MDR-TB) cases among notified TB patients in 2011 (WHO, 2012b), most cases arising from a combination of physician error and patient non-compliance during treatment of susceptible TB (Ormerod, 2005). Treatment for MDR-TB is

longer, lasting 20 months, and requires more expensive and toxic drugs (WHO, 2012b). There is therefore an urgent need to discover and develop new anti-TB drugs.

1.1.2 Methicillin-resistant *Staphylococcus aureus* (MRSA) infections

Methicillin-resistant *Staphylococcus aureus* (MRSA) is one of the most significant human pathogens that can cause a wide range of infectious diseases, such as superficial skin infections, deep-skin abscesses, bone and joint infections, pneumonia, bacteraemia and endocarditis (Al-Haj *et al*., 2009; Raghukumar *et al*., 2010). MRSA was first reported in 1961 in the United Kingdom, 2 years after methicillin (a β-lactam antibiotic) was introduced into clinical usage (Livemore, 2000; Raygada and Levine, 2009). It is now well-known for causing healthcare-associated nosocomial infections in hospitalised, predisposed patients such as the elderly, immuno compromised or those undergoing surgery. There has also been an increase in the number of people infected with MRSA (causing skin and soft tissue infections, ranging in severity from furuncles to necrotising fasciitis) amongst healthy individuals in the community (Maeda *et al*., 2008; Otto, 2012).

MRSA represents an enormous burden on healthcare systems since it leads to long hospitalisation stays, and high morbidity and mortality (Raghukumar *et al*., 2010; Kejela and Bacha, 2013). It has been reported that MRSA is responsible for 18,000 deaths annually (Moore *et al*., 2010), and MRSA infections are even implicated in more deaths than AIDS each year in the US (Kejela and Bacha, 2013). In Europe, the number of MRSA-associated nosocomial infections alone has been estimated at more than 150,000 annually (Kock *et al*., 2010).

The treatment of MRSA infections requires a variety of oral antibiotics, including clindamycin, trimethoprim-sulfamethoxazole, tetracyclines such as doxycycline or minocycline, rifampin, and occasionally fluoroquinolones. For more serious infections requiring hospitalisation, some parenteral antibiotics such as vancomycin, daptomycin, linezolid and tigecycline need to be used (Moellering, 2008). However, these drugs present a number of limitations as some *S. aureu*s strains have become resistant not only to the regularly used penicillin-related (β-lactam) antibiotics, but also to some tetracyclines, daptomycin, rifampicin and even vancomycin (Al-Haj *et al*., 2009; Raghukumar *et al*., 2010). In this context, the treatment of MRSA infections has become more difficult. Discovering and developing alternative anti-MRSA agents remains a priority.

1.2 Antimicrobial natural products

Natural products are greatly used in the field of pharmaceutical drug discovery and drug design (Molinari, 2009). A wide range of natural products have been reported to possess significant antimicrobial activity. Major antimicrobial natural products include alkaloids, coumarins and tannins, flavonoids, iridoids and iridoid glycosides, lignans, polypeptides and lectins, quinones, saponins, simple phenolics, steroids, terpenes and terpenoids and xanthones (Cowan, 1999; Ciocan and Bara, 2007; Saleem *et al*., 2010).

1.2.1 Alkaloids

Alkaloids are heterocyclic nitrogen-containing compounds. Many alkaloids have been identified and documented for their antimicrobial activity. For example, two alkaloids (dihydrochelerythrine and dihydrosanguinarine), isolated from *Bocconia*

arborea, displayed good antimicrobial activity against several Gram-positive and Gram-negative bacteria and antifungal activity against *Candida albicans* (Navarro and Delgado, 1999). The alkaloid holarrifine-24-ol, isolated from the stem bark of *Holarrhena antidysenterica*, had good activity against ten pathogenic bacteria and six phytopathogenic fungi (Raman *et al*., 2004). Some cyclostellettamine, indoloquinoline, diterpenoid and indole-derived alkaloids also exhibited good antimicrobial activity (Oliveira *et al.*, 2006; Karou *et al.*, 2006; Tanaka *et al.*, 2006; Ki-Bong *et al.*, 2006). 8-Hydroxydihydrosanguinarine and 8-hydroxydihydrochelerythrine, isolated from *Chelidonium majus* Linn, were potently active against MRSA strains (Zuo *et al*., 2008). Evocarpine isolated from *Tetradium ruticarpum* demonstrated strong activity aganist MRSA with an MIC value of 8 μg/mL (Pan *et al*., 2013). Cepharanone B, piperolactam A and cepharadione B, isolated from *Piper sanctum*, displayed activity against *M. tuberculosis* $H_{37}Rv$ with MIC values of 12, 8 and 32 μg/mL , respectively (Mata *et al*., 2004). Bisbenzylisoquinoline alkaloids, tiliacorinine, 2'-nortiliacorinine and tiliacorine (from *Tiliacora triandra*), were active against multidrug-resistant *M. tuberculosis* isolates, with MICs ranging from 0.7 to 6.2 μg/mL (Sureram *et al*., 2012).

1.2.2 Coumarins and tannins

Coumarins are phenolic compounds with a fused benzene and α-pyrone. They possess antimicrobial, antithrombotic, anti-inflammatory and vasodilatory properties (Namba *et al*., 1988). It has been reported that the antibacterial effect of coumarins is affected by their substitution patterns (Souzaa *et al*., 2005; Stein *et al*., 2006). Antibacterial effects have been documented for xanthotoxin, daphnetin, rhodonin, herniarin, umbelliferone and scopoletin, and antifungal activity for umbelliferone, scopoletin, coumarin and prenyletin (Kayser and Kolodziej, 1997; Kwon *et al*., 1997;

Stein *et al*., 2006; Shakeel-u-Rehman *et al*., 2010). Moreover, five known coumarins (imperatorin, isoimperatorin, heraclenol, oxypeucedanin hydrate and heraclenin) were also reported effective against six Gram-positive and negative bacteria (*Enterobacter cloacae*, *Escherichia coli*, *Klebsiella pneumonia*, *Pseudomonas aeruginosa*, *S. aureus* and *Staphylococcus epidermidis*) and two oral pathogens (*Streptococcus mutans* and *Streptococcus viridians*) (Widelski *et al*., 2009). A naturally occurring chlorinated coumarin ethyl 6-chloro-2-oxo-4-phenyl-2H-chromen-3-carboxylate, isolated from *Fomitopsis officinalis*, displayed specific activity against both replicating and non-replicating *M. tuberculosis* as well as *M. tuberculosis* isolates with mono-resistance to rifampin, isoniazid, streptomycin, kanamycin or cycloserine (Hwang *et al*., 2012).

Tannins are categorised into hydrolysable and condensed tannins. The latter are polymeric phenolic compounds, formed by polymerisation of flavan units. Hydrolyzable tannins are based on gallic acid, usually as multiple esters with D-glucose (Cowan, 1999). Tannins display a range of biological properties, including antimicrobial and immunostimulating activity (Haslam, 1996). Some tannins can inhibit *S. aureus*-induced plasma coagulation (Akiyama *et al*., 2001). Some condensed tannins showed activity against pathogens involved in mastitis (Min *et al*., 2008). Tannins isolated from *Solanum trilobatum* exhibited activity against *Escherichia coli, Proteus vulgaris*, *Pseudomonas aeruginosa*, *Salmonella typhi*, *S. aureus* and *Streptococcus pyrogen* (Doss *et al*., 2009). Corilagin and tellimagrandin I (from *Arctostaphylos uvaursi* and *Rosa canina*, respectively) reduced the MIC of β-lactams in MRSA (Shimizu *et al*., 2001; Shiota *et al*., 2004; Hatano *et al*., 2005). Punicalagin, isolated from *Terminalia brachystemma* leaf, was active against three *Candida* species (Liu *et al*., 2009).

1.2.3 Flavonoids

Flavonoids (or bioflavonoids) are hydroxylated phenolic compounds containing two benzene rings linked by a linear three carbon chain. These include compounds such as flavones and flavonols. Flavones are a class of flavonoids which have the backbone of 2-phenylchromen-4-one. The substitution of the 3-hydroxyl group in flavones produces flavonols. The flavonols diversify from each other with the different position of the phenolic OH groups. Flavonoids can complex with the proteins of bacterial cell walls to inhibit microorganisms (Cowan, 1999).

The antimicrobial activity of flavonoids has been largely documented. Glycosylated derivatives of mono and dihydroxylated in B ring flavonoids had antibacterial activity against *Escherichia coli*, *Pseudomonas aeruginosa*, *Shigella* species and *Staphylococcus aureus* (Herna´ndez *et al.*, 2000). Apigenin, identified from *Scutellaria barbata*, exhibited a potent activity (MIC 3.9~15.6 µg/mL) against 20 strains of MRSA (Sato *et al.*, 2000). Galangin (3, 5, 7-trihydroxyflavone), isolated from propolis collected from Croatia, displayed strong activity against MRSA, multiple-resistant *Enterococcus spp.* and *Pseudomonas aeruginosa* (Stjepan and Ivan, 2003). Pinobanksin-3-*O*-acetate and pinocembrin, isolated from Jordanian propolis, were also active against MRSA (Darwish *et al.*, 2010). Flavonoids 3,4'-dimethoxykaempferol and 5,6,7-trihydroxy-3,4'-dimethoxyflavone, reported from the Mexican medicinal plant *Larrea divaricata*, both displayed an MIC of 50 µg/mL towards *M. tuberculosis* $H_{37}Rv$ (Rivero-Cruz *et al.*, 2005). An isoflavonoid laburnetin, isolated from *Ficus chlamydocarpa*, exhibited potent inhibitory activity against *Mycobacterium smegmatis* and *M. tuberculosis*, with MICs of 0.61 and 4.88 µg/mL, respectively (Kuete *et al.*, 2008). Other flavonoids with antitubercular activity include luteolin, quercetin, 5,4'-dihydroxy-3,7,8,3'-tetramethoxyflavone, 5,4'-dihydroxy-3,7,8-trimethoxyflavone, baicalein, myricetin and hispidulin

(Favela-Hernán *et al*., 2012; Yadav *et al*., 2013).

Flavonoids are also active against fungi and viruses. Polymethoxylated flavonoids (from *Citrus* spp. peels) exhibited activity against *Microsporum canis* and *Trichophyton mentagrophytes* (Johann *et al.*, 2007). Gnaphaliin A, isolated from *Pseudognaphalium robustum*, was fungitoxic against *Botrytis cinerea* with IC_{50}=45.5 μg/mL (Cotoras *et al*., 2011). It was reported that chrysin was active against the HIV virus (Critchfield *et al.*, 1996), moralbanone (from *Morus alba*) was active against the herpes simplex type 1 virus (HSV-1) (Du *et al*., 2003), some flavonoids from *Aesculus chinensis* were active against the respiratory syncytial virus (RSV), parainfluenza type 3 virus (PIV 3) and influenza type A virus (Flu A) (Wei *et al*., 2004), and baicalein displayed potent activity aginst the Japanese Encephalitis Virus (JEV) with IC_{50}=14.28 μg/mL (Johari *et al*., 2012).

1.2.4 Iridoid and iridoid glycosides

Iridoids are compounds consisting of a cyclopentane ring combined with a six-membered oxygen heterocycle. They are typically found in plants as glycosides. Iridoids and iridoid glycosides are known for their biological activities, including antimicrobial property (Tundis *et al*., 2008). Plumieride, protoplumericin A and plumieride acid, from *Plumeria alba*, were reported active against *Bacillus subtilis*, *Candida albicans*, *Escherichia coli* and *S.aureus* (Afifi *et al*., 2006). Agnuside and negundoside, from *Vitex negundo*, both inhibited the growth of *Cryptococcus neoformans*, *Klebsiella pneumonia* and *Trichophyton mentagrophytes*, and the latter also showed activity against *Aspergillus fumigatus*, *Escherichia coli*, *Pseudomonas aeruginosa* and *Staphylococcus aureu* (Sathiamoorthy *et al*., 2007). Pulchelloside from *Eremostachys laciniata* was against *Bacillus cereus*, penicillin-resistant *Escherichia coli*, *Proteus mirabilis* and *S. aureus* with MIC values of 50.0 μg/mL

(Modaressi *et al*., 2009). Two iridoid lactones, plumericin and isoplumericin from *Plumeria bicolor*, exhibited strong activity against *M. tuberculosis* $H_{37}Rv$ and four MDR strains with MICs ranging from 1.3 to 2.6 μg/mL (Kumar *et al*., 2013).

1.2.5 Lignans

Lignans are polyphenolic compounds derived from phenylalanine through dimerization of substituted cinnamic alcohols. Their antimicrobial activity has been well documented. A lignan, (+)-lyoniresinol 3α-*O*-β-D-glucopyranoside, isolated from the root bark of *Lycium chinense*, was reported active against *S. aureus* (MIC=2.5~5.0 μg/mL) and three human-pathogenic fungi, *Candida albicans*, *Saccharomyces cerevisiae* and *Trichosporon beigelii* (MICs=5.0, 5.0 and 10.0 μg/mL, respectively) (Lee *et al*., 2005). Hopeanolin, obtained from the stem bark of *Hopea exalata*, demonstrated high antifungal activity against *Alternaria solani*, *Colletotrichum lagenarium*, *Fusarium oxysporum*, *Pyricularia oryzae* and *Valsa mali* (Ge *et al*., 2006). Heyneanol A, from the root extract of *Vitis sp.* (grape vine), was active against *Enterococcus faecium*, *S. aureus*, *Streptococcus agalactiae*, *Streptococcus pyogenes* and MRSA (MIC=2.0 μg/mL) (Peng *et al*., 2008). Eupomatenoid-5 from *Piper regnellii* and dihydroguaiaretic acid from *Larrea tridentata* were also active against MRSA (Marcal *et al*., 2010; Favela-Hernández *et al*., 2012). The dihydroguaiaretic acid as well as another two lignans 4-epi-larreatricin and 3'-demethoxy-6-*O*-demethylisoguaiacin (from *Larrea tridentata*) had acitivity towards multidrug-resistant strains of *M. tuberculosis* with MICs of 12.5~50, 50, 12.5 μg/mL, respectively (Favela-Hernández *et al*., 2012).

1.2.6 Polypeptides and lectins

Antimicrobial peptides are usually low molecular weight cationic proteins with

disulfide bonds (Zhang and Lewis, 1997; Izadpanah and Gallo, 2005), which can form ion channels on bacterial cell membranes (Dong *et al.*, 2002; Ganz, 2004; Rogan *et al.*, 2006) or can bind to bacterial endotoxins (Rogan *et al*., 2006). Many antibacterial peptide families have been isolated from plants. For example, a 47-residue peptide (fabatin) from the beans of *Vicia faba* inhibited *E. coli*, *Enterococcus hirae* and *P. aeruginosa* (Zhang and Lewis, 1997). Other plant peptides such as circulins A and B, cyclopsychotride A, Ib-AMP1 and Ib-AMP4, have also been reported effective against *Bacillus subtilis*, *Escherichia coli*, *Klebsiella oxytoca*, *Micrococcus luteus*, *Proteus vulgaris*, *Pseudomonas aeruginosa*, *S. aureus* or *Streptococcus faecalis* (Pelegrini *et al*., 2011).

Lectins are nonimmunogenic proteins/glycoproteins with at least one noncatalytic domain that can bind carbohydrate residues selectively and reversibly (Zhao *et al.*, 2009; Costa *et al.*, 2010). Owing to their binding to the specific carbohydrates on the surfaces of microorganisms, some lectins have been reported to possess substantial activity particularly against *Bacillus subtilis*, *Enterococcus faecalis*, *Escherichia coli*, *Klebsiella pneumoniae*, *Proteus morganii*, *Staphylococcus epidermidis*, *Streptococcus faecalis* and *Xanthomonas axonopodis. pv. passiflorae* (Riera *et al.*, 2003; Costa *et al.*, 2010; Barbosa *et al.*, 2010); antifungal activity against *Fusarium lateritium* and *Rhizoctonia solani* and antiviral activity against White Spot Syndrome Virus (Zhao *et al*., 2009).

1.2.7 Quinones and derivatives

Quinones are aromatic compounds with two ketone substitutients. The exchange between diphenol and diketone occurs easily. This can explain for many biological activities of quinones. Quinones are also able to irreversibly combine with nucleophilic groups such as amino acids to make a protein inactive or non-functional,

which is considered to account for the potential antimicrobial activity of quinones (Stern *et al.*, 1996).

Reports have shown that naphthoquinones from *Fusarium solani*, *F. oxysporum* and *Cassia italica* were active against *Bacillus anthracis*, *Corynebacterium pseudodiphthericum*, *Pseudomonas aeruginosa*, *Pseudomonas pseudomalliae*, *Staphylococcus aureus* and *Streptococcus pyogenes* (Baker *et al.*, 1989; Kazmi *et al.*, 1994). 6-(4,7-Dihydroxy-heptyl) quinone obtained from *Pergularia daemia* was also effective against some pathogenic bacterial strains (Ignacimuthu *et al*., 2009). Mansonone F, a sesquiterpenoid quinone isolated from *Ulmus davidiana var. japonica*, displayed antibacterial acitvity against MRSA comparable to that of vancomycin (Shin *et al*., 2000). Alkannin and shikonin from *Arnebia euchroma* were active against MRSA with MICs of 6.25 μg/mL (Shen *et al*., 2002). 3-Methoxyjuglone, isolated from *Engelhardia roxburghiana*, exhibited activity against *M. tuberculosis* $H_{37}Rv$ (MIC=6.25 μg/mL) (Lin *et al*., 2005). Royleanones horminone, 6β,7α-dihydroxyroyleanone and 6,7-dehydroroyleanone displayed activity against multidrug-resistant *M. tuberculosis* strains (MICs≤12.5 μg/mL), and 7α-acetoxy-6β-hydroxyroyleanone was active against *M. tuberculosis* $H_{37}Rv$ strain (MIC=25 μg/mL) (Rijo *et al*., 2010). Naturally derived quinones also demonstrated good to moderate antifungal activity against *Colletotrichum spp*. (Meazza *et al*., 2003).

1.2.8 Saponins

Saponins are glycosides containing one or more sugar chains on a triterpene or steroid aglycone backbone. They have been reported to possess a wide range of biological properties, including antimicrobial activity (Güçlü-Üstündağ and Mazza, 2007). Dioscin, a steroidal saponin isolated from *Smilacina atropurpurea*, displayed

activity against *Candida albicans* and *Candida glabrata* (Zhang *et al*., 2006). (25R)-5α-Spirostan-3β,6β-diol-3-*O*-{β-Dglucopyranosyl-(1/2)-*O*-[β-D-xylopyranosyl-(1/3)]-*O*-β-D-glucopyranosyl-(1/4)-β-D-galactopyranoside} and aginoside, from *Allium leucanthum*, were active against seven Candida strains with a minimum fungicidal concentration (MFC) ranging from 6.25 to 12.5 μg/mL (Mskhiladze *et al*., 2008). Scrokoelziside A from *Scrophularia ningpoensis* was effective against β-haemolytic streptococci strain (Li *et al*., 2009). Ilekudinchosides A and B, two triterpenoid saponins obtained from *Ilex kudincha*, exhibited activity against *S.aureus* and MRSA (Zuo *et al*., 2011).

1.2.9 Simple phenolics and derivatives

Compounds in this group have a phenolic ring which can be substituted with more than one hydroxyl groups. The site and number of hydroxyl groups on the ring are speculated to be related to antimicrobial activity. Catechol, caffeic acid and cinnamic acid are common compounds in this category.

Studies have shown that catechol had antibacterial activity against three bacterial strains (*Corynebacterium xerosis*, *Pseudomonas putida* and *Pseudomonas pyocyanea*) and two fungi (*Fusarium oxysporum* and *Penicillium italicum*) (Kocacalıskana *et al*., 2006). Catechol and its derivatives, isolated from *Diospyros kaki* Thunb. roots, were also reported to be effective against some pathogenic intestinal bacteria (Jeonga *et al*., 2009). Caffeic acid, isolated from herbs such as tarragon and thyme, was active against bacteria, viruses and fungi (Brantner and Grein, 1994; Sher, 2009). Caffeic acid and its esters, isolated from propolis, displayed activity against seven Gram-positive, four Gram-negative bacteria and one fungus (Kartala *et al*., 2003). Leaf extracts of rosemary and lavender also exhibited activity against some phytopathogens, which was mainly ascribed to caffeic acid, rosmarinic acid and

some other simple phenolic derivatives (Widmer and Laurent, 2006). Cinnamic acid has a long history as antitubercular agent used along with known antibiotics such as isoniazid, rifampin, ofloxacine or clofazimine. Studies showed that gradual improvement was observed when the TB-patients were treated with cinnamic acid isolated from storax (resinous exudate of the tree *Liquidambar orientalis*). Ethylcinnamate and benzylcinnamate have also been reported as anti-TB agents (De *et al*., 2012a).

1.2.10 Steroids

Steroids are compounds that contain a characteristic arrangement of four cycloalkane rings that are joined to each other. Some steroids have been reported with antitubercular activity. A mixture of two ketosteroids stigmasta-4-en-3-one and stigmasta-4-22-dien-3-one, isolated from *Morinda citrifolia*, exhibited strong activity against *M. tuberculosis* (MIC<2.0 μg/mL) (Saludes *et al*., 2002). Several sterols from *Ruprechtia triflora* were active against *M. tuberculosis* with MIC values ranging from 2-128 μg/mL, with 5α,8α-epidioxyergost-6,22-dien-3β-ol, 5α,8α-epidioxystigmasta-6,22-dien-3β-ol and stigmast-4-en-6β-ol-3-one being the most active, each with an MIC value of 2 μg/mL (Woldemichael *et al*., 2003). Two tirucallane-skeleton sterols isolated from the stem bark of *Amphipterygium adstringens*, (14b,24e)-3-hydroxylanosta-7,24-dien-26-oic acid and (14b,24e)-3-oxolanosta-7,24-dien-26-oic acid, revealed activity against *M. tuberculosis* $H_{37}Rv$ with MICs of 64 and 32 μg/mL, respectively (Rivero-Cruz *et al*., 2005). Other steroids showing antitubercular acitivity include cholesterol, sitosterol, ergosterol, stigmasterol, ergosterol peroxide, chondrilasterol (Rugutt and Rugutt, 2012), and stigmast-5-en-3β-ol-7-one, stigmast-4-ene-6β-ol-3-one, stigmast-5,22-dien-3β-ol-7-one and stigmast-4, 22-dien-6-ol-3β-one (Gutierrez-Lugo *et al*., 2005).

1.2.11 Terpenes and terpenoids

Terpenes are naturally occurring hydrocarbons based on combinations of the isoprene unit. Terpenes chemical modification such as by oxidation or rearrangement of the carbon skeleton produces terpenoids (Cowan, 1999). Terpenes and terpenoids are the primary constituents of the essential oils produced by plants as a defense mechanism against insects, fungi and other invaders (Tsao and Coats, 1995). Terpenes are classified into monoterpenes (C_{10}), sesquiterpenes (C_{15}), diterpenes (C_{20}), triterpenes (C_{30}) and tetraterpenes (C_{40}).

Studies have shown that terpenes exhibit strong antimicrobial activity (Baratta *et al.*, 1998; Kalemba and Kunicka, 2003; Pasqua *et al.*, 2005; Adiguzel *et al.*, 2007; Luangnarumitchai *et al.*, 2007; Dayisoylu *et al.*, 2009), and many terpenoids are also active against bacteria, fungi, viruses and protozoa (Hasegawa *et al.*, 1994; Xu *et al.*, 1996; Ghoshal *et al.*, 1996; Singh and Singh, 2003; Can-Aké *et al.*, 2004; Rahman *et al.*, 2005; Daisy *et al.*, 2008). Terpenes ferruginol, hinokiol, 15-copaenol, cubenol and torreyol, from *Pilgerodendron uviferum* (D. Don) Florin, were reported effective against *Bacillus subtilis*, *Pseudomonas aureginosa* and *S. aureus* (Solis *et al*., 2004). Linalyl acetate, (+) menthol and thymol displayed strong activity against *Escherichia coli* and *S. aureus* (Trombetta *et al*., 2005). A triterpenoid 3-acetyl aleuritolic acid, from *Spirostachys Africana* bark, exhibited activity against *Escherichia coli*, *Salmonella typhy*, *Shigella dysenteriae*, *S. aureus* and *Vibrio cholera* (Mathabe *et al*., 2008). Carvacrol, thymol, geraniol and eugenol were reported active against *S. aureus* methicillin sensitive (MSSA) and MRSA (Gallucci *et al*., 2010). A new terpenoid isolated from *Mentha pulegium* and identified as 1α, 6β-dimethyl-5β-hydroxy-4β-(prop-1-en-2-yl)-decahydronaphthalen-2-one, also displayed activity against MRSA (IC_{50}=8.5 μg/mL) (Ibrahim, 2013).

(+)-Bornyl piperate, a monoterpene ester isolated from the underground roots of *Piper aff. Pedicellatum*, inhibited the growth of *M. tuberculosis* $H_{37}Ra$ with MIC of 25 μg/mL (Rukachaisirikul *et al*., 2004). Totarol, from *Juniperus communis*, exhibited activity against *M. tuberculosis* $H_{37}Rv$ and the isoniazid-, streptomycin-, and moxifloxacin-resistant variants (MIC of 73.7, 38.4, 83.4 and 60.0 μM, respectively) (Gordien *et al*., 2009). Other terpenes or terpenoids with anti-TB activity include cabralealactone, cabraleahydroxylactone, *allo*-aromadendrane-10β, 14-diol, *allo*-aromadendrane-10α, 14-diol, *allo*-aromadendrane-10β, 13, 14-triol, eichlerialactone, cabraleadiol, friedelin, 9-hydroxy-13(14)-labden-15,16-olide and isoambreinolide (Phongmaykin *et al*., 2008; Mann *et al*., 2011; Tiwari *et al*., 2013).

1.2.12 Xanthones and derivatives

Xanthones are polyphenolic compounds structurally similar to bioflavonoids, with a six-carbon conjugated ring characterized by multiple double carbon bonds. Compounds in this category have fewer side-effects and a low probability to cause pathogen resistance compared with conventional antibiotics and synthetic antimicrobial agents. Natural xanthones are known for their potent anti-MRSA activity (Saleem *et al*., 2010).

Two tetraoxygenated xanthones (mangostanin and amangostin), isolated from *Garcinia cowa*, exhibited activity against methicillin-sensitive *S. aureus* (MSSA, ATCC 25923) and MRSA with MIC values of 4.0 μg/mL and 8.0 μg/mL, respectively (Panthong *et al*., 2006). γ-Mangostin from *Garcinia mangostana* displayed antibacterial activity against MRSA, MSSA, vancomycin-resistant *Enterococcus* (VRE) and vancomycin-sensitive *Enterococcus* (VSE) strains at MICs 3.13, 6.25, 6.25 and 6.25 μg/mL (Dharmaratne *et al*., 2013). Formoxanthone C, macluraxanthone, xanthone V1 and gerontoxanthone I from the roots of *Cratoxylum*

formosum were reported active against *Bacillus subtilis*, *Enterococcus faecalis*, *Salmonella typhi* and *S. aureus* (Boonsri *et al*., 2006). Prenylated xanthones α- and β-mangostins and garcinone B, obtained from the fruits of *Garcinia mangostana*, exhibited strong inhibitory effect against *M. tuberculosis* (MIC=6.25 μg/mL) (Suksamrarn *et al*., 2003).

1.3 Medicinal plants

Plants have been traditionally used worldwide for centuries to treat many illnesses, including infectious diseases (Kumarasamy *et al.*, 2002). Plants have developed a stunning array of protective mechanisms to combat invading "ennemies" like herbivorous insects and pathogenic microbes (Freeman and Beattie, 2008). One of these mechanisms of defence is the production of abundant antimicrobial substances. These compounds are often also active against microbial pathogens causing diseases in human. This gives a rationale for the use of plants in traditional medicine as remedies for various infections (Rios and Recio, 2005; Gonzalez-Lamothe *et al*., 2009). Studies have shown that plants contain a wide variety of bioactive natural products, some of which possess good *in vitro* antimicrobial activity (Sher, 2009). Medicinal plants thus represent an important source of natural 'hits' which could be optimised to afford new antimicrobial drug leads. There has been an increase in recent years in the search for novel antimicrobial agents from medicinal plants (Namita and Mukesh, 2012).

In Scotland, many plants have a long history of traditional use for the treatment of infections (e.g. influenza, diphtheria, typhoid, smallpox, leprosy, pneumonia, scrofula) (Table 1.1) (Darwin, 1996; Mabberleg, 2003).

Table 1.1 Medicinal plants commonly used in Scotland

Species	Common Name	Family	Medicinal use
Arctium lappa L.	Burdock	Asteraceae	diuretic, diaphoretic, antimicrobial and to purify blood
Tussilago farfara L.	Coltsfoot	Asteraceae	suppress cough, treat lung ailments and skin diseases
Bellis perennis L.	Common daisy	Asteraceae	treat joint pains, arthritis or joint inflammation, liver and kidney disorders
Taraxacum officinale L.	Common dandelion	Asteraceae	diuretic ,laxative; treat gallbladder/liver ailments, diabetes
Achillea millefolium L.	Yarrow	Asteraceae	treat inflammations; stop bleeding; sedative
Chamomilla recutita L.	German chamomile	Asteraceae	treat stomachache and irritable bowel syndrome; laxative; anti-inflammatory and bactericidal
Angelica sylvestris L.	Wild angelica	Apiaceae	antispasmodic, diaphoretic, diuretic, expectorant, stomachic and tonic
Foeniculum vulgare Mill.	Fenne	Apiaceae	analgesic, anti-inflammatory, antispasmodic, diuretic, expectorant, laxative and stomachic
Allium ursinum L.	Wild garlic	Alliaceae	antibacterial, antifungal, antioxidant
Alliaria petiolata M. Bieb.	Garlic mustard	Brassicaceae	antiasthmatic, antiscorbutic, deobstruent, diaphoretic
Capsella bursa-pastoris L.	Shepherd's purse	Brassicaceae	antiscorbutic, astringent, diuretic, haemostatic, hypotensive

Table 1.1 (continued) Medicinal plants commonly used in Scotland

Species	Common Name	Family	Medicinal use
Empetrum nigrum L.	Crowberry	Ericaceae	treat diarrhea and stomach problems
Hyssopus officinalis L.	Hyssop	Lamiaceae	cough suppressant
Thymus praecox L.	Wild thyme	Lamiaceae	disinfectant, sedative, antispasmodic, diaphoretic, expectorant and tonic
Salvia officinalis L.	Sage	Lamiaceae	antibiotic, antifungal, astringent, antispasmodic and tonic
Rosmarinus officinalis L.	Rosemary	Lamiaceae	antioxidant, lower the risk of strokes and neurodegenerative diseases
Malva moschata L.	Musk-mallow	Malvaceae	antiphlogistic, astringent, demulcent, diuretic, expectorant, laxative
Chelidonium majus L.	Greater celandine	Papaveraceae	analgesic, cholagogic, sedative, antimicrobial
Agropyron repens L.	Cough grass	Poaceae	treat urinary tract infections and kidneys conditions; antimicrobial
Prunus padus L.	Bird cherry	Rosaceae	anodyne, diuretic, febrifuge and sedative, combat colds and feverish conditions
Verbena officinalis L.	Common vervain	Verbenaceae	diaphoretic, improve digestion, treat depression
Valeriana officinalis L.	Valerian	Valerianaceae	sedative, treat insomnia

1.3.1 *Arctium lappa* L.

1.3.1.1 Botanical description

A. lappa L. is a biennial herbaceous plant commonly named "burdock" or "lappa burdock" (Peirce, 1999). It belongs to the Asteraceae family. Burdock is generally 3-4 feet high. Its stem has multiple branches. Its leaves are dark green, wavy and heart-shaped. When in bloom from July to October, Burdock has round crimson-violet prickly flowerheads (Figure 1.1). The roots are brownish-green or nearly black with a very horny, longitudinally wrinkled bark (Kemper *et al*., 1999).

Figure 1.1 Flowerheads of *Arctium lappa* L. [(a)]

a: http://en.wikipedia.org/wiki/File:Villtakjas_2008.jpg (picture not copyright protected)

1.3.1.2 Traditional uses

A. lappa L. is a traditional herbal remedy, which has been used worldwide for a long time to treat a range of diseases. In 14th century Europe, burdock was used to treat leprosy and later to combat fevers and treat skin infections, syphilis and gonorrhea (Kemper *et al*., 1999). In China, burdock roots are used mixed with other herbs to treat upper respiratory tract infections (Sun *et al*., 1992), while dried fruits are used

to promote eruption, relieve a sore throat and alleviate swelling (Kamkaen *et al*., 2006). In Korea, the seeds are traditionally used as a diuretic, anti-inflammatory and detoxifying agent (Park *et al*., 2007). In Brazil, the leaves and roots are used for their diuretic and antiseptic properties (Barbosa-Filho *et al*., 1993). American herbalists use burdock root to treat arthritis, urinary tract-related problems, ringworms, and eczema (Kemper *et al*., 1999). In Britain, the root of burdock has been used against scurvy, diabetes and rheumatism (Williams and Wilkins, 1999). Burdock roots, seeds and leaves are also used as traditional anti-TB medicine (Ritchason, 1995).

1.3.1.3 Previous chemical work on *Arctium lappa* L.

Various phytochemicals, such as lignans, terpenoids, carbohydrates, sterols and polyphenols, have been mainly isolated from the roots, seeds and fruits of burdock (Table 1.2).

1.3.1.4 Previous biological work on *Arctium lappa* L.

Burdock extracts and some isolated phytochemicals showed antimicrobial activity. The *n*-hexane, butanol and ethyl acetate extracts of burdock leaf inhibited some bacteria related to endodontic pathogens (e.g. *Bacillus subtilis*, *Enterococcus faecalis*, *Pseudomonas aeruginosa* and *S. aureus*,) (Pereira *et al.*, 2005). Burdock root ethanol extract was active *in vitro* against *Escherichia coli, Shigella flexneri* and *Shigella sonnei* (Moskalenko, 1986). An aqeous-ethanolic root extract also displayed activity against *Proteus mirabilis* (Keyhanfar *et al*., 2011). Burdock peel extract was effective against *Vibrio parahemolyticus* (He *et al*., 2012). Burdock fruit extract inhibited the growth of *Aspergillus parasiticus* (Bahk and Marth, 1983). Some polyacetylenes isolated from the roots exhibited potent antibacterial and antifungal properties (Takasugi *et al*., 1987). Chlorogenic acid isolated from the leaves showed inhibitory effects on *Escherichia coli*, *Micrococcus luteus* and *S. aureus* (Lin *et al.*,

2004). Arctigenin, isolated from the seeds, fruits, leaves and roots, exhibited activity against HIV-1 (Schroder *et al*., 1990; Eich *et al*., 1996) while caffeic acid and chlorogenic acid strongly inhibited herpes simplex viruses (HSV-1, HSV-2) and adenoviruses (ADV-3, ADV-11) (Chiang *et al*., 2002).

Other biological properties reported for *A. lappa* include anti-inflammotory, anti-cancer and anti-diabetic activity. Experiments showed that its roots antagonised PFA (platelet activating factor) in rabbits (Iwakami *et al*., 1992). Burdock reduced the *in vitro* release of inflammatory mediators through inhibition of degranulation and leukotriene release, and decreased carageenan-induced edema in rodents (Lin *et al*., 1996). Studies also revealed that its seed extracts ameliorated high fat/cholesterol diet-induced vascular dysfunction through protection of vascular relaxation and suppression of inflammation (Lee *et al*., 2012). The sesquiterpene lactone onopordopicrin enriched fraction of burdock exerted marked protective effects in acute experimental colitis (de-Almeida *et al*., 2013). Arctiin, a lignan isolated from *A. lappa*, displayed anti-cancer activity in humans and rats (Hirose *et al.*, 2002; Huang *et al.*, 2004; Matsuzaki *et al.*, 2008). Studies also revealed that the oral administration of an ethanolic extract of burdock root significantly decreased blood glucose and increased insulin level in streptozotocin-induced diabetic rats (Cao *et al*., 2012).

Table 1.2 Some phytochemicals previously isolated from *A. lappa*

Classification	Compound	Parts of the plant	Reference
Lignans	Arctigenin 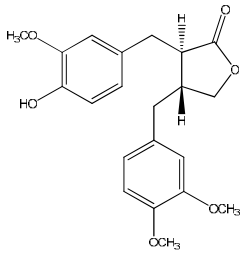	Seeds, fruits, leaves, roots	(Liu *et al*., 2005; Ishihara *et al.*, 2006; Kamkaen *et al.*, 2006; Matsumoto *et al.*, 2006; Tsai *et al*., 2011)
	3'-Demethyl arctigenin 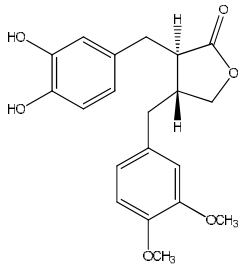	Seeds	(Kamkaen *et al*., 2006)
	Arctiin 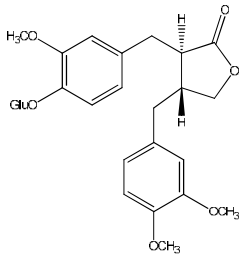	Seeds, fruits, leaves, roots	(Liu *et al*., 2005; Ishihara *et al*., 2006; Kamkaen *et al*., 2006)

Table 1.2 (continued) Some phytochemicals previously isolated from *A. lappa*

Classification	Compound	Parts of the plant	Reference
	Matairesinol 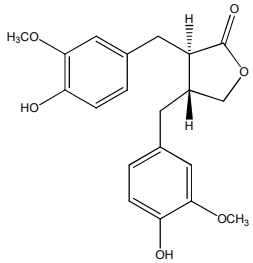	Fruits, seeds	(Wang and Yang, 1993; Matsumoto *et al*., 2006)
	Trachelogenin 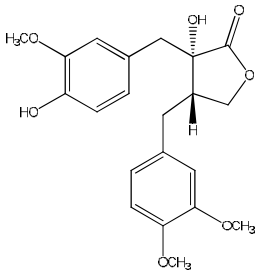	Fruits	(Chan *et al*., 2011)
	Diarctigenin 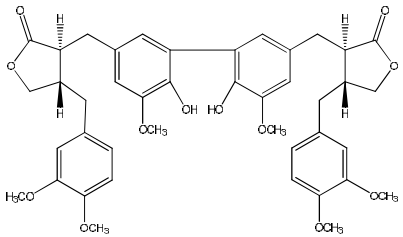	Seeds	(Park *et al*., 2007; Kim *et al*., 2008)

Table 1.2 (continued) Some phytochemicals previously isolated from *A. lappa*

Classification	Compound	Parts of the plant	Reference
	Lappaol A 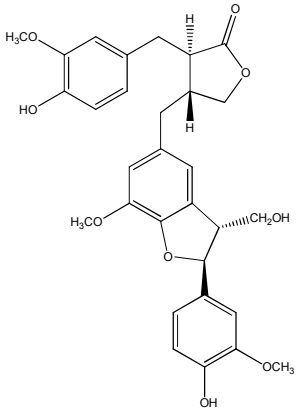	Seeds	(Ichihara *et al*., 1976; Ming *et al*., 2004)
	Lappaol B 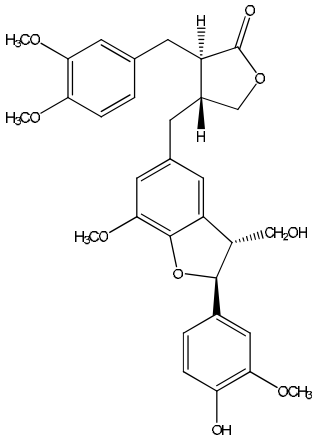	Seeds	(Ichihara *et al*., 1976)

Table 1.2 (continued) Some phytochemicals previously isolated from *A. lappa*

Classification	Compound	Parts of the plant	Reference
	Lappaol C 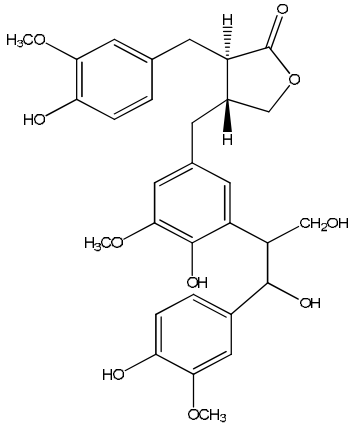	Seeds	(Ming *et al*., 2004; Park *et al*., 2007)
	Isolappaol C 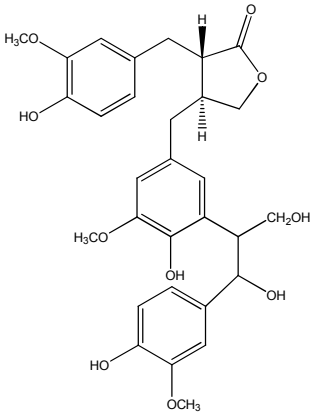	Seeds	(Park *et al*., 2007)

Table 1.2 (continued) Some phytochemicals previously isolated from *A. lappa*

Classification	Compound	Parts of the plant	Reference
	Lappaol D	Seeds	(Park *et al*., 2007)
	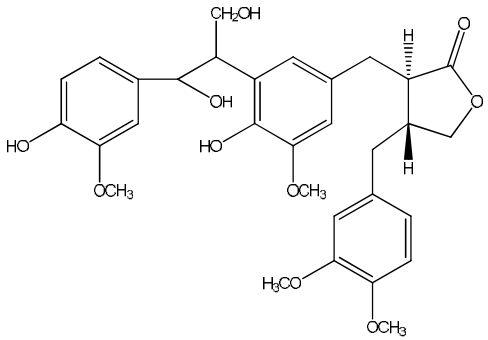		
	Lappaol F	Seeds	(Ming *et al*., 2004)
	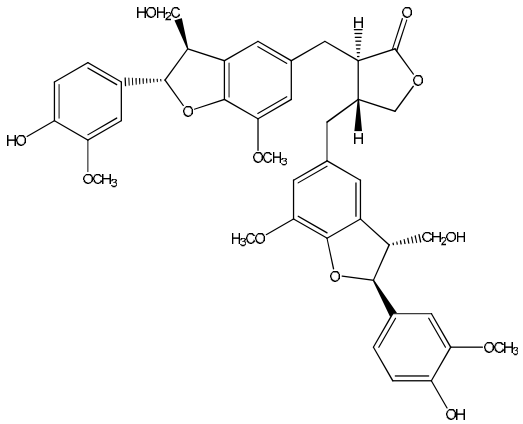		

Table 1.2 (continued) Some phytochemicals previously isolated from *A. lappa*

Classification	Compound	Parts of the plant	Reference
Sterols	β-sitosterol	Seeds	(Ming *et al*., 2004)
	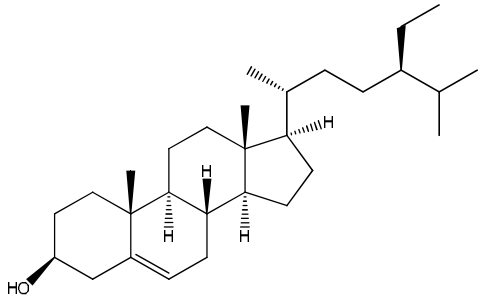		
	Sitosterol-β-D-glucopyranoside	Roots, seeds	(Ming *et al*., 2004; Mizushina *et al*., 2006)
	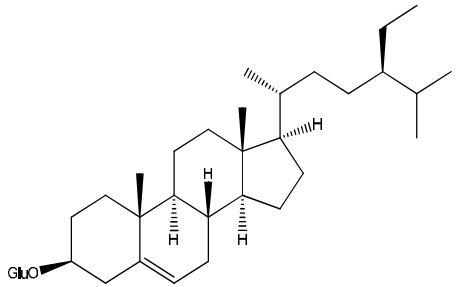		
Terpenoids	β-eudesmol	Fruits, leaves	(Tsuneki *et al*., 2005)
	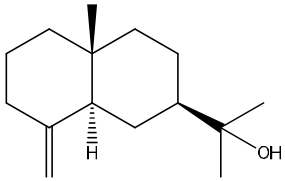		

Table 1.2 (continued) Some phytochemicals previously isolated from *A. lappa*

Classification	Compound	Parts of the plant	Reference
	Costus acid 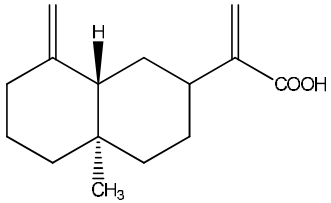	Leaves	(Barnes *et al*., 2007)
	Dehydrocostus lactone 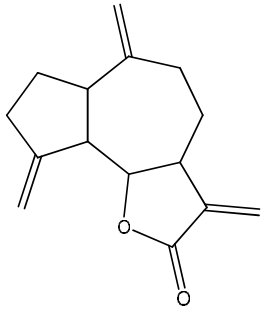	Leaves	(Barnes *et al*., 2007)
	Onopordopicrin 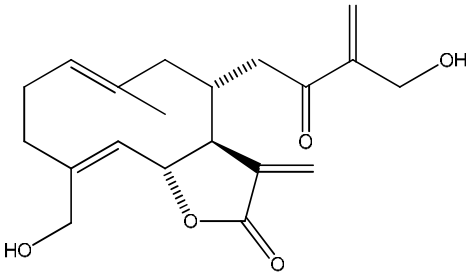	Leaves	(Costa *et al*., 1993)

Table 1.2 (continued) Some phytochemicals previously isolated from *A. lappa*

Classification	Compound	Parts of the plant	Reference
Polyphenols	Caffeic acid 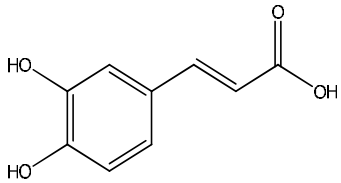	Roots, leaves, seeds	(Bhat *et al*., 2007; Pari and Prasath, 2008)
	Chlorogenic acid 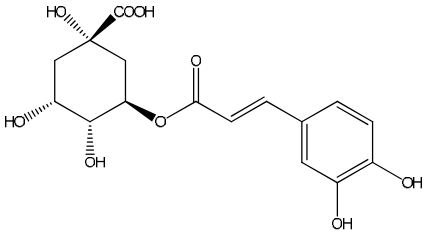	Roots, leaves, seeds	(Chen *et al*., 2004; Lin *et al*., 2004)
	Cynarin 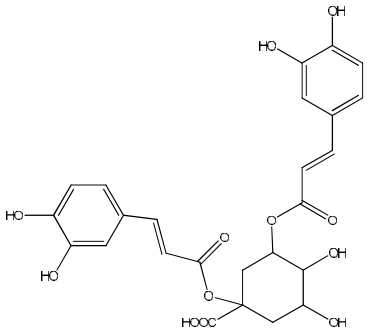	Roots, leaves, seeds	(Ferracane *et al*., 2010)

Table 1.2 (continued) Some phytochemicals previously isolated from *A. lappa*

Classification	Compound	Parts of the plant	Reference
	1-*O*-,5 -*O*-dicaffeoyl-3-*O*-succinylquinic acid	Roots	(Maruta *et al*., 1995)
	1-*O*-,5 -*O*-dicaffeoyl-4-*O*-succinylquinic acid	Roots	(Maruta *et al*., 1995)

Table 1.2 (continued) Some phytochemicals previously isolated from *A. lappa*

Classification	Compound	Parts of the plant	Reference
	1-*O*-,5 -*O*-dicaffeoyl-3-*O*-, 4-*O*-disuccinylquinic acid	Roots	(Maruta *et al*., 1995)
	Luteolin	Roots, leaves	(Ferracane *et al*., 2010)
	Quercetin	Roots, leaves	(Ferracane *et al.*, 2010)

Table 1.2 (continued) Some phytochemicals previously isolated from *A. lappa*

Classification	Compound	Parts of the plant	Reference
	Quercitrin 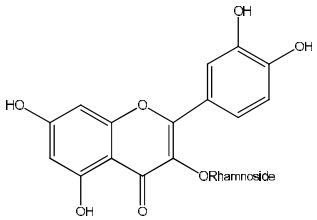	Roots, leaves	(Ferracane *et al*., 2010)
	Kaempferol 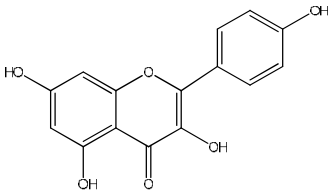	Roots	(Chen *et al*., 2011)
Carbohydrates	ALF (Fructan) 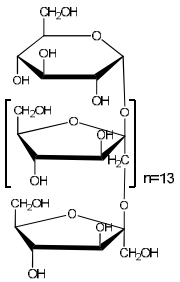	Roots	(Shi, 2009)

1.3.2 *Tussilago farfara* L.

1.3.2.1 Botanical description

T. farfara L. is a low-growing evergreen perennial plant from the Asteraceae family. It is commonly named as coltsfoot, coughwort, clayweed, horsefoot or foalfoot (Bond *et al.*, 2007). It grows 7.5-30 cm tall and is covered by upright pink scales and loose cottony fluff. The leaves are 10-20 cm across, round or heart-shaped and slightly toothed, with a downy whitish underside and a smooth sea-green upper surface. The crushed flowers are solitary, in bright yellow color and look like dandelion (fluffy white ball, seeding between May and July) (Figure 1.2). The woolly leaf stems are in clumps without scales, and each arises directly from a separate root bud (Church, 2008).

Figure 1.2 Flowers of *Tussilago farfara* L. [(b)]

b: http://en.wikipedia.org/wiki/File:Coltsfoot.jpg (picture not copyright protected)

1.3.2.2 Traditional uses

Coltsfoot is a well-known herbal remedy. Its flower buds and leaves have been commonly used for over 2000 years in Europe and Asia to treat throat and lung illnesses, such as bronchitis, asthma, emphysema, pertussis and chronic cough

including TB (Culvenor *et al*., 1976; Didry, 1982; Duke, 2002; Bensky *et al.*, 2004). In Britain,the leaves (more rarely, the roots) soaked in water have been used to treat asthma (Allen and Hatfield, 2004), and an ointment made from the roots used with other ingredients to relieve sprains and swellings (Allen and Hatfield, 2004). In China, coltsfoot leaves and flowers are used to suppress cough (Liu *et al*, 2006). American Indians use preparations of coltsfoot roots as a blood purifier and forgout, liver and kidney problems (Church, 2008).

1.3.2.3 Previous chemical work on *Tussilago farfara* L.

T. farfara mainly contains terpenoids, flavonols, alkaloids, essential oils, tannins, acids and carbohydrates (Table 1.3).

1.3.2.4 Previous biological work on *Tussilago farfara* L.

Coltsfoot extracts displayed antimicrobial activity against several bacteria and yeasts. Fresh leaf extracts and dried flower extracts displayed activity against *Bordetella pertussis*, *Proteus hauseri, Proteus vulgaris* and *Pseudomonas aeruginosa*, (Leven *et al.*, 1979). Leaf ethanolic extracts revealed moderate activity against *Candida albicans*, *Escherichia coli*, *Klebsiella pneumoniae*, *Kluyveromyces fragilis*, *Mycobacterium smegmatis*, *Rhodotorula rubra* and *S. aureus* (Dulger and Gonuz, 2004). Ethanolic extracts from the aerial parts and the roots exhibited activity against *Bacillus cereus and* S. *aureus* (Kokoska *et al.*, 2002; Janovska *et al.*, 2003). Aqueous extracts of leaves showed activity against *Staphylococcus epidermidis and Staphylococcus pyogenes* (Turker and Usta, 2008). Ethanolic extracts of flowers and stems were active against *Lactobacillus rhamnosus*, *Saccharomyces cerevisiae* and *Serratia rubidaea* (Kačániová *et al*., 2013).

Anti-inflammatory activity has been documented against carrageenan-induced oedema in the rat paw (Benoit *et al*., 1976). A bisabolene epoxide from *T. farfara*

displayed inhibition of nitric oxide synthesis in lipopolysaccharide-activated macrophages (Ryu *et al*., 1999). Tussilagone, isolated from the flower buds, exhibited anti-inflammatory activity in murine macrophages by inducing heme oxygenase-1 (HO-1) expression (Lim *et al.*, 2008; Hwangbo *et al.*, 2009). Tussilago water extracts exhibited anti-inflammatory activity by inhibiting IFN-γ and IL-5 production (Jeong *et al*., 2013). Studies also displayed that coltsfoot extracts can inhibit PAF (platelet activating factor) (Hwang *et al*., 1987), act as a cardiovascular and respiratory stimulant (Li and Wang, 1988) and have neuroprotective and antioxidative effects (Cho *et al*., 2005).

Table 1.3 Some phytochemicals previously isolated from *T. farfara*

Classification	Compound	Parts of the plant	Reference
Terpenoids	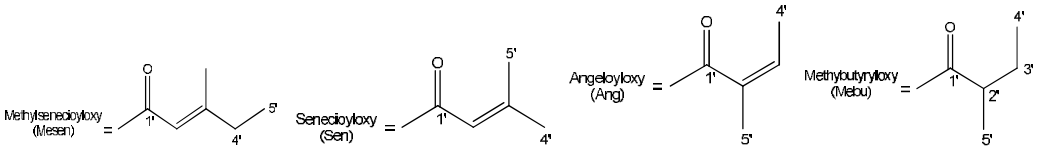		
	Sesquiterpenes:	Flower buds	(Kikuchi and Suzuki, 1992; Ryu *et al*., 1999; Yaoita *et al*., 1999 ; Yaoita *et al*., 2001; Liu *et al*., 2006; Park *et al*., 2008)
	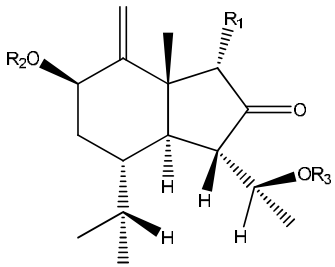		

R_1	R_2	R_3
1. H	Mesen	Ac
2. OMebu	Mesen	Ac
3. H	Mesen	H
4. H	Ang	Ac
5. H	Sen	Ac
6. OMebu	Mesen	H

1. 14-Acetoxy-7β-(3-ethyl crotonoyloxy) notonipetranone (Tussilagonone)

2. 14-Acetoxy-7β-(3-ethyl-cis-crotonoyloxy)-1α-(2-methylbutyryloxy)-notonipetranone

3. 7β-(3-Ethyl-cis-crotonoyloxy)-14-hydroxy-notonipetranone

4. 14-Acetoxy-7β-angeloyloxy-notonipetranone

5. 14-Acetoxy-7β-senecioyloxy-notonipetranone

6. 7β-(3-Ethyl-cis-crotonoyloxy)-14-hydroxy-1α-(2-methylbutyryloxy)-notonipetranone

Table 1.3 (continued) Some phytochemicals previously isolated from *T. farfara*

Classification	Compound	Parts of the plant	Reference
	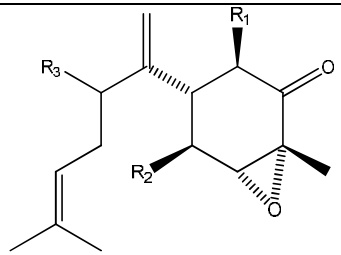		

	R_1	R_2	R_3
7.	H	H	H
8.	OAc	OH	OAng

7. (3R,4R,6S)-3,4-Epoxybisabola-7(14),10-dien-2-one

8. (1R,3R,4R,5S,6S)-1-Acetoxy-8-angeloxoyloxy-3,4-epoxy-5-hyroxbisalcola-7(14),10-dien-2-one

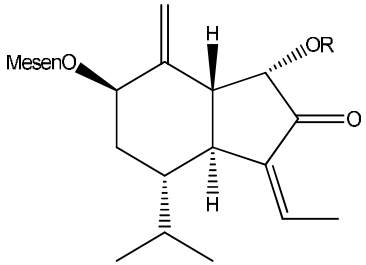

	R
9.	Mebu
10.	Ang
11.	Mesen

9. 1α-(2-Methylbutyryloxy)-7β-(4-methylsenecioyloxy)oplopa-3(14)Z,8(10)- dien-2-one

10.1α-Angeloyloxy-7β-(4-methylsenecioyloxy)oplopa-3(14)Z,8(10)-dien-2-one

11. lα-7β-Di(4-methulsenecioyloxy)oplopa-3(14)Z,8(10)-dien-2-one

Table 1.3 (continued) Some phytochemicals previously isolated from *T. farfara*

Classification	Compound	Parts of the plant	Reference
	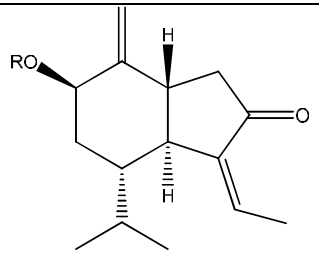 **R** **12**. Sen **13**. Mesen **14**. Ang **12**. 7β-Senecioyloxyoplopa-3(14)Z,8(10)-dien-2-one **13**. 7β-(4-Methylsenecioyloxy)oplopa-3(14)Z,8(10)-dien-2-one **14**. 7β-Angeloyloxyoplopa-3(14)*Z*,8(10)-dien-2-one		
	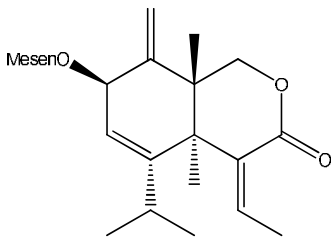 **15** 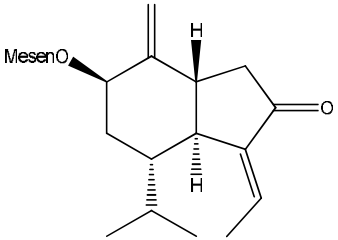 **16** **15**. 7β-(3-Ethyl-cis-crotonoyloxy)-5,6-dehydro-3,14-dehydro-Z-notonipetralactone **16**. 7β-(4-Methylsenecioyloxy)oplopa-3(14)E,8(10)-dien-2-one		

Table 1.3 (continued) Some phytochemicals previously isolated from *T. farfara*

Classification	Compound	Parts of the plant	Reference
	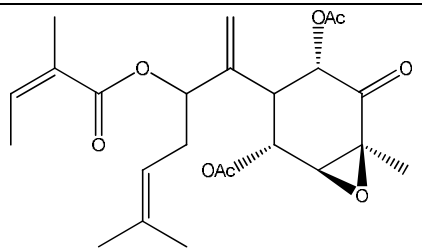 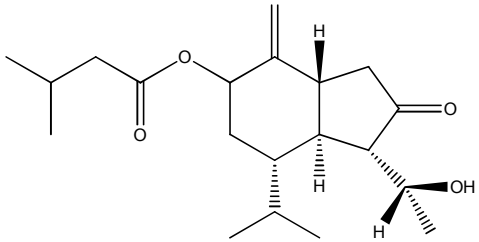 **17** **18**		
	17. 1α,5α-Bisaeetoxy-8-angeloyloxy-3β,4β-epoxy-bisabola-7(14),10-dien-2-one		
	18. 14(R)-Hydroxy -7β-isovaleroyloxyoplop-8(10)-en-2-one		
	Triterpenoids:	Flower buds	(Yaoita and Masao, 1998; Liu *et al*., 2006)
	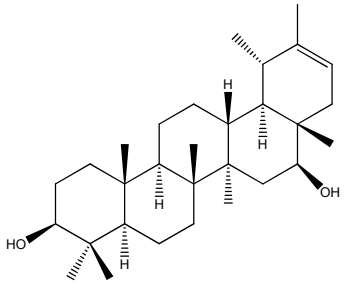 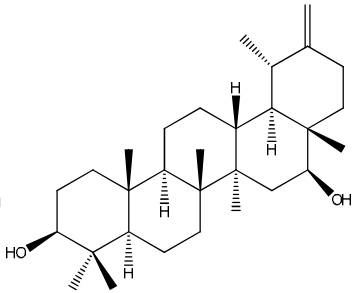 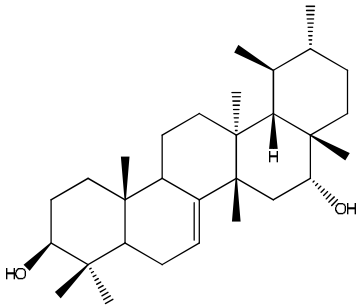 **19**. Faradiol **20**. Arnidiol **21**. Bauer-7-ene-3β,16α-diol		

Table 1.3 (continued) Some phytochemicals previously isolated from *T. farfara*

Classification	Compound				Parts of the plant	Reference
	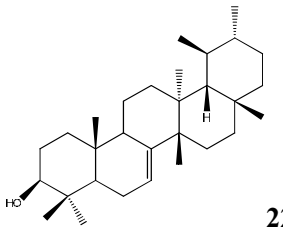 **22**. Bauerenol					
	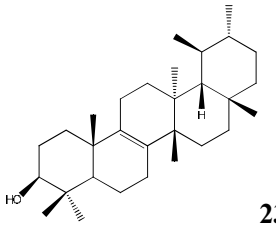 **23**. Isobauerenol					
	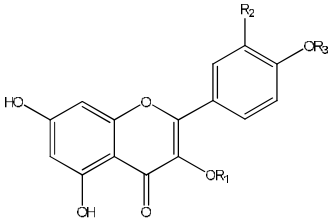				Flower buds	(Liu *et al*., 2006)
Flavonols		**R_1**	**R_2**	**R_3**		
	24. Kaempferol	H	H	H		
	25. Rutin	rut	OH	H		
	26. Hyperin	gal	OH	H		
	27. Quercetin	H	OH	H		
	28. Quercetin-3-*O*-arabinoside	ara	OH	H		
	29. Kaempferol-3-*O*-arabinoside	ara	H	H		
	30. Quercetin-4'-*O*-glucoside	H	OH	glu		
	31. Kaempferol-3-*O*-glucoside	glu	H	H		
	32. Kaempferol-3-*O*-rutinoside	rut	H	H		

Table 1.3 (continued) Some phytochemicals previously isolated from *T. farfara*

Classification	Compound				Parts of the plant	Reference
Alkaloids	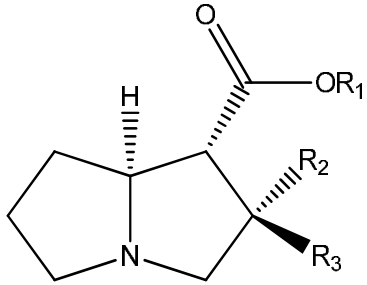				Flower buds	(Luethy *et al.*, 1980; Roder and Wiedenfeld, 1981; Liu *et al.*, 2006)
		R_1	**R_2**	**R_3**		
	33. Tussilagine	Me	OH	Me		
	34. Isotussilagine	Me	Me	OH		
	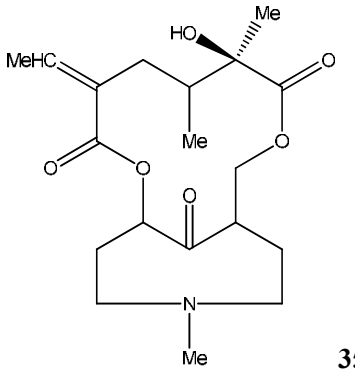 **35**. Senkirkine		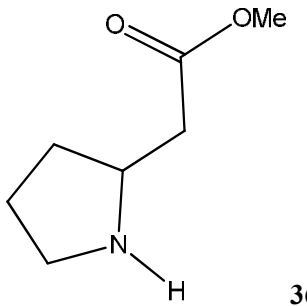 **36**. 2-Methylpyrrolidine			

Table 1.3 (continued) Some phytochemicals previously isolated from *T. farfara*

Classification	Compound					Parts of the plant	Reference
Phenolic derivatives	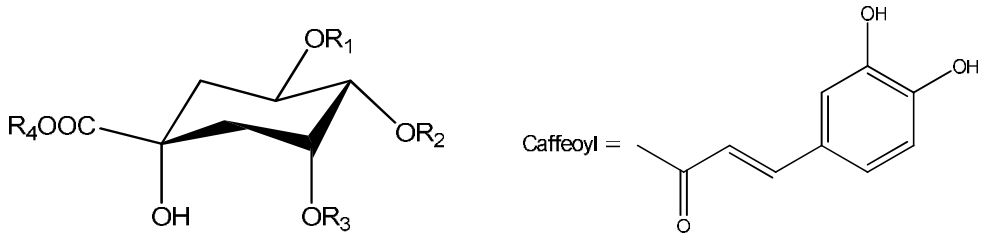					Flower buds	(Liu *et al*., 2007)
		R_1	**R_2**	**R_3**	**R_4**		
	37. Methyl 3,4-*O*-dicaffeoylquinate	Caffeoyl	Caffeoyl	H	CH_3		
	38. Methyl 3,5-*O*-dicaffeoylquinate	Caffeoyl	H	Caffeoyl	CH_3		
	39. Methyl 4,5-*O*-dicaffeoylquinate	H	Caffeoyl	Caffeoyl	CH_3		
	40. 3,5-*O*-Dicaffeoylquinic acid	Caffeoyl	H	Caffeoyl	H		
	41. Methyl 3-*O*-caffeoylquinate	Caffeoyl	H	H	CH_3		
	42. 3-*O*-Caffeoylquinic acid	Caffeoyl	H	H	H		

1.3.3 *Verbascum thapsus* L.

1.3.3.1 Botanical description

V. thapsus L. is a hairy biennial plant from the Scrophulariaceae family. Its common names include mullein, common mullein, great mullein, wooly mullein and white mullein (Strange, 1977; Darwin, 1996). In its first year of growth, it produces a large rosette of leaves up to 60 cm long, and the second year a single unbranched and stout flowering stem 0.3-2.0 m tall is normally bolted from the rosette of leaves (Gross and Werner, 1978). On flowering plants the thick and decurrent leaves are alternately arranged up the stem, with much variable leaf shapes from oblong to oblanceolate between the upper and lower leaves on the stem, and the leaves are gradually reduced up the stem and densely woolly with branched hairs (Millspaugh, 1974). The hairs are not confined to the leaves alone, but are also on every part of the stem, on the calyces and on the outside of the corollas, which makes the whole plant appears whitish or grey (Gross and Werner, 1978). Its small yellow flowers are densely grouped on a tall stem, with five stamens, a 5-lobed calyx tube and a 5-petalled corolla. The flowers are almost sessile with very short pedicles less than 2 mm and slightly irregular with rotate corollas (Millspaugh, 1974). Stamens are irregular and attached to the corolla, and three upper filaments are shorter and covered by yellow or whitish hairs, while the lower two are longer and glabrous with larger anthers (Gross and Werner, 1978).

Figure 1.3 Whole plants of *Verbascum thapsus* L. [(c)]

c: http://en.wikipedia.org/wiki/File:Starr_040723-0030_Verbascum_thapsus.jpg (picture not copyright protected)

1.3.3.2 Traditional uses

The plant has been used since ancient times as a remedy for the treatment of skin disorders, inflammatory conditions, bleeding of the lungs and bowels, piles and diarrhoea (Darwin, 1996). Mullein leaves and flowers have expectorant and demulcent properties and preparations were traditionally employed to treat repisratory tract-related disorders such as bronchitis, dry coughs, spasmodic cough, whooping cough, asthma and TB (Grieve, 1981; Berk, 1996). In Europe, a sweetened infusion of the flowers used to be a remedy against mild catarrhs and colic. Flowers were also reputed for burns, erysipelas, and ringworms (Millspaugh, 1974; Grieve 1981). A leaf decoction was used traditionally as a cardiostimulant, while a root decoction was used to alleviate toothaches, cramps, convulsions and migraines. Crushed roots directly rubbed on skin were traditionally used to remove warts (Tyler, 1993; 1994).

1.3.3.3 Previous chemical work on *Verbascum thapsus* L.

Previous studies regarding the chemical constituents of *V. thapsus* revealed the presence of saponins, iridoids, iridoid glycosides, phenylethanoid glycosides, flavonoids, steroids, sesquiterpenes, diterpenes and several phenolic acid derivatives (Table 1.4).

1.3.3.4 Previous biological work on *Verbascum thapsus* L.

V. thapsus extracts and some isolated compounds showed antimicrobial activity. A leaf methanolic extract displayed activity against *Escherichia coli*, *Mycobacterium phlei* and *S. aureus* (McCutcheon *et al*., 1992) and antifungal activity against *Fusarium graminearum*, *Macrophomina phaseolina*, *Microsporum cookerii* and *M. gypseum* (McCutcheon *et al*., 1994; Vogt *et al*., 2010). Leaf aqueous extracts were active against *Klebsiella pneumoniae* and *S. aureus*. An extract prepared from flowers (treated with olive oil) was found effective against *E. coli*, *K. pneumoniae*, *Pseudomonas aeruginosa* and *S. aureus* (Turker and Camper, 2002). The essential oil obtained from the dried flowering aerial parts exhibited activity against *Aspergillus niger*, *Bacillus subtilis, P. aeruginosa*, *Salmonella typhi* and *S. aureus* (Morteza-Semnaniab *et al*., 2012).

A decoction of flowers showed antiviral activity on A_2 and B-type influenza viruses (Skwarek, 1979). A methanolic extract exhibited activity against the pseudorabies virus strain RC/79 (PrV) (Escobar *et al*., 2012). Aucubin isolated from *V. thapsus* was found to suppress the DNA replication of the hepatitis B virus (Chang, 1997). *V. thapsus* extracts also displayed anthelmintic activity against roundworms (*Ascaridia galli*) and tapeworms (*Raillietina spiralis*) (Ali *et al*., 2012).

It was also reported that a methanolic extract of flowers improved wound healings by reducing swelling and inflammation (Mehdinezhad *et al*., 2011). Verbascoside was

found to inhibit the formation of 5-HETE and leucotriene B_4 in human polymorphonuclear leukocytes (Kimura *et al*., 1987), have anti-inflammatory activity against D-galactosamine and lipopolysaccharide-induced hepatitis in mice (Xiong *et al*., 1999), and suppress carrageenan-induced rat paw oedema (Schapoval *et al*., 1998). Verbascoside was also reported to increase heart rate in perfused rats (Pennacchio *et al*., 1999), but induce a dose-dependent decrease in systolic, diastolic, mean arterial blood pressure and heart rate when administered intravenously to normotensive pentothal anaesthetized rats (Ahmad *et al*., 1995).

Table 1.4 Some phytochemicals previously isolated from *V. thapsus*

Classification	Compound	Parts of the plant	Reference
Saponins	Saikogenin A	Fruit capsules	(De-Pascual-Teresa *et al*., 1980)
	3-*O*-fucopyranosylsaikogenin F	Aerial parts	(Zhao *et al*., 2011)

Table 1.4 (continued) Some phytochemicals previously isolated from *V. thapsus*

Classification	Compound	Parts of the plant	Reference
	Thapsuine A 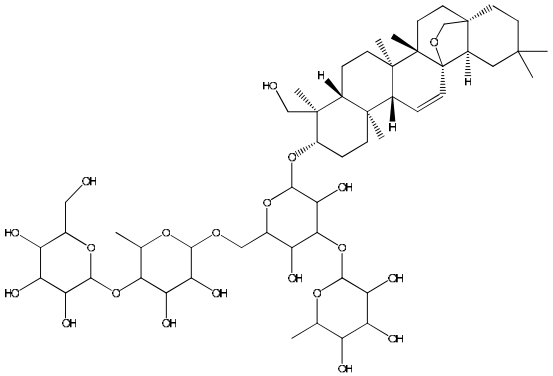	Fruit capsules	(De-Pascual-Teresa *et al*., 1980)
	Hydroxythapsuine A 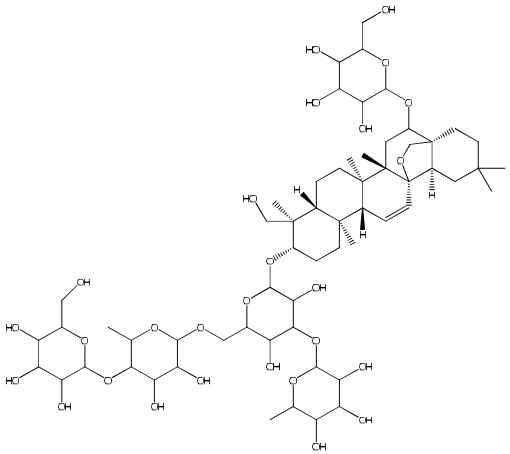	Fruit capsules	(De-Pascual-Teresa *et al*., 1980)

Table 1.4 (continued) Some phytochemicals previously isolated from *V. thapsus*

Classification	Compound	Parts of the plant	Reference
Iridoids	Jioglutolide 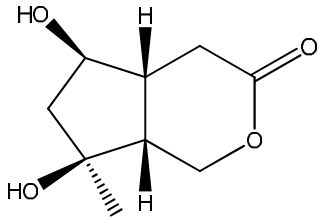	Aerial parts	(Zhao *et al*., 2011)
	Genipin 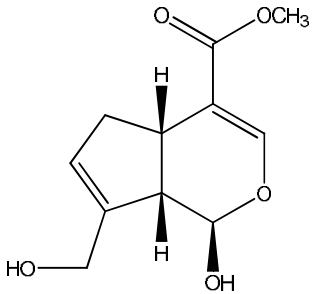	Whole plant	(Hussain *et al*., 2009)
	β-Gardiol 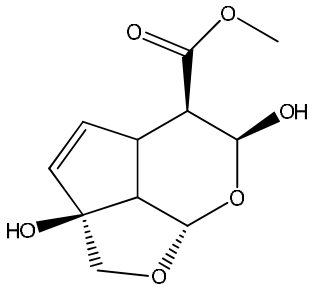	Whole plant	(Hussain *et al*., 2009)

Table 1.4 (continued) Some phytochemicals previously isolated from *V. thapsus*

Classification	Compound	Parts of the plant	Reference
	α-Gardiol 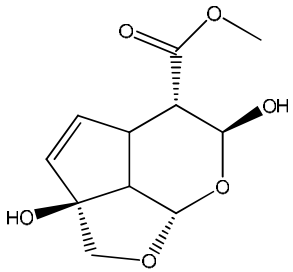	Whole plant	(Hussain *et al*., 2009)
Iridoid glycosides	Aucubin 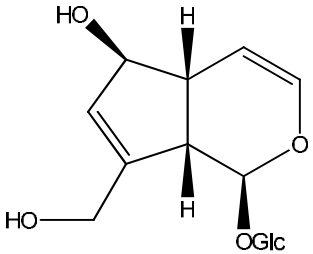	Whole plant, Roots	(Khuroo *et al*., 1988; Pardo *et al*., 1998)
	Ajugol 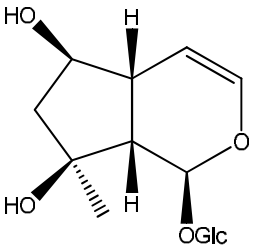	Whole plant, Roots, Aerial parts	(Warashina *et al*., 1991; Pardo *et al*., 1998; Hussain *et al*., 2009; Zhao *et al*., 2011)

Table 1.4 (continued) Some phytochemicals previously isolated from *V. thapsus*

Classification	Compound	Parts of the plant	Reference
	Catalpol 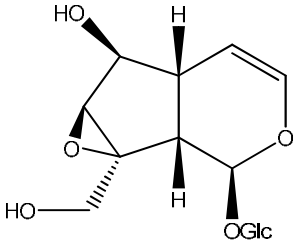	Whole plants	(Seifert *et al*., 1985)
	Harpagoside 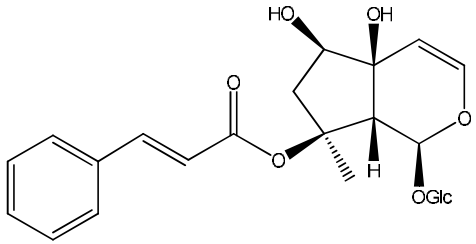	Whole plant, Roots, Aerial parts	(Warashina *et al*., 1991; Pardo *et al*., 1998; Hussain *et al*., 2009; Zhao *et al*., 2011)
	Laterioside 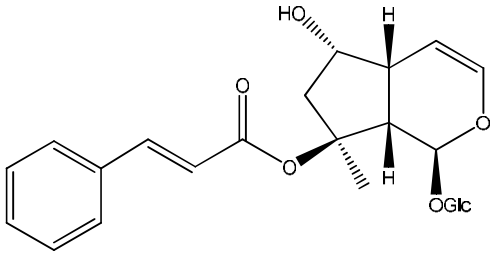	Whole plant, Roots,	(Warashina *et al*., 1991; Pardo *et al*., 1998; Hussain *et al*., 2009)

Table 1.4 (continued) Some phytochemicals previously isolated from *V. thapsus*

Classification	Compound	Parts of the plant	Reference
	Picroside	Whole plant	(Hussain *et al*., 2009)
Phenylethanoid glycosides	Verbascoside	Whole plant	(Hussain *et al*., 2009)

Table 1.4 (continued) Some phytochemicals previously isolated from *V. thapsus*

Classification	Compound	Parts of the plant	Reference
	Arenarioside	Whole plant	(Warashina *et al*., 1992)
	Alyssonoside	Whole plant	(Warashina *et al*., 1992)

Table 1.4 (continued) Some phytochemicals previously isolated from *V. thapsus*

Classification	Compound	Parts of the plant	Reference
	Leucosceptoside B	Whole plant	(Warashina *et al*., 1992)
	Cistanoside B	Whole plant	(Warashina *et al*., 1992)

Table 1.4 (continued) Some phytochemicals previously isolated from *V. thapsus*

Classification	Compound	Parts of the plant	Reference
	Forsythoside B	Whole plant	(Warashina *et al*., 1992)
Flavonoids	Verbacoside	Whole plant	(Mehrotra *et al*., 1989)
	Apigetrin	Aerial parts	(Zhao *et al*., 2011)

Table 1.4 (continued) Some phytochemicals previously isolated from *V. thapsus*

Classification	Compound	Parts of the plant	Reference
	Amentoflavone	Whole plant	(Hussain *et al*., 2009)
	Luteolin	Whole plant, Aerial parts	(Zhao *et al*., 2011)
Steroids	Ergosta-7-en-3-*β*-ol	Fruit capsules	(De-Pascual-Teresa *et al*., 1978b)

Table 1.4 (continued) Some phytochemicals previously isolated from *V. thapsus*

Classification	Compound	Parts of the plant	Reference
	24α-methyl-5α-cholestan-3-one	Whole plant	(Khuroo *et al*., 1988)
	24α-ethyl-5α(β)-cholestan-3-one	Whole plant	(Khuroo *et al*., 1988)
	24α-ethyl-5α-cholestan-7-en-3-one	Whole plant	(Khuroo *et al*., 1988)

Table 1.4 (continued) Some phytochemicals previously isolated from *V. thapsus*

Classification	Compound	Parts of the plant	Reference
	24α-ethyl-5α(β)-cholestan-22-en-3-one	Whole plant	(Khuroo *et al*., 1988)
	24α-ethyl-5α-cholestan-$\Delta^{7,22}$-dien-3-one	Whole plant	(Khuroo *et al*., 1988)
	α-Spinasterol	Fruit capsules	(De-Pascual-Teresa *et al*., 1978a)

Table 1.4 (continued) Some phytochemicals previously isolated from *V. thapsus*

Classification	Compound	Parts of the plant	Reference
Sesquiterpens/ Diterpenes	Buddlinderterpene A 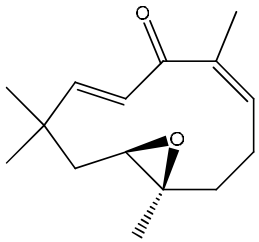	Whole plant	(Hussain *et al*., 2009)
	Buddlinderterpene B 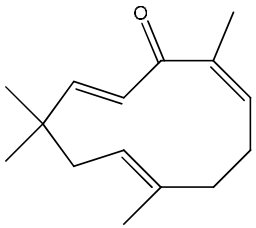	Whole plant	(Hussain *et al*., 2009)
	Buddlinderterpene C 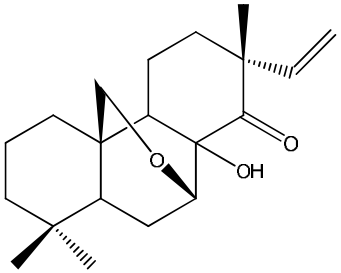	Whole plant	(Hussain *et al*., 2009)

1.4 Aims and Objectives

The purpose of this study was to phytochemically investigate three medicinal plants (*A. lappa*, *T. farfara* and *V. thapsus*) and test some of the isolated compounds for antibacterial activity. The plant parts investigated were selected on the basis of their traditional use in the treatment of infectious diseases, including TB.

The objectives of the work were to:

- develop suitable methods to purify phytochemicals from selected plant extracts, using techniques such as thin layer chromatography, vacuum liquid chromatography, open column chromatography, size exclusion chromatography and preparative thin layer chromatography;
- elucidate the structures of isolated compounds using ^{1}H and ^{13}C nuclear magnetic resonance, including extensive two-dimensional ^{1}H-^{1}H homonuclear (COSY, NOESY, TOCSY) and ^{1}H-^{13}C heteronuclear (HMBC, HSQC) experiments and mass spectrometry;
- screen extracts and some isolated compounds for activity against two microorganisms (*M. tuberculosis* and Methicillin-resistant *S. aureus*) using agar dilution and broth microdilution assays.

CHAPTER 2

MATERIALS AND METHODS

2 Materials and methods

2.1 General

2.1.1 Solvents

- *n*-Hexane (HPLC grade)
- Dichloromethane (HPLC grade)
- Ethyl acetate (HPLC grade)
- Methanol (HPLC grade)
- *n*-Butanol (HPLC grade)
- Acetone (HPLC grade)
- Acetic acid (Analytical grade)

Solvents listed above were used during different process of extraction, chromatographic separation and analytical TLCs. They were obtained in 2.5 L glass bottle from Fisher Scientific UK Ltd. All the solvents were stored at room temperature and transferred to 500 mL solvent bottles for routine use.

Deuterated (99.9%) solvents ($CDCl_3$, DMSO-d_6, CD_3OD and Acetone-d_6) were purchased from Sigma-Aldrich UK Ltd, and they were used for the NMR analysis.

2.1.2 Reagents and chemicals

- *p*-Anisaldehyde (Sigma-Aldrich, UK)
- Vanillin (BDH, UK)
- Dragendorf's reagent (Sigma-Aldrich, UK)
- TLC grade silica gel coated aluminum sheet (Precoated Silica gel PF_{254}, Merck, Germany)
- Silica gel 60 PF_{254} containing gypsum for preparative TLC (Merck,

Germany)

- TLC grade silica gel 60H (Merck, Germany)
- Column grade silica gel (Silica gel 60, mesh size 0.063-0.200mm, Merck, Germany)
- Lipophilic Sephadex® (LH-20100, Sigma-Aldrich, UK)
- Vancomycin (Sigma-Aldrich, UK)
- Oxacillin (Sigma-Aldrich, UK)
- MTT (Sigma-Aldrich, UK)

2.1.3 Plant materials

Dried aerial parts of *A. lappa*, *T. farfara* and *V. thapsus* were purchased from GBaldwin & Co (London, UK). The plants were ground to a fine power using a grinder (IKA® Werke GmbH & Co. KG, Germany) for extraction.

2.2 Extraction and partitioning

The plant material (around 1 kg) was extracted in a Soxhlet apparatus using solvents of increasing polarity starting with *n*-hexane and followed by ethyl acetate and methanol (3.5 L each). Each extraction stage was carried out to exhaustion. All extracts obtained were evaporated at 40°C under vacuum using a rotary evaporator. Hexane and ethyl acetate extracts obtained were stored at -20°C prior to analysis. The methanol extract was re-dissolved in a solution of 2.5% ethanol in distilled water and partitioned sequentialy with dichloromethane and *n*-butanol to afford three phases. Dichloromethane and *n*-butanol phases were first dried over anhydrous sodium sulphate and then evaporated using rotary evaporator. The remaining aqueous phase was freeze dried. All dried phases were stored at -20°C in glass flasks or

beakers.

2.3 Chromatographic techniques

Several chromatographic techniques were used for the isolation of compounds from crude extracts.

2.3.1 Thin layer chromatography

Thin layer chromatography (TLC) was used to i) screen the plant material for the presence of compounds; ii) determine the best eluting system for column chromatography and iii) monitor fractions during column chromatography. Plant extracts, fractions or pure compounds were dissolved in an appropriate solvent and spotted approximately 1cm above the bottom edge of a TLC plate. Spots were applied as bands to allow for an easy and accurate visualisation and the bands were kept as narrow as possible to reduce the overlapping of compounds. Solvent combinations of *n*-hexane/dichloromethane, *n*-hexane/ethyl acetate or ethyl acetate/methanol were used as mobile phases depending on the expected polarity of the sample under analysis.

Plates were first examined under UV light using short (λ=254 nm) and long wavelengths (λ=366 nm). Short UV is useful to detect aromatic compounds while compounds with conjugated double bonds are visible under long UV light. Then plates were sprayed with either anisaldehyde-sulphuric acid or vanillin-sulphuric acid reagents which allow visualisation of most compounds (phenols, terpenes, sterols, pigments and sugars) or with Dragendorff's reagent for alkaloids. Various colours were observed after spraying with anisaldehyde-sulphuric acid or vanillin-sulphuric

acid reagent and heating for 1~2 minutes with a hotgun. Alkaloids were detected as orange spots against a yellow background after treating with Dragendorff's reagent (Sherma and Fried, 1996).

2.3.2 Vacuum liquid chromatography

Vacuum liquid chromatography (VLC) was performed in a sintered glass funnel attached to a water pump. Silica gel 60H (TLC grade) was loaded into the funnel and vacuum was applied to compress silica gel to a hard layer. The least polar solvent was allowed to run through the column to check whether the column was homogenously packed.

Samples were dissolved in an appropriate solvent, absorbed on a small amount of silica gel 60 (mesh size 0.063~0.200 mm) and dried to achieve a free flowing powder. The powder was loaded and packed as a uniform thin layer on the top of the compressed silica gel column and the thin layer was covered with filter paper. The column was eluted starting with *n*-hexane followed by ethyl acetate/*n*-hexane mixtures of increasing polarity and finally with mixtures of ethyl acetate and methanol. The column was allowed to dry completely between fractions to improve resolution and separation of compounds. Each fraction was collected, evaporated to dryness at 40°C under vacuum using a rotary evaporator. Then the fractions were checked by TLC and pooled according to similar chemical profiles (Coll and Bowden, 1986; Pelletier *et al*., 1986).

2.3.3 Size exclusion chromatography

Gel Filtration (GF) or molecular sieve chromatography is a form of liquid chromatography in which molecular can be separated according to their molecular

size. Lipophilic Sephadex® LH20100 was used for this purpose. When solvent passes through a Sephadex® column, small molecules have a greater tendency to diffuse into the porous gel particles so remain trapped in the column and elute after bigger molecules.

For non-polar fractions, Sephadex® was soaked in a solution of 5% *n*-hexane in dichloromethane or 50% dichloromethane in methnol for several hours. The slurry was then poured and packed in glass chromatography column of appropriated size. Samples were dissolved in a small volume of 5% *n*-hexane in dichloromethane or 50% dichloromethane in methnol solution. The concentrated sample was loaded at the top of the column. Elution was started with 5% *n*-hexane in dichloromethane or 50% dichloromethane in methnol. If needed, elution was continued with 100% dichloromethane or 100% methanol, respectively. For relatively polar fractions, Sephadex® was soaked in methanol and the column was then eluted with the same solvent. When column finished, Sephadex® was washed several times with methanol and kept dried for re-use (Determann and Brewer, 1975; Kremmer and Boross, 1979).

2.3.4 Silica gel column chromatography

Open Column Chromatography (CC) was performed on silica gel 60 (mesh size 0.063~0.200 mm). The column was packed using the wet packing technique. Silica gel 60 was made into slurry using the least polar solvent of the eluting system and then poured and packed in a glass chromatography column of appropriate size. Air bubbles were eliminated by taping. Excess solvent was allowed to run through and the column was left to settle down. Samples were dissolved in a suitable solvent and adsorbed on a small amount of silica gel 60 (mesh size 0.063~0.200 mm), then loaded at the top of the column. A cotton plug or filter paper was applied over the

sample to prevent any distortion when the solvent drops came from solvent reservoir. Elution was carried out either isocratically or using a gradient. The collected fractions were analyzed by TLC and pooled according to similar chemical profiles (Ravindranath, 1989; Braithwaite and Smith, 1996).

2.3.5 Preparative thin layer chromatography

Preparative thin layer chromatography (PTLC) was mostly used when compounds reuired to be purified from fractions in low amounts. TLC plates of 0.5 mm thickness were prepared by vigorously mixing 20 g of silica gel (silica gel 60 PF_{254} containing gypsum) with 40 mL of distilled water (normally a ratio of 1:2) and applying the paste as a thin layer to glass plates with a TLC applicator. The plates were allowed to air dry and then activated in an oven at 76°C.

Samples to be purified were dissolved in a suitable solvent and spotted on the prepared plates as a narrow streak about 2.5 cm from the bottom. The plate was allowed to dry and then developed in an appropriate solvent system. After drying, the plate was observed under UV light (sometimes sprayed at one side with a suitable reagent) and compounds were marked for collection and carefully scraped with a spatula. Compounds were recovered from the silica gel by washing the silica gel through a cotton wool or filter paper with *n*-hexane, ethyl acetate and methanol (Sherma and Fried, 1996).

2.4 Isolation protocols

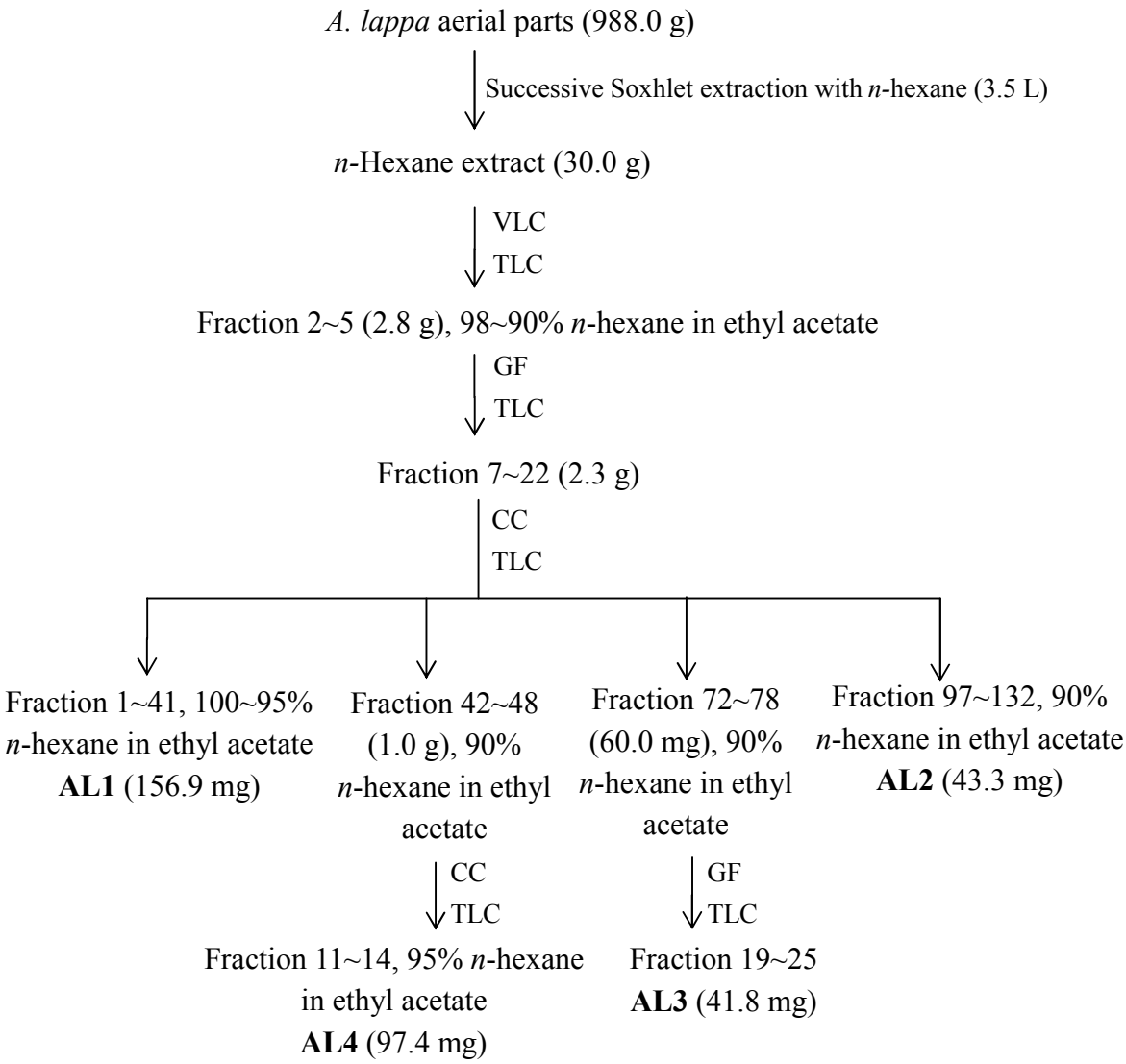

VLC: eluted with 100% *n*-hexane, increasing polarity by gradual increase of ethyl acetate followed by methanol, 400 mL of each solvent mixture used, column size 13 cm (diameter) ×10 cm (height); GF: eluted with 5% *n*-hexane in dichloromethane, around 2 mL collected for each fraction, column size 2 cm (diameter) ×100 cm (height); CC: eluted with 100% *n*-hexane, increasing polarity by gradual increase of ethyl acetate, 300~500 mL of each solvent mixture used, "large" volume collected for the first several fractions and then roughly 4 mL collected for each fraction, column size 4 cm (diameter) ×60 cm (height); TLC: pooling fractions with similar chemical profiles.

Protocol 1: Isolation of compounds from the *n*-hexane extract of *A. lappa*

A. lappa aerial parts (988.0 g)

↓ Successive Soxhlet extraction with ethyl acetate (3.5 L)

Ethyl acetate extract (30.0 g)

↓ VLC, TLC

Fraction 15A (2.0 g), 70% ethyl acetate in methanol

↓ GF, TLC

Fraction 91~125 solid, **AL6** (42.7 mg)

VLC: eluted with 100% *n*-hexane, with the gradual increase of ethyl acetate, followed by the increase of methanol, 300 mL of each solvent mixture used and each solvent mixture repeated three times, column size 13 cm (diameter) ×10 cm (height); GF: eluted with 100% methanol and aroud 2 mL collected for each fraction, column size 2 cm (diameter) ×100 cm (height); TLC: pooling fractions with similar chemical profiles.

Protocol 2: Isolation of compounds from the ethyl acetate extract of *A. lappa*

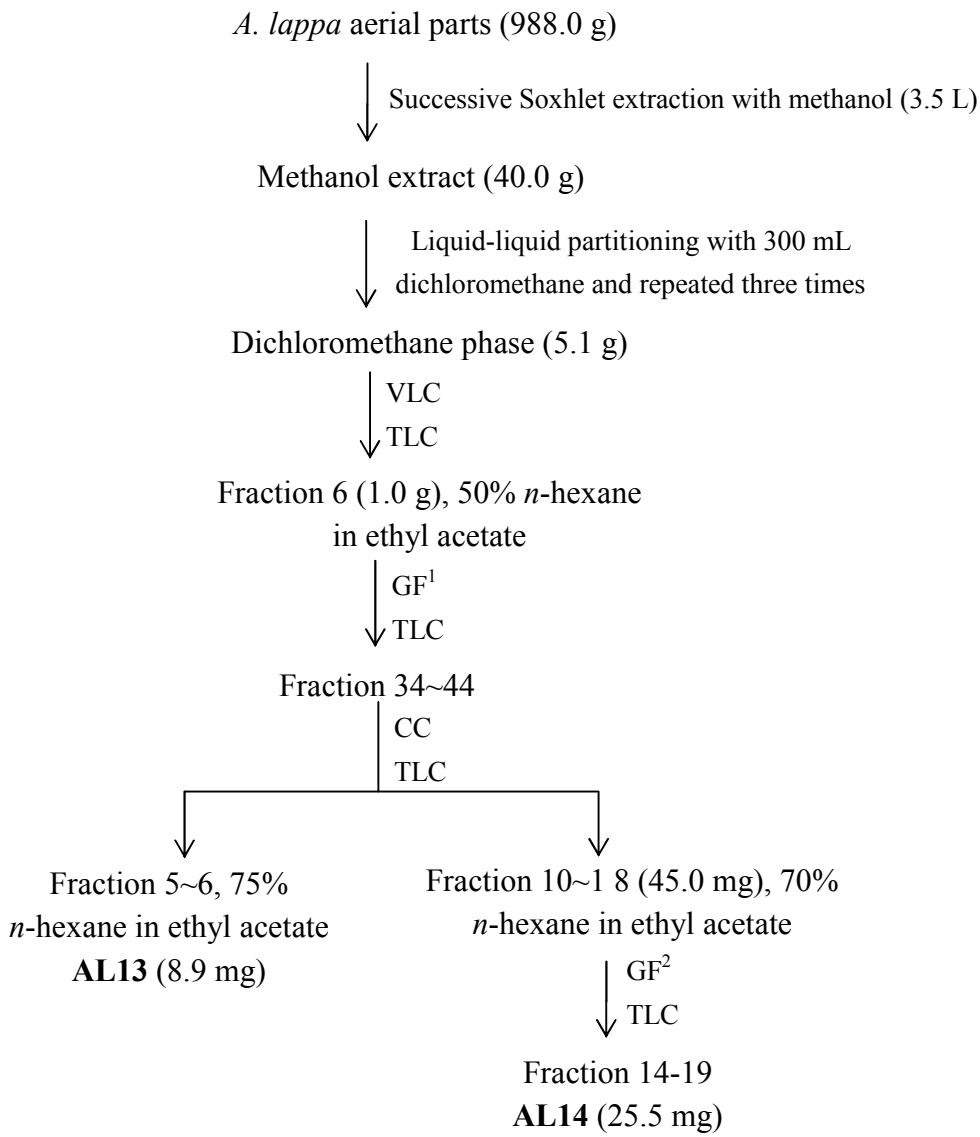

VLC: eluted with 100% *n*-hexane, with the gradual increase of ethyl acetate, 200 mL of each solvent mixture used and each solvent mixture repeated twice, column size 4 cm (diameter) ×16 cm (height); GF^1: eluted with 100% methanol and around 2 mL collected for each fraction, column size 2 cm (diameter) ×100 cm (height); GF^2: eluted with 100% ethyl acetate and around 1 mL collected for each fraction, column size 1 cm (diameter) ×30 cm (height); CC: eluted with 100% *n*-hexane, increasing polarity by gradual increase of ethyl acetate, 50~300 mL of each solvent mixture used and roughly 1~2 mL collected for each fraction, column size 1 cm (diameter) ×30 cm (height); TLC: pooling fractions with similar chemical profiles.

Protocol 3: Isolation of compounds from the dichloromethane phase of *A. lappa* methanol extract

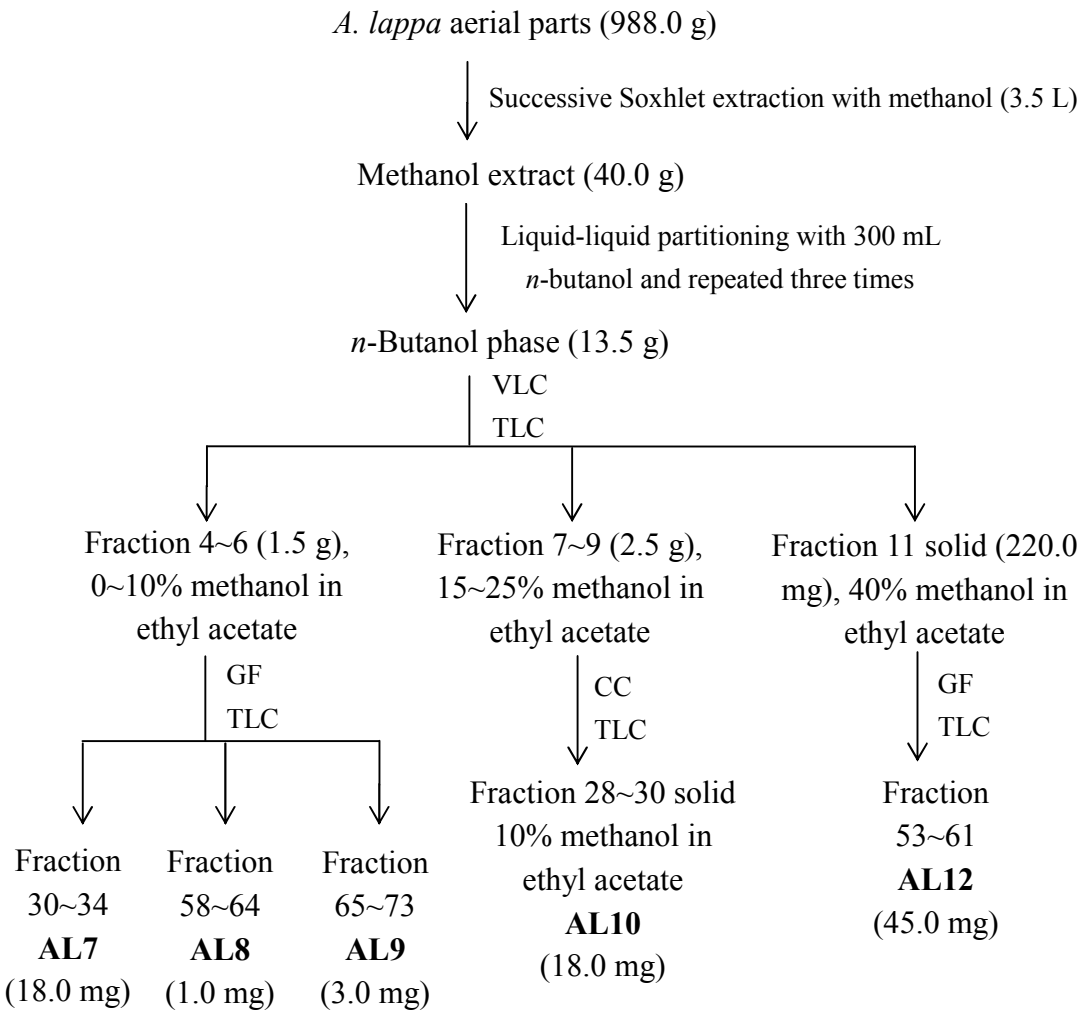

VLC: eluted with 50% *n*-hexane in ethyl acetate, with the gradual increase of ethyl acetate followed by methanol, 300 mL of each solvent mixture used and each solvent mixture repeated twice, column size 13 cm (diameter) ×10 cm (height); GF: eluted with 100% methanol and around 2 mL collected for each fraction, column size 2 cm (diameter) ×100 cm (height); CC: eluted with 100% ethyl acetate, increasing polarity by gradual increase of methanol, 200 mL of each solvent mixture used and roughly 4 mL collected for each fraction, column size 4 cm (diameter) ×60 cm (height); TLC: pooling fractions with similar chemical profiles.

Protocol 4: Isolation of compounds from the *n*-butanol phase of *A. lappa* methanol extract

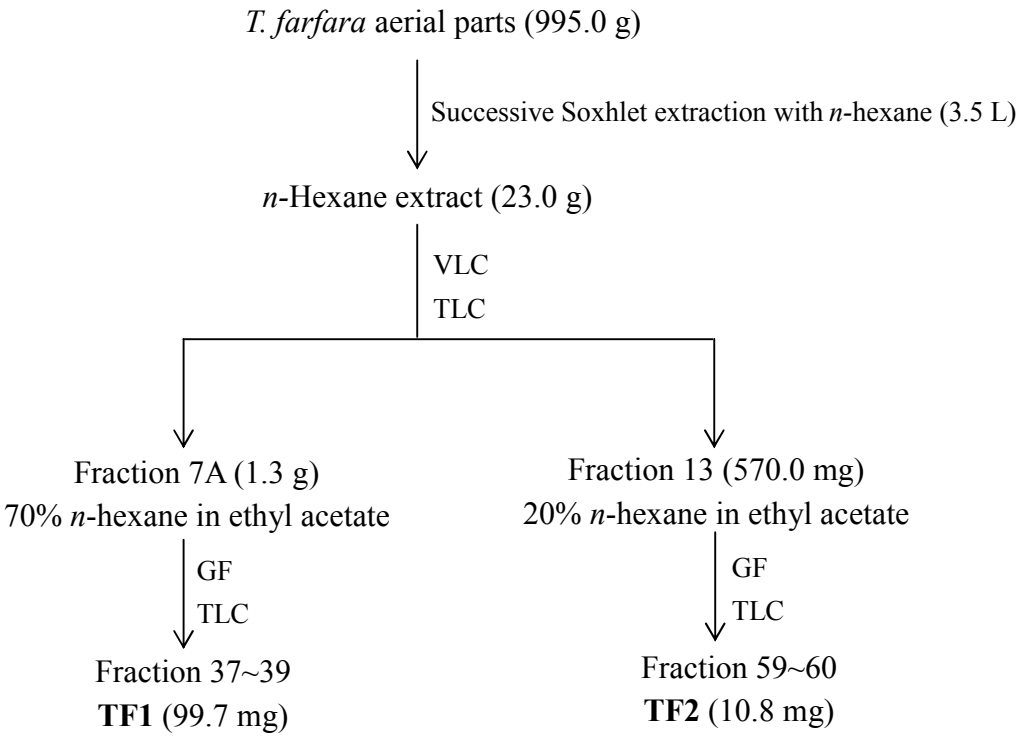

VLC: eluted with 100% *n*-hexane, increasing polarity by gradual increase of ethyl acetate, 400 mL of each solvent mixture used and each solvent mixture repeated twice, column size 13 cm (diameter) ×10 cm (height); GF: eluted with 5% *n*-hexane in dichloromethane and around 2 mL collected for each fraction, column size 2 cm (diameter) ×100 cm (height); TLC: pooling fractions with similar chemical profiles.

Protocol 5: Isolation of compounds from the *n*-hexane extract of *T. farfara*

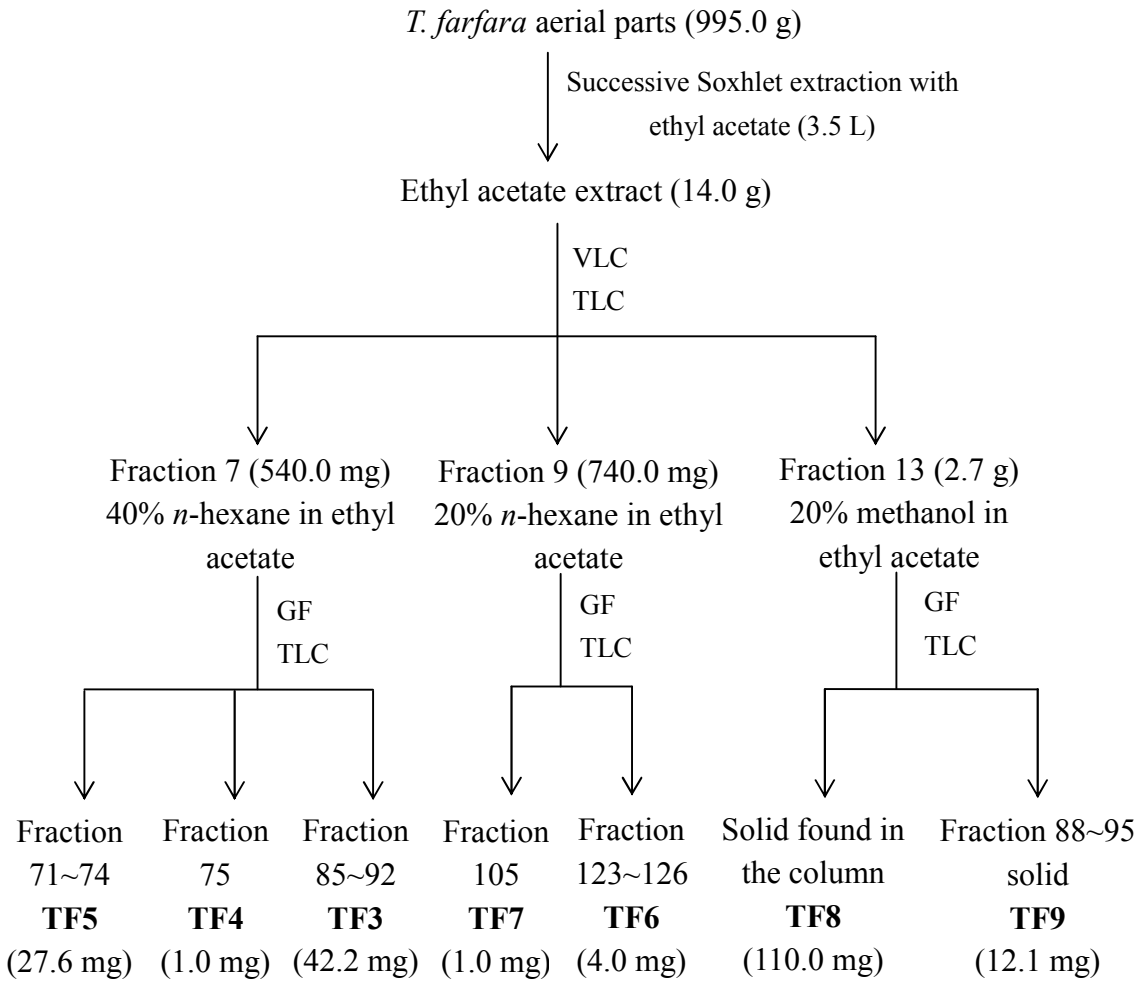

VLC: eluted with 100% *n*-hexane, with the gradual increase of ethyl acetate, followed by the increase of methanol, 400 mL of each solvent mixture used and each solvent mixture repeated twice, column size 13 cm (diameter) ×10 cm (height); GF: eluted with 100% methanol and around 2 mL collected for each fraction, column size 2 cm (diameter) ×100 cm (height); TLC: pooling fractions with similar chemical profiles.

Protocol 6: Isolation of compounds from the ethyl acetate extract of *T. farfara*

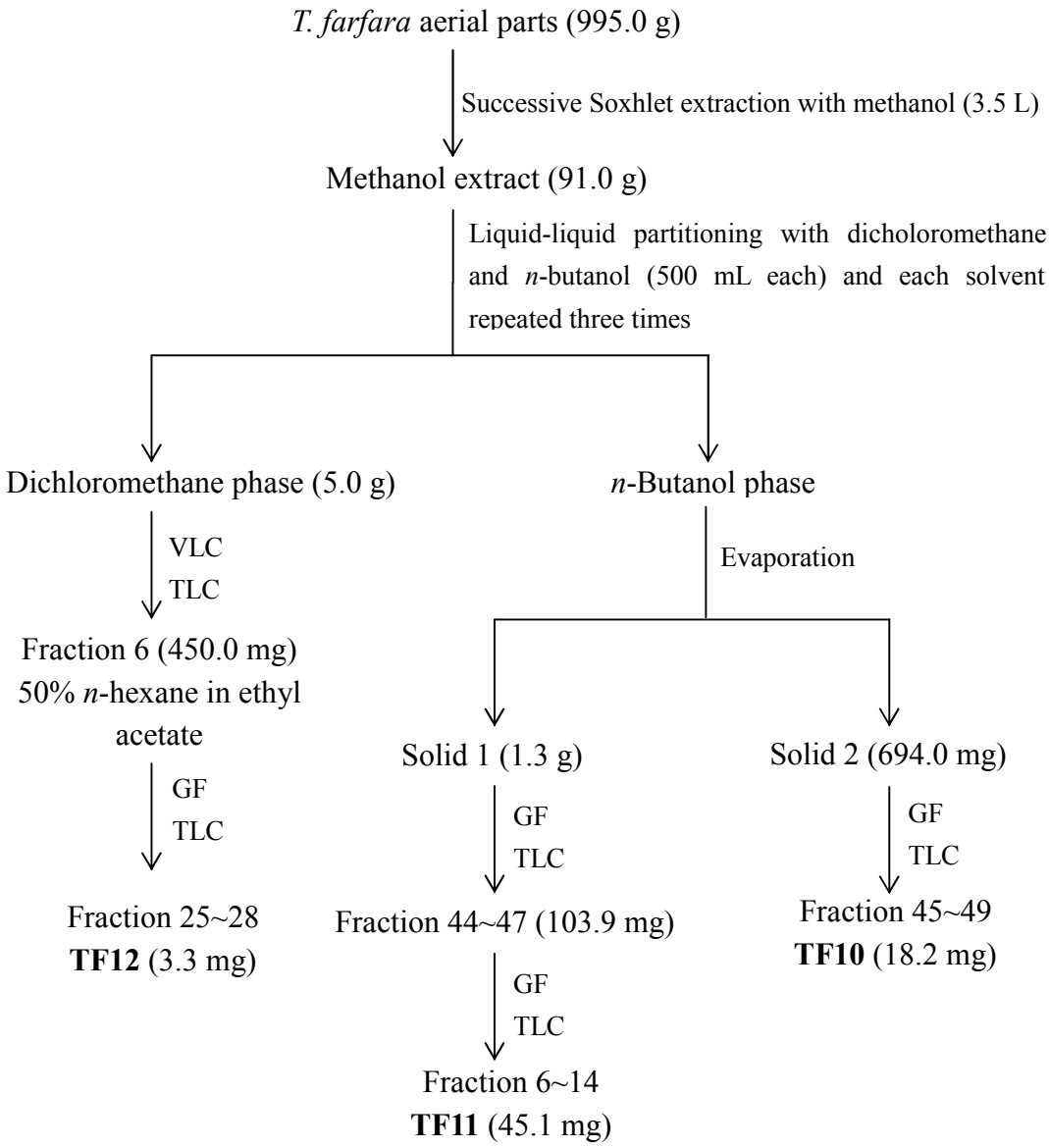

VLC: eluted with 100% *n*-hexane, with the gradual increase of ethyl acetate, followed by the increase of methanol, 300 mL of each solvent mixture used and each solvent mixture repeated twice, column size 7 cm (diameter) ×15 cm (height); GF: eluted with 100% methanol and around 2 mL collected for each fraction, column size 2 cm (diameter) ×100 cm (height); TLC: pooling fractions with similar chemical profiles.

Protocol 7: Isolation of compounds from the methanol extract of *T. farfara*

V. thapsus aerial parts (998.0 g)

↓ Successive Soxhlet extraction with *n*-hexane (3.5 L)

n-Hexane extract (10.6 g)

↓ VLC, TLC

Fraction 6A (550.0 mg)
80% *n*-hexane in ethyl acetate

↓ GF, TLC

Fraction 31~43
VT1 (81.7 mg)

VLC: eluted with 100% *n*-hexane, with the gradual increase of ethyl acetate, followed by the increase of methanol, 500 mL of each solvent mixture used and each solvent mixture repeated three times, column size 7 cm (diameter) ×15 cm (height); GF: eluted with 50% dichloromethane in methanol and around 2 mL collected for each fraction, column size 2 cm (diameter) ×100 cm (height); TLC: pooling fractions with similar chemical profiles.

Protocol 8: Isolation of compounds from the *n*-hexane extract of *V. thapsus*

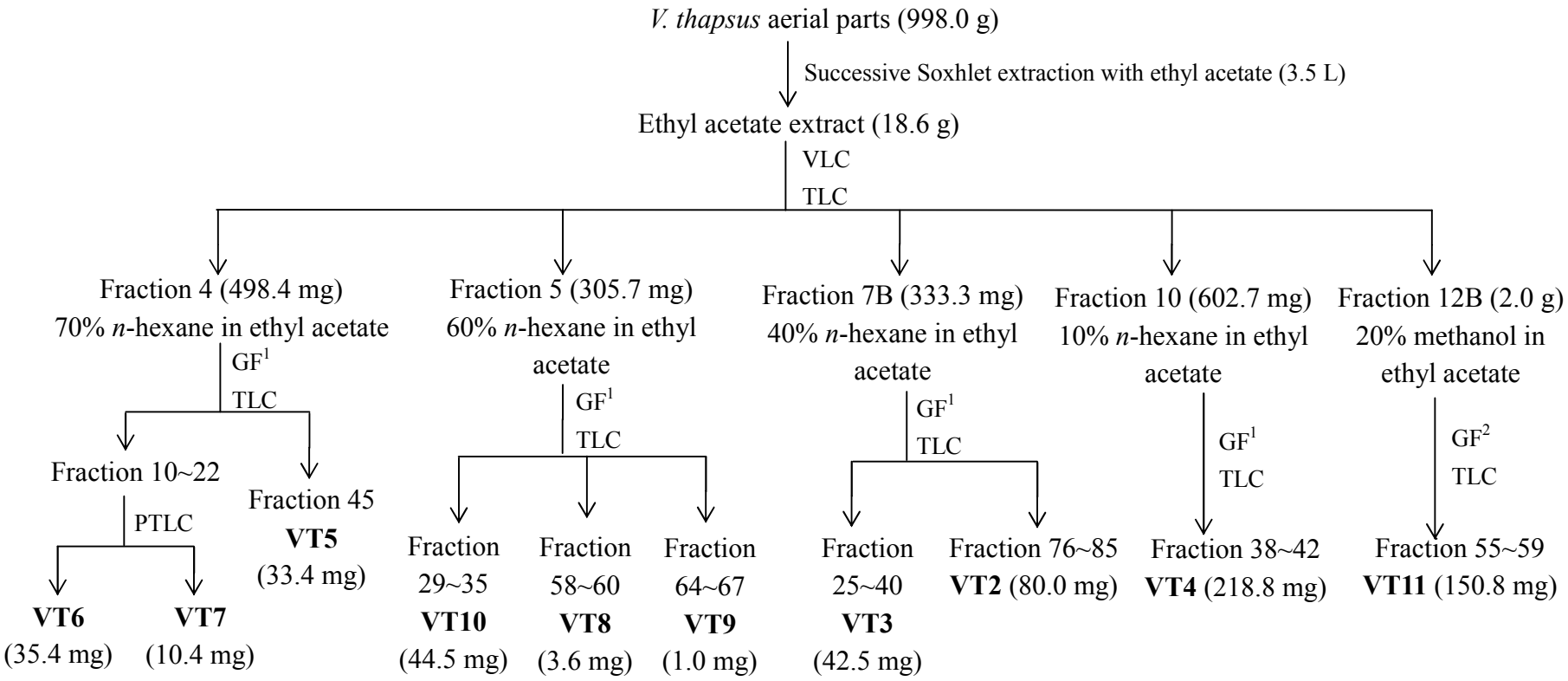

VLC: eluted with 100% *n*-hexane, with the gradual increase of ethyl acetate, followed by the increase of methanol, 400 mL of each solvent mixture used and each solvent mixture repeated twice, column size 7 cm (diameter) ×15 cm (height); GF^1: eluted with 50% dichloromethane in methanol and around 2 mL collected for each fraction, column size 2 cm (diameter) ×100 cm (height); GF^2: eluted with 100% methanol and around 2 mL collected for each fraction, column size 2 cm (diameter) ×100 cm (height); PTLC: Plates were developed twice in 80% *n*-hexane in Ethyl acetate (200 mL); TLC: pooling fractions with similar chemical profiles.

Protocol 9: Isolation of compounds from the methanol extract of *V. thapsus*

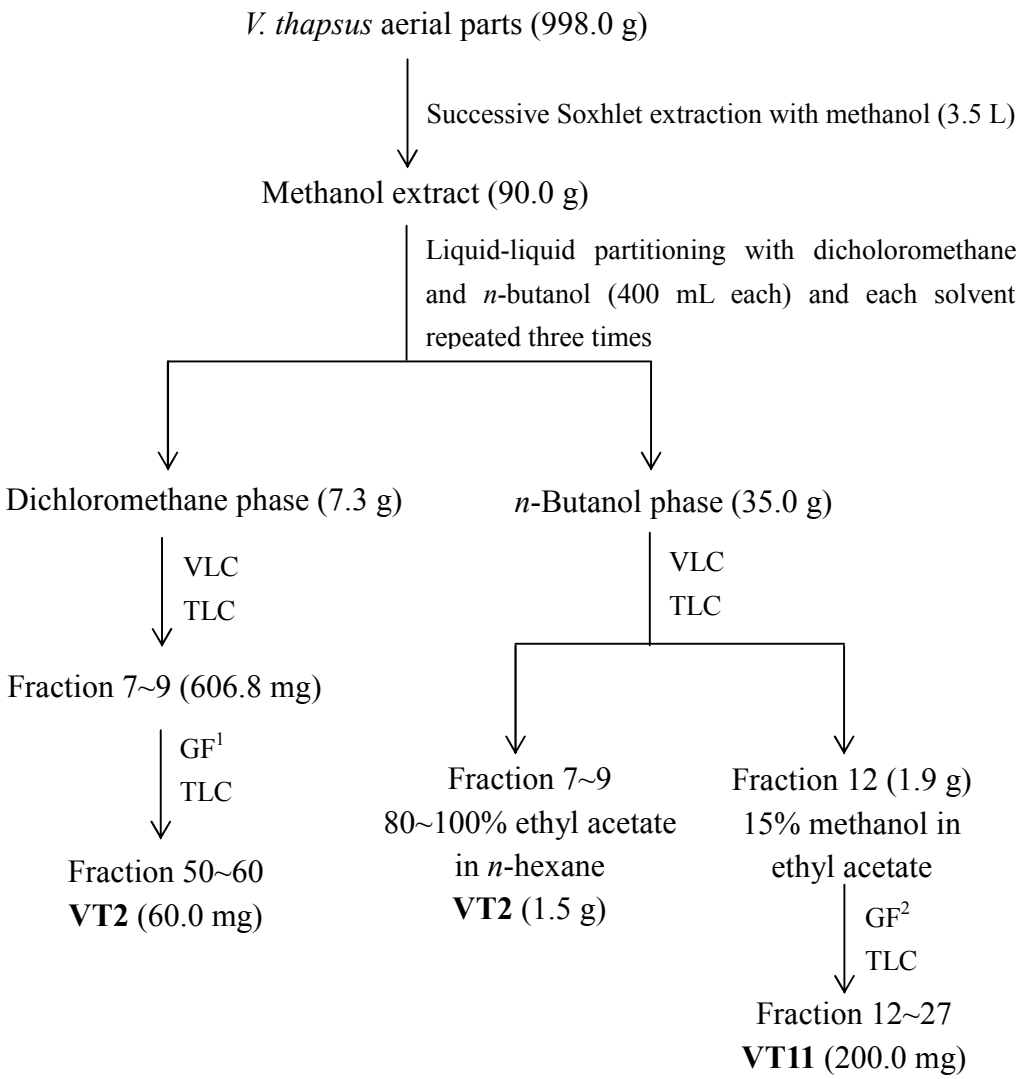

VLC: eluted with 100% *n*-hexane, with the gradual increase of ethyl acetate, followed by the increase of methanol, 500 mL of each solvent mixture used and each solvent mixture repeated twice, 7 cm (diameter) ×15 cm (height); GF^1: eluted with 50% dichloromethane in methanol and around 2 mL collected for each fraction, column size 2 cm (diameter) ×100 cm (height); GF^2: eluted with 100% methanol, around 2 mL collected for each fraction, column size 2 cm (diameter) ×100 cm (height); TLC: pooling fractions with similar chemical profiles.

Protocol 10: Isolation of compounds from the methanol extract of *V. thapsus*

2.5 Structure elucidation

2.5.1 NMR spectroscopy

1D and 2D ^{1}H and ^{13}C NMR experiments were carried out on a JEOL (JNM LA400) 400 MHz and a Bruker 500 or 400 MHz instruments. NMR tubes (5 mm) purchased from Wilmad-labglass were used for routine NMR experiments. Samples were dissolved in about 0.6 mL of suitable deuterated solvent and taken in NMR tubes. Adding too little or too much of solvent was avoided to prevent shimming problems and long experimental hours, respectively.

The identification of pure compounds was first carried out by one dimensional ^{1}H and ^{13}C NMR spectroscopy. Spectra obtained for known compounds were identified following comparison with published spectral data. Further 2D experiments were carried out when necessary to accurately assign proton and carbon chemical shifts and determine relative stereochemistry in some cases.

2.5.1.1 ^{1}H NMR

^{1}H NMR experiment was carried out for all compounds isolated and was used as the primary means of structural identification. It provided information on the protons present in the molecule, their chemical shifts, multiplicity (coupling information) and estimated numbers from the integration. The spectra obtained were used to assess the purity of any isolated compounds. The ^{1}H NMR was also used to detect the relative molar ratio of any components present as a mixture (Breitmaier, 1993; Williams and Fleming, 2008).

2.5.1.2 ^{13}C NMR

This gave information on the number and type of carbons present in a compound. The spectra obtained were either broad band-decoupled or *J*-modulated. In broad band-decoupled spectra, the ^{1}H nuclei are irradiated during the ^{13}C acquisition so all protons are fully decoupled from the ^{13}C nuclei. When this is done each distinct ^{13}C environment in the molecule gives rise to a separate singlet signal.

The *J*-modulated experiment helps distinguish the carbons according to the extent of their proton attachments (C, CH, CH_2 and CH_3). DEPT spectrum is a pulse sequenced experiment that transforms the information of CH signal multiplicity and spin-spin coupling into phase relationship (Becconsall, 2005). In a DEPT 135 spectrum, CH_3 and CH are directed towards the positive phase of the spectrum while CH_2 is facing the negative phase. A DEPTQ 135 spectrum is the same as a DEPT 135 spectrum except the quaternary carbons are present and 180 degree out of phase with respect to the CH/CH_3 carbons. The obvious advantage of the DEPTQ 135 spectrum over a standard broad band-decoupled carbon spectrum is that using this technique it is possible to distinguish C/CH_2 carbons from CH/CH_3 carbons in one experiment. The other advantage is that it is 4 times more sensitive as it uses ^{1}H-^{13}C polarization transfer (Breitmaier, 1993; Becconsall, 2005).

2.5.1.3 Correlation spectroscopy (COSY)

This 2D experiment gives ^{1}H-^{1}H coupling in a molecule and it is possible to reveal all coupling relationships in one experiment using a suitable pulse sequence. The proton shifts are plotted on both axes with the contour plot along the diagonal of the square, and the correlations are shown as cross peaks with the diagonal corresponding to the ordinary ^{1}H NMR spetrum. Thus the cross peaks refer to the

spin-spin coupled protons. The correlations observed are due to germinal (^2J) and vicinal (^3J) protons. But ^4J and ^5J couplings or allylic couplings can also be observed in a COSY spectrum (Breitmaier, 1993; Williams and Fleming, 2008).

2.5.1.4 Heteronuclear Single Quantum Correlation (HSQC)

This 2D ^{1}H-^{13}C experiment shows one-bond (^1J) direct correlations. The pulse sequence applied in this experiment uses a time delay set to 1/2*J* where *J* is the value similar to that of one-bond ^{1}H-^{13}C coupling. In an HSQC spectrum, the ^{1}H and ^{13}C (or DEPT) spectrum is plotted along the abscissa and ordinate, respectively (or vice versa). Cross-peaks indicate proton and carbons that are directly connected to each other (Claridge, 2006; Williams and Fleming, 2008).

2.5.1.5 Heteronuclear Multiple Bond Correlation (HMBC)

The spectra obtained from this experiment reveal heterounclear shift correlations *via* long-range couplings ($^2J_{CH}$ and $^3J_{CH}$). The proton spectrum is arranged on one axis and the carbon on the other, and the correlations are displayed as cross peaks. The time delay (1/2*J*) used in the pulse sequence is kept such that to *J* value in the range of $^3J_{CH}$ and $^2J_{CH}$. Unless otherwise stated, the HMBC experiment carried out for different samples in the present study used a time delay of 0.07s (e.g. J_{CH}=7Hz). Since this pulse programme uses ^{1}H-^{13}C polarization transfer, the detection is four times more sensitive than a ^{13}C NMR experiment (Breitmaier, 1993; Claridge, 2006; Williams and Fleming, 2008).

2.5.1.6 Nuclear Overhauser Enhancement spectroscopy (NOESY)

In this experiment, all correlations between protons showing Nuclear Overhauser Effect (NOE) are recorded two-dimensionally. A NOESY spectrum measures ^{1}H-^{1}H

interactions arising from through space dipolar coupling. The spectrum obtained is similar to a COSY spectrum (scalar through bonds coupling), but a correctly-phased NOESY spectrum will show cross-peaks representing NOE correlations. The NOESY experiment is useful in determining compound structure and relative stereochemistry (Williams and Fleming, 2008).

2.5.1.7 Total Correlation Spectroscopy (TOCSY)

A TOCSY helps identifying networks of mutually-coupled protons. The magnetisation of the first proton in the spin system is transferred to the next and so forth in a relay manner, until the network is blocked by a quaternary carbon or another atom, magnetisation can no longer be relayed to the protons on the side. Therefore, a whole network of protons can be detected by tracing the cross-peaks arising from specific protons. The relay distance is dependent on the mixing time (Williams and Fleming, 2008). The spectrum generated resembles a COSY spectrum. In this study, the TOCSY experiment was used to assist in the assignment of the disaccharide protons of compound VT11.

2.5.2 Mass spectrometry

High resolution electron impact (HREI) mass spectra were recorded on a JEOL 505HA spectrometer using direct probe at elevated temperature (110~160°C) at 70 eV. Positive ion and negative ion mode ESI experiments were performed on a Thremo Finnigan LCQ-Decaiontrap or Orbitrap HRESI mass spectrometer (mass analyser set up at 100,000 ppm, externally calibrated at 3 ppm). In this study, the choice of any particular mode was mainly based on the polarity of isolated compounds. Generally, positive ion HRESI-MS analysis was chosen for less polar

compounds, and negative ion HRESI mode was selected for relatively more polar (e.g. phenolic) componds. According to the polarity, samples were dissolved in acetonitrile, methanol or water (HPLC grade) or in a binary mixture of these solvents to get a concentration of 100 μg/mL. Sample solution (10~20 μL) was injected along with a direct infusion of 0.1% formic acid in acetonitrile: water (90:10) at a flow rate of 200 μL/min. The main parameters used for mass spectral analysis are presented in Table 2.1. MS data acquisition was carried out by Dr. Tong Zhang and Dr. Gavin Blackburn.

Table 2.1 Main parameters for the ESI mass spectral analysis*

Attribute	Positive mode		Negative mode
Capillary Temp (°C)		220.00	
Sheath Gas flow (bar)		30.00	
Auxiliary Gas flow (bar)		10.00	
Source voltage (kV)	4.00		3.10
Source current (μA)		100.00	
Capillary voltage (V)	35.50		-48.00
Tube Lens (V)	90.00		-145.00

*May vary slightly from experiment to experiment

2.6 Antibacterial screening

2.6.1 Screening against *Mycobacterium tuberculosis*

2.6.1.1 Spot-culture growth inhibition assay

A high-throughput version of the spot culture growth inhibition (SPOTi) assay (Evangelopoulos and Bhakta, 2010; Gupta and Bhakta, 2012; Guzman *et al*., 2013) was used by Dr. Dimitrios Evangelopoulos and Dr. Sanjib Bhakta (Department of Biological Sciences, University of London, UK) for *M. tuberculosis* screening.

M. tuberculosis $H_{37}Rv$ (ATCC27294) was initiated from a cryopreserved glycerol stock, passaged twice for growth uniformity and grown at 37°C in 10 mL Middlebrook 7H9 liquid medium supplemented with 10% (v/v) oleic acid/albumin/dextrose/catalase until the log phase (OD600≈0.7). Mycobacterial cultures were first checked for quality control using cold Ziehl-Neelsen staining. The mycobacterial suspension was then prepared by dilution to achieve 1×10^5 CFU/mL inoculum for further use.

Extracts/compounds were dissolved in DMSO. Serial dilution was performed in a sterile, thin 96-well frosted subskirted microtitre plate. A column containing only DMSO was also included as negative control. 2 µL of each of the diluted extracts/compounds were then transferred into sterile 96-well plates. The plates were filled up to 200 µL with Middlebrook 7H10 agar medium enriched with 10% (v/v) oleic acid/albumin/dextrose/catalase. The agar-based media were prevented from solidifying by using a hot plate at 50°C with constant stirring. The distribution of the agar media into the 96 wells was achieved using the MultidropCombi microplate dispenser (Thermo-Fisher Scientific). Plates were dried and 2 µL prepared mycobacterial suspension was spotted (10^5 CFU/mL) at the centre of each well by

either the use of a single pipettor or by using the MultidropCombi. The plates were then swirled and left with the cover open for 5 min to absorb the culture within the medium. Then the plates were incubated in sealed bags at 37°C for 2 weeks.

MICs were determined as the lowest concentration of extracts/compounds showing no visible mycobacterial growth. The first-line anti-TB drugs isoniazid and rifampicin were included as antibiotic controls.

2.6.1.2 Microplate Alamar Blue assay

The activity against *M. tuberculosis* $H_{37}Rv$ (ATCC 27294) was also assessed by MS Baojie Wan (ITR, Chicago, USA) according to a method based on the microplate Alamar Blue assay (MABA) (Collins and Franzblau, 1997).

Stock solutions of extracts/compounds were prepared in DMSO and added, at a concentration of 100 or 50 µg/mL, to two wells of a microplate containing Middlebrook 7H12 broth. One well was inoculated with broth containing 2×10^4 CFU/mL *M. tuberculosis* $H_{37}Rv$. The second well received only media in order to assess background fluorenscence. Isonizid, rifampicin, streptomycin, capreomycin and PA-824 (a nitroimidazopyran-derived experimental antitubercular drug candidate) were included as antibiotic controls. Additional controls consisted of growth control (bacteria+DMSO) and sterility control (media only). For MICs, tow-fold serial dilutions were performed in 7H12 media. Each microplate was incubated for 5 days at 37°C in a 5% CO_2 atmosophere in a sealed plastic bag. After 5 days of incubation at 37°C, one control growth was developed with a mixture of Alamar Blue solution (20 µL) (Trek Diagnostics, Westlake Ohio, USA) and sterile 10% Tween 80 (12 µL). The plates were re-incubated at 37°C for 24 h.

After this, if the well turned pink, the dye mixture was placed in to all wells and the paltes were re-incubated for an additional 34 h. The mean fluorescence units (FU) of media-only wells were subtracted from all other wells. Each sample was assayed in duplicate. Results were expressed in terms of percentage of inhibition defined as follows:

$$\%\ \text{inhibition} = \left(1 - \frac{\text{test well FU}}{\text{mean FU of triplicate wells containg only bacteria}}\right) \times 100$$

The MIC was defined as the lowest concentration effecting a reduction in fluorescence of ≥90% relative to bacteria only controls. Each sample was tested in duplicate.

2.6.2 Screening against Methicillin-resistant *Staphylococcus aureus*

The activity against Methicillin-resistant *S. aureus* (MRSA) was evaluated by Mr Simon Mylrea using an MTT assay (Seidel *et al.*, 2008). An epidemic EMRSA-15 strain of MRSA (isolated from a clinical sample obtained from the New Royal Infirmary, Edinburgh, UK), was used in this study. The strain (coded LF78) was reported resistant to ampicillin, oxacillin, cefotaxime, cefuroxime and ciprofloxacin (Raghukumar *et al.*, 2010). Stock solutions of compounds were prepared in DMSO and diluted with Tryptic Soy Broth (TSB) to achieve required concentrations.

Bacterial colonies from cultures freshly grown on Tryptic Soy Agar (TSA) plates were transferred in sterile TSB (5 mL). Following incubation at 37°C overnight in a shaker, dilutions were prepared in TSB to achieve a bacterial inoculum of 1×10^5 CFU/mL.

The assay was performed in flat-bottomed 96-well plates containing 100 μL of TSB in each well. Vancomycin (Sigma-Aldrich, UK) and oxacillin (Sigma-Aldrich, UK) were used as antibiotic controls. Samples (100 μL) were added (initial concentration of 1 mg/mL) and two-fold serial dilutions were carried out. The bacterial inoculum (100 μL) was added to each well to achieve a final concentration of 0.5×10^5 CFU/mL. Plates were incubated at 37°C overnight.

After the end of the incubation period, 20 μL of MTT (5 mg/mL in ethanol) was added to each well and the plates were re-incubated for 20 min. A change in colour from yellow to purple/black indicated the presence of visible bacteria. The MIC was determined as the lowest sample concentration that prevented this change and exhibited complete inhibition of macroscopic growth. All samples were screened in duplicate and on two separate days.

CHAPTER 3

RESULTS AND DISCUSSION

3 Results and discussion

Part A Phytochemical studies

3.1 Terpenoids and steroids

3.1.1 Characterisation of TF2 as loliolide

TF2 was isolated from the *n*-hexane extract of *T. farfara* as a colourless oil **(Section 2.4: Protocol 5, 0.0011% yield)**. This compound was not active under short wave UV light but turned pink upon spraying the TLC plate with anisaldehyde-sulphuric acid reagent and heating.

The positive ion mode HRESI-MS spectrum showed a quasi-molecular ion $[M+H]^+$ at *m/z* 197.1172, suggesting a molecular formula of $C_{11}H_{16}O_3$ (DBE=4).

The ^{1}H NMR spectrum **(Figure 3.3, Table 3.1)** displayed an olefinic proton at δ5.72 (1H, *s*), an oxymethine proton at δ4.35 (1H, *m*) and three methyl groups at δ1.29 (*s*), δ1.49 (*s*) and δ1.79 (*s*). Some other signals were also detected at δ1.56 (1H, *dd*, *J*=3.6, 14.6 Hz), δ1.82 (1H, *dd*, *J*=14.5, 4.0 Hz), δ2.01 (1H, *dt*, *J*=14.6, 5.3, 2.8 Hz) and δ2.49 (1H, *dt*, *J*=14.1, 5.3, 2.6 Hz), and with the aid of the HSQC experiment they were identified as two pairs of methylene protons (δ1.56/δ2.01 and δ1.82/δ2.49).

In the COSY spectrum, the oxymethine proton exhibited correlations to two methylene groups. The methyl group at δ1.79 correlated to one pair of methylene protons at δ1.82/δ2.49, and the methyl at δ1.49 correlated to the other pair of methylene protons at δ1.56/δ2.01.

The ^{13}C NMR spectrum **(Table 3.1)** displayed three methyls at δ26.5, δ27.0, δ30.7,

two methylenes at δ45.7, δ47.3, one oxymethine at δ67.1 and one olefinic carbon at δ113.0. With the aid of the HMBC experiment, the presence of four quaternary carbons was also established with signals at δ35.8, δ86.8, δ172.1 and δ182.2.

In the HMBC spectrum **(Figure 3.4)**, the olefinic proton at δ5.72 (H-7) displayed correlations to quaternary carbons at δ35.8 (C-1), δ86.8 (C-5) and δ182.2 (C-6) and to the carbonyl at δ172.1 (C-8). The methyls at δ1.29 (Me-10) and δ1.49 (Me-9) were identified as geminal methyls as they correlated to the same quaternary carbon at δ35.8 (C-1). Both methyls also showed ^{3}J correlations to the methylene carbon at δ47.3 (C-2) and the quaternary carbon at δ182.2 (C-6). The third methyl group at δ1.79 (Me-11) revealed a ^{3}J coupling to the methylene carbon at δ45.7 (C-4) and to the quaternary carbon at δ182.2 (C-6). One of the methylene protons at δ2.49 (H-4a) correlated to carbons at δ47.3 (C-2) and δ67.1 (C-3).

In the NOESY spectrum **(Figure 3.5)**, the oxymethine proton at δ4.35 (H-3) showed correlations to the protons at δ1.56 (H-2b) and δ1.82 (H-4b), and at the deep level it also correlated to the methyl at δ1.29 (Me-10), suggesting that H-3, H-2b, H-4b and Me-10 were on the same side of the plane. The methyl at δ1.79 (Me-11) showed correlations to the methyl at δ1.49 (Me-9) and the proton at δ2.49 (H-4a), indicating that Me-9, Me-11 and H-4a were on the other side of the plane.

The above NMR results were consistent with previous reports for loliolide (Fernandez *et al*., 1993; Kimura and Maki, 2002; Lee *et al*., 2009; Erosa-Rejón *et al*., 2009). Although another study assigned C-6 at δ172.8 and C-8 at δ182.3 (Valdes III, 1986), this was not supported by our HMBC data. This is the first report of the isolation of loliolide from *T. farfara*.

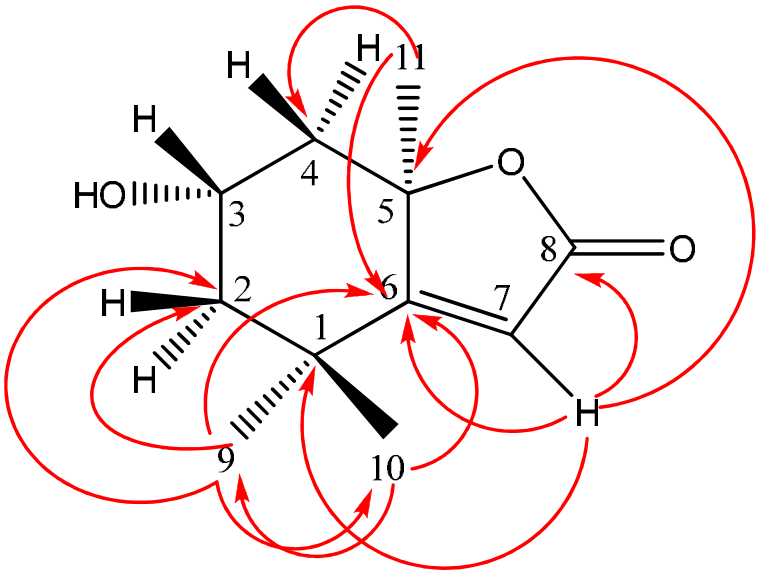

Figure 3.1 Structure of TF2 with selected HMBC correlations

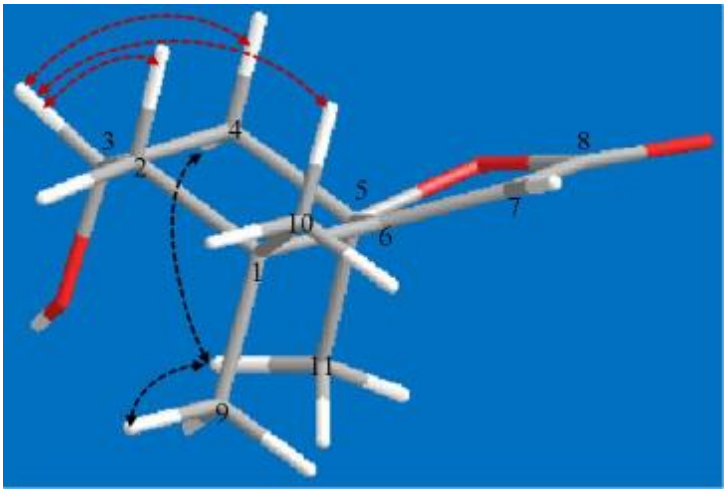

Figure 3.2 3D Structure of TF2 with important NOESY correlations

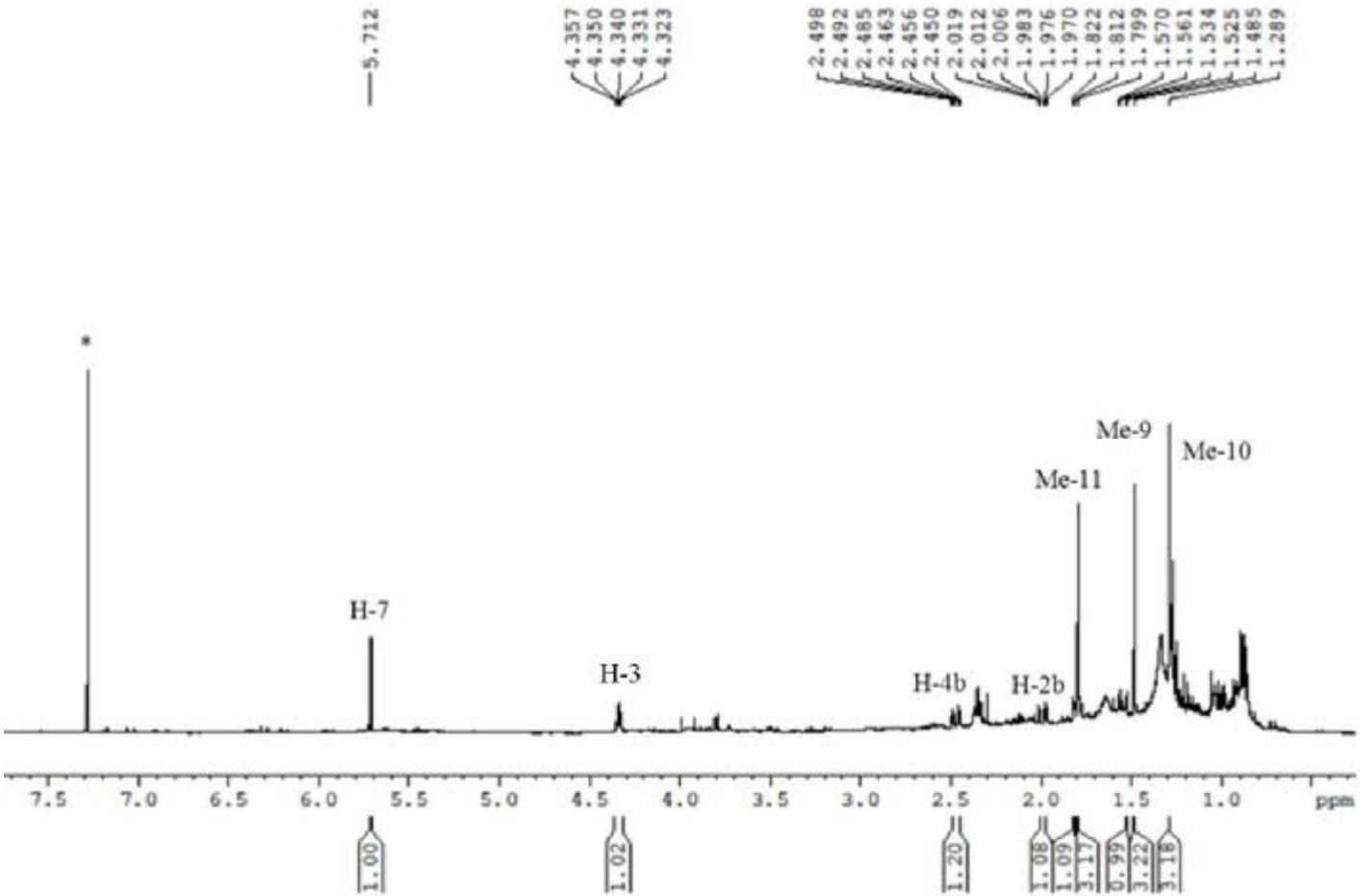

Figure 3.3 ^{1}H NMR spectrum (400 MHz) of TF2 in $CDCl_3$ (*)

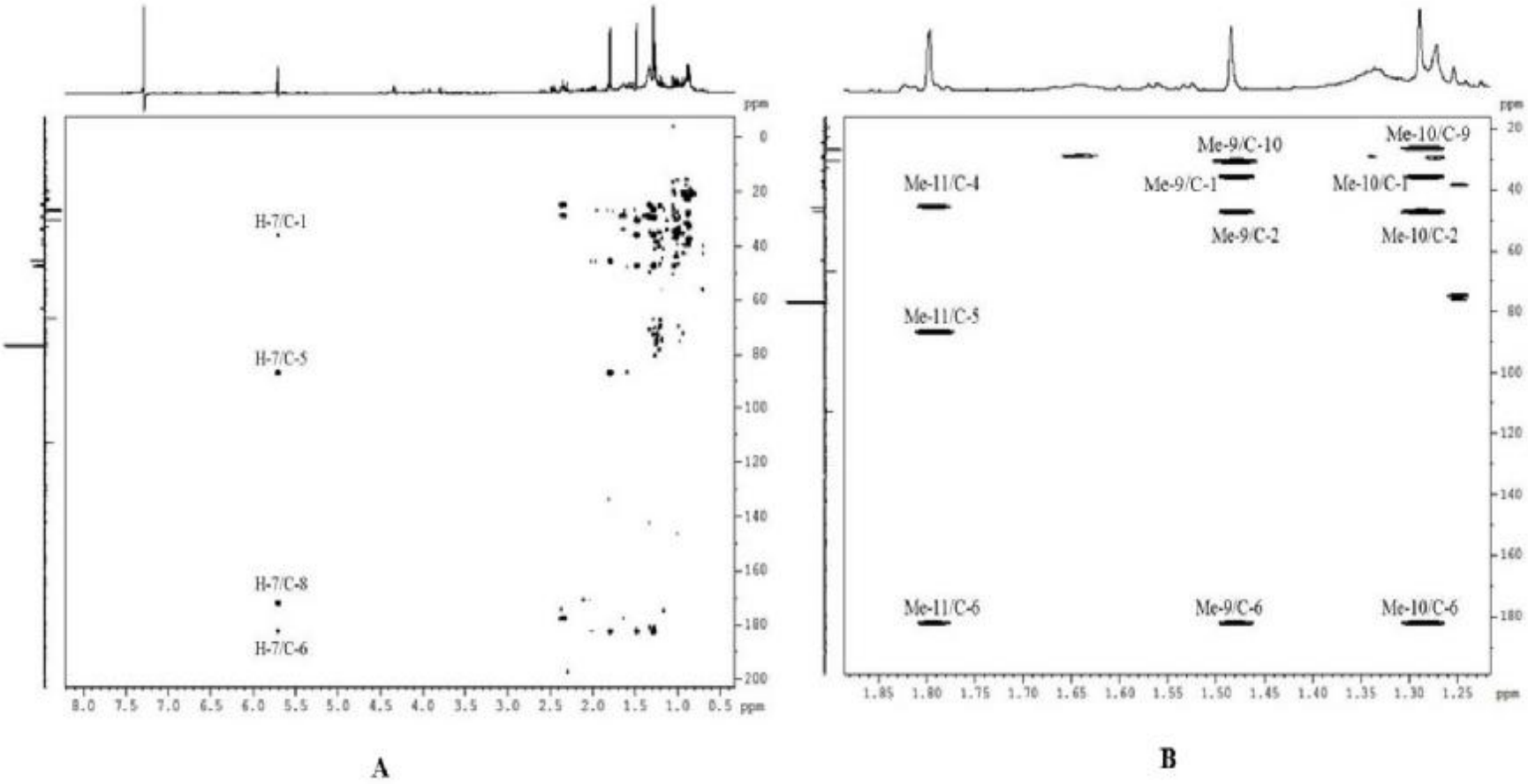

Figure 3.4 HMBC spectra (400 MHz) of TF2 in $CDCl_3$

A: Full HMBC spectrum; B: Selected expansion of HMBC spectrum

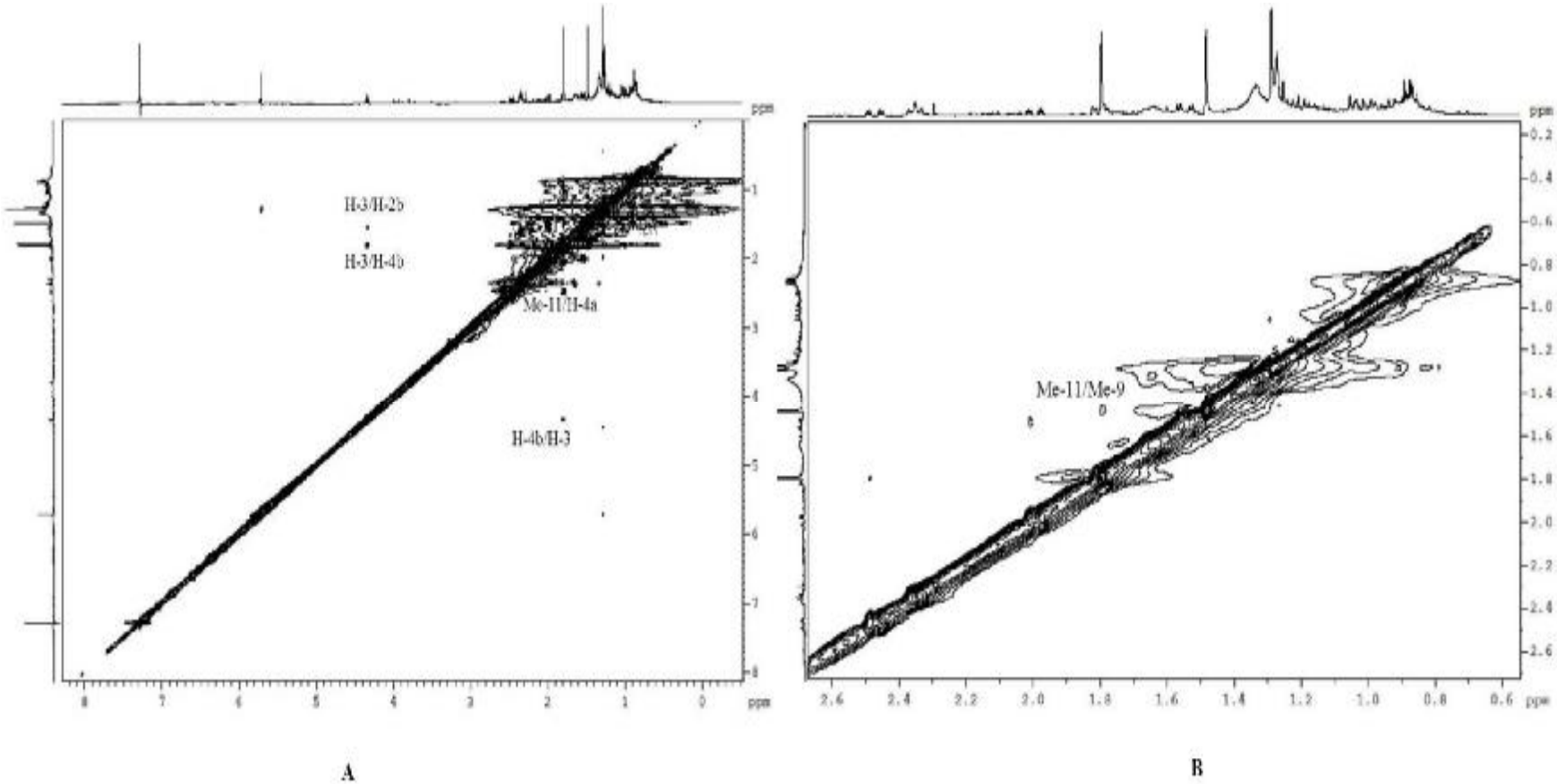

Figure 3.5 NOESY spectra (400 MHz) of TF2 in $CDCl_3$

A: Full NOESY spectrum; B: Selected expansion of NOESY spectrum

3.1.2 Characterisation of AL13 as isololiolide

AL13 was isolated from the methanol extract of *A. lappa* as a colourless oil **(Section 2.4: Protocol 3, 0.0009% yield)**. TLC analysis showed a pink spot after spraying with anisaldehyde-sulphuric acid reagent and heating.

The positive ion mode HRESI-MS spectrum gave a quasi-molecular ion $[M+H]^+$ at *m/z* 197.1172, suggesting a molecular formula of $C_{11}H_{16}O_3$ (DBE=4).

The ^{1}H NMR spectrum **(Figure 3.8, Table 3.1)** revealed similar features to the one obtained for **TF2.** An olefinic proton displayed at δ5.72 (1H, *s*), an oxymethine proton at δ4.13 (1H, *m*), three methyl groups at δ1.27 (3H, *s*), δ1.32 (3H, *s*), δ1.59 (3H, *s*) and two methylene groups at δ1.32 (1H, *dd*, *J*=12.0, 12.1 Hz)/δ2.03 (1H, *dt*, *J*=10.1, 3.6, 1.7 Hz) and δ1.50 (1H, *dd*, *J*=11.7, 11.8 Hz)/δ2.53 (1H, *dt*, *J*=11.3, 4.8, 2.4 Hz). With the aid of the COSY experiment, the proton at δ4.13 was attributed to H-3; protons at δ1.32/δ2.03 were assigned as H-2 and protons at δ1.50/δ2.53 as H-4.

The ^{13}C NMR spectrum **(Figure 3.9, Table 3.1)** displayed the presence of 11 carbons, including three methyls at δ25.1, δ25.5 and δ29.9, two methylenes at δ47.9 and δ49.8, one oxymethine at δ64.9, one olefinic carbon at δ113.2, and four quaternary carbons at δ35.0, δ86.8, δ171.7 and δ181.0.

In the HMBC spectrum **(Figure 3.10)**, the olefinic proton and three methyls exhibited similar correlations to those observed for **TF2** (loliolide). The methylene protons at δ1.32 (H-2a)/δ2.03 (H-2b) were detected with couplings to carbons at δ25.1 (C-9), δ29.9 (C-10), δ47.9 (C-4), δ181.0 (C-6), δ64.9 (C-3) and δ35.1 (C-1).

The NOESY spectrum **(Figure 3.11)** for **AL13** showed that the oxymethine proton at

δ4.13 (H-3) correlated to the methyls at δ1.33 (Me-10) and δ1.59 (Me-11) as well as to two protons at δ2.03 (H-2b) and δ2.53 (H-4b), which indicated that H-3, Me-10, Me-11, H-2b and H-4b were on the same side of the ring plane.

The above information led to the characterisation of **AL13** as isololiolide. The NMR data showed good agreement with previously published data (Kimura and Maki, 2002). This is the first report of the isolation of isololiolide from *A. lappa*.

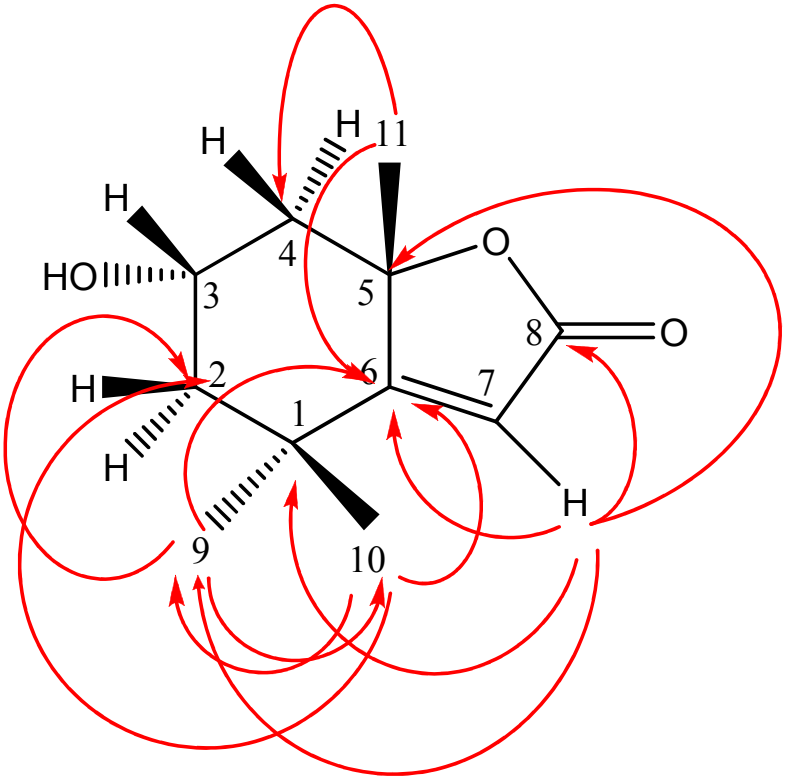

Figure 3.6 Structure of AL13 with selected HMBC correlations

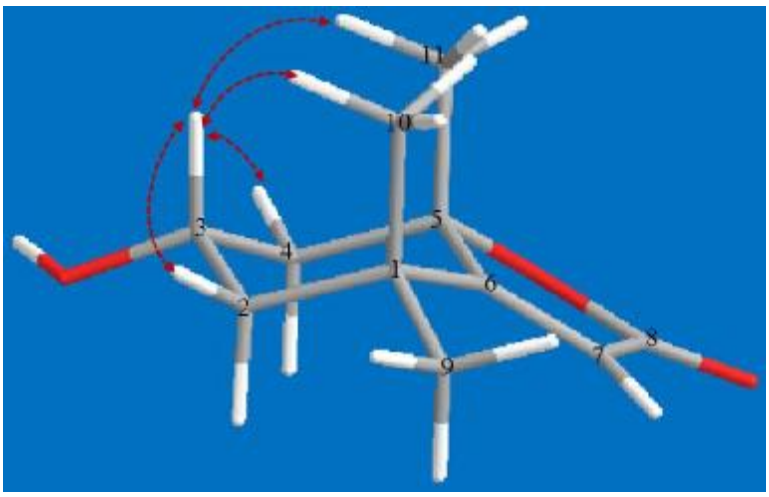

Figure 3.7 3D Structure of AL13 with important NOESY correlations

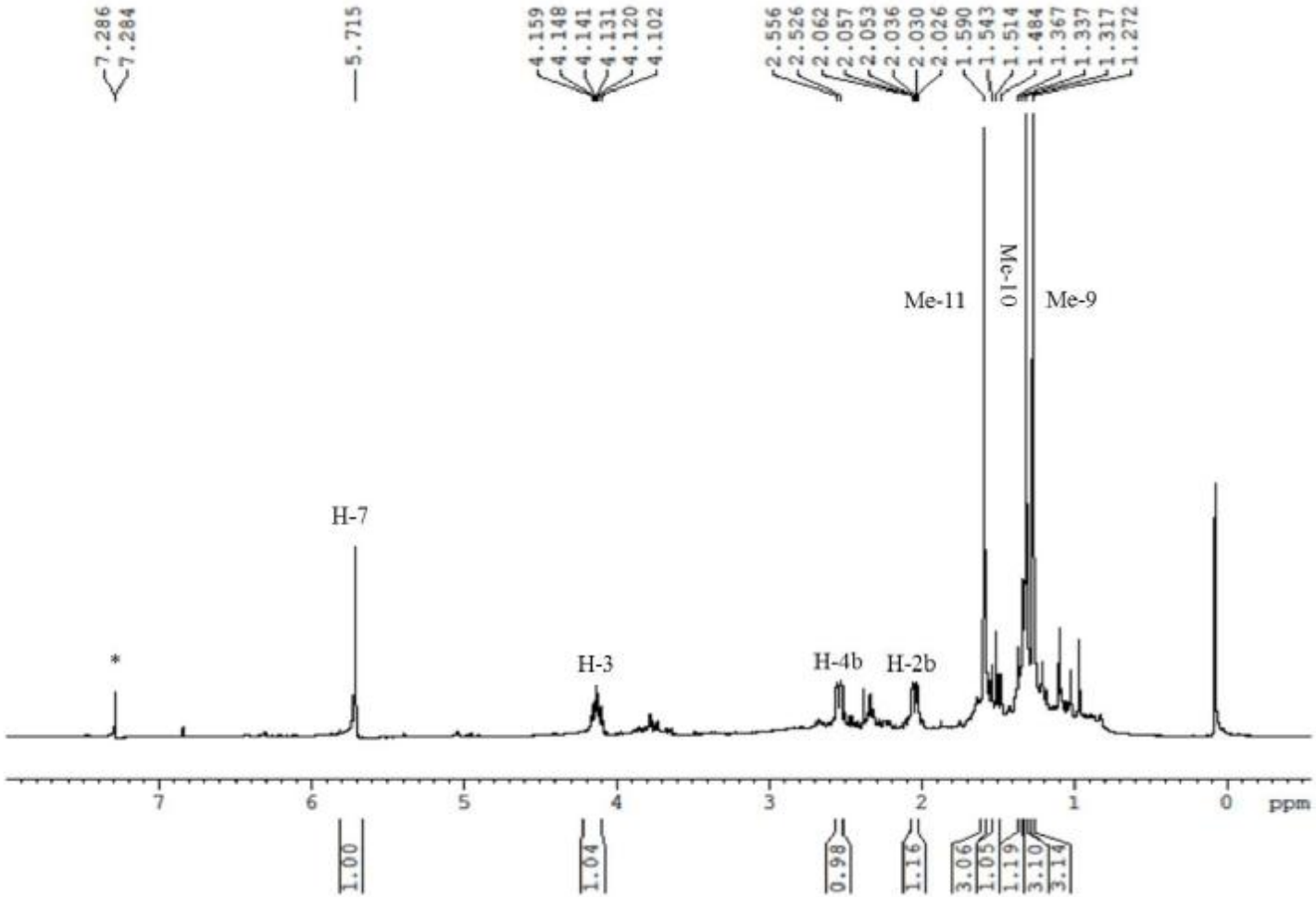

Figure 3.8 ^{1}H NMR spectrum (400 MHz) of AL13 in $CDCl_3$ (*)

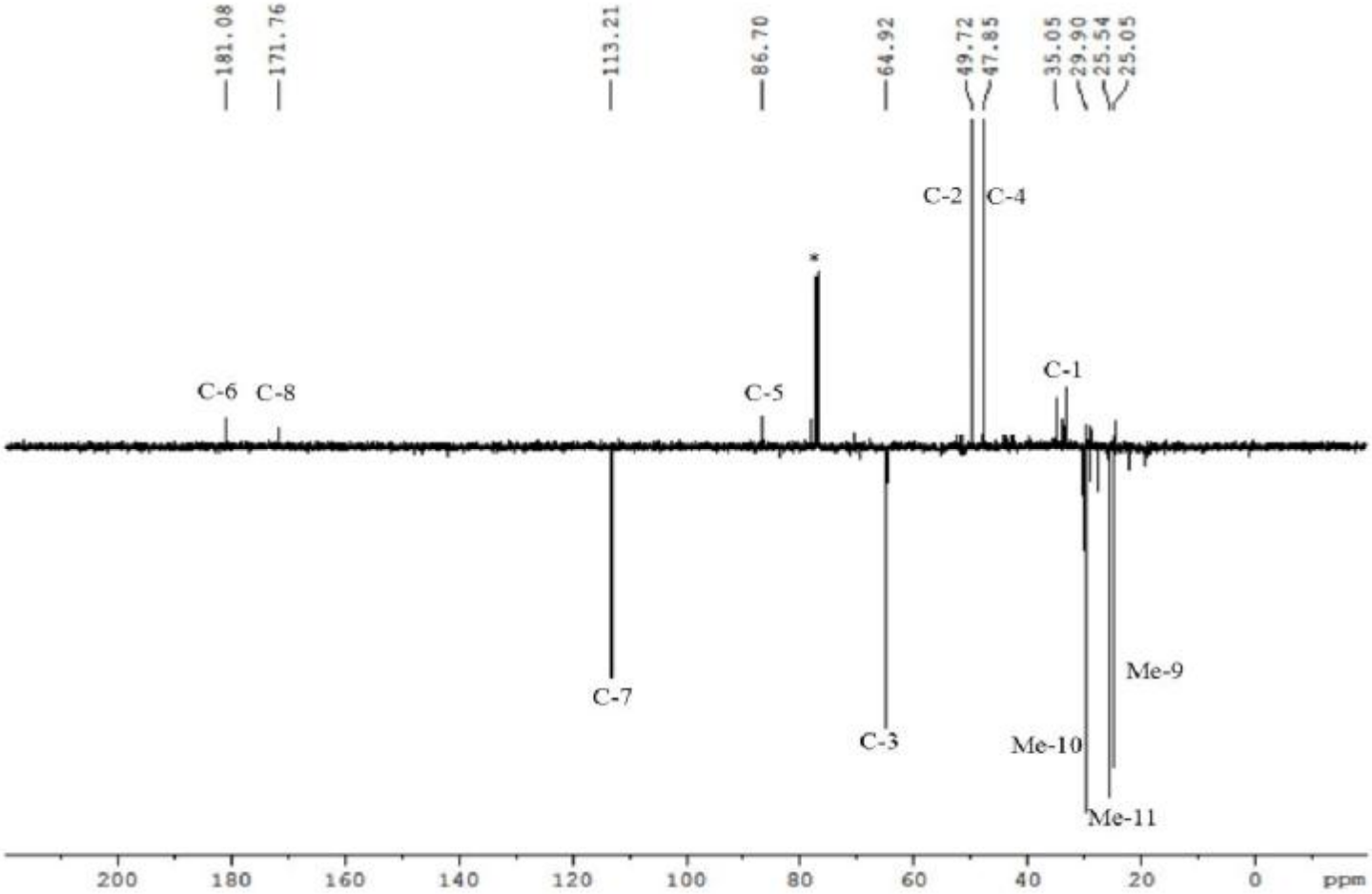

Figure 3.9 DEPTQ 135 ^{13}C NMR spectrum (100 MHz) of AL13 in $CDCl_3$ (*)

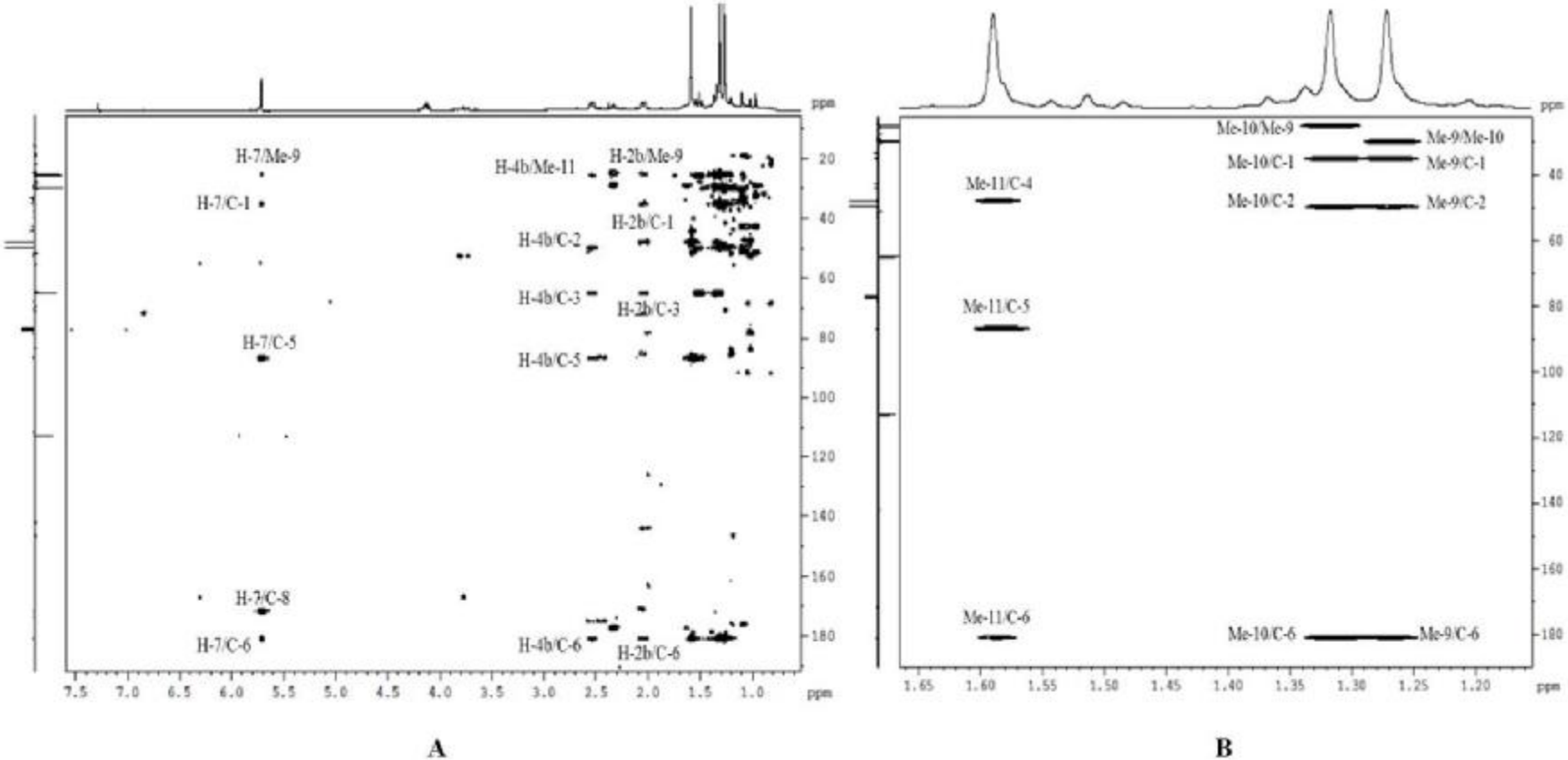

Figure 3.10 HMBC spectra (400 MHz) of AL13 in $CDCl_3$

A: Full HMBC spectrum; B: Selected expansion of HMBC spectrum

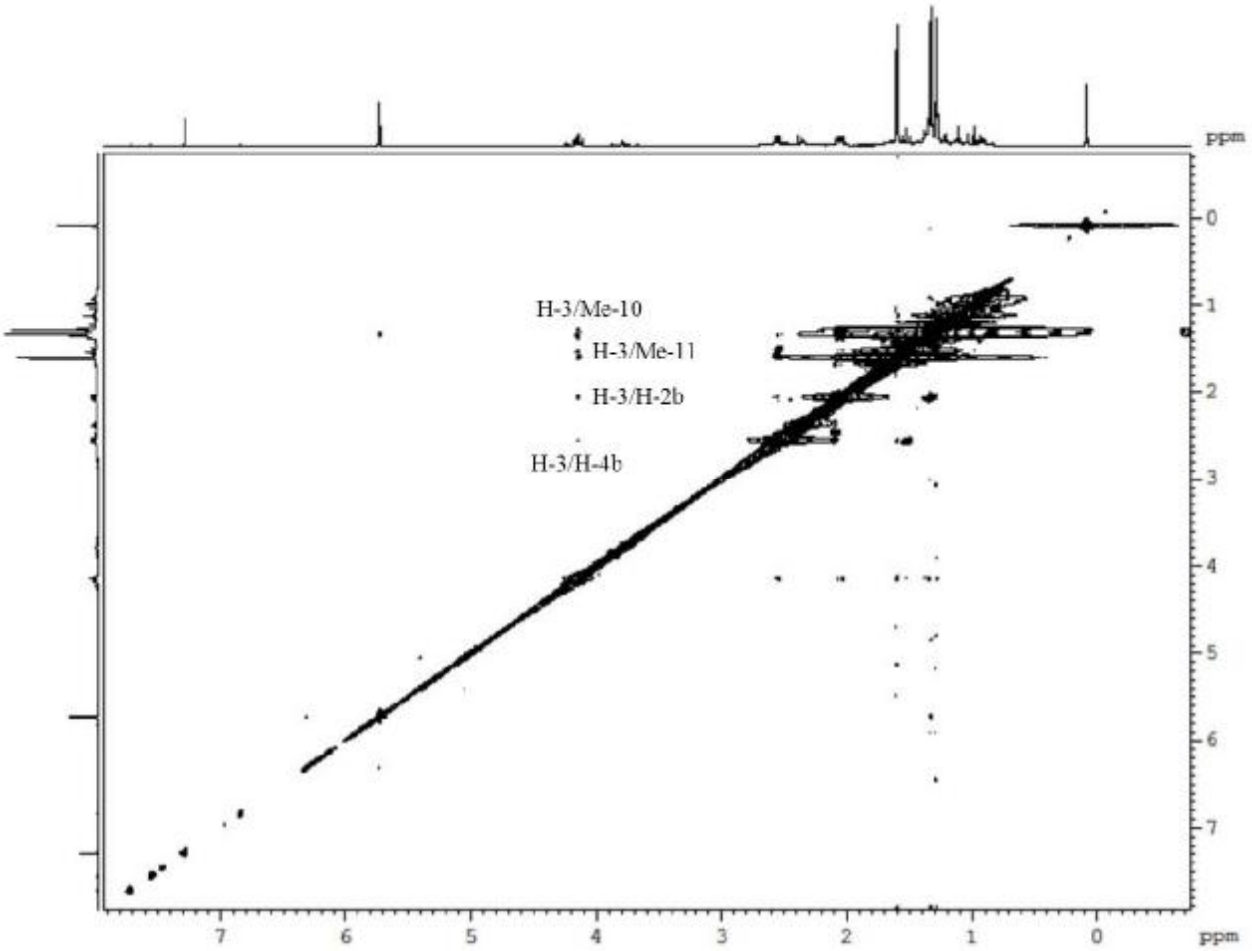

Figure 3.11 NOESY spectrum (400 MHz) of AL13 in $CDCl_3$

Table 3.1 ^{1}H (400 MHz) and ^{13}C (100 MHz) NMR data of TF2 and AL13 in $CDCl_3$

Position	TF2		AL13	
	H (δ)	C (δ)	H (δ)	C (δ)
1	-	35.8	-	35.0
2	1.56 (1H, *dd*, *J*=3.6, 14.6 Hz)	47.3	1.32 (1H, *dd*, *J*=12.0, 12.1 Hz)	49.8
	2.01 (1H, *dt*, *J*=14.6, 5.3, 2.8 Hz)		2.03 (1H, *dt*, *J*=10.1, 3.6, 1.7 Hz)	
3	4.35 (1H, *m*)	67.1	4.13 (1H, *m*)	64.9
4	1.82 (1H, *dd*, *J*=14.5, 4.0 Hz)	45.7	1.50 (1H, *dd*, *J*=11.7, 11.8 Hz)	47.9
	2.49 (1H, *dt*, *J*=14.1, 5.3, 2.6 Hz)		2.53 (1H, *dt*, *J*=11.3, 4.8, 2.4 Hz)	
5	-	86.8	-	86.8
6	-	182.2	-	181.0
7	5.72 (1H, *s*)	113.0	5.72 (1H, *s*)	113.2
8	-	172.1	-	171.7
9	1.49 (3H, *s*)	26.5	1.27 (3H, *s*)	25.1
10	1.29 (3H, *s*)	30.7	1.32 (3H, *s*)	29.9
11	1.79 (3H, *s*)	27.0	1.59 (3H, *s*)	25.5

3.1.3 Characterisation of AL14 as melitensin

AL14 was isolated from the methanol extract of *A. lappa* as a colourless oil **(Section 2.4: Protocol 3, 0.0026% yield)**. A pink spot was detected on the TLC plate after treatment with anisaldehyde-sulphuric acid reagent followed by heating.

The positive ion mode HRESI-MS data gave a quasi-molecular ion $[M+H]^+$ at *m/z* 267.1591, suggesting a molecular formula of $C_{15}H_{22}O_4$ (DBE=5).

The ^{1}H NMR spectrum **(Figure 3.14, Table 3.2)** displayed an olefinic proton at δ5.77 (1H, *dd*, *J*=17.4, 10.7 Hz), a pair of exomethylenes at δ5.00 (1H, *d*, *J*=17.4 Hz)/δ5.04 (1H, *d*, *J*=10.5 Hz) and δ5.38 (1H, *s*)/δ4.94 (1H, s), two methine protons at δ2.63 (1H, *dd*, *J*=12.1, 6.9 Hz) and δ2.39 (1H, *d*, *J*=11.7 Hz) and two methyls at δ1.10 (3H, *s*), δ1.37 (3H, *d*, *J*=6.9 Hz). With the aid of the HSQC experiment, another two methylenes and three methines were identified with signals at δ4.05 (1H, *d*, *J*=13.9 Hz)/δ3.98 (1H, *d*, *J*=14.5 Hz), δ1.81 (1H, *m*)/δ1.60 (1H, *m*), δ4.18 (1H, *t*, *J*=11.0 Hz), δ3.96 (1H, *ddd*, *J*=10.5, 6.8, 4.2 Hz) and δ1.77 (1H, *m*).

The COSY experiment revealed a coupling between the olefinic proton at δ5.77 and the methylene protons at δ5.00/δ5.04, and a coupling between the methine signal at δ2.63 and the methyl group at δ1.37.

The ^{13}C NMR spectrum **(Figure 3.15, Table 3.2)** showed the presence of 15 carbons with two methyls, six methines including one olefinic methine and two oxymethines, four methylenes including two exomethylenes and one oxymethylene, and three quaternary carbons including one carbonyl.

In the HMBC spectrum **(Figure 3.16, Table 3.2)**, the olefinic proton at δ5.77 (H-1)

displayed ^{3}J correlations to a methyl at δ18.8 (C-14), a methylene at δ49.3 (C-9) and a methine at δ50.3 (C-5). The exomethylene protons at δ5.38/δ4.94 (H-3a/b) revealed ^{3}J couplings to the methine at δ50.3 (C-5) and an oxymethylene at δ67.2 (C-15). The other exomethylene at δ5.00/δ5.04 (H-2a/b) ^{3}J correlated to a quaternary carbon at δ41.7 (C-10). The oxymethine at δ4.18 (H-6) coupled to a methine at δ41.6 (C-11), an oxymethine at δ68.8 (C-8), a methine at δ50.3 (C-5) and a quaternary carbon at δ144.4 (C-4). The oxymethylene at δ4.05/δ3.98 (H-15a/b) correlated to the methine at δ50.3 (C-5) and the exomethylene at δ114.5 (C-3). Correlations between the oxymethine at δ3.96 (H-8) and carbon signals at δ41.6 (C-11), δ41.7 (C-10) and δ78.9 (C-6) were also observed. The methine proton at δ2.63 (H-11) showed correlations to a methyl at δ14.3 (C-13), an oxymethine at δ68.8 (C-8) and the carbonyl at δ179.1 (C-12). The methine proton at δ2.39 (H-5) correlated via ^{3}J couplings to a methyl at δ18.8 (C-14), an oxymethylene at δ67.2 (C-15), an olefinic methine at δ146.4 (C-1), a exomethylene at δ114.5 (C-3) and a methine at δ58.2 (C-7). The methylene protons at δ1.81/δ1.60 (H-9a/b) ^{3}J correlated to a methyl at δ18.8 (C-14) and a methine at δ58.2 (C-7), and the methine proton at δ1.77 (H-7) displayed ^{3}J correlations to a methyl at δ14.3 (C-13) and a methine at δ50.3 (C-5). The methyl doublet at δ1.37 (Me-13) correlated to two methines at δ41.6 (C-11) and δ58.2 (C-7) and the carbonyl at δ179.1 (C-12), and the other methyl singlet at δ1.10 (Me-14) correlated to carbon signals at δ41.7 (C-10), δ50.3 (C-5) and δ146.4 (C-1).

The H-6 proton (δ4.18, *t*, *J*=11.0 Hz) appeared as a triplet with a large coupling constant, allowing the assignment of H-5, H-6 and H-7 as axial, and also the large coupling constant for H-8 (δ 3.96, *ddd*, *J*=10.5, 6.8, 4.2 Hz) allowed it to be assigned as axial. In the NOESY spectrum **(Figure 3.17)**, the methyl at δ1.10 (Me-14) displayed correlations to protons at δ1.81 (H-9a), δ3.96 (H-8) and δ4.18 (H-6). H-6 also coupled to the proton at δ2.63 (H-11) and H-8 correlated to the proton H-9a. On

the other hand, the olefinic proton at δ5.77 (H-1) correlated to the protons at δ1.60 (H-9b) and δ2.39 (H-5), and the latter (H-5) also coupled to the proton at δ1.77 (H-7). The methyl at δ1.37 (Me-13) correlated to the proton at δ1.77 (H-7). This established that Me-14, H-8, H-6, H-11 and H-9a were on the same side of the plane (e.g. on the β side), while Me-13, H-1, H-5, H-7 and H-9b were on the other side (α).

Based on the above information, **AL14** was identified as melitensin.The results were in good agreement with previous reports (Picher *et al*., 1984; Cardona *et al*., 1989; Medjroubi *et al*., 2003). This is the first report of the isolation of melitensin from *A. lappa*.

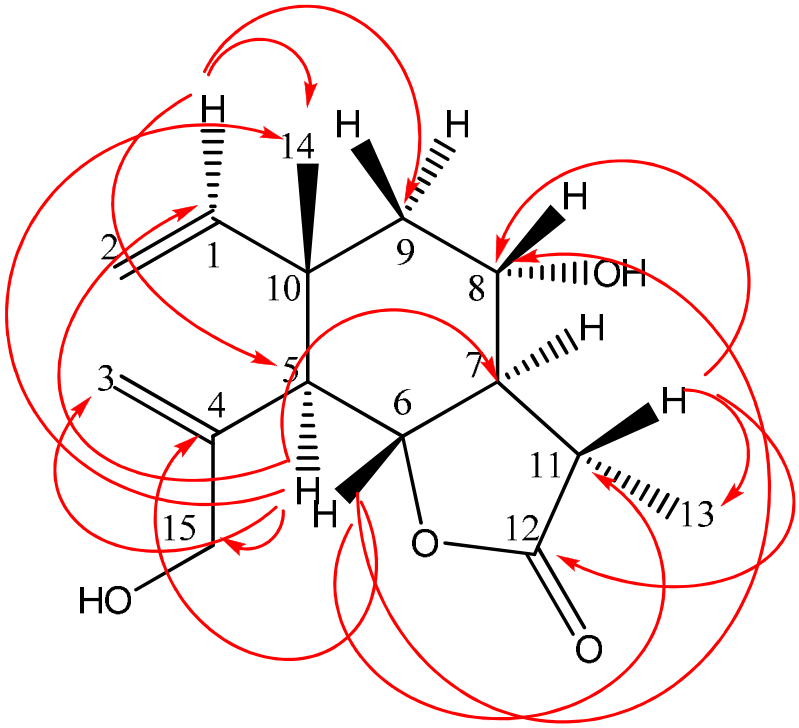

Figure 3.12 Structure of AL14 with selected HMBC correlations

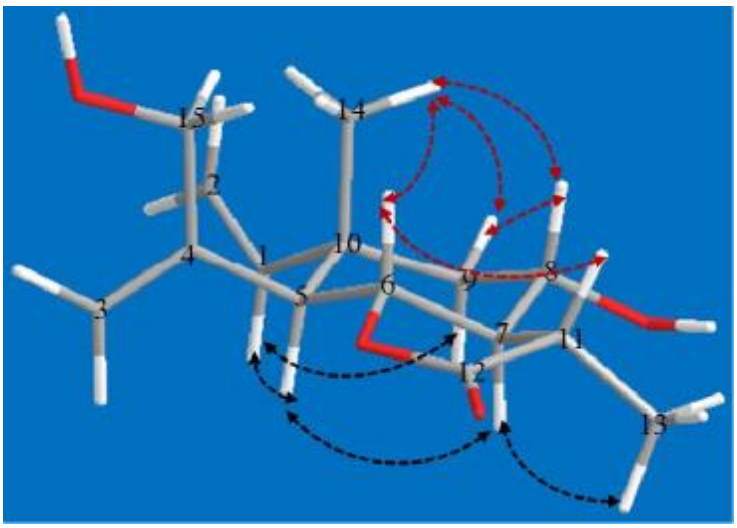

Figure 3.13 3D Structure of AL14 with important NOESY correlations

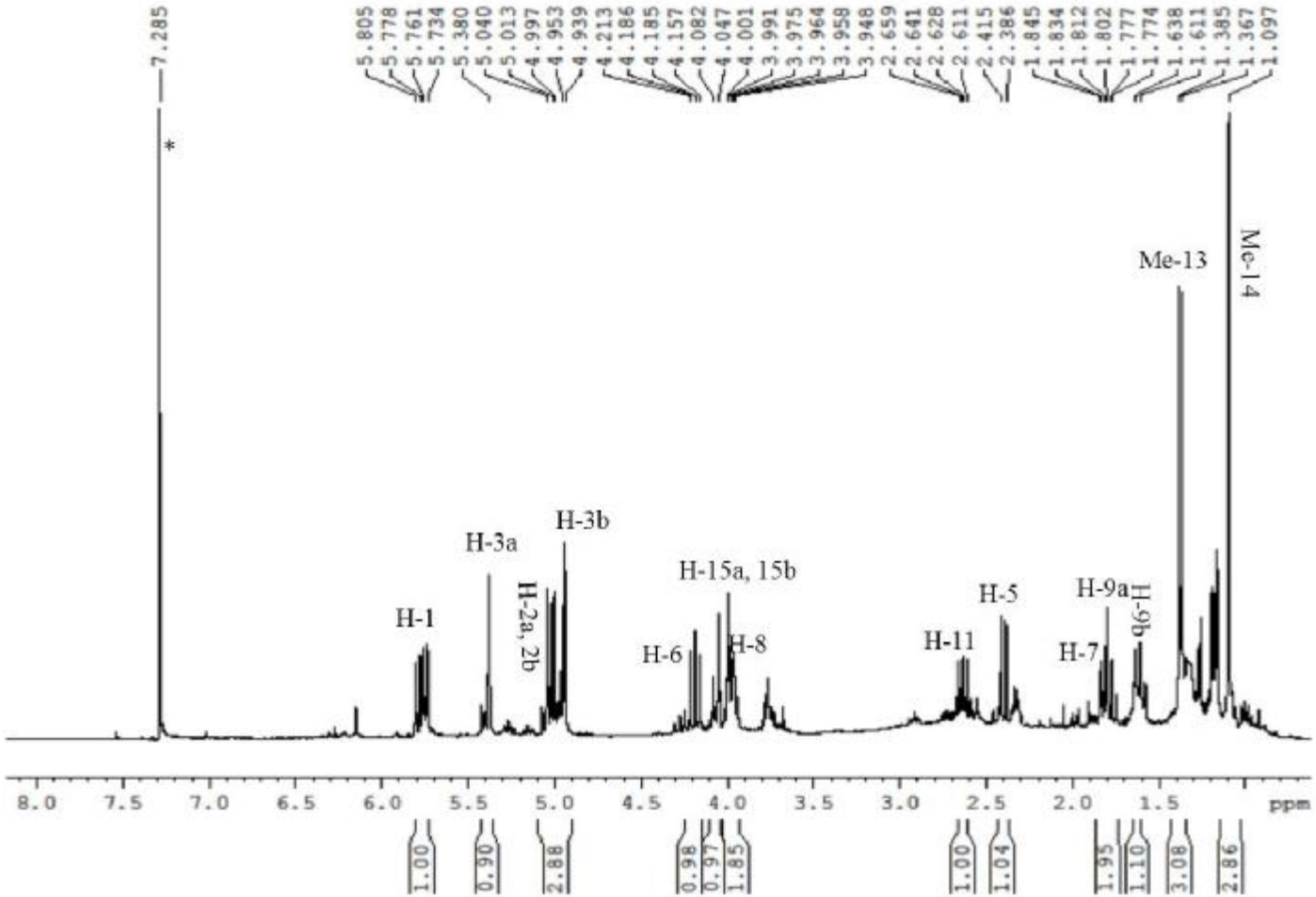

Figure 3.14 ^{1}H NMR spectrum (400 MHz) of AL14 in $CDCl_3$ (*)

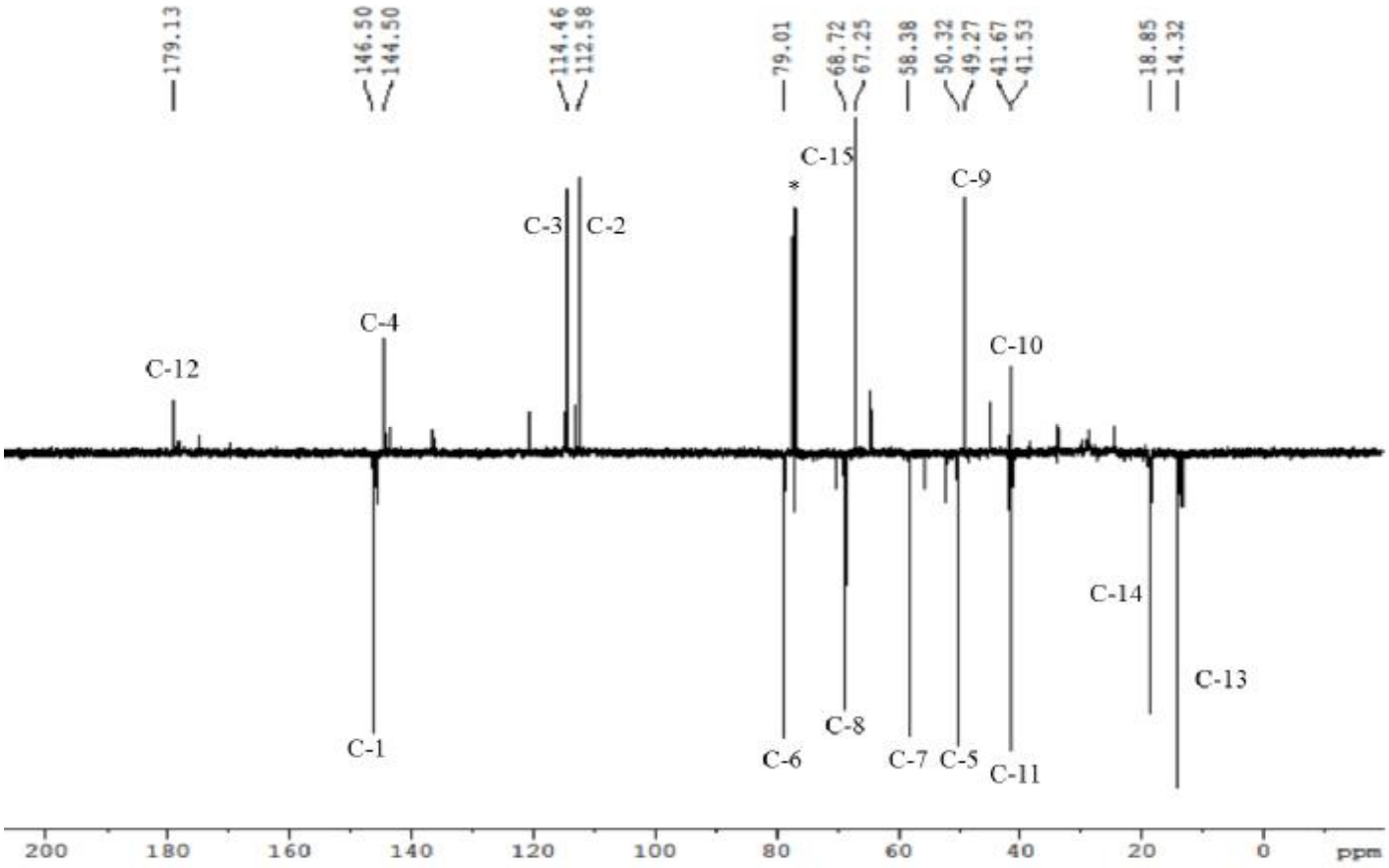

Figure 3.15 DEPTQ 135 ^{13}C NMR spectrum (100 MHz) of AL14 in $CDCl_3$ (*)

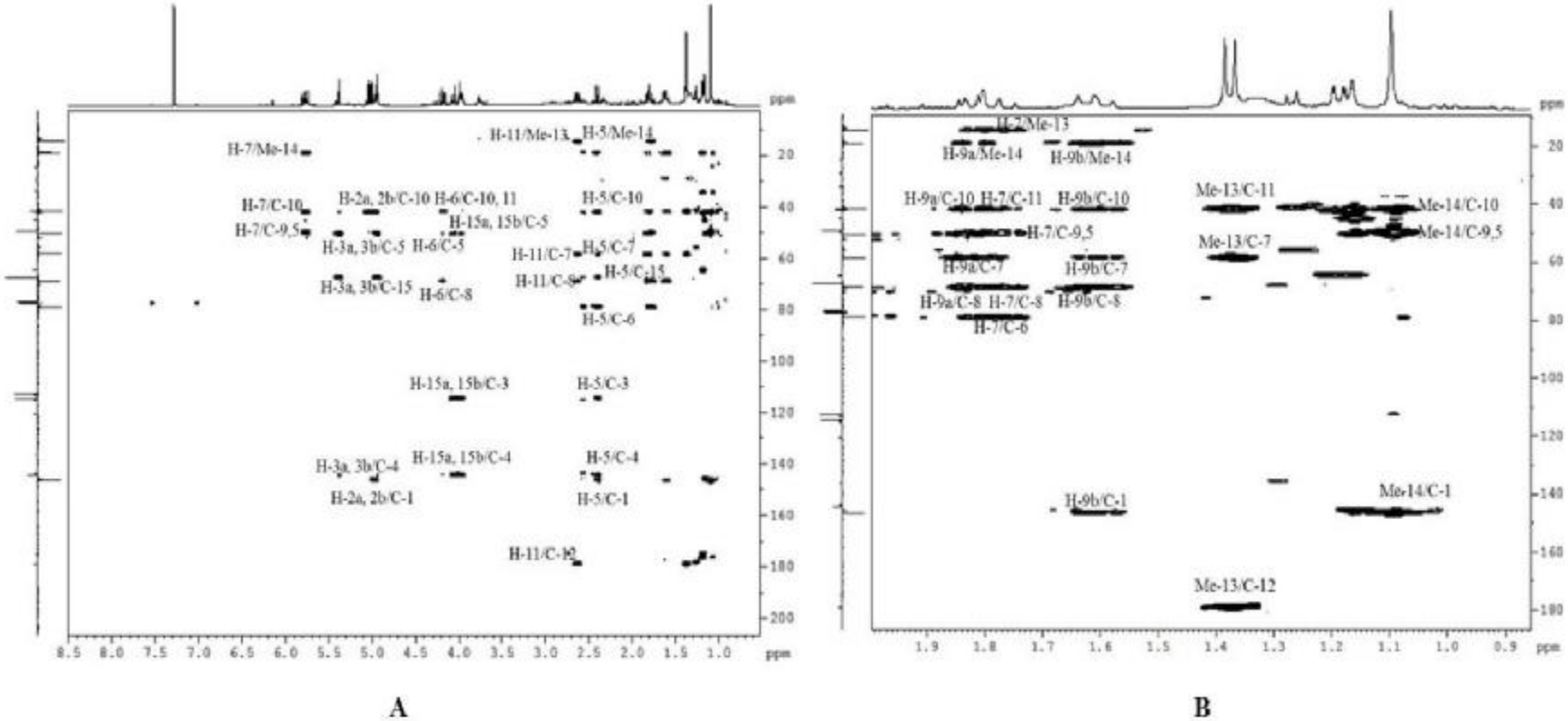

Figure 3.16 HMBC spectra (400 MHz) of AL14 in $CDCl_3$

A: Full HMBC spectrum; B: Selected expansion of HMBC spectrum

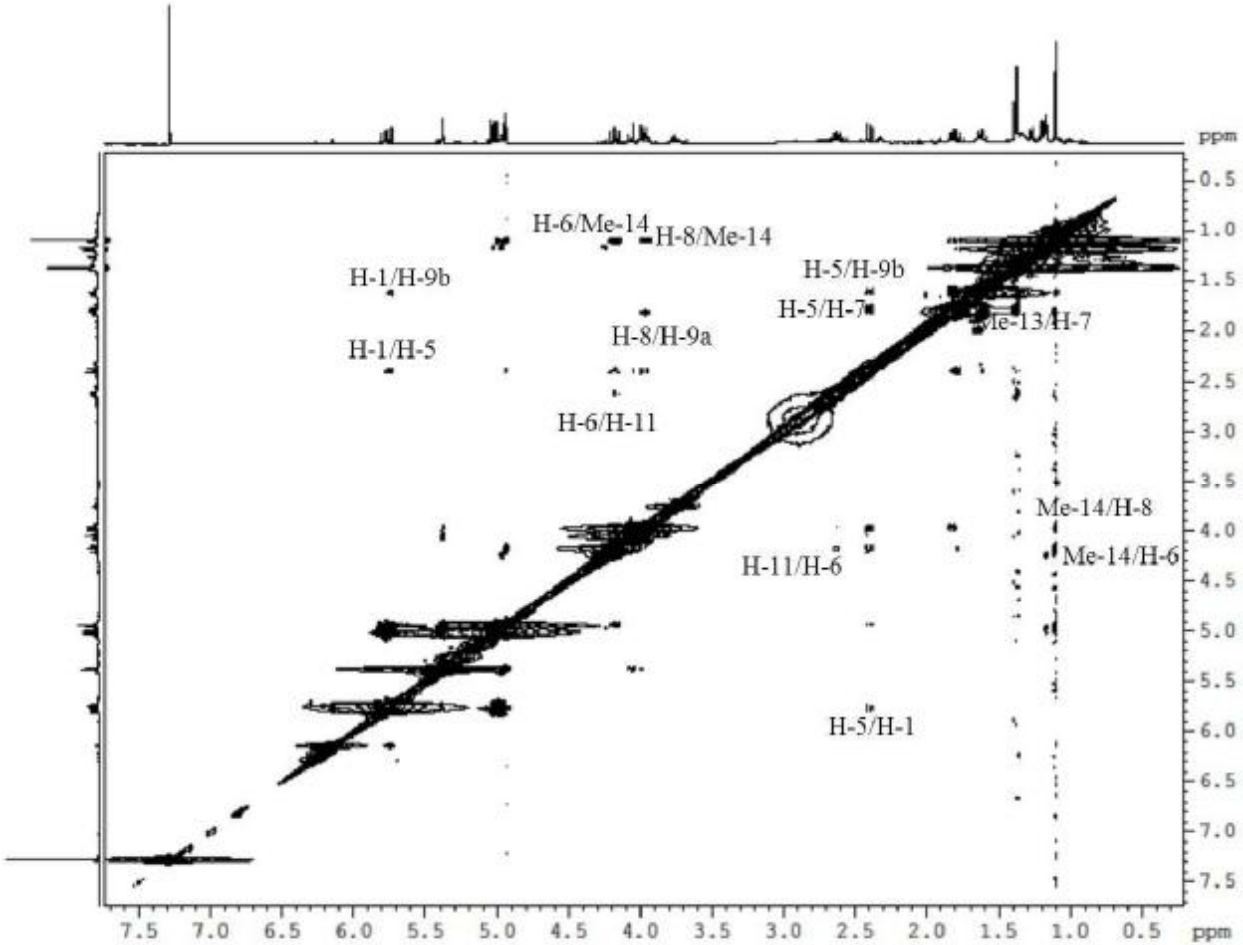

Figure 3.17 NOESY spectrum (400 MHz) of AL14 in $CDCl_3$

Table 3.2 ^{1}H (400 MHz) and ^{13}C (100 MHz) NMR data of AL14 in $CDCl_3$

Position	H (δ)	C (δ)	HMBC correlations
1	5.77 (1H, *dd*, *J*=17.4, 10.7 Hz)	146.4	Me-14, C-5, C-9, C-10
2	5.00 (1H, *d*, *J*=17.4 Hz)	112.4	C-10, C-1
	5.04 (1H, *d*, *J*=10.5 Hz)		
3	5.38 (1H, *s*)/4.94 (1H, s)	115.5	C-5, C-15, C-4
4	-	144.4	
5	2.39 (1H, *d*, *J*=11.7 Hz)	50.3	C-1, C-3, C-7, Me-14, C-15, C-10, C-4, C-6
6	4.18 (1H, *t*, *J*=11.0 Hz)	78.9	C-11, C-8, C-4, C-5
7	1.77 (1H, *m*)	58.2	Me-13, C-11, C-5, C-8, C-6
8	3.96 (1H, *ddd*, *J*=10.5, 6.8, 4.2 Hz)	68.8	C-11, C-10, C-7
9	1.81 (1H, *m*)/1.60 (1H, *m*)	49.3	Me-14, C-7, C-10, C-8
10	-	41.7	
11	2.63 (1H, *dd*, *J*=12.1, 6.9 Hz)	41.6	C-8, Me-13, C-7, C-12
12	-	179.1	
13	1.37 (3H, *d*, *J*=6.9 Hz)	14.3	C-7, C-12, C-11
14	1.10 (3H, *s*)	18.8	C-1, C-5, C-10
15	4.05 (1H, *d*, *J*=13.9 Hz)	67.2	C-3, C-4
	3.98 (1H, *d*, *J*=14.5 Hz)		

3.1.4 Characterisation of AL3 as taraxasterol

AL3 was isolated from the *n*-hexane extract of *A. lappa* as a white powder **(Section 2.4: Protocol 1, 0.0042% yield)**. A pink spot was observed after spraying with anisaldehyde-sulphuric acid reagent and heating.

The ^{1}H NMR spectrum **(Figure 3.20, Table 3.3)** diaplayed a doublet of doublet at δ4.64 (2H, *dd*, *J*=2.2, 4.9 Hz) being identified as an exomethylene with the aid of the HSQC experiment, a doublet of doublet at δ3.22 (1H, *dd*, *J*=5.5, 10.9 Hz) indicating the presence of an oxymethine, five singlets at δ0.81 (3H), δ0.90 (6H), δ0.97 (3H) , δ1.01(3H) and δ1.07(3H) and one doublet at δ1.05 (3H, *J*=7 Hz) indicating the presence of seven methyls.

The ^{13}C NMR spectrum **(Table 3.3)** revealed the presence of 30 carbons including seven methyls, eleven methylenes, five methines, one oxymethine and six quaternary carbons but no carbonyl group. On this basis, a molecular formula of $C_{30}H_{50}O$ was deduced for **AL3**. This was confirmed with the positive ion mode HRESI-MS data which gave a base peak at *m/z* 409.3825 $[(M-H_2O) +H]^+$ and thus a molecular formula of $C_{30}H_{50}O$ (DBE=6).

In the HMBC spectrum **(Figure 3.21)**, the exomethylene protons (H-30) at δ4.64 displayed ^{3}J correlations to a methine at δ39.0 (C-19) and a methylene at δ25.6 (C-21) and ^{2}J correlation to an olefinic quaternary carbon at δ154.5 (C-20). The oxymethine at δ3.22 (H-3) ^{3}J coupled to methyl carbons at δ15.4 (C-24) and 28.2 (C-23) and ^{2}J correlated to the quaternary carbon at δ38.8 (C-4). The methyl groups at δ0.81 (Me-24) and δ1.01 (Me-23) with ^{2}J correlations to the quaternary carbon at δ38.8 (C-4) were identified as geminal methyls. They both also showed ^{3}J correlations to the carbons at δ55.6 (C-5) and δ79.1(C-3). The signal at δ0.90 (Me-25) correlated to the carbons at δ55.6 (C-5) and δ50.7 (C-9) while the singlet at δ0.90 (Me-28)

exhibited correlations to carbons at δ38.4 (C-16) and δ38.9 (C-22).

The large coupling constant observed for H-3 (*J*=5.5, 10.9 Hz) established the *trans-diaxial* orientation of H-2, H-3 protons. In the NOESY spectrum **(Figure 3.22)**, the oxymethine displayed correlations to one of the two geminal methyl groups at δ1.01 (Me-23) and the proton at δ0.73 (H-5) whilst the other methyl group at δ0.81 (Me-24) correlated to the methyl at δ0.90 (Me-25), which led to the conclusion that H-3, H-5 and Me-23 were on the α side of the plane. Other correlations were observed at δ1.05 (Me-26)/δ0.90 (Me-25), at δ2.13 (H-19)/δ1.05 (Me-26) and at δ1.63 (H-13)/δ2.13 (H-19)/δ0.90 (Me-28), thus Me-24, Me-25, Me-26, H-13, H-19 and Me-28 were all on the β side of the plane. The large couping constant for H-19 (*J*=6.9, 13.8 Hz) indicated H-19 and H-18 were *trans-diaxial* protons and H-18 was on the α side of the plane.

Based on the above information, **AL3** was identified as taraxasterol. The NMR data were in agreement with previous reports (Takaoka and Hiroi, 1976; Mahato and Kundu, 1994). This compound has previously been isolated from *A. lappa* roots and leaves (Vachalkova *et al.*, 2004).

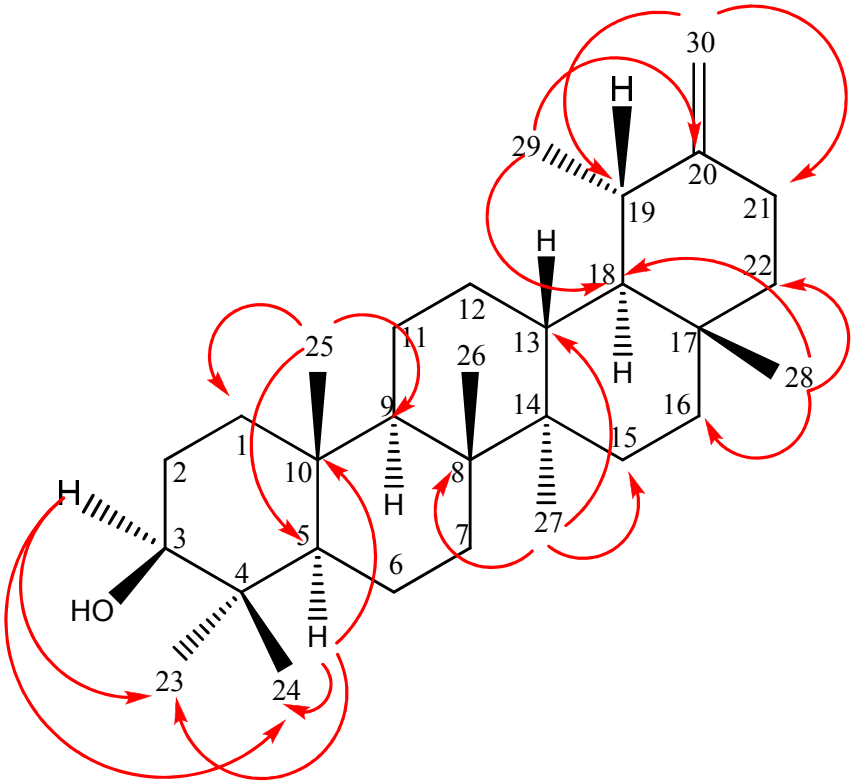

Figure 3.18 Structure of AL3 with selected HMBC correlations

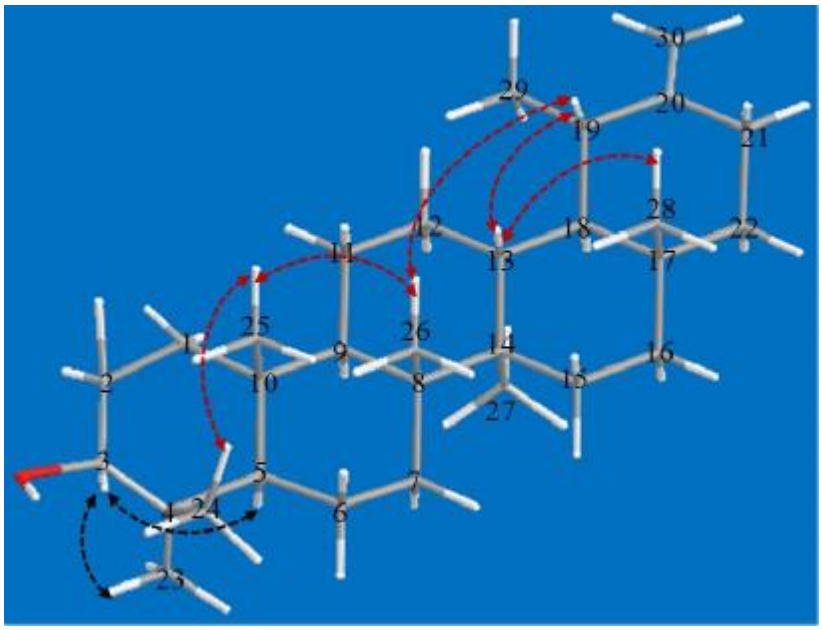

Figure 3.19 3D Structure of AL3 with important NOESY correlations

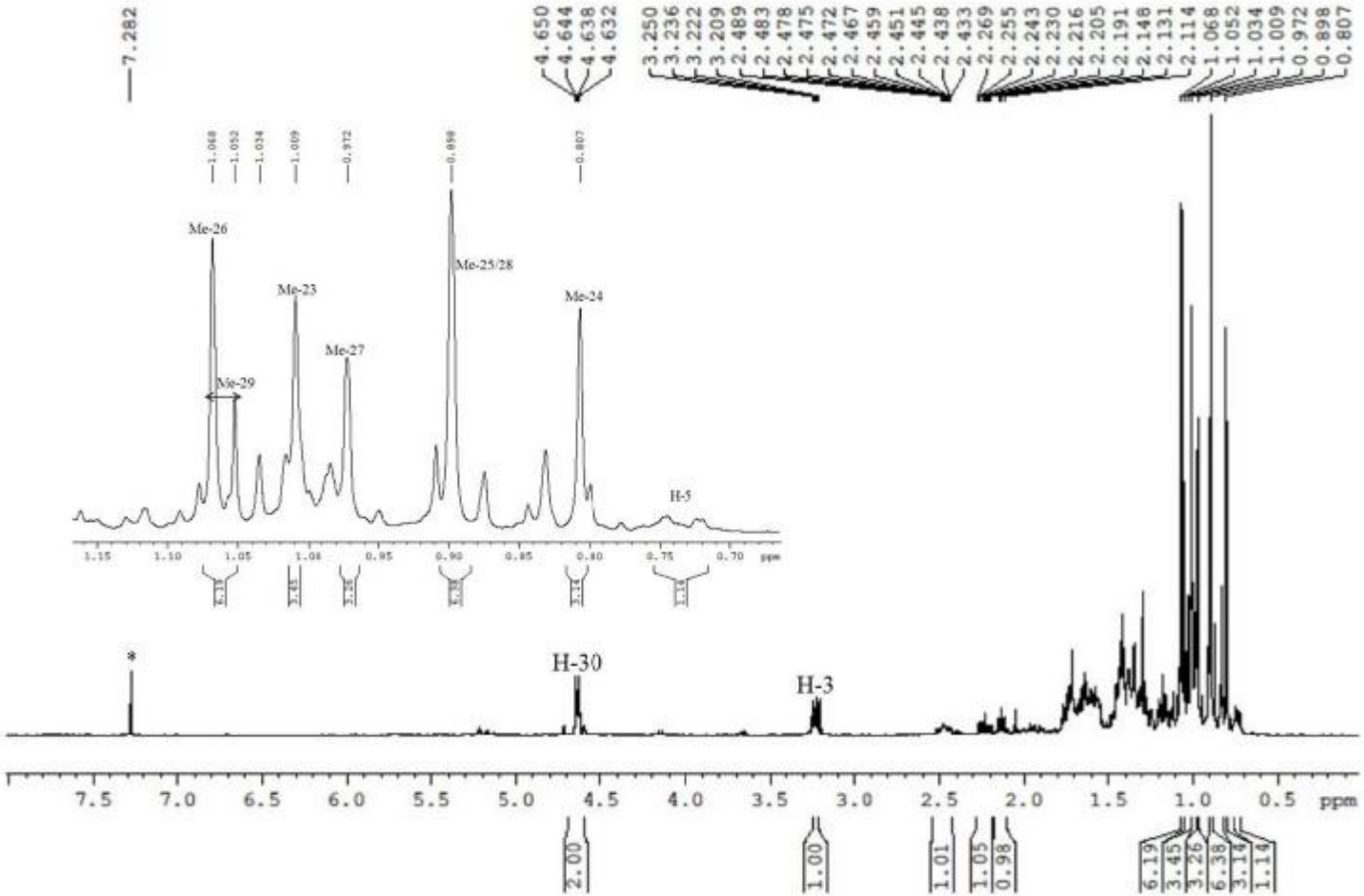

Figure 3.20 ^{1}H NMR spectrum (400 MHz) of AL3 in $CDCl_3$ (*)

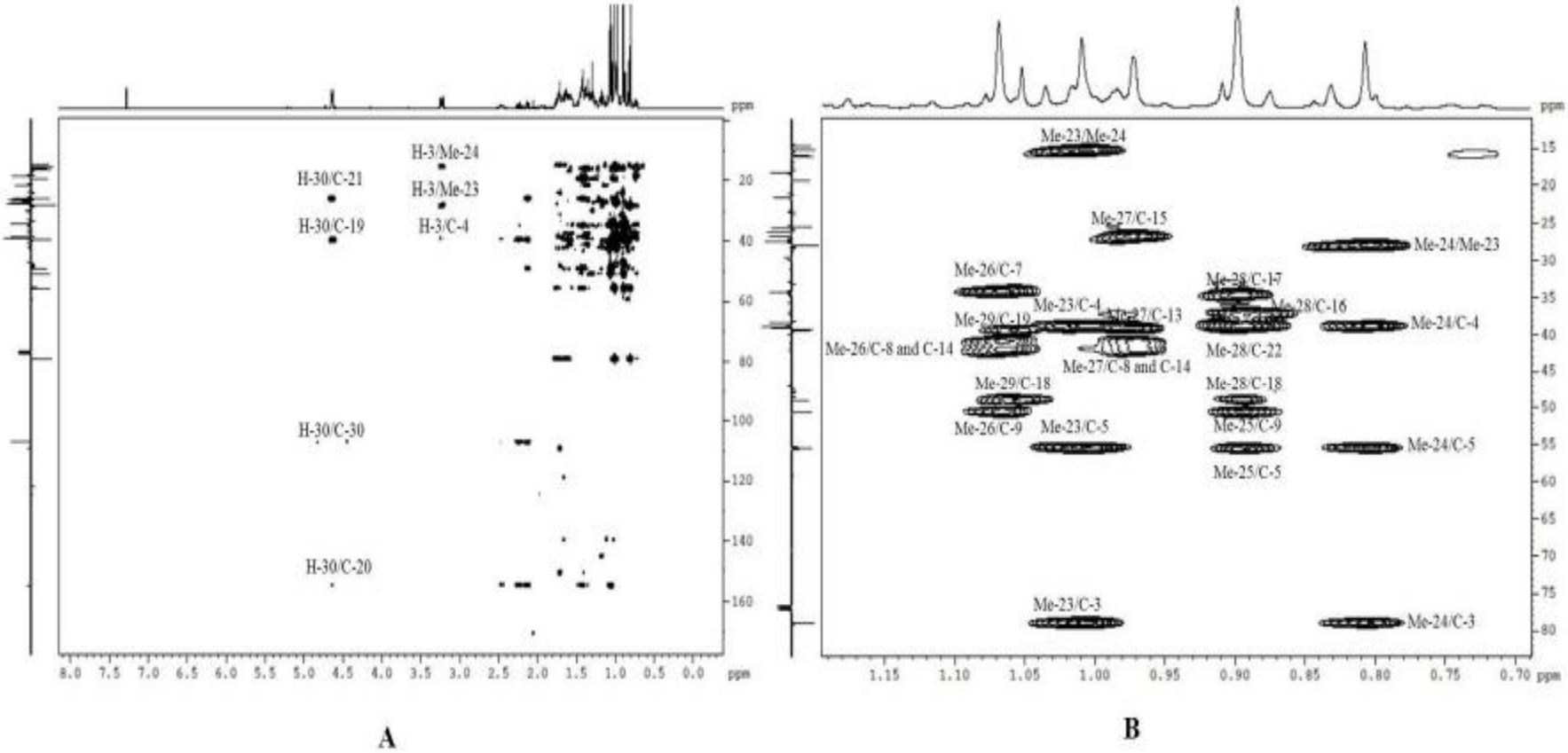

Figure 3.21 HMBC spectra (400 MHz) of AL3 in $CDCl_3$

A: Full HMBC spectrum; B: Selected expansion of HMBC spectrum

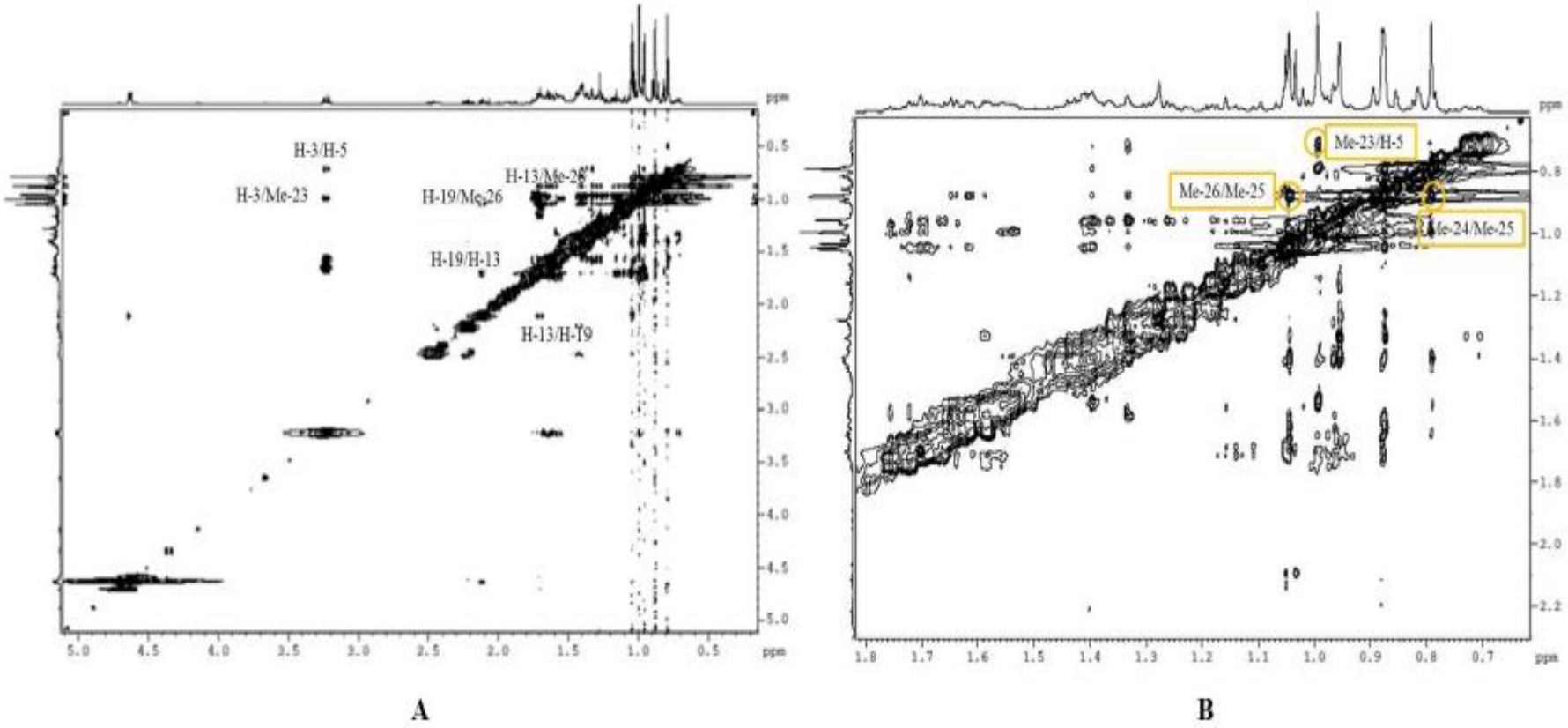

Figure 3.22 NOESY spectra (400 MHz) of AL3 in $CDCl_3$

A: Full NOESY spectrum; B: Selected expansion of NOESY spectrum

3.1.5 Characterisation of AL4 as taraxasterol acetate

AL4 was isolated from the *n*-hexane extract of *A. lappa* as a white amorphous solid **(Section 2.4: Protocol 1, 0.0099% yield)**. A pink spot appeared on the TLC plate upon spraying with anisaldehyde-sulphuric acid reagent and heating.

The ^{1}H NMR data **(Figure 3.24, Table 3.3)** of **AL4** were similar to that of **AL3**. The main difference was the presence of a highly deshielded oxymethine at δ4.49 (1H, *dd*, *J*=5.4, 10.7 Hz) compared with δ3.22 **(AL3)**. This suggested that the oxymethine was esterified. An extra downfield shift of δ2.05 (3H, *s*) established the presence of acetyl protons. Due to the large coupling constant (*J*=10.7 Hz), H-3 was assigned as axial.

The ^{13}C NMR spectrum **(Figure 3.25, Table 3.3)** displayed 32 carbons including eight methyls, eleven methylenes, five methines, one oxymethine and seven quaternary carbons. The presence of a quaternary carbon at δ171.1 and a methyl at δ21.3, confirmed the presence of an acetyl unit in **AL4**. The above information indicated a molecular formula of $C_{32}H_{52}O_2$. The positive ion mode HRESI-MS data for **AL4** gave a base peak at *m/z* 409.3831 accounting for $[(M-CH_3COOH) +H]^+$ and thus a molecular formula of $C_{32}H_{52}O_2$ (DBE=7) for **AL4**.

The HMBC spectrum **(Figure 3.26)** exhibited similar correlations to those observed for **AL3**. The main difference was that both the oxymethine at δ4.49 (H-3) and the methyl at δ21.3 (Me-32) coupled to a carbonyl at δ171.1 (C-31), establishing the presence of an acetyl unit in C-3.

On the basis of the above data and by comparison with previous reports, **AL4** was identified as taraxasterol acetate. The spectroscopic data were consistent with previously published data (Khalilov *et al*., 2003). This compound has previously been isolated from *A. lappa* leaves (Committee on Herbal Medicinal Products, 2010).

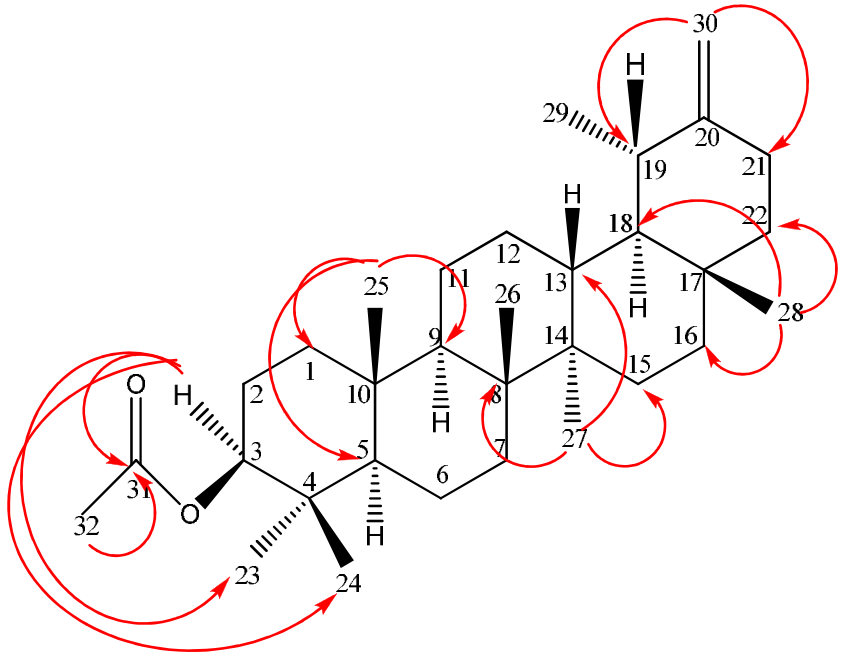

Figure 3.23 Structure of AL4 with selected HMBC correlations

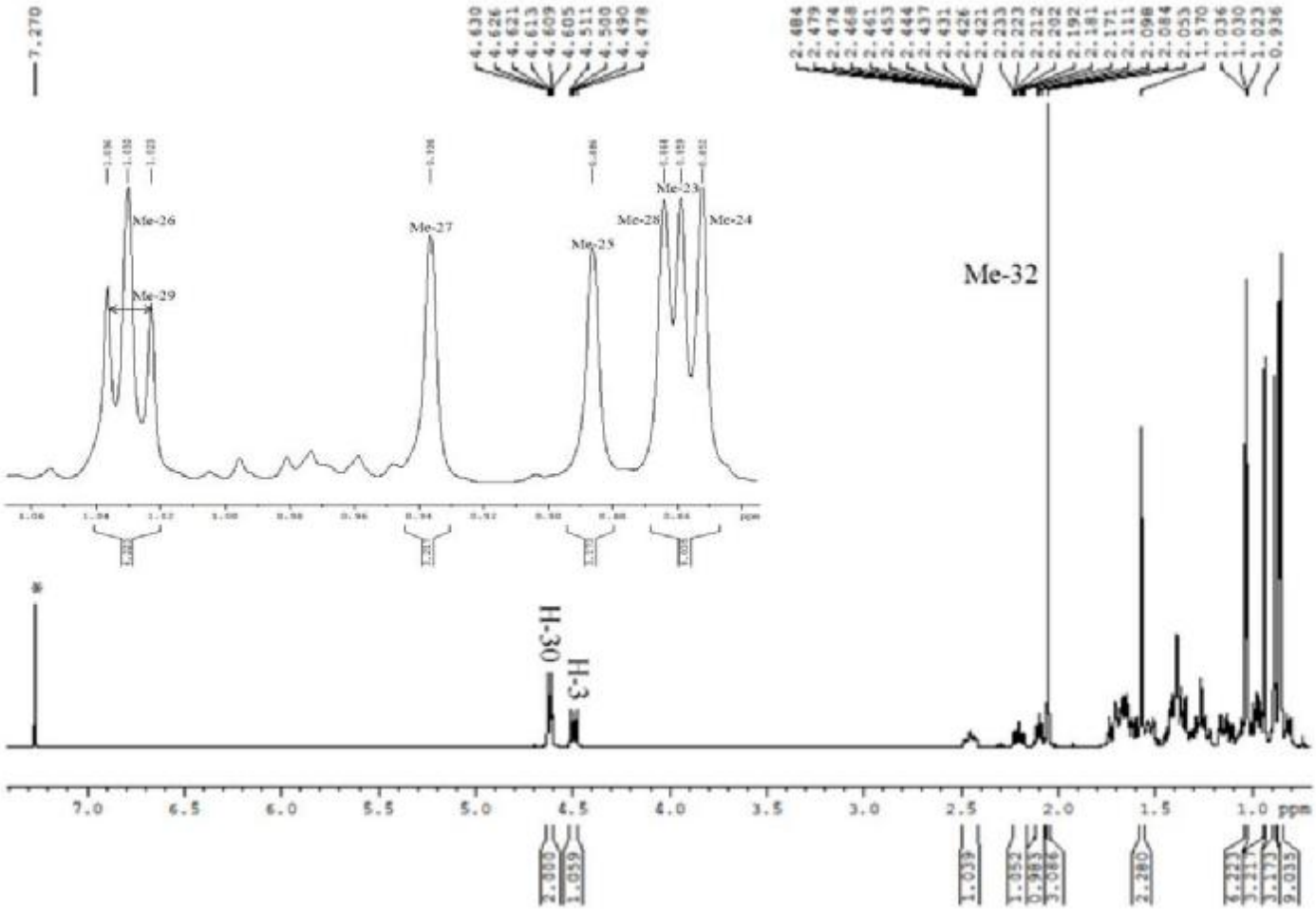

Figure 3.24 ^{1}H NMR spectrum (500 MHz) of AL4 in $CDCl_3$ (*)

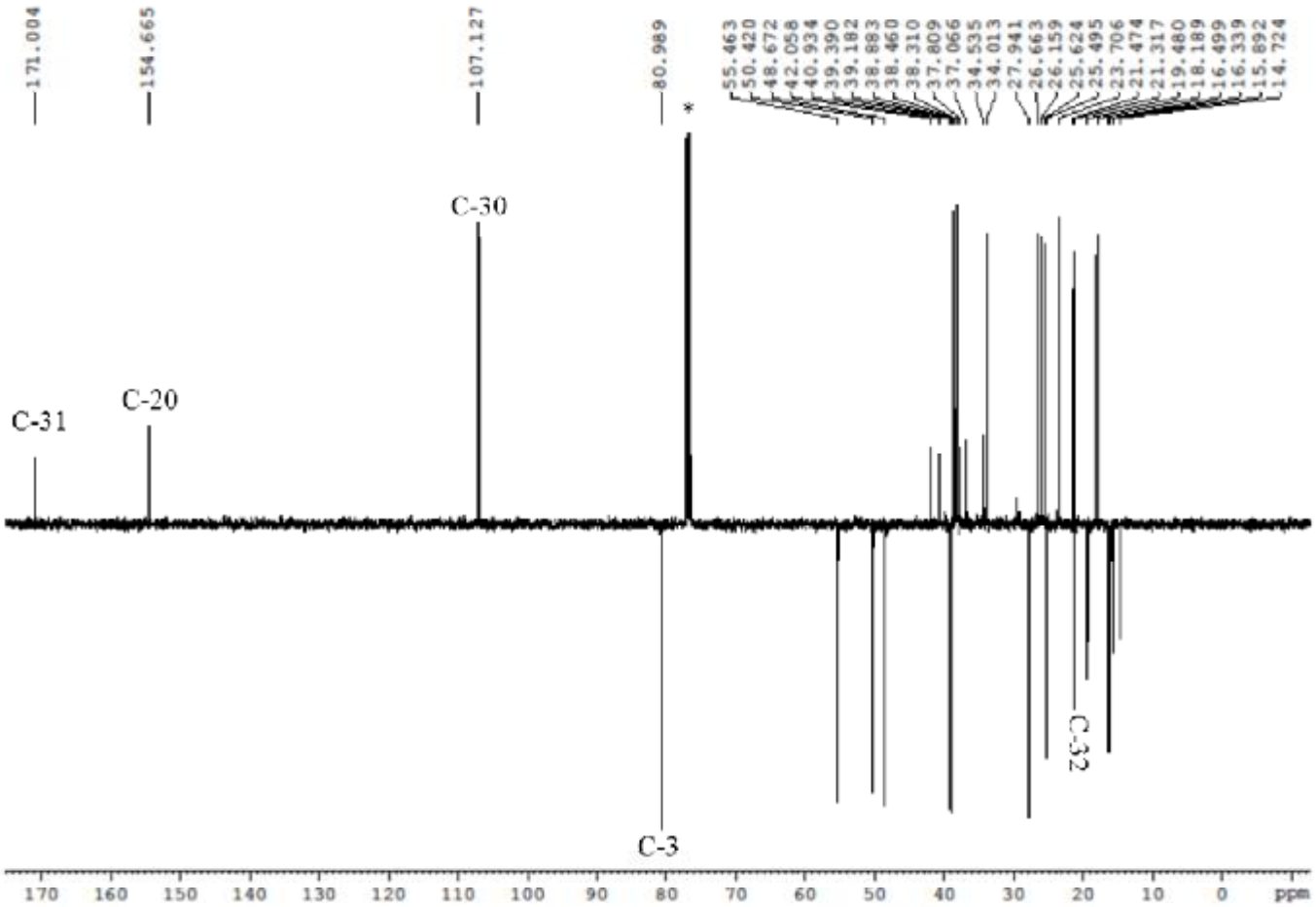

Figure 3.25 Jmod ^{13}C NMR spectrum (125 MHz) of AL4 in $CDCl_3$ (*)

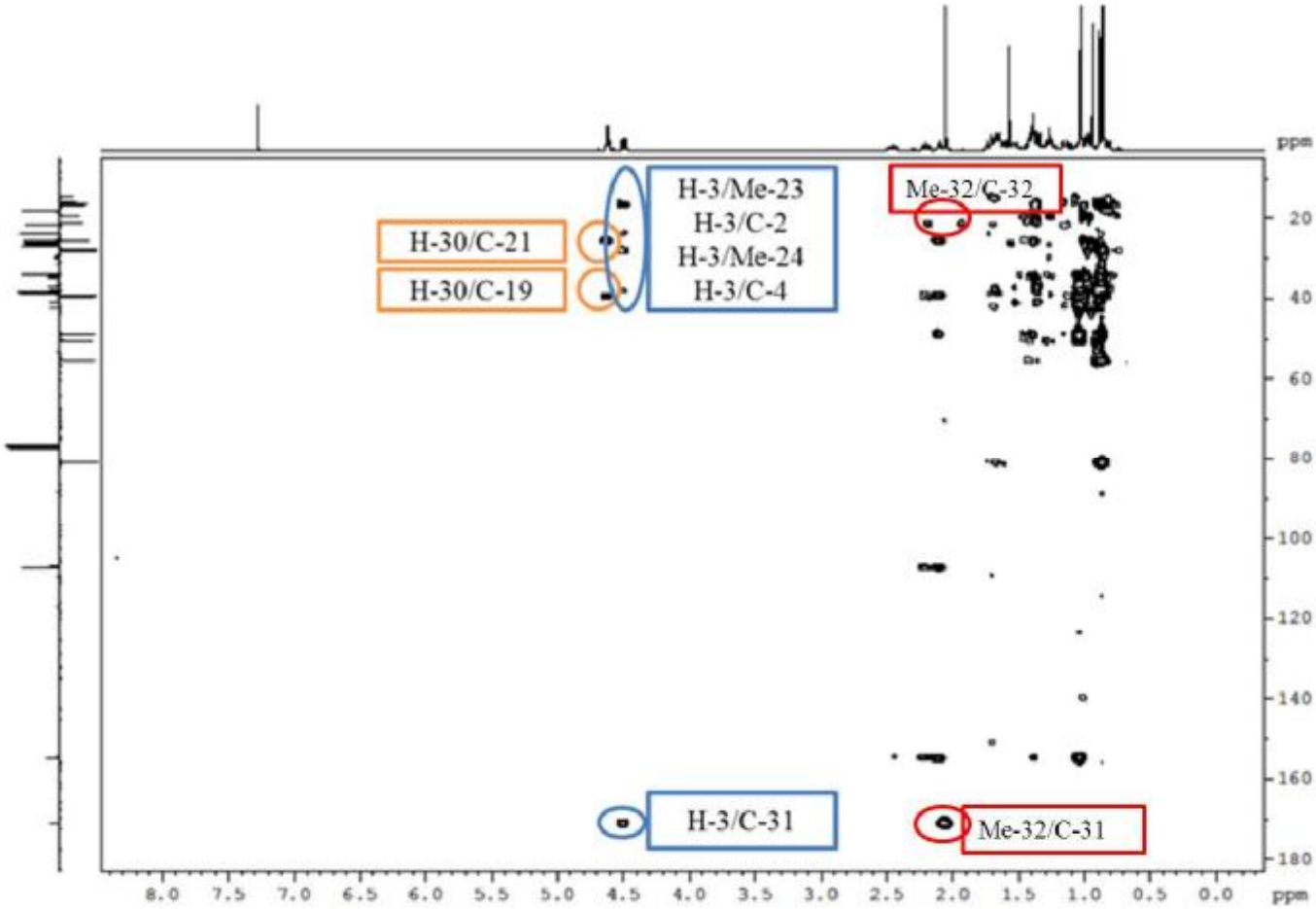

Figure 3.26 HMBC spectrum (500 MHz) of AL4 in $CDCl_3$

Table 3.3 ^{1}H and ^{13}C NMR data of AL3 and AL4 in $CDCl_3$

Position	AL3		AL4	
	H (δ, 400 MHz)	C (δ, 100 MHz)	H (δ, 500 MHz)	C (δ, 125 MHz)
1	1.29 (1H, *m*)/1.19 (1H, *m*)	38.4	1.22 (1H, *m*)/1.14 (1H, *m*)	38.3
2	1.66 (1H, *m*)/1.60 (1H, *m*)	27.4	1.66 (1H, *m*)/1.61(1H, *m*)	23.7
3	3.23 (1H, *dd*, *J*= 5.5, 10.9 Hz)	79.0	4.49 (1H, *dd*, *J*=5.4, 10.7 Hz)	81.0
4	-	38.9	-	37.8
5	0.73 (1H, *m*)	55.6	0.81 (1H, *m*)	55.5
6	1.56 (1H, *m*)/1.42 (1H, *m*)	18.4	1.51 (1H, *m*)/1.38 (1H, *m*)	18.2
7	1.45 (1H, *m*)/1.40 (1H, *m*)	34.2	1.39 (1H, *m*)/1.37 (1H, *m*)	34.0
8	-	41.0	-	40.9
9	1.35 (1H, *m*)	50.6	1.34 (1H, *m*)	50.4
10	-	37.3	-	37.1
11	1.58 (1H, *m*)/1.31 (1H, *m*)	21.5	1.54 (1H, *m*)/1.26 (1H, *m*)	21.5
12	1.75 (1H, *m*)/1.70 (1H, *m*)	26.2	1.69 (1H, *m*)/1.65 (1H, *m*)	26.2
13	1.63 (1H, *m*)	39.0	1.59 (1H, *m*)	39.1
14	-	42.1	-	42.1
15	1.02 (1H, *m*)/1.98 (1H, *m*)	26.7	1.71 (1H, *m*)/1.65 (1H, *m*)	26.7
16	1.74 (1H, *m*)/1.00 (1H, *m*)	38.9	1.74 (1H, *m*)/1.71 (1H, *m*)	38.5

Table 3.3 (continued) ^{1}H and ^{13}C NMR data of AL3 and AL4 in $CDCl_3$

Position	AL3		AL4	
	H (δ, 400 MHz)	C (δ, 100 MHz)	H (δ, 500 MHz)	C (δ, 125 MHz)
17	-	34.6	-	34.5
18	1.01 (1H, *m*)	48.9	0.97 (1H, *m*)	48.6
19	2.12 (1H, *dd*, *J* =7.0, 14.0 Hz)	39.4	2.10 (1H, *dd*, *J*= 6.9, 13.8 Hz)	39.4
20	-	154.6	-	154.6
21	2.48 (1H, *m*)/2.23 (1H, *m*)	25.7	2.43 (1H, *m*)/2.18 (1H, *m*)	25.6
22	1.45 (1H, *m*)/1.40 (1H, *m*)	39.0	1.43 (1H, *m*)/1.35 (1H, *m*)	38.9
23	1.01 (3H, *s*)	28.0	0.86 (3H, *s*)	28.0
24	0.81 (3H, *s*)	15.4	0.85 (3H, *s*)	16.5
25	0.90 (3H, *s*)	16.2	0.89 (3H, *s*)	16.4
26	1.07 (3H, *s*)	15.9	1.03 (3H, *s*)	16.0
27	0.97 (3H, *s*)	14.7	0.94 (3H, *s*)	14.7
28	0.90 (3H, *s*)	19.4	0.86 (3H, *s*)	19.5
29	1.05 (3H, *d*, *J*=7 Hz)	25.5	1.03 (3H, *d*, *J*= 6.8 Hz)	25.5
30	4.64 (2H, *dd*, *J*=2.2, 4.9 Hz)	107.1	4.62 (2H, *dd*, *J*=2.3, 5.0 Hz)	107.1
31			-	171.1
32			2.05 (3H, *s*)	21.3

3.1.6 Characterisation of VT1 as α-spinasterol

VT1 was isolated from the *n*-hexane extract of *V. thupasus* as colourless needles **(Section 2.4: Protocol 8, 0.0082% yield)**. A purple spot appeared on the TLC plate upon spraying with vanillin-sulphuric acid reagent and heating.

HREI-MS analysis indicated a molecular ion $[M]^+$ at *m/z* 412 and some fragments at *m/z* 81, 83, 107, 147, 255, 273, 300, suggesting a molecular formula of $C_{29}H_{49}O$ (DBE=6).

The ^{1}H NMR spectrum **(Figure 3.28, Table 3.4)** displayed six methyl groups, two tertiary methyl groups as singlets at δ0.57 and δ0.82 which were assigned to Me-18 and Me-19, respectively. The signals of two secondary methyls were observed as doublets at δ1.04 (*J*=6.6 Hz) and δ0.86 (*J*=6.4 Hz) which were assigned to Me-21 and Me-26, respectively. The signal of another secondary methyl (Me-27) at δ0.82 was overlapped with a triplet signal of Me-29 at δ0.83 which belonged to a primary methyl group, so their *J* value were ambiguous. Two olefinic-proton resonances at δ5.18 (*dd*, *J*=8.6, 15.1 Hz) and δ5.05 (*dd*, *J*=8.6, 15.2 Hz) were attributed to the *trans*-olefinic protons H-22 and H-23, respectively, and the other olefinic proton appeared at δ5.18 (*brs*) with assignment to H-7. One oxymethine proton resonated at δ3.62 (*ddd*, *J*=11.1, 6.6 and 4.5 Hz). The large coupling constant (*J*=11.1 Hz) suggested that H-3 was axial (i.e. on the α side of the ring plane).

The ^{13}C NMR spectrum **(Figure 3.29, Table 3.4)** suggested the presence of 29 carbons including six methyls, nine methylenes, eleven methines with one oxymehine and three olefinic methines, and three quaternary carbons.

In the HMBC spectrum **(Figure 3.30, Table 3.4)**, the methyl at δ1.04 (Me-21)

displayed ^{3}J correlations to carbons at δ55.9 (C-17), δ138.2 (C-22) and a ^{2}J correlation to the carbon at δ40.8 (C-20). The proton at δ5.18 (H-22) ^{3}J correlated to the carbon at δ55.9 (C-17), indicating that the side chain in compound **VT1** was linked to the C-17 of the main skeleton. In addition, the methyl at δ0.57 (Me-18) showed ^{3}J couplings to carbons at δ39.5 (C-12), δ55.1 (C-14), δ55.9 (C-17) and a ^{2}J coupling to the carbon at δ43.3 (C-13). The methyl at δ0.82 (Me-19) exhibited ^{3}J correlations to carbons at δ37.2 (C-1), δ40.2 (C-5), δ49.4 (C-9) and a ^{2}J correlation to the carbon at δ34.3 (C-10). The proton at δ1.82 (H-14) displayed correlations to the carbons at δ117.5 (C-7) and δ139.6 (C-8), suggesting a double bond was positioned in C-7. This was also confirmed with ^{3}J correlations between the signal at δ5.18 (H-7) and carbons at δ40.2 (C-5) and δ49.4 (C-9). The signals at δ5.18 (H-22) and δ5.05 (H-23) both coupled to carbons at δ40.8 (C-20) and δ51.2 (C-24), and the former also correlated to a methyl at δ21.4 (C-21) while the latter coupled to a methylene at δ25.4 (C-28), confirming the locations of H-22 and H-23.

The above information suggested the identification of **VT1** as either α-spinasterol or chondrillasterol. The latter differs from α-spinasterol in the stererochemistry at C-24 and differences in C-2, C-4, C-26 and C-27 chemical shifts. The ^{13}C NMR results (**Table 3.5)** obtained for **VT1** were in agreement with published data for α-spinasterol (Ragasa and Lim, 2005) rather than chondrillasterol (Wandji *et al*., 2002). Other NMR data were in agreement with previous reports (Mehrotra *et al*., 1989; Turker and Gurel, 2005). This compound has been isolated from *V. thapsus* fruits (De-Pascual-Teresa *et al*., 1978a), and this is first report from the aerial parts.

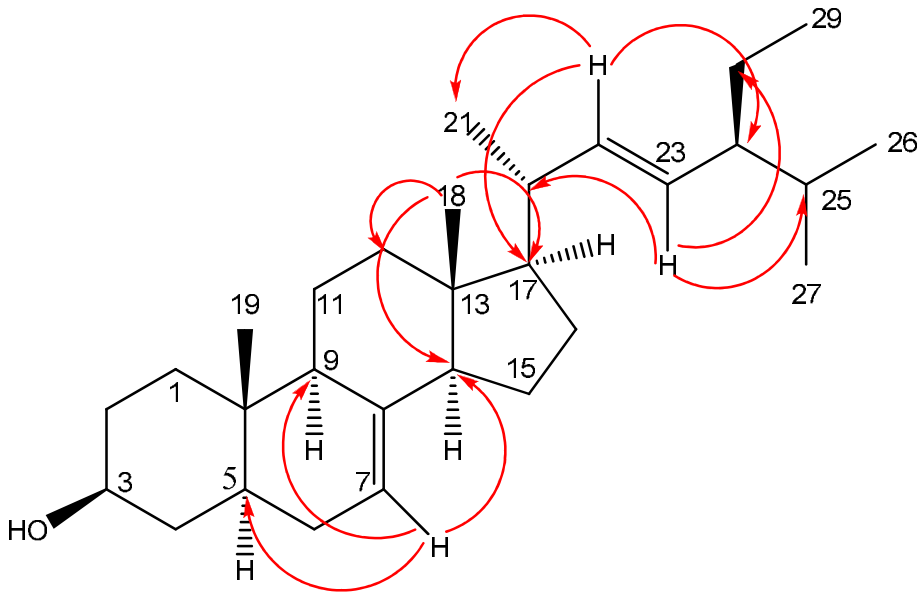

Figure 3.27 Structure of VT1 with selected HMBC correlations

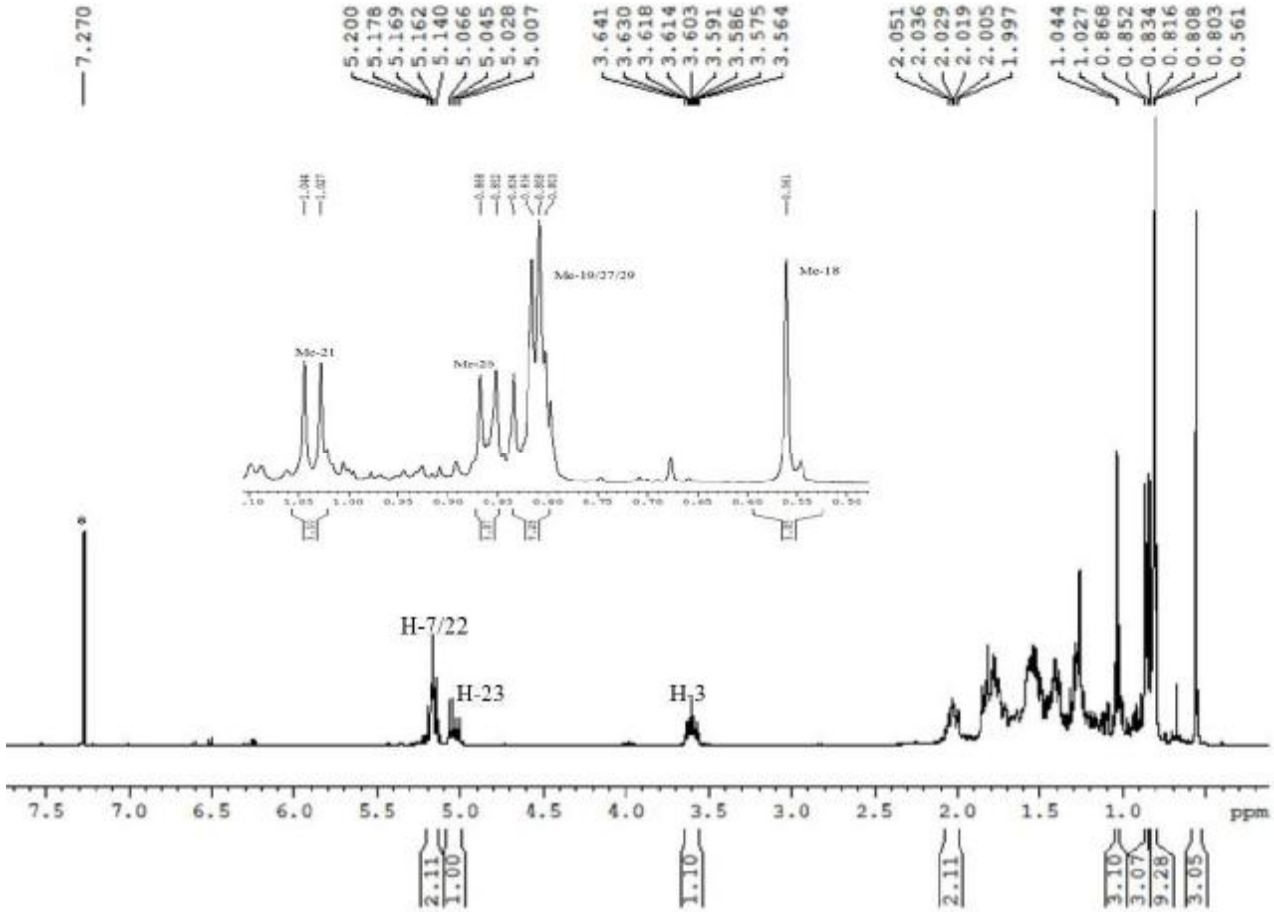

Figure 3.28 ^{1}H NMR spectrum (400 MHz) of VT1 in $CDCl_3$ (*)

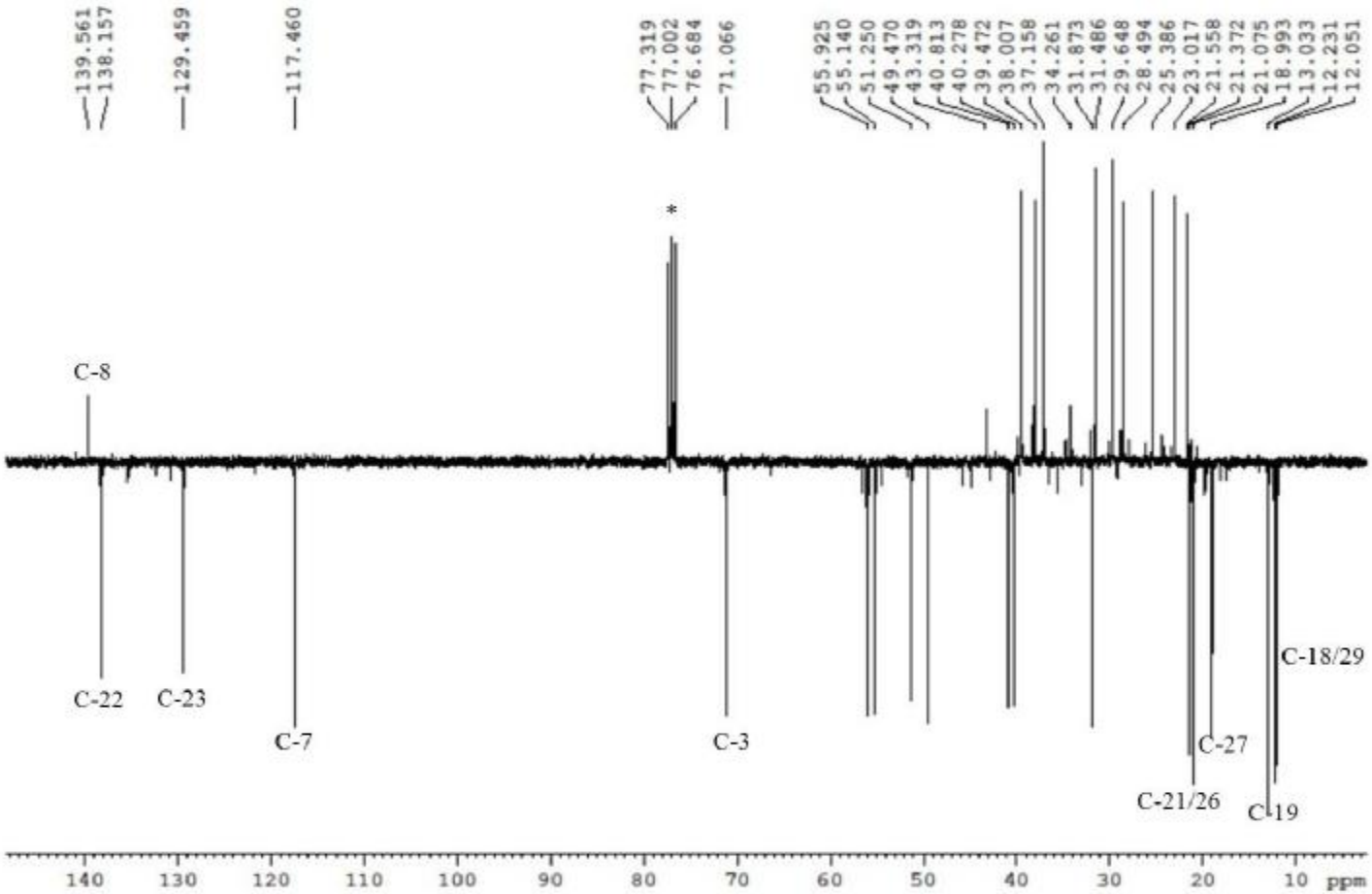

Figure 3.29 DEPTQ 135 ^{13}C NMR spectrum (100 MHz) of VT1 in $CDCl_3$ (*)

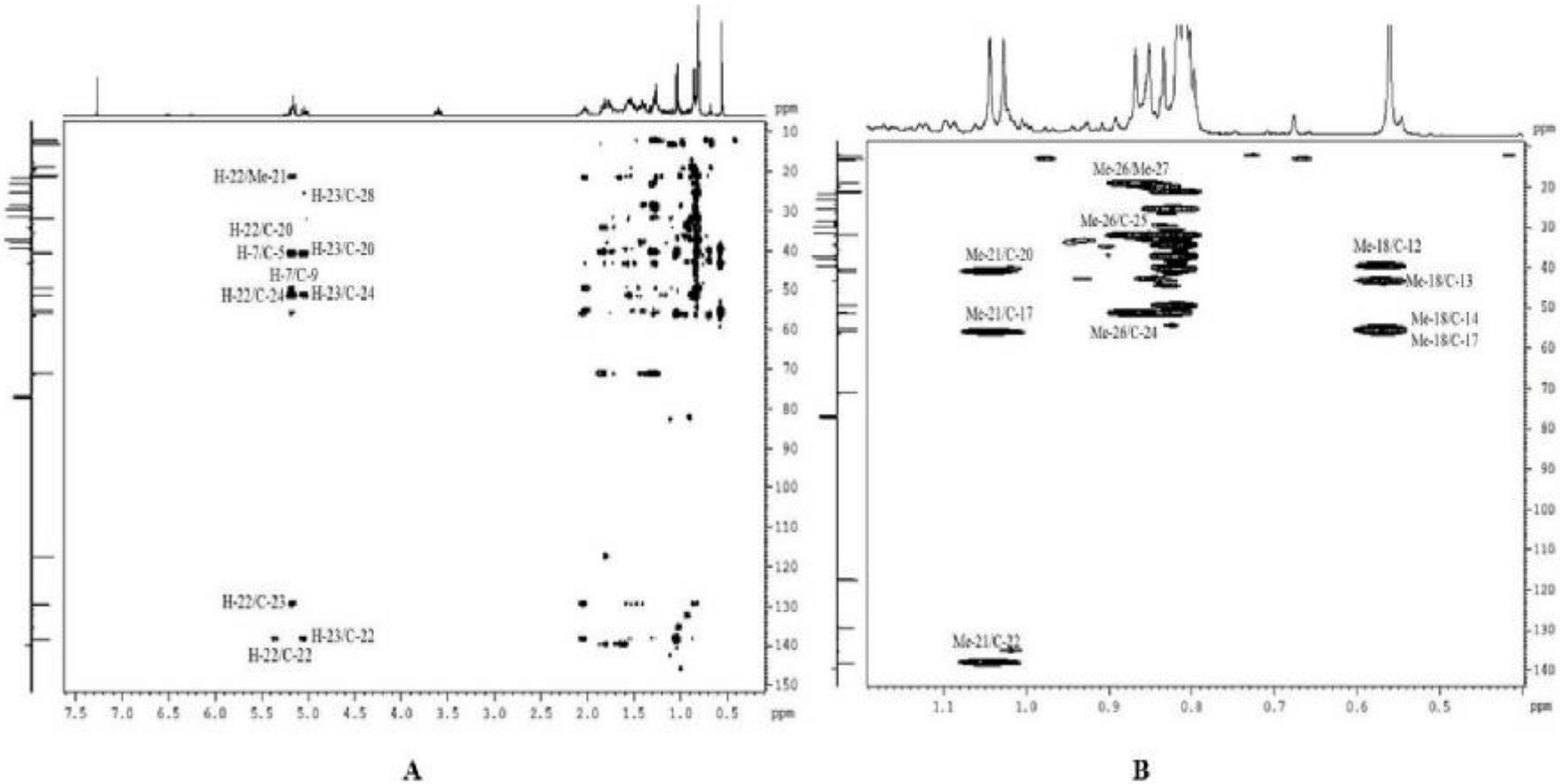

Figure 3.30 HMBC spectra (400 MHz) of VT1 in $CDCl_3$

A: Full HMBC spectrum; B: Selected expansion of HMBC spectrum

Table 3.4 ^{1}H (400 MHz) and ^{13}C NMR (100 MHz) data of VT1 in $CDCl_3$

Position	H (δ)	C (δ)	Selected HMBC correlations
1	1.10 (1H, *m*)/1.84 (1H, *m*)	37.2	
2	1.40 (1H, *m*)/1.81 (1H, *m*)	31.5	
3	3.62 (1H, *ddd*, *J*=11.1, 6.6 and 4.5 Hz)	71.1	
4	1.27 (1H, *m*)/1.73 (1H, *m*)	38.0	C-3, C-6, C-5
5	1.41 (1H, *m*)	40.2	
6	1.27 (1H, *m*)/1.78 (1H, *m*)	29.7	
7	5.18 (1H, *brs*)	117.5	C-5, C-9, C-14, C-6
8	-	139.6	
9	1.66 (1H, *m*)	49.4	
10	-	34.3	
11	1.49 (1H, *m*)/1.58 (1H, *m*)	21.5	
12	1.25 (1H, *m*)/2.01 (1H, *m*)	39.5	
13	-	43.3	
14	1.82 (1H, *m*)	55.1	
15	1.40 (1H, *m*)/1.51 (1H, *m*)	23.0	
16	1.28 (1H, *m*)/1.76 (1H, *m*)	28.6	
17	1.27 (1H, *m*)	55.9	C-13, C-14, C-15, C-20, C-21
18	0.57 (3H, *s*)	12.1	C-12, C-14, C-17, C-13
19	0.82 (3H, *s*)	13.1	C-1, C-5, C-9, C-10
20	2.04 (1H, *m*)	40.8	
21	1.04 (3H, *d*, *J*=6.6 Hz)	21.4	C-17, C-20, C-22
22	5.18 (1H, *dd*, *J*=8.6, 15.1 Hz)	138.2	C-17, C-24, C-21, C-20, C-23
23	5.05 (1H, *dd*, *J*=8.6, 15.2 Hz)	129.5	C-20, C-22, C-24, C-25, C-28
24	1.54 (1H, *m*)	51.2	
25	1.55 (1H, *m*)	31.9	
26	0.86 (3H, *d*, *J*=6.4 Hz)	21.2	Me-27, C-24, C-25
27	0.82 (3H)	19.0	Me-26, C-24, C-25
28	1.18 (1H, *m*)/1.43 (1H, *m*)	25.4	
29	0.83 (3H)	12.3	C-24, C-28

Table 3.5 Comparison of ^{13}C NMR spectral data of compounds VT1, α-spinasterol and chondrillasterol in $CDCl_3$

Position	α-spinasterol (δ, 100 MHz)	chondrillasterol (δ, 75 MHz)	VT1 (δ, 100 MHz)
1	37.2	37.1	37.2
2	31.5	26.1	31.5
3	71.1	71.0	71.1
4	38.0	34.2	38.0
5	40.3	40.2	40.2
6	29.7	29.6	29.7
7	117.5	117.4	117.5
8	139.6	139.6	139.6
9	49.5	49.4	49.4
10	34.2	34.2	34.3
11	21.6	21.5	21.5
12	39.6	39.4	39.5
13	43.3	43.3	43.3
14	55.1	55.1	55.1
15	23.0	23.0	23.0
16	28.5	28.5	28.6
17	55.9	55.9	55.9
18	12.0	12.0	12.1
19	13.0	13.0	13.1
20	40.8	40.8	40.8
21	21.4	21.1	21.4
22	138.1	138.2	138.2
23	129.5	129.4	129.5
24	51.2	51.2	51.2
25	31.9	31.9	31.9
26	21.2	19.0	21.2
27	19.0	21.4	19.0
28	25.4	25.4	25.4
29	12.2	12.2	12.3

3.1.7 Characterisation of AL6/TF8 as daucosterol

AL6 was isolated from the ethyl acetate extract of *A. lappa* **(Section 2.4: Protocol 2, 0.0043% yield)**, and **TF8** was isolated from the ethyl acetate extract of *T. farfara* **(Section 2.4: Protocol 6, 0.0111% yield)**. They both revealed a purple spot on the TLC plate after treatment with anisaldehyde-sulphuric acid reagent followed by heating.

The ^{1}H NMR spectrum **(Figure 3.32, Table 3.6)** indicated the presence of a phytosterol skeleton (Iida *et al*., 1980). It was considered to be β-sitosterol due to the distinctive olefinic signal at δ5.33 (1H, *d*, *J*=4.6 Hz) and six methyl groups at δ0.66 (3H, *s*), δ0.79 (3H, *s*), δ0.81 (3H, *s*), δ0.83 (3H, *s*), δ0.91 (3H, *d*, *J*=6.4 Hz) and δ0.96 (3H, *s*). The multiplicity and *J* values for H-3 were ambiguous because of signal overlapping in the ^{1}H NMR spectrum. However in the HSQC spectrum the cross-correlation peak for H-3/C-3 was relatively stretched (3.38-3.51 ppm or 52 Hz), indicating that H-3 was axial (i.e. on the α side of the ring plane). The proton spectrum also suggested the presence of a sugar unit with an anomeric proton at δ4.22 (1H, *d*, *J*=7.8 Hz) with an H-1'/H-2' *trans*-diaxial configuration. With the aid of HSQC and COSY experiments, the proton signals for a β-D-glucosyl unit were identified.

The ^{13}C NMR assignments **(Table 3.6)** were extracted from the HMBC spectrum. A total of 35 carbons were identified including the anomeric carbon at δ101.4 (C-1') and olefinic carbons at δ121.7 (C-6) and δ 140.9 (C-5). In the HMBC spectrum **(Figure 3.33, Table 3.6)**, the anomeric proton at δ4.22 (H-1') displayed ^{3}J coupling to the methine carbon at δ77.3 (C-3), and other correlations included Me-18 to C-12, C-13, C-14, C-17; Me-19 to C-1, C-9 and Me-21 to C-20, C-22, C-17.

The presence of the glucose moiety was also confirmed from the positive ion mode HRESI-MS experiment. The data revealed a base peak at *m/z* 397.3830 attributable to the fragment ion $[M-C_6H_{12}O_6+H]^+$ and another ion peak at *m/z* 181.0632 for the fragment $[C_6H_{12}O_6+H]^+$, thus indicating a molecular formula of $C_{35}H_{60}O_6$ (DBE=6).

The above information identified **AL6/TF8** as daucosterol and the NMR data were in good agreement with previous reports (Lee *et al*., 2002; Saxena and Albert, 2005; Saeidnia *et al*., 2011).This compound has been isolated from *A. lappa* seeds and roots (Mizushina *et al*., 2006) and *T. farfara* flower buds (Wu *et al*., 2008). This is the first report in *A. lappa* aerial parts.

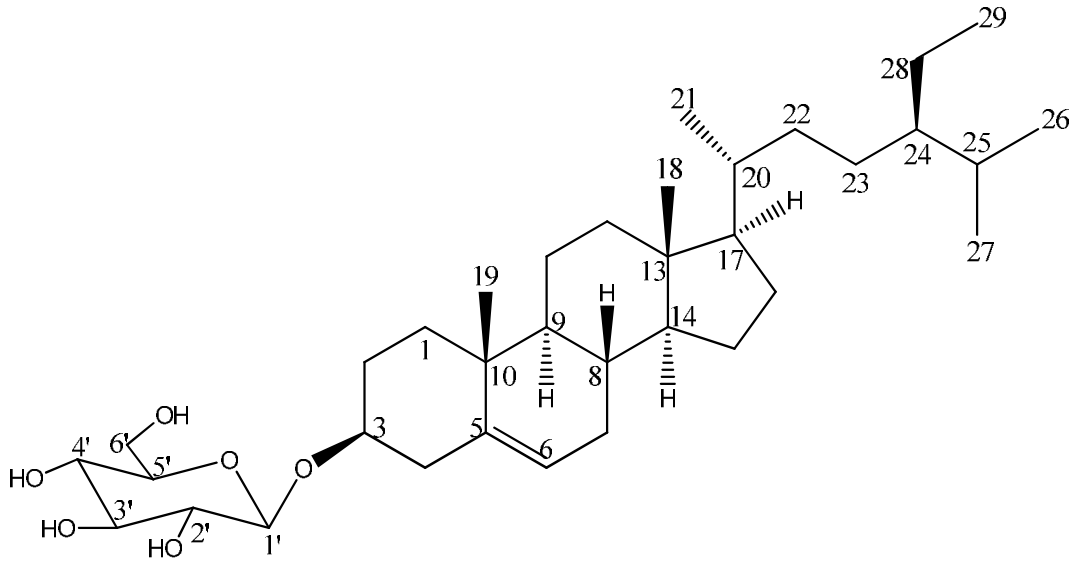

Figure 3.31 Structure of AL6/TF8

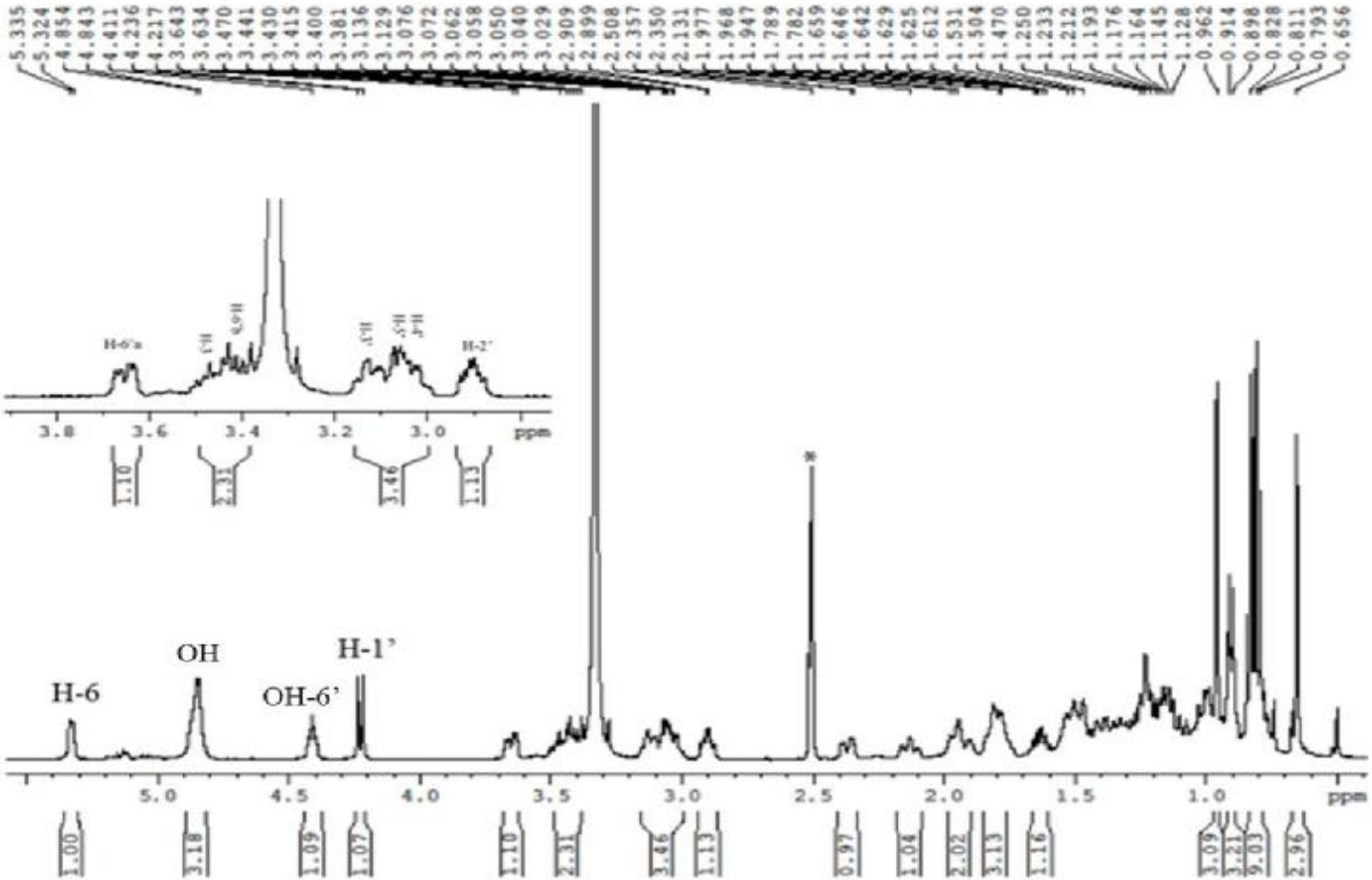

Figure 3.32 ^{1}H NMR spectrum (400 MHz) of AL6/TF8 in DMSO-d_6 (*)

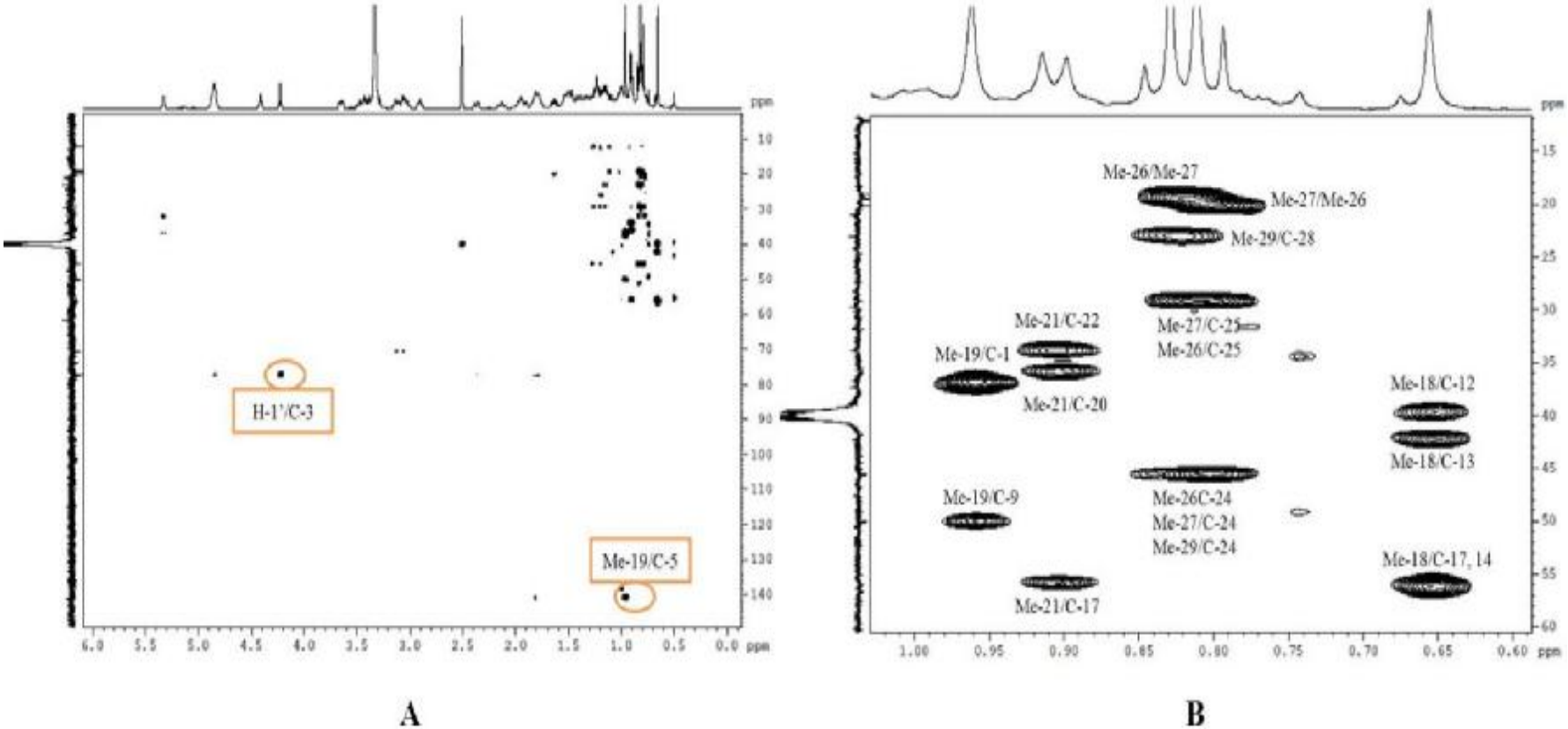

Figure 3.33 HMBC spectra (400 MHz) of AL6/TF8 in DMSO-d_6

A: Full HMBC spectrum; B: Selected expansion of HMBC spectrum

Table 3.6 ^{1}H (400 MHz) and ^{13}C NMR (100 MHz) data of AL6/TF8 in DMSO-d$_6$

Position	H (δ)	C (δ)	Selected HMBC correlations
1	1.00 (1H, *m*)/1.79 (1H, *m*)	37.3	C-3
2	1.48 (2H, *m*)	29.6	
3	3.46 (1H, *m*, *J*>10 Hz)	77.2	C-1’
4	2.13 (1H, *m*)/2.36 (1H, *m*)	38.6	C-3, C-6, C-5
5	-	140.9	
6	5.33 (1H, *d*, *J*=4.6 Hz)	121.7	C-8
7	1.92 (2H, *m*)	31.9	
8	1.39 (1H, *m*)	31.9	
9	0.88 (1H, *m*)	50.1	
10	-	36.6	
11	1.39 (1H, *m*)/1.50 (1H, *m*)	21.1	
12	1.14 (1H, *m*)/1.95 (1H, *m*)	39.6	
13	-	41.0	
14	1.09 (1H, *m*)	55.9	
15	1.03 (1H, *m*)/1.54 (1H, *m*)	24.3	
16	1.80 (1H, *m*)/1.54 (1H, *m*)	28.2	
17	0.98 (1H, *m*)	56.6	C-12, C-13, C-14, C-17
18	0.66 (3H, *s*)	12.2	C-1, C-9
19	0.96 (3H, *s*)	19.4	
20	1.34 (1H, *m*)	35.8	
21	0.91 (3H, *d*, *J*=6.4 Hz)	19.1	C-17, C-20, C-22
22	1.00 (1H, *m*)/1.31 (1H, *m*)	33.9	
23	1.16 (2H, *m*)	25.9	
24	0.91 (1H, *m*)	45.7	
25	1.63 (1H, *m*)	29.2	
26	0.81 (3H, *s*)	12.2	Me-27, C-24, C-25
27	0.79 (3H, *s*)	19.2	Me-26, C-24, C-25
28	1.48 (1H, *m*)/1.81 (1H, *m*)	29.7	
29	0.83 (3H, *s*)	20.3	C-24, C-28
1’	4. 22 (1H, *d*, *J*=7.8 Hz)	101.4	C-3
2’	2.90 (1H, *m*)	73.8	
3’	3.14 (1H, *m*)	77.1	
4’	3.03 (1H, *m*)	70.5	
5’	3.06 (1H, *m*)	77.1	
6’	3.42 (1H, *m*)/3.65 (1H, *m*)	61.6	

3.1.8 Characterisation of AL2/TF1 as a mixture of β-sitosterol (a) and stigmasterol (b)

AL2 was isolated from the *n*-hexane extract of *A. lappa* as white solid **(Section 2.4: Protocol 1, 0.0044% yield)**, and **TF1** was isolated from the *n*-hexane extract of *T. farfara* **(Section 2.4: Protocol 5, 0.0100% yield)**. They both revealed a purple spot after treatment with anisaldehyde-sulphuric acid reagent and heating.

The ^{1}H NMR spectrum **(Figure 3.34)** demonstrated a signal at δ5.36 (2H) attributed to the olefinic protons H-6 of sitosterol (a) and stigmasterol (b). Two signals at δ5.15 and δ5.05 were assigned to the olefinic protons H-22 and H-23 of stigmasterol (b). A signal at δ3.55 (2H) was assigned to the oxymethine protons H-3 of sitosterol (a) and stigmasterol (b). The spectrum also showed two singlets at δ1.01 and δ0.69 attributable to Me-19 and Me-18, respectively, and four doublets at δ0.93 (Me-21), δ0.85 (Me-26), δ0.83 (Me-29) and δ0.81 (Me-27).

The ^{13}C NMR **(Figure 3.35)** displayed some distinctive signals at δ140.8 (C-5) and 121.8 (C-6). Two other signals at δ138.4 and δ129.1 were assigned to C-22 and C-23 of stigmasterol (b), respectively. A carboxymethine, attributable to C-3, was observed at δ71.9. The remaining carbon signals presented chemical shifts between δ11 and δ57, including the C-22 and C-23 of β-sitosterol (a) at δ34.0 and δ26.1, respectively.

Based on the above data and by comparion with previous reports (Wright *et al.*, 1978; Pateh *et al.*, 2008), **AL2/TF1** was characterised as a mixture of β-sitosterol and stigmasterol in a 1:1 ratio, because the integration of protons at δ5.36 (H-6), δ5.15 (H-22), δ5.05 (H-23) and δ3.55 (H-3) were found ratioed at 2:1:1:2. β-Sitosterol has been previously reported from *A. lappa* seeds (Ming *et al*., 2004) and *T. farfara* flower buds (Wu *et al*., 2008).

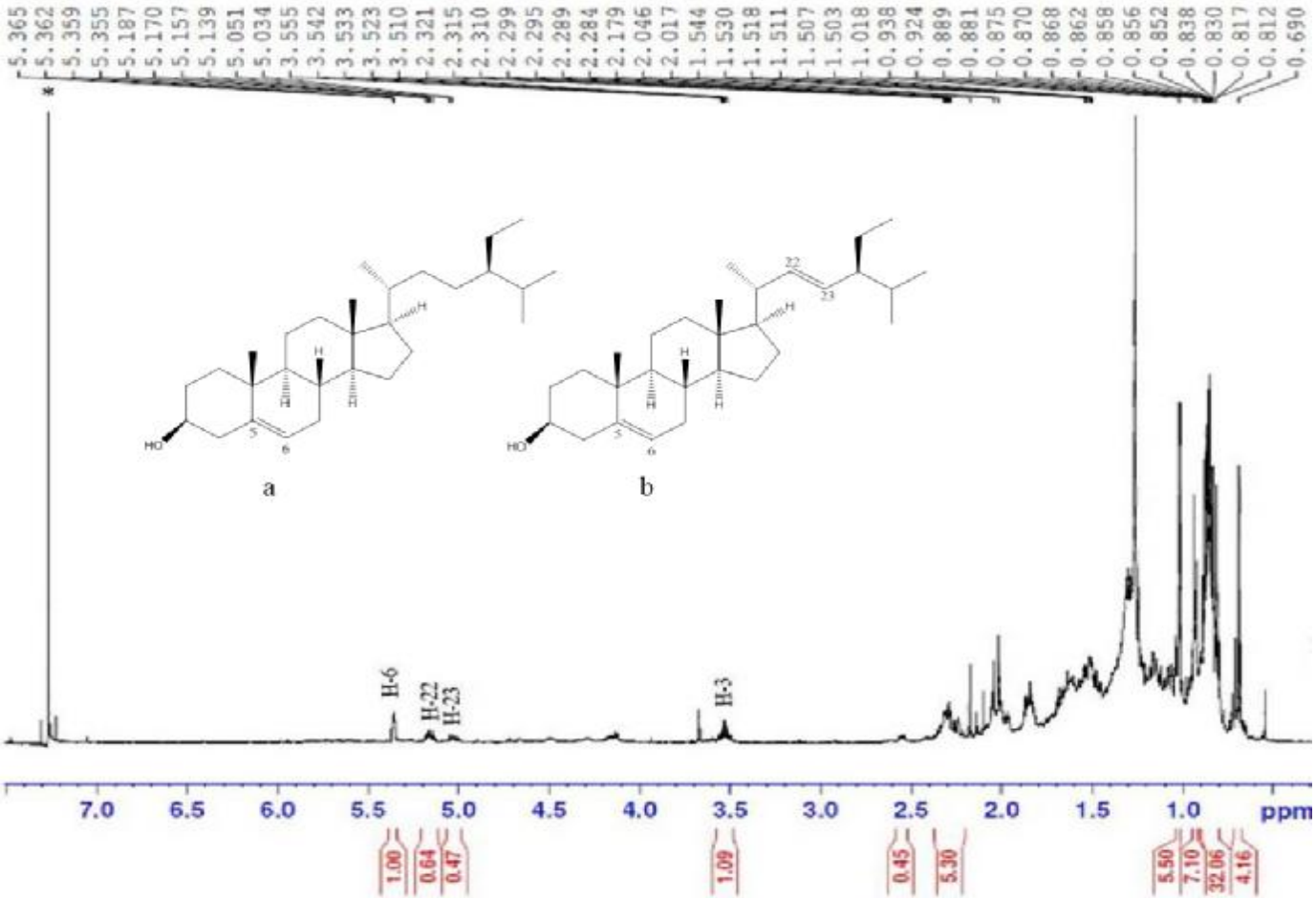

Figure 3.34 ^{1}H NMR spectrum (400 MHz) of AL2/TF1 in $CDCl_3$ (*)

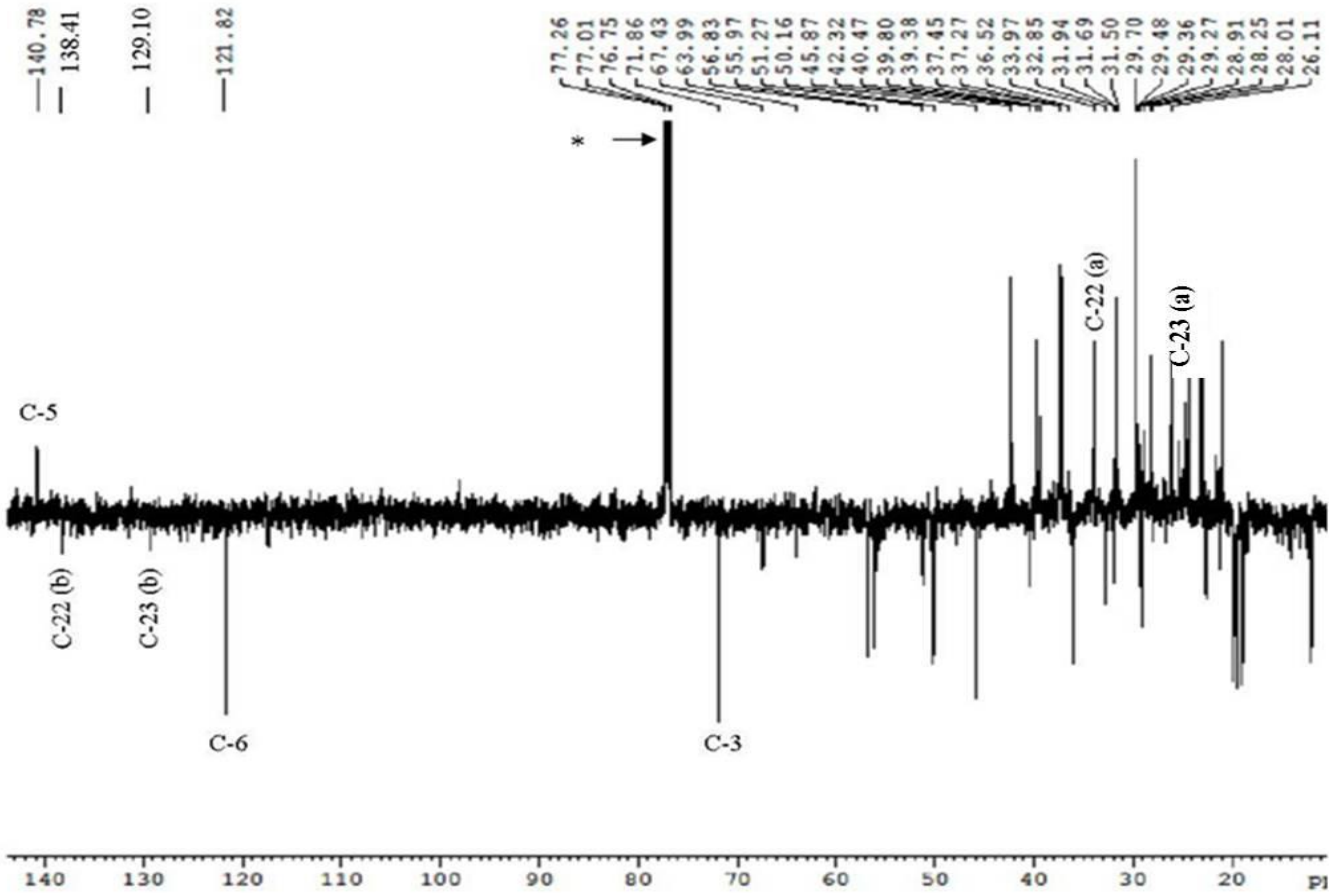

Figure 3.35 DEPTQ 135 ^{13}C NMR spectrum (400 MHz) of AL2/TF1 in $CDCl_3$ (*)

3.2 Pheophorbides and pheophytins

3.2.1 Common spectroscopic features

These compounds were isolated from the ethyl acetate extract of *V. thapsus* as dark-green or black amorphous solids **(Section 2.4: Protocol 9; VT3 0.0044% yield, VT6 0.0035% yield, VT7 0.0010% yield, VT10 0.0045% yield)**. They gave a quenching spot under short UV light and a red fluorescence under long UV. The spot turned green to yellowish-green when treated with vanillin-sulphuric acid reagent and heating.

The ^{1}H NMR spectra **(Table 3.7 and 3.9, Figure 3.37 and 3.38)** revealed three proton singlets in the region of δ8.50~10.10 and a fourth singlet at around δ6.30. They also showed two multiplets between δ6.15 and δ6.30 and another one at around δ7.90 accounting for a -CH=CH_2 group. In the region of δ3.00~4.00, some sharp singlets were observed for methyl or methoxy groups, and some methyl singlets were also detected between δ1.60 and δ1.90.

The ^{13}C NMR spectra **(Table 3.7 and 3.9, Figure 3.39 and 3.40)** displayed four olefinic methines between δ90.0 and δ130.0, one olefinic methylene at around δ123.0, three methines and one methoxy in the region of δ50.0~65.0, and some methyls between δ10.0 and δ25.0. The spectra also exhibited three methylenes between δ19.0 and δ35.0, and some carbonyls were observed in the region of δ165.0~190.0.

3.2.2 Characterisation of VT3 as pheophorbide A

The positive ion mode HRESI-MS data for **VT3** gave a quasi-molecular ion $[M+H]^+$

at *m/z* 593.2750, suggesting a molecular fomula of $C_{35}H_{36}O_5N_4$ (DBE=19).

The ^{1}H NMR spectrum **(Table 3.7, Figure 3.37)** exhibited four protons as singlets at δ9.43, δ9.27, δ8.56 and δ6.27. It also displayed a deshielded methine at δ7.90 (1H, *dd*, *J*=11.5, 17.8 Hz), two methines at δ4.23 (1H, *brd*, *J*=8.7 Hz) and δ4.48 (1H, *br d*, *J*=7.2 Hz), and three methylenes at δ3.60 (2H, *m*), δ2.28 (1H, *m*)/δ2.65 (1H, *m*) and δ2.32 (1H, *m*)/δ2.59 (1H, *m*), and one exomethylene at δ6.23 (1H, *d*, *J*=17.8 Hz)/δ6.15 (1H, *d*, *J*=11.5 Hz). Three methyl singlets at δ3.66, δ3.37 and δ3.16 and one methoxy singlet at δ3.90 were also observed. Another two methyls were detected upfield at δ1.84 (3H, *d*, *J*=7.3 Hz) and δ1.66 (3H, *t*, *J*=3.6 Hz).

In the COSY spectrum **(Figure 3.41)**, a cross peak between the methine at δ7.90 and the exomethylene at δ6.23/δ6.15 was observed, suggesting the presence of a -CH=CH_2 group. The methylene protons at δ3.60 revealed correlations to a methyl triplet at δ1.66, which established the presence of a -CH_2CH_3 group. The methine at δ4.48 correlated to the methyl doublet at δ1.84, and correlations between the methine at δ4.23 and the methylene at δ2.28/δ2.65 were also observed.

The ^{13}C NMR spectrum **(Table 3.7, Figure 3.39)** of **VT3** demonstrated 35 carbons including five methyls, one methoxy at δ52.9, seven methines including four olefinic carbons at δ129.0, δ97.5, δ104.4 and δ93.1, three methylenes at δ19.4, δ29.7 and δ30.9, one exomethylene at δ122.7 and eighteen quaternary carbons including three carbonyls at δ189.8, δ177.7 and δ169.7.

In the HMBC spectrum **(Table 3.8)**, the singlet at δ9.43 (H-10) displayed ^3J correlations to quaternary carbons at δ145.2 (C-8) and δ128.8 (C-12). Two methyls at δ1.66 (Me-8^2) and δ3.16 (Me-7^1) also correlated via ^3J couplings to C-8. Another

methyl at δ3.66 (Me-12^1) coupled to C-12. The methyl (Me-8^2) also showed a ^2J correlation to the methylene at δ19.4 (C-8^1), establishing that the -CH_2CH_3 group was attached in C-8. The singlet at δ8.56 (H-20) revealed ^3J couplings to a quaternary carbon at δ131.9 (C-2) and a methine at δ50.2 (C-18). Two methyls at δ3.37 (Me-2^1) and δ1.84 (Me-18^1) correlated to the quaternary carbon at δ131.9 (C-2) and the methine at δ50.2 (C-18), respectively. The proton at δ7.90 (H-3^1) revealed ^3J and ^2J correlations, respectively, to the quaternary carbons at δ131.9 (C-2) and δ136.1 (C-3), establishing that the -CH=CH_2 group was attached to C-3. The singlet at δ6.27 (H-13^2) ^3J correlated to quaternary carbons at δ128.9 (C-13) and δ149.7 (C-14), and ^2J coupled to carbonyls at δ189.8 (C-13^1) and δ169.7 (C-13^3) and a quaternary carbon at δ105.1 (C-15). A ^3J correlation between the methoxy at δ3.90 and the carbonyl at δ169.7(C-13^3) established the assignment of the methoxy group as MeO-13^4. The proton at δ4.48 (H-18) revealed ^3J and ^2J couplings, respectively, to a methylene at δ29.7 (C-17^1) and a methine at δ51.1 (C-17); the proton at δ4.23 (H-17) displayed ^3J correlation to another methylene at δ30.9 (C-17^2); the methylene protons at δ2.28/δ2.65 (H-17^1a/b) correlated via ^3J coupling to the carbonyl at δ177.7 (C-17^3). This established the presence of a -CH_2CH_2COOH side-chain in C-17.

In the NOESY spectrum **(Figure 3.42)**, a more intense cross peak between the singlet at δ6.27 (H-13^2) and the methylene protons at δ2.28/δ2.65 (H-17^1a/b) was observed compared to the less intense cross peak between H-13^2 and the methine proton at δ4.23 (H-17), which indicated a compound with H-13^2 and H-17^1 located on the same side of the plane (Lai *et al*., 2010). In addition, the methine at δ4.23 (H-17) correlated to the methyl at δ1.84 (Me-18^1) suggesting H-17 and Me-18^1 were on the other side of the plane.

On the basis of above information, **VT3** was identified as pheophorbide A. The NMR

data were in good agreement with pulished data for this compound (Hargus *et al*., 2007; Lai *et al*., 2010). This is the first report of the isolation of pheophorbide A from *V. thapsus*.

3.2.3 Characterisation of VT10 as pheophorbide A ethyl ester

The positive ion mode HRESI-MS data for **VT10** gave a quasi-molecular ion $[M+H]^+$ at *m/z* 621.3065, indicating a molecular fomula of $C_{37}H_{40}O_5N_4$ (DBE=19).

The ^{1}H NMR spectrum **(Table 3.7, Figure 3.37)** was similar to the data obtained for **VT3**, suggesting another pheophorbide template with three highly deshielded protons at δ9.39 (1H, *s*, H-10), δ9.21 (1H, *s*, H-5) and δ8.57 (1H, *s*, H-20) and a singlet at δ6.31 (1H, *s*, H-13^2). The main difference was the presence of two signals identified as an oxymethylene at δ4.08 (2H, *m*) and a methyl at δ1.16 (3H, *t*, *J*=7.1 Hz). The COSY spectrum established that these two signals coupled with each other, suggesting the presence of an $-OCH_2CH_3$ group.

The ^{13}C NMR spectrum **(Table 3.7, Figure 3.39)** revealed 37 carbons. Two extra carbons ccompared to **VT3** were found at δ60.7 and δ14.2, further confirming the presence of an $-OCH_2CH_3$ group. All other carbon chemical shifts were in agreement with the data obtained for **VT3** except that the carbonyl shift was found at δ173.1 rather than δ177.7, strongly suggesting that the carbon was esterified by the the $-OCH_2CH_3$ group.

Selected HMBC correlations are shown in **Table 3.8**. A ^3J correlation between the methylene at δ2.37/δ2.68 (H-17^{1}a/b) and the carbonyl at δ173.1 was observed. The methyl group at δ1.16 (Me-17^5) coupled to the carbon at δ60.7 (C-17^4). The oxymethylene at δ4.08 (H-17^4) displayed a ^3J correlation to the carbonyl at δ173.1.

This confirmed that the -OCH_2CH_3 group was attached to the carbonyl at δ173.1 (C-17^3).

The NOESY results for **VT10 (Figure 3.42)** were similar to those obtained for **VT3**. A more intense correlation between H-13^2 at δ6.31 and H-17^1a/b at δ2.37/δ2.68 was observed compared to the less intense correlation between the H-13^2 and H-17 at δ4.25, thus H-13^2 and H-17^1 were on the same side of the plane.

Based on the above information and by comparison with the data obtained for **VT3**, **VT10** was identified as pheophorbide A ethyl ester. The NMR results were in good agreement with pulished data for this compound (Nakamura *et al*., 1996; Wongsinkongman *et al*., 2002). Pheophorbide A ethyl ester is reported for the first time in *V. thapsus*.

3.2.4 Characterisation of VT6 as pheophytin A

The positive ion mode HRESI-MS data for **VT6** gave a quasi-molecular ion $[M+H]^+$ at *m/z* 871.5715, indicating a molecular fomula of $C_{55}H_{74}O_5N_4$ (DBE=20).

The ^{1}H NMR spectrum **(Table 3.9, Figure 3.38)** demonstrated some similar features to the data obtained for **VT3** and **VT10**, suggesting the presence of a pheophorbide derivative with three highly deshielded protons at δ9.52 (1H, *s*, H-10), δ9.38 (1H, *s*, H-5) and δ8.58 (1H, *s*, H-20) and another three deshielded signals at δ6.00~8.00 for H-3^1, H-3^2 and H-13^2, respectively. In addition, an oxymethylene multiplet at δ4.50, a triplet at δ5.16 assigned as an olefinic proton attached to a methylene and some methyl signals at δ0.81 (6H, *d*), δ0.87 (6H, *d*) and δ1.60 (3H, *s*) were observed, suggesting the presence of a phytol group.

The ^{13}C NMR spectrum **(Table 3.9, Figure 3.40)** displayed a total of 55 carbons. 35 carbons were similar to those in **VT3** with a carbonyl at δ173.0 (C-17^3) in **VT6**, suggesting an esterified position. The other 20 carbons could be attributed to the phytol moiety with one olefinic methine (δ117.7), one oxymethylene (δ61.5), five methyls (δ16.3, δ19.6, δ19.7, δ22.6 and δ22.7), nine methylenes (three at δ24.00~25.00, four at δ36.50~37.50 and two at δ39.4 and δ39.8), and three methines (δ28.0, δ32.6 and δ32.7) as well as one quaternary carbon (δ142.9).

The HMBC spectrum **(Table 3.10)** gave all typical correlations as in **VT3** and **VT10** confirming the presence of a pheophorbide derivative. The oxymethylene protons of the phytol group at δ4.50 showed a ^3J correlation to the carbonyl at δ173.0, establishing the position of the phytol moiety in C-17^3.

The above information as well as comparison with the data obtained for **VT3** and **VT10** led to the characterisation of **VT6** as pheophytin A. The NMR data were in good agreement with published data of this compound (Hargus *et al*., 2007; Fang and Xu, 2008). This is the first report of the isolation of pheophytin A from of *V. thapsus*.

3.2.5 Characterisation of VT7 as pheophytin B

The positive ion mode HRESI-MS data for **VT7** revealed a quasi-molecular ion $[M+H]^+$ at *m/z* 885.5508, indicating a molecular fomula of $C_{55}H_{72}O_6N_4$ (DBE=21).

The ^1H NMR spectrum **(Table 3.9, Figure 3.38)** was similar to the data obtained for **VT6**, suggesting a pheophorbide derivative with a phytol moiety. The main difference was that there were four deshielded protons at δ10.86 (1H, *s*), δ10.04 (1H, *s*), δ9.27 (1H, *s*) and δ8.54 (1H, *s*) instead of three in **VT6**, and two methyls instead of three at δ3.00~4.00. Altogether, this suggested that one of the methyls had been

substituted by a CHO group in **VT7**.

The ^{13}C NMR spectrum **(Table 3.9, Figure 3.40)** revealed 55 carbons as in **VT6**. However, some of the observed chemical shifts were different. The main difference was that one additional highly-deshielded methine was detected at δ187.4, establishing the presence of an aldehyde group. Additionally, the methyl at δ11.3 (observed in **VT6)** was not observed in **VT7**.

The HMBC correlations **(Table 3.10)** were similar to those obtained for **VT6**. The extra deshielded proton at δ10.86 (H-7^1) instead of the methyl at δ3.23 (Me-7^1) in **VT6** ^3J correlated to the quaternary carbon at δ150.7 (C-6), establishing that the CH_3 group attached in C-7 in **VT6** was substituted by a CHO group in **VT7**.

On the basis of the above data and by comparison with the data obtained for **VT6**, **VT7** was identified as pheophytin B. The NMR data were in agreement with a previous report (Fang and Xu, 2008). Pheophytin B is reported from *V. thapsus* for the first time.

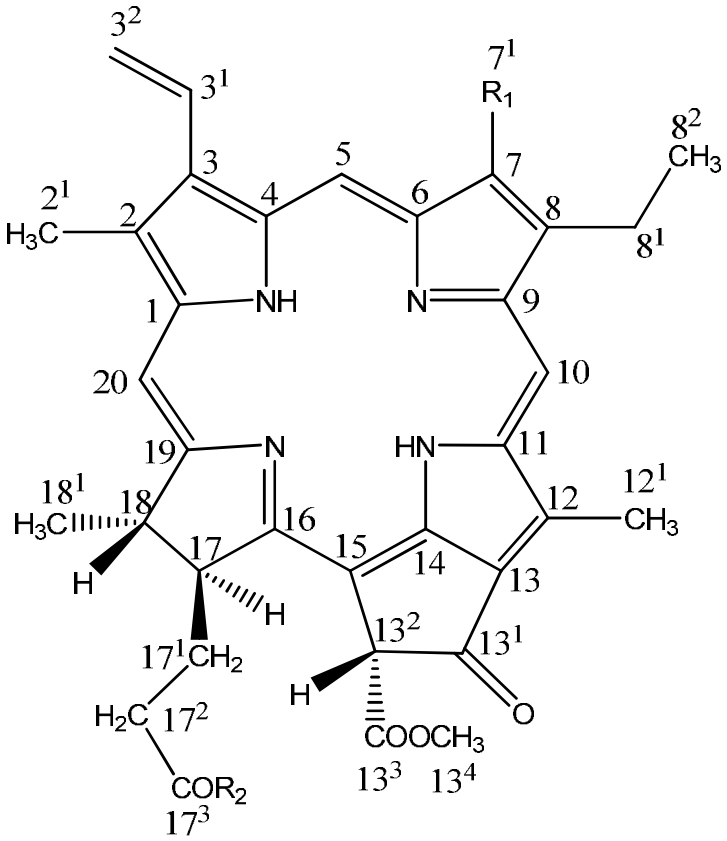

Phytol=

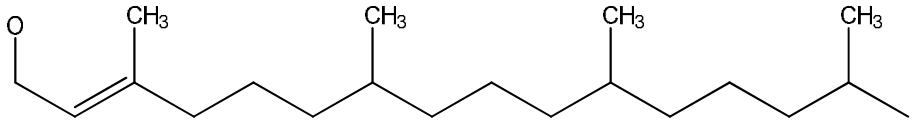

R_1=CH_3, R_2=OH, Pheophorbide A (**VT3**)

R_1=CH_3, R_2=OCH_2CH_3, Pheophorbide A ethyl ester (**VT10**)

R_1=CH_3, R_2=Phytol, Pheophytin A (**VT6**)

R_1=CHO, R_2=Phytol, Pheophytin B (**VT7**)

Figure 3.36 Structures of VT3, VT10, VT6 and VT7

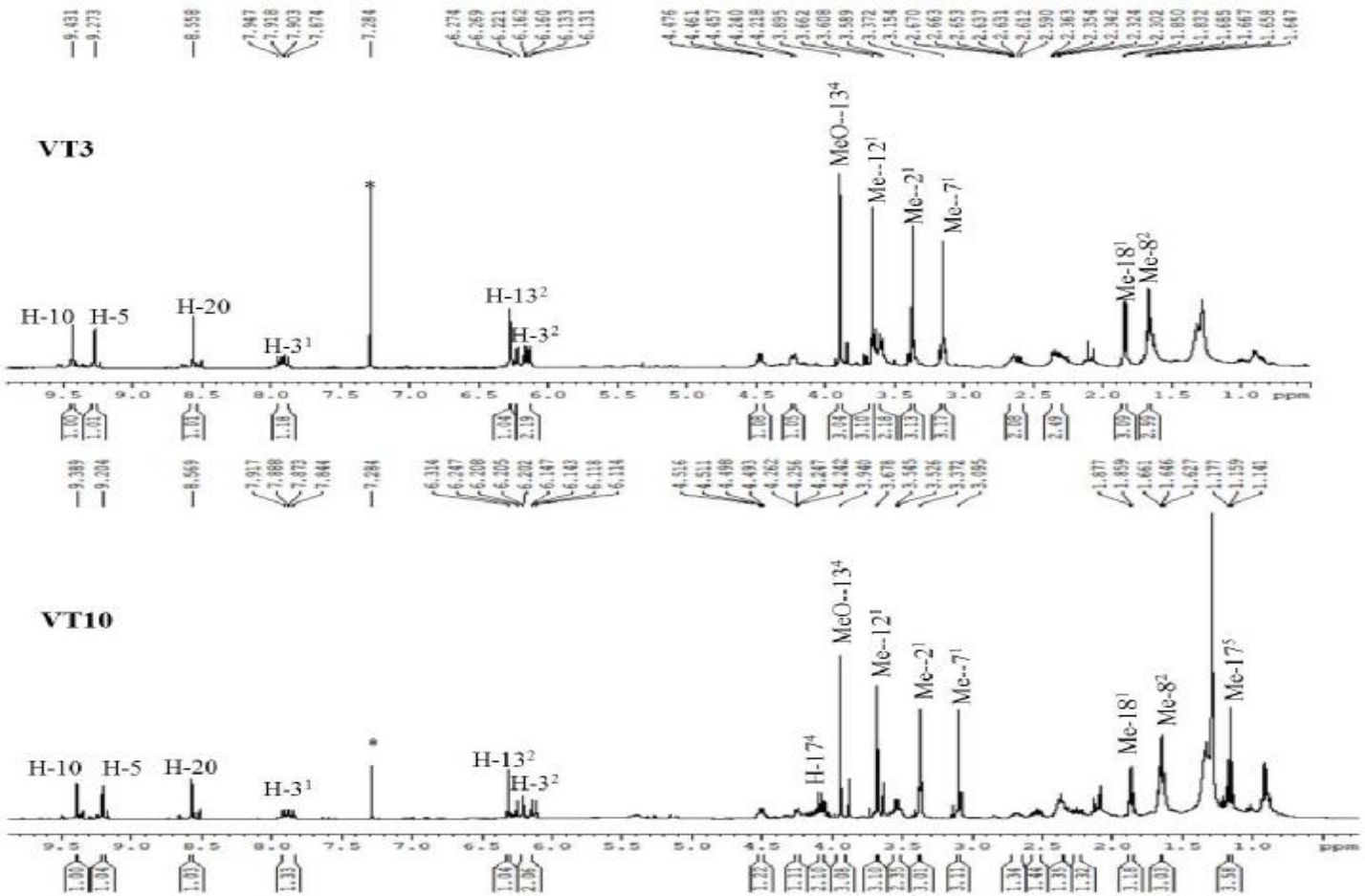

Figure 3.37 ^{1}H NMR spectra (400 MHz) of VT3 and VT10 in $CDCl_3$ (*)

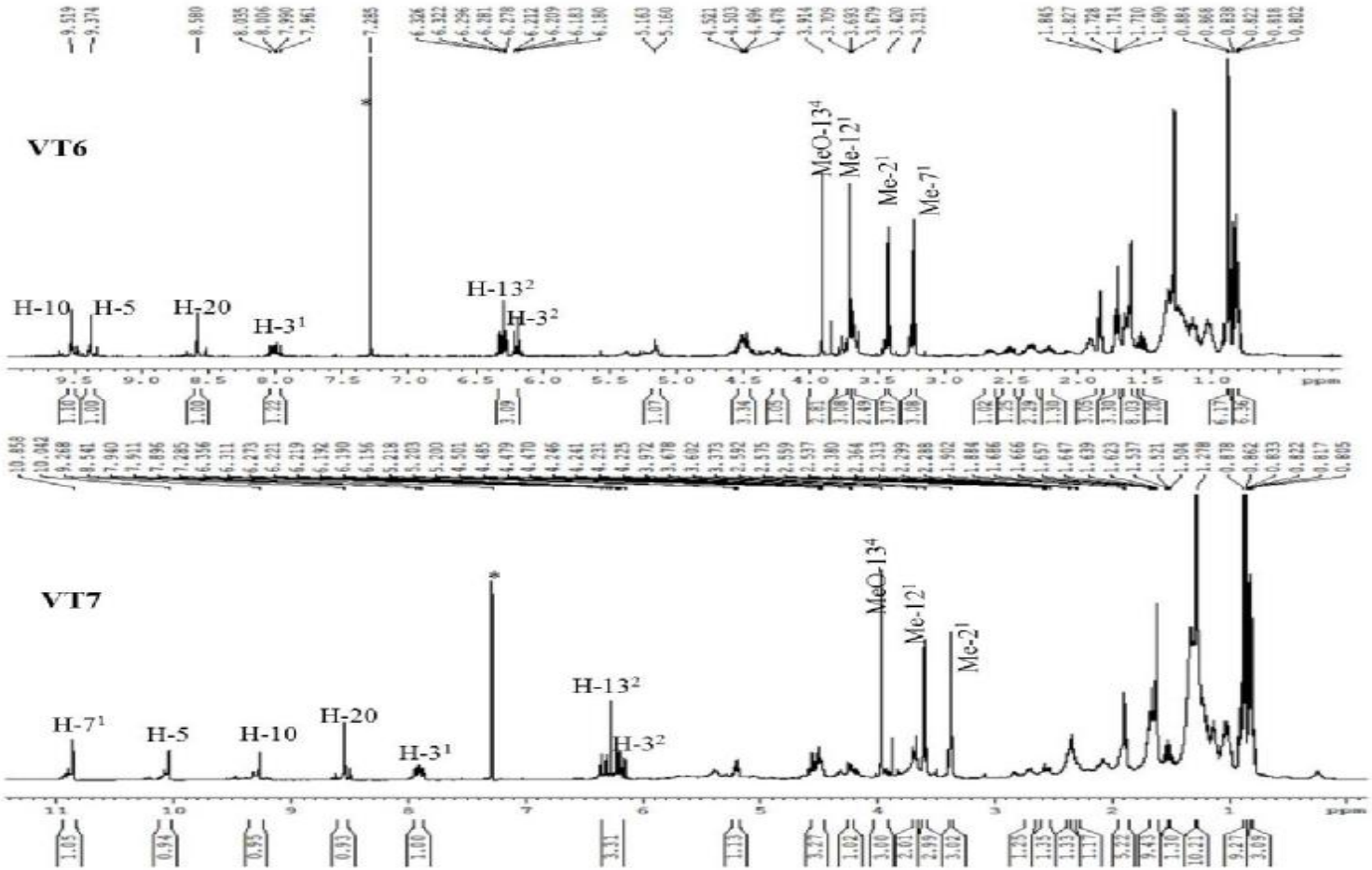

Figure 3.38 ^{1}H NMR spectra (400 MHz) of VT6 and VT7 in $CDCl_3$ (*)

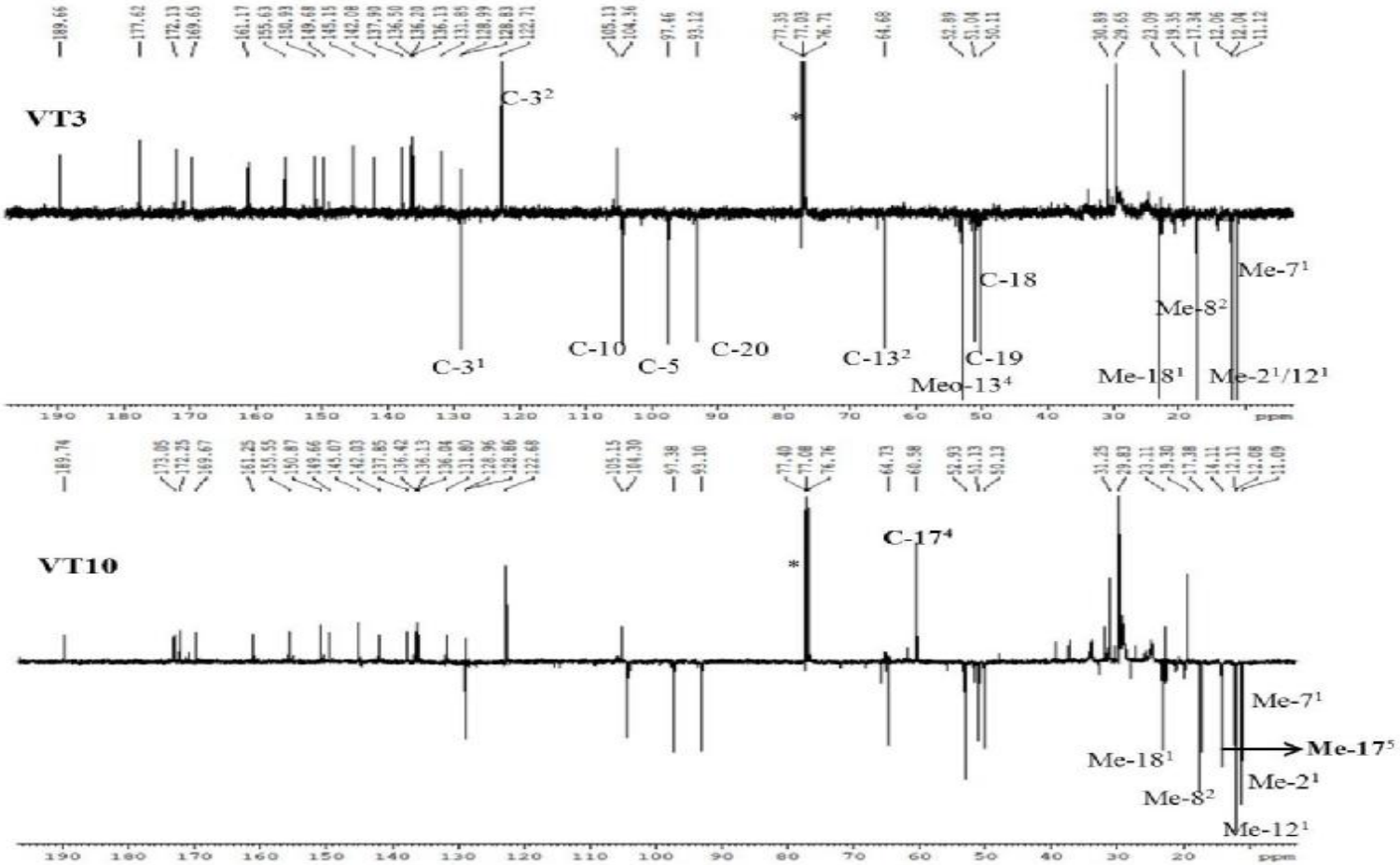

Figure 3.39 DEPTQ 135 ^{13}C NMR spectra (100 MHz) of VT3 and VT10 in $CDCl_3$ (*)

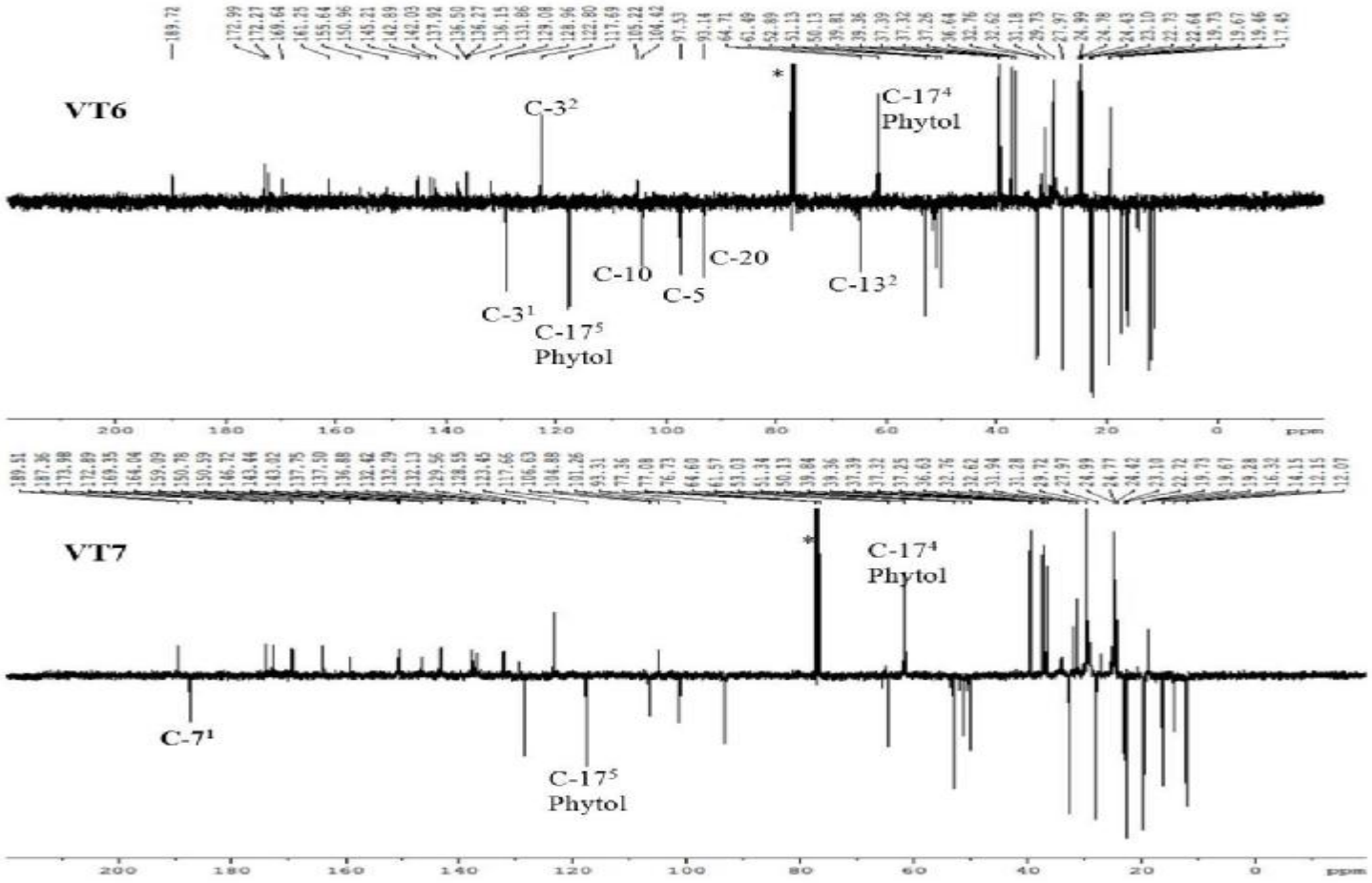

Figure 3.40 DEPTQ 135 ^{13}C NMR spectra (100 MHz) of VT6 and VT7 in $CDCl_3$ (*)

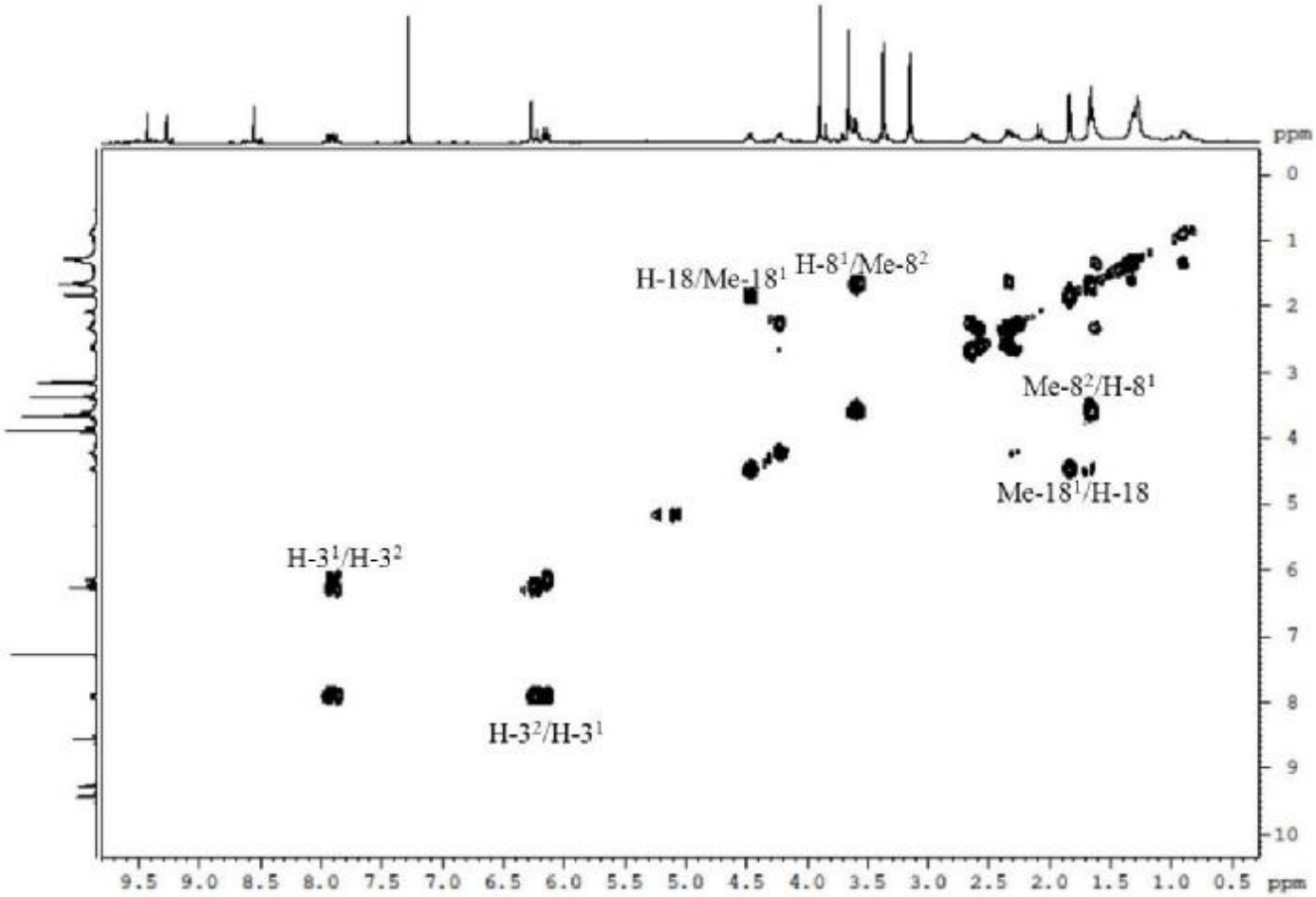

Figure 3.41 COSY spectrum (400 MHz) of VT3 in $CDCl_3$

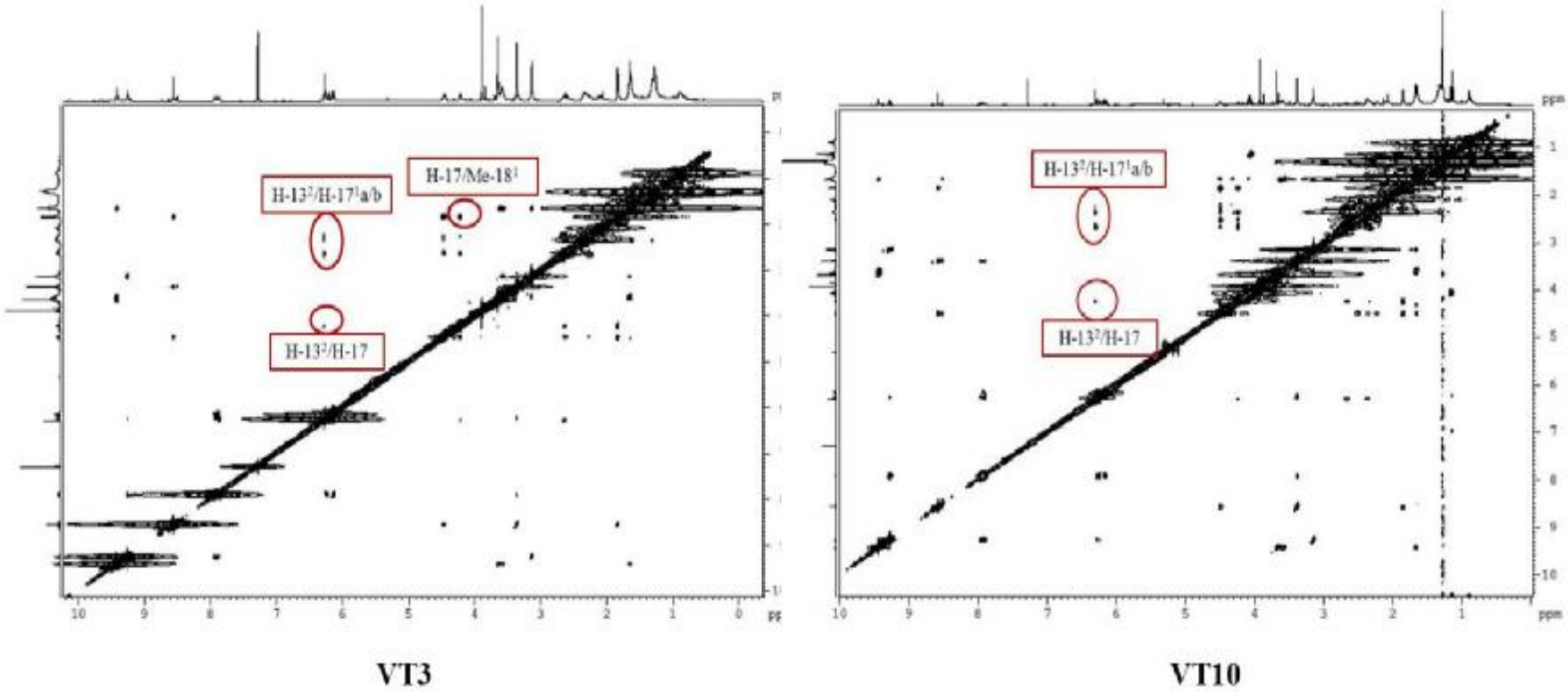

Figure 3.42 NOESY spectra (400 MHz) of VT3 and VT10 in $CDCl_3$

Table 3.7 ^{1}H (400 MHz) and ^{13}C NMR (100 MHz) data of VT3 and VT10 in $CDCl_3$

	VT3		VT10	
Position	**H (δ)**	**C (δ)**	**H (δ)**	**C (δ)**
1	-	142.1	-	142.3
2	-	131.9	-	131.9
2^1	3.37 (3H, *s*)	12.1	3.37 (3H, *s*)	12.1
3	-	136.1	-	136.1
3^1	7.90 (1H, *dd*, *J*=11.5, 17.8 Hz)	129.0	7.87 (1H, *dd*, *J*=11.6, 17.7 Hz)	129.0
3^2	6.15 (1H, *d*, *J*=11.5 Hz) /6.23 (1H, *d*, *J*=17.8 Hz)	122.7	6.13 (1H, *d*, *J*=11.5 Hz) /6.22 (1H, *d*, *J*=17.8 Hz)	122.8
4	-	136.5	-	136.5
5	9.27 (1H, *s*)	97.5	9.21 (1H, *s*)	97.4
6	-	155.6	-	155.6
7	-	136.2	-	136.2
7^1	3.16 (3H, *s*)	11.1	3.10 (3H, *s*)	11.1
8	-	145.2	-	145.2
8^1	3.60 (2H, *m*)	19.4	3.53 (2H, *m*)	19.4
8^2	1.66 (3H, *t, J*=3.6 Hz)	17.3	1.65 (3H, *t*, *J*=6.0 Hz)	17.4
9	-	150.9	-	150.9
10	9.43 (1H, *s*)	104.4	9.39 (1H, *s*)	104.4
11	-	137.9	-	137.9
12	-	128.8	-	128.8
12^1	3.66 (3H, *s*)	12.1	3.68 (3H, *s*)	12.1
13	-	128.9	-	128.9
13^1	-	189.8	-	189.8
13^2	6.27 (1H, *s*)	64.7	6.31 (1H, *s*)	64.7
13^3	-	169.7	-	169.7
13^4	3.90 (3H, s)	52.9	3.93 (3H, *s*)	53.1
14	-	149.7	-	149.7
15	-	105.1	-	105.1
16	-	161.2	-	161.3
17	4.23 (1H, *d*, *J*=8.7 Hz)	51.1	4.25 (1H, *d*, *J*=6.0 Hz)	51.1
17^1	2.28 (1H, *m*) /2.65 (1H, *m*)	29.7	2.37 (1H, *m*) /2.68 (1H, *m*)	29.8
17^2	2.32 (1H, *m*) /2.59 (1H, *m*)	30.9	2.25 (1H, *m*) /2.54 (1H, *m*)	31.2
17^3	-	177.7	-	173.1
18	4.48 (1H, *d*, *J*=7.2 Hz)	50.2	4.51 (1H, *d*, *J*=7.3 Hz)	50.1
18^1	1.84 (3H, *d*, *J*=7.3 Hz)	23.1	1.87 (3H, *d*, *J*=7.3 Hz)	23.2
19	-	172.1	-	172.3
20	8.56 (1H, *s*)	93.1	8.57 (1H, *s*)	93.1
17^4			4.08 (2H, *m*)	60.7
17^5			1.16 (3H, *t*, *J*=7.1 Hz),	14.2

Table 3.8 Selected HMBC correlations of VT3 and VT10 in $CDCl_3$

Position	VT3 HMBC correlations (H→C)	VT10 HMBC correlations (H→C)
1		
2		
2^1	H-2^1/C-2, C-1, C-3, C-2^1	H-2^1/C-2, C-1, C-3, C-2^1
3		
3^1	H-3^1/C-3^2, C-2, C-4	H-3^1/C-3^2, C-2, C-4
3^2	H-3^2/C-3, C-3^1	H-3^2/C-3, C-3^1
4		
5	H-5/C-7, C-3, C-4	H-5/C-7, C-3, C-4
6		
7		
7^1	H-7^1/C-6, C-8, C-7, C-9, C-7^1	H-7^1/C-6, C-8, C-7, C-9, C-7^1
8		
8^1	H-8^1/C-8^2, C-9, C-7	H-8^1/C-8^2, C-9, C-7, C-8
8^2	H-8^2/C-8^1, C-8	H-8^2/C-8^1, C-8
9		
10	H-10/C-12, C-11, C-8	H-10/C-12, C-11, C-8, C-10
11		
12		
12^1	H-12^1/C-11, C-13, C-12	H-12^1/C-11, C-13, C-12, C-10
13		
13^1		
13^2	H-13^2/C-16, C-15, C-13, C-14, C-13^1, C-13^3	H-13^2/C-16, C-13, C-14, C-13^1, C-13^3
13^3		
13^4	H-13^4/C-13^3	H-13^4/C-13^3
14		
15		
16		
17	H-17/C-18^1, C-17^1, C-17^2, C-16, C-19	H-17/C-18^1, C-17^1, C-17^2, C-16
17^1	H-17^1/C-17^3	H-17^1/C-17^2, C-18, C-17^3
17^2	H-17^2/C-17^3	H-17^2/C-17^1, C-17, C-17^3
17^3		
18	H-18/C-18^1, C-17^1, C-17, C-16, C-19	H-18/C-18^1, C-17^1, C-17, C-16,
18^1	H-18^1/C-17, C-18, C-19	H-18^1/C-17, C-18, C-19
19		
20	H-20/C-2, C-18, C-1	H-20/C-2, C-18, C-1
17^4		H-17^4/C-17^3, C-17^5
17^5		H-17^5/C-17^4

Table 3.9 ^{1}H (400 MHz) and ^{13}C NMR (100 MHz) data of VT6 and VT7 in $CDCl_3$

	VT6		VT7	
Position	**H (δ)**	**C (δ)**	**H (δ)**	**C (δ)**
1	-	142.1	-	143.4
2	-	131.9	-	132.1
2^1	3.42 (3H, *s*)	12.1	3.37 (3H, *s*)	12.1
3	-	136.3	-	137.5
3^1	7.99 (1H, *dd*, *J*=11.5, 17.8 Hz)	129.1	7.90 (1H, *dd*, *J*=11.6, 17.8 Hz)	128.6
3^2	6.19 (1H, *d*, *J*=11.5 Hz) /6.30 (1H, *d*, *J*=17.8 Hz)	122.8	6.20 (1H, *d*, *J*=11.5 Hz) /6.33 (1H, *d*, *J*=17.8 Hz)	123.4
4	-	136.5	-	136.9
5	9.38 (1H, *s*)	97.5	10.04 (1H, *s*)	101.3
6	-	155.6	-	150.7
7	-	136.1	-	132.4
7^1	3.23 (3H, *s*)	11.3	10.86 (1H, *s*)	187.4
8	-	145.2	-	159.1
8^1	3.67 (2H, *m*)	19.5	3.69 (2H, *m*)	18.8
8^2	1.71 (3H, *t*, *J*=7.6 Hz)	17.5	1.67 (3H, *t*, *J*=7.9 Hz)	19.3
9	-	150.9	-	146.6
10	9.52 (1H, *s*)	104.5	9.27 (1H, *s*)	106.6
11	-	137.9	-	137.7
12	-	129.0	-	132.2
12^1	3.71 (3H, *s*)	12.2	3.60 (3H, *s*)	12.2
13	-	128.9	-	129.6
13^1	-	189.6	-	189.5
13^2	6.30 (1H, *s*)	64.8	6.27 (1H, *s*)	64.7
13^3	-	169.5	-	169.3
13^4	3.91 (3H, *s*)	52.9	3.97 (3H, *s*)	53.1

Table 3.9 (continued) ^{1}H (400 MHz) and ^{13}C NMR (100 MHz) data of VT6 and VT7 in $CDCl_3$

	VT6		VT7	
Position	**H (δ)**	**C (δ)**	**H (δ)**	**C (δ)**
14	-	149.7	-	150.6
15	-	105.2	-	104.9
16	-	161.4	-	164.1
17	4.24 (1H, *d*, *J*=8.0 Hz)	51.2	4.23 (1H, *d*, *J*=6.2 Hz)	51.4
17^1	2.36 (1H, *m*) /2.66 (1H, *m*)	29.7	2.37 (1H, *m*) /2.69 (1H, *m*)	29.7
17^2	2.22 (1H, *m*) /2.51 (1H, *m*)	31.3	2.31 (1H, *m*) /2.56 (1H, *m*)	31.3
17^3	-	173.0	-	172.9
18	4.49 (1H)	50.2	4.48 (1H)	50.1
18^1	1.84 (3H, *d*, *J*=7.3 Hz)	23.1	1.88 (3H, *d*, *J*=7.3 Hz)	23.1
19	-	172.1	-	174.0
20	8.58 (1H, *s*)	93.2	8.54 (1H, *s*)	93.4
Phytol	**Protons**: 4.50 (CH_2), 5.16 (CH), 1.91 (CH_2), 1.28 ($3CH_2$), 1.22/1.02 ($4CH_2$), 1.13 (CH_2), 1.33 (2CH), 1.52 (CH), 0.81 (CH_3, *d*), 0.82 (CH_3, *d*), 0.86 (CH_3, *d*), 0.87 (CH_3, *d*), 1.60 (CH_3, *t*)		**Protons**: 4.52 (CH_2), 5.20 (CH), 1.92 (CH_2), 1.31 ($3CH_2$), 1.22/1.02 ($4CH_2$), 1.12 (CH_2), 1.33 (2CH), 1.51 (CH), 0.81 (CH_3, *d*), 0.82 (CH_3, *d*), 0.86 (CH_3, *d*), 0.87 (CH_3, *d*), 1.62 (CH_3, *t*)	
	Carbons: 61.5, 117.7, 142.9, 39.9, 25.0, 37.4, 32.7, 37.3, 24.8, 37.2, 32.6, 36.6, 24.4, 39.4, 28.0. 22.7, 22.6, 19.6, 19.5, 16.3		**Carbons**: 61.6, 117.7, 143.0, 39.8, 24.9, 37.2, 32.6, 37.3, 24.4, 37.4, 32.7, 36.6, 24.8, 39.4, 28.0. 22.7, 22.6, 19.6, 19.7, 16.3	

Table 3.10 Selected HMBC correlations of VT6 and VT7 in $CDCl_3$

Position	VT6 HMBC correlations (H→C)	VT7 HMBC correlations (H→C)
1		
2		
2^1	H-2^1/C-2, C-1, C-3, C-2^1	H-2^1/C-2, C-1, C-3, C-2^1
3		
3^1	H-3^1/C-3, C-2, C-4	H-3^1/C-3^2, C-2, C-4
3^2	H-3^2/C-3, C-3^1	H-3^2/C-3, C-3^1
4		
5	H-5/C-7, C-3, C-4	H-5/C-7, C-3, C-4
6		
7		
7^1	H-7^1/C-6, C-8, C-7	H-7^1/C-6, C-7, C-7^1
8		
8^1	H-8^1/C-8^2, C-9, C-7, C-8	H-8^1/C-8^1, C-8^2, C-9, C-7, C-8
8^2	H-8^2/C-8^1, C-8	H-8^2/C-8^1, C-8
9		
10	H-10/C-12, C-11, C-8	H-10/C-12, C-11, C-8
11		
12		
12^1	H-12^1/C-11, C-13, C-12	H-12^1/C-11, C-13, C-12
13		
13^1		
13^2	H-13^2/C-15, C-14, C-13^1, C-13^3	H-13^2/C-16, C-15, C-14, C-13^1, C-13^3
13^3		
13^4	H-13^4/C-13^3	H-13^4/C-13^3
14		
15		
16		
17	H-17/C-17^1, C-17^2, C-16	H-17/C-18^1, C-17^1, C-17^2, C-16
17^1		C-17^3
17^2		C-17^1, C-17, C-17^3
17^3		
18	H-18/C-18^1, C-17^2	H-18/C-18^1, C-17^1, C-19, C-16,
18^1	H-18^1/C-17, C-18, C-19	H-18^1/C-17, C-18, C-19
19		
20	H-20/C-2, C-18, C-1	H-20/C-2, C-18, C-1
Phytol	4.50/117.7, 142.9, 173.0 (C-17^3) 5.16/16.3, 39.9	4.52/117.7, 143.0, 172.9(C-17^3) 5.20/16.3, 39.8

3.3 Flavonoids

3.3.1 Common spectroscopic features

AL8, **AL9** and **AL10** were isolated from the methanol extract of *A. lappa* **(Section 2.4: Protocol 4; AL8 0.0001% yield, AL9 0.0003% yield, AL10 0.0018% yield)**, **TF3**, **TF6** and **TF9** were isolated from the ethyl acetate extract of *T. farfara* **(Section 2.4: Protocol 6; TF3 0.0042% yield, TF6 0.0004% yield, TF9 0.0012% yield)**, and **VT2** was isolated from the ethyl acetate and methanol extracts of *V. thapsus* **(Section 2.4: Protocol 9 and 10, 0.1643% yield)**. All compounds were obtained as yellow amorphous solids. TLC analysis revealed a quenching spot under short UV light which turned yellow after treatment with anisaldehyde-sulphuric acid (**AL8**, **AL9**, **AL10**, **TF3**, **TF6** and **TF9**) or vanillin-sulphuric acid (**VT2**) reagent followed by heating.

The ^{1}H NMR spectra **(Table 3.11 and 3.12, Figure 3.44 and 3.45)** suggested the presence of two aromatic spin systems with one system common in all compounds showing two *meta*-coupled protons typical of A ring protons H-6 and H-8. The other aromatic system (B ring) exhibited either a 4'-monosubstitution or a 3', 4'-disubstitution. Sharp singlets in the region of δ12.17 to 12.97 were observed for all compounds, typical of the 5-OH of flavonoids which can form hydrogen bond in solvent DMSO-d_6 and Acetone-d_6.

The ^{13}C NMR spectra **(Table 3.11 and 3.12, Figure 3.46 and 3.47)** indicated that **AL8/TF3**, **AL9/TF6** and **VT2** had 15 carbons, whilst **AL10/TF9** presented 21 carbons with six carbons typical of a glucose including the anomeric methine at δ104.0 and the oxymethylene at δ61.9. Signals at δ175.7~182.1, typical of a C-4 carbonyl group in flavonoids, were also detected for all compounds.

3.3.2 Characterisation of AL8/TF3 as kaempferol

The negative ion mode HRESI-MS data for **AL8/TF3** gave a quasi-molecular ion $[M-H]^-$ at *m/z* 285.0409, suggesting a molecular fomula of $C_{15}H_{10}O_6$ (DBE=11).

In the ^{1}H NMR spectrum **(Table 3.11, Figure 3.44)**, the A ring of a flavonol structure was identified with two *meta*-coupled protons at δ6.28 (1H, *d*, *J*=2.0 Hz, H-6) and δ6.54 (1H, *d*, *J*=2.0 Hz, H-8). A pair of signals showing *ortho*, *meta*-couplings at δ7.03 (2H, *dd*, *J*=2.1, 8.0 Hz, H-3'/5') and δ8.17 (2H, *dd*, *J*=2.1, 8.0 Hz, H-2'/6') established the presence of a 1, 4-para disubtituted B ring.

In the HMBC spectrum **(Table 3.11)**, both protons at δ6.28 (H-6) and δ6.54 (H-8) showed ^3J correlations to the same quaternary carbon at δ103.5 (C-10) and ^2J correlations to the highly-deshielded quaternary carbon at δ164.1 (C-7); the former (H-6) also ^2J correlated to another highly-deshielded quaternary carbon at δ161.5 (C-5), and the latter (H-8) displayed a ^2J coupling to the carbon at δ156.9 (C-9) and a ^4J 'W' coupling to the carbonyl at δ175.7 (C-4). The protons at δ7.03 (H-3'/5') and δ8.17 (H-2'/6') displayed ^2J and ^3J correlations, respectively, to the oxygen-bearing quaternary carbon at δ159.4 (C-4'), indicating the presence of a -OH substituent in C-4' on the B ring. Protons at δ8.17 (H-2'/6') also exhibited ^3J coupling to another highly-deshieled carbon at δ146.2 (C-2) and ^2J correlation to a quaternary carbon at δ122.6 (C-1'). Couplings between the -OH in C-5 and its neighbouring carbons were also detected, including a ^3J correlation to C-6 at δ98.4, C-10 at δ103.5, and a ^4J correlation to C-7 (δ164.1).

Based on the above data, **AL8/TF3** were unambiguously characterised as kaempferol. The NMR data were in agreement with published data of this compound (Chen *et al*., 2001; Xiao *et al*., 2006; Lee *et al*., 2009). This compound has previously been

isolated from *A. lappa* roots (Chen *et al*., 2011) and *T. farfara* flower buds and leaves (Liu *et al*., 2006; Chanaj-kaczmarek *et al*., 2013). This is the first report of its presence in *A. lappa* aerial parts.

3.3.3 Characterisation of AL9/TF6 as quercetin

The negative ion mode HRESI-MS data for **AL9/TF6** revealed a quasi-molecular ion $[M-H]^-$ at *m/z* 301.0357, suggesting a molecular fomula of $C_{15}H_{10}O_7$ (DBE=11).

The ^{1}H NMR spectrum **(Table 3.12, Figure 3.45)** of **AL9/TF6** was similar to that of **AL8/TF3** with the presence of two *meta*-coupled protons at δ6.19 (1H, *d*, *J*=2.0 Hz, H-6) and δ6.40 (1H, *d*, *J*=2.0 Hz, H-8) on the A ring. The presence of an ABX substitution pattern on the B ring was established with signals for protons at δ6.89 (1H, *d*, *J*=8.5 Hz, H-5'), δ7.54 (1H, *dd*, *J*=2.2, 8.5 Hz, H-6') and δ7.67 (1H, *d*, *J*=2.2 Hz, H-2').

Based on the ^{1}H and ^{13}C NMR data **(Table 3.12)** and by comparision with **AL8/TF3** NMR data as well as published data (Guvenalp and Demirezer, 2005; Xiao *et al*., 2006; Xiang *et al*., 2011), **AL9/TF6** was characterised as quercetin and the identification was also further confirmed with the HMBC analysis **(Table 3.12)**. Quercetin has previously been isolated from *A. lappa* roots and leaves (Ferracane *et al*., 2010) and *T. farfara* flower buds (Liu *et al*., 2006).

3.3.4 Characterisation of VT2 as luteolin

The negative ion mode HRESI-MS data for **VT2** gave a quasi-molecular ion $[M-H]^-$ at *m/z* 285.0409, suggesting a molecular fomula of $C_{15}H_{10}O_6$ (DBE=11).

The ^{1}H NMR spectrum **(Table 3.12, Figure 3.45)** of **VT2** displayed similarity to that of **AL9/TF6**, with two A ring *meta*-coupled protons at δ6.20 (H-6) and δ6.45 (H-8) and three protons at δ6.90 (1H, *d*, *J*=8.1 Hz), δ7.40 (1H, *m*) and δ7.43 (1H, *m*) suggesting an ABX substitution pattern on the B ring. But the multiplicity and *J* values of the protons at δ7.40 and δ7.43 could not be established unambiguously because of signal overlapping in the region of δ7.40~7.43. An extra signal was also detected at δ6.67 (1H, s), which was attributed to H-3 on the C ring. The above information suggested the identification of **VT2** as luteolin.

In the HMBC spectrum **(Table 3.12)**, the correlations observed were similar to those detected for **AL9/TF3** (quercetin). However, the additional signal at δ6.67 (1H, s, H-3) was found to correlate via a ^{3}J coupling to two quaternary carbons at δ104.2 (C-10) and δ122.0 (C-1'). A ^{4}J 'W' coupling to the oxygen-bearing quaternary carbon at δ161.9 (C-5) was also observed. On the basis of the above information, **VT2** was identified as luteolin and the NMR data were in agreement with a previous report (Saeidnia *et al*., 2009). Luteolin has previously been isolated from *V. thapsus* aerial parts (Zhao *et al*., 2011).

3.3.5 Characterisation of AL10/TF9 as kaempferol-3-*O*-glucoside (astragalin)

The negative ion mode HRESI-MS data for **AL10/TF9** displayed a quasi-molecular ion peak $[M-H]^-$ at *m/z* 447.0938, suggesting a molecular fomula of $C_{21}H_{20}O_{11}$ (DBE=12).

The ^{1}H NMR spectrum **(Table 3.11, Figure 3.44)** of **AL10/TF9** revealed an A ring and a B ring similar to that of **AL8/TF3** with A ring protons at δ6.30 (H-6) and δ6.53 (H-8) and B ring protons at δ6.98 (2H, *dd*, *J*=2.1, 8.0 Hz, H-3'/5') and δ8.15 (2H, *dd*, *J*=2.1, 8.0 Hz, H-2'/6'). The spectrum also indicated the presence of a sugar unit,

with an anomeric proton at δ5.26 (1H, *d*, *J*=7.5 Hz, H-1''), an oxymethylene at δ3.53 (1H, *m*, H-6a'')/δ3.66 (1H, *m*, H-6b'') and four oxymethines at δ3.29 (1H, *m*, H-3''), δ3.37 (1H, *m*, H-5''), δ3.45 (1H, *m*, H-2'') and δ3.49 (1H, *m*, H-4''). The large coupling constant observed for H-1'' (*J*=7.5 Hz) indicated that H-1'' and H-2'' were *trans*-diaxial. On this basis, the sugar unit was identified as β-D-glucopyranoside.

The HMBC spectrum **(Table 3.11)** demonstrated the same correlations for A & B ring protons as those observed for **AL8/TF3**. An additional ^{3}J correlation was observed for the anomeric proton of the glucose unit at δ5.26 (H-1'') to the quaternary carbon at δ134.5 (C-3). The above data led to the identification of **AL10/TF9** as kaempferol-3-*O*-glucoside (astragalin). The NMR data were in agreement with published data (Xiao *et al*., 2006; Lee *et al*., 2009). This compound has previously been isolated from *T. farfara* flower buds and leaves (Liu *et al*., 2006; Chanaj-kaczmarek *et al*., 2013); this is its first report from *A. lappa*.

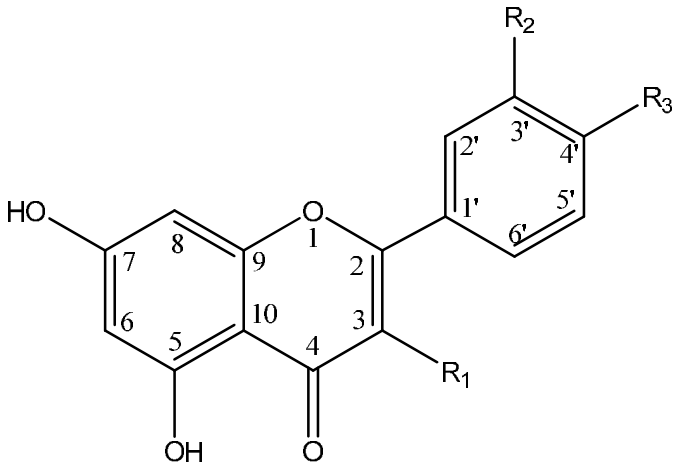

R_1=R_3=OH, R_2=H, Kaempferol (**AL8/TF3**)

R_1=R_2=R_3=OH, Quercetin (**AL9/TF6**)

R_1=H, R_2=R_3=OH, Luteolin (**VT2**)

R_1=OGlu, R_2=H, R_3=OH, Kaempferol-3-*O*-glucoside (**AL10/TF9**)

Figure 3.43 Structures of AL8/TF3, AL9/TF6, AL10/TF9 and VT2

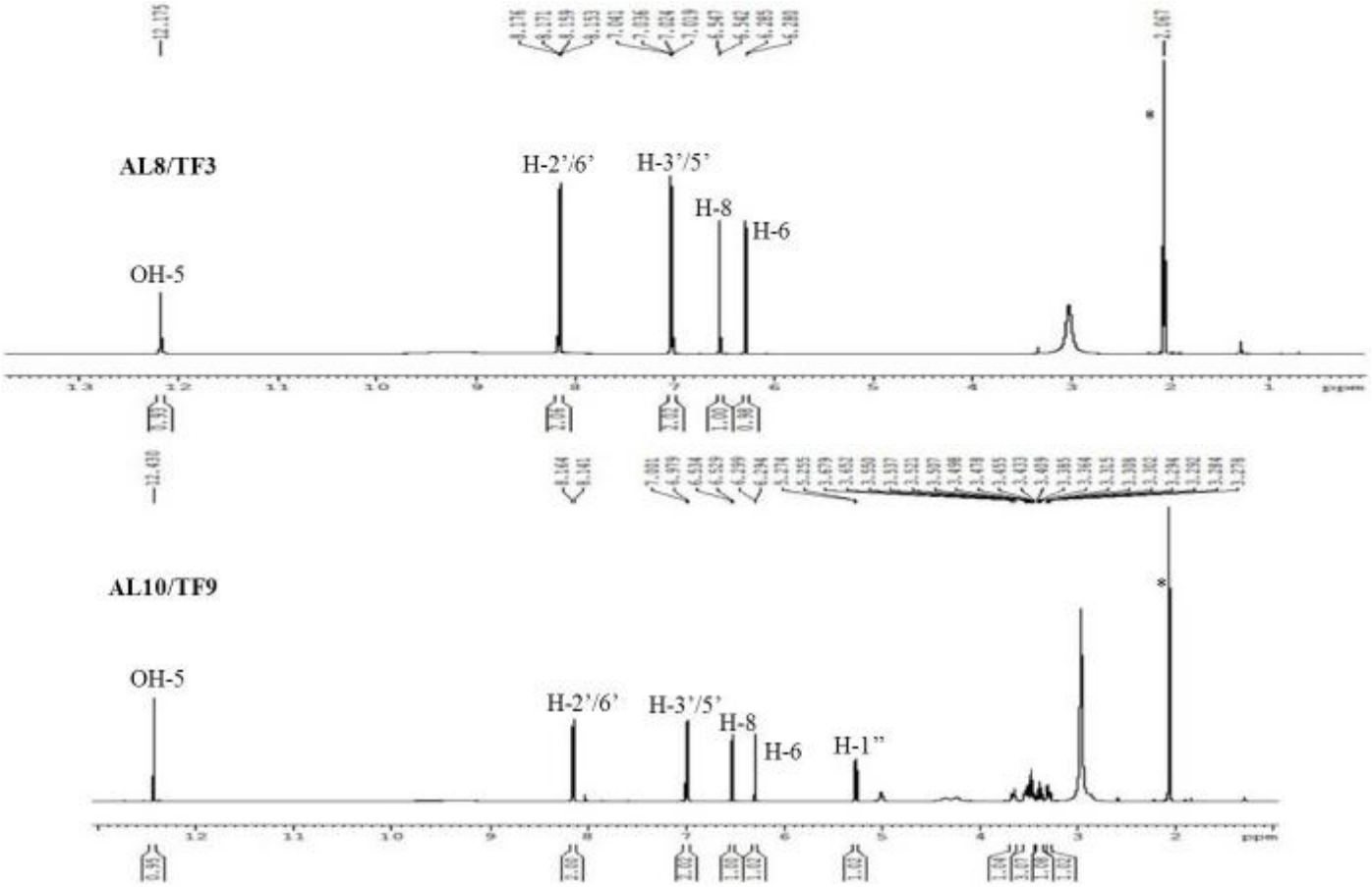

Figure 3.44 ^{1}H NMR spectra (400 MHz) of AL8/TF3 and AL10/TF9 in Acetone-d_6 (*)

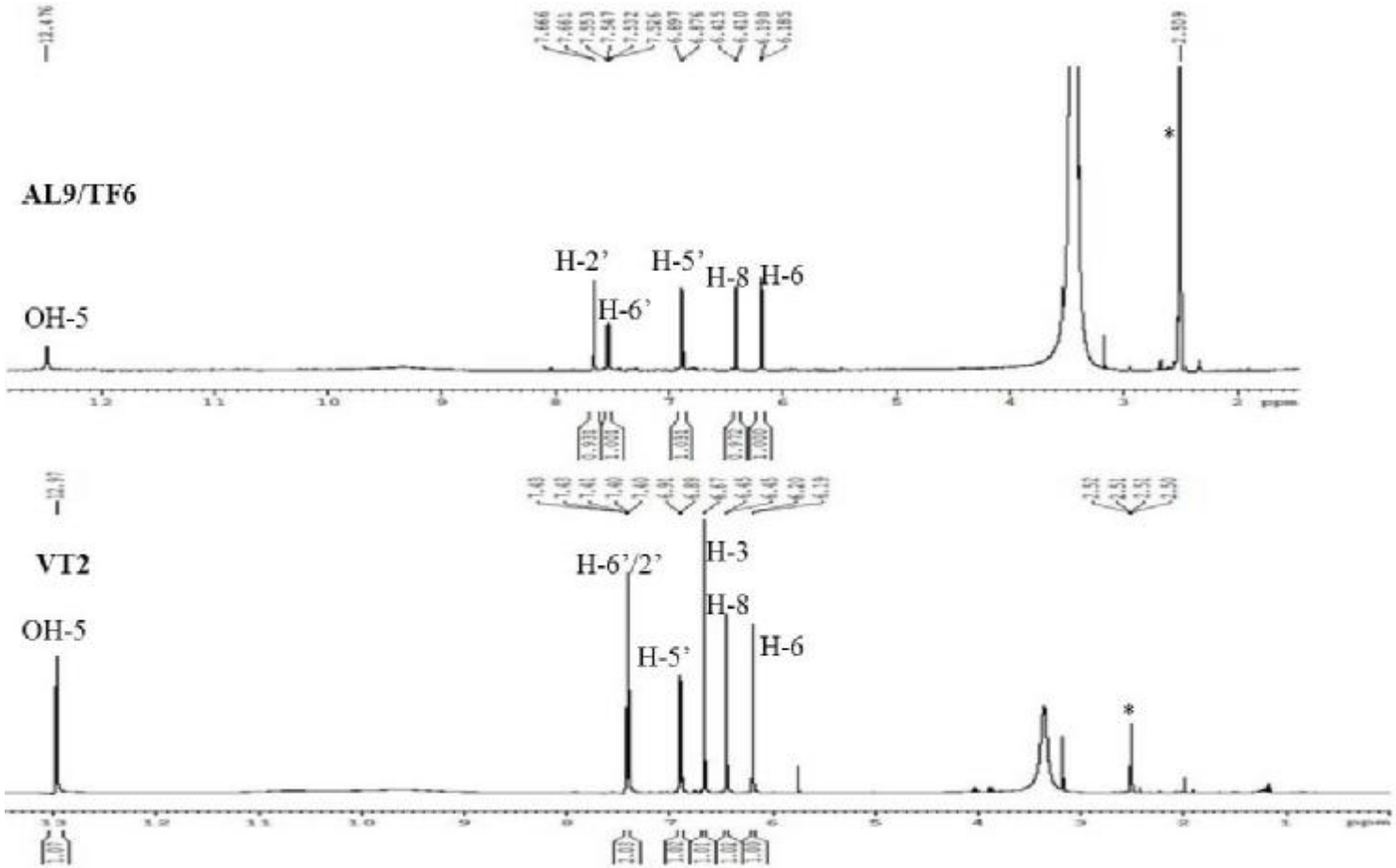

Figure 3.45 ^{1}H NMR spectrua (400 MHz) of AL9/TF6 and VT2 in DMSO-d_6 (*)

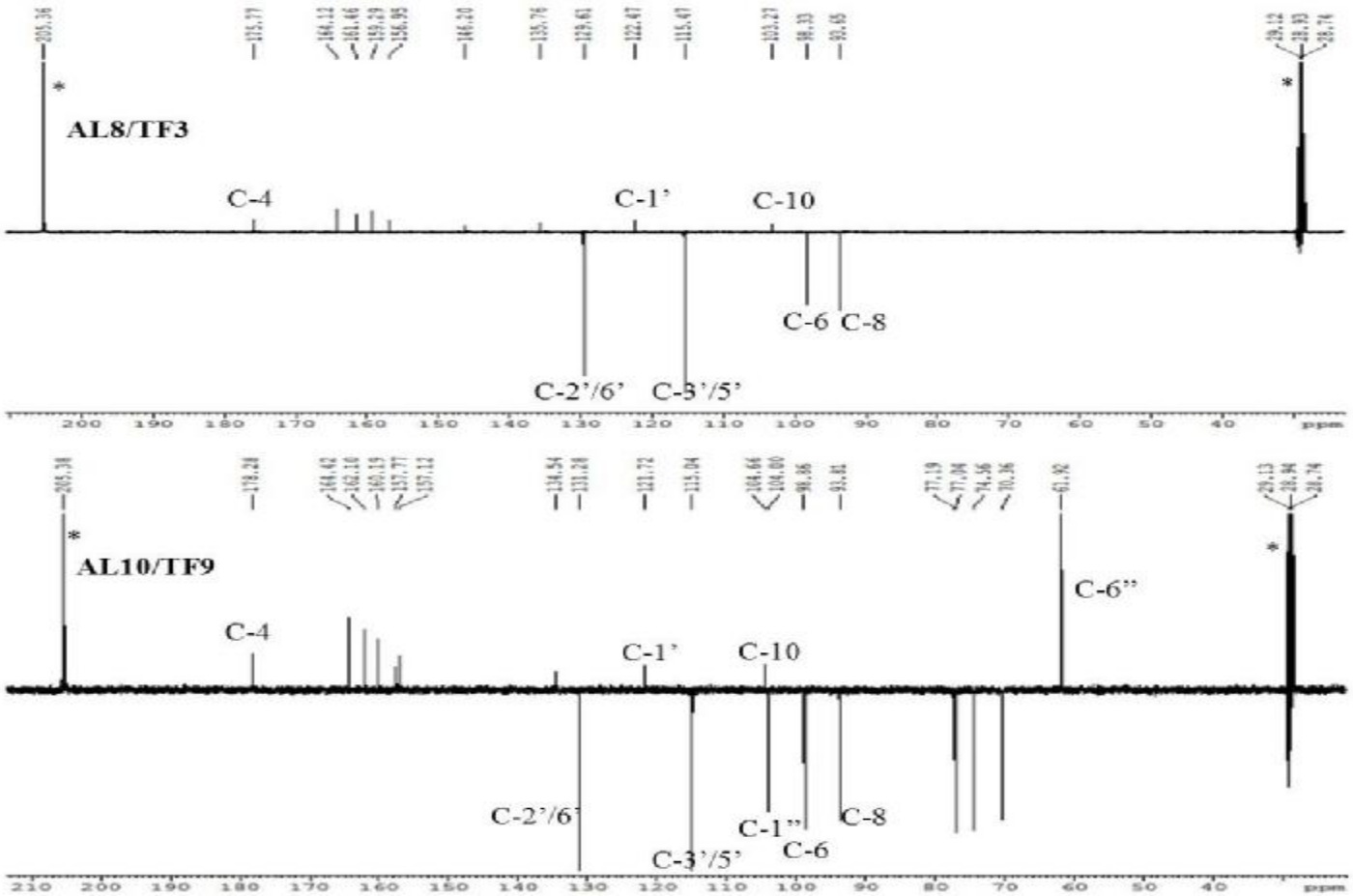

Figure 3.46 DEPTQ 135 ^{13}C NMR spectra (100 MHz) of AL8/TF3 and AL10/TF9 in Acetone-d_6 (*)

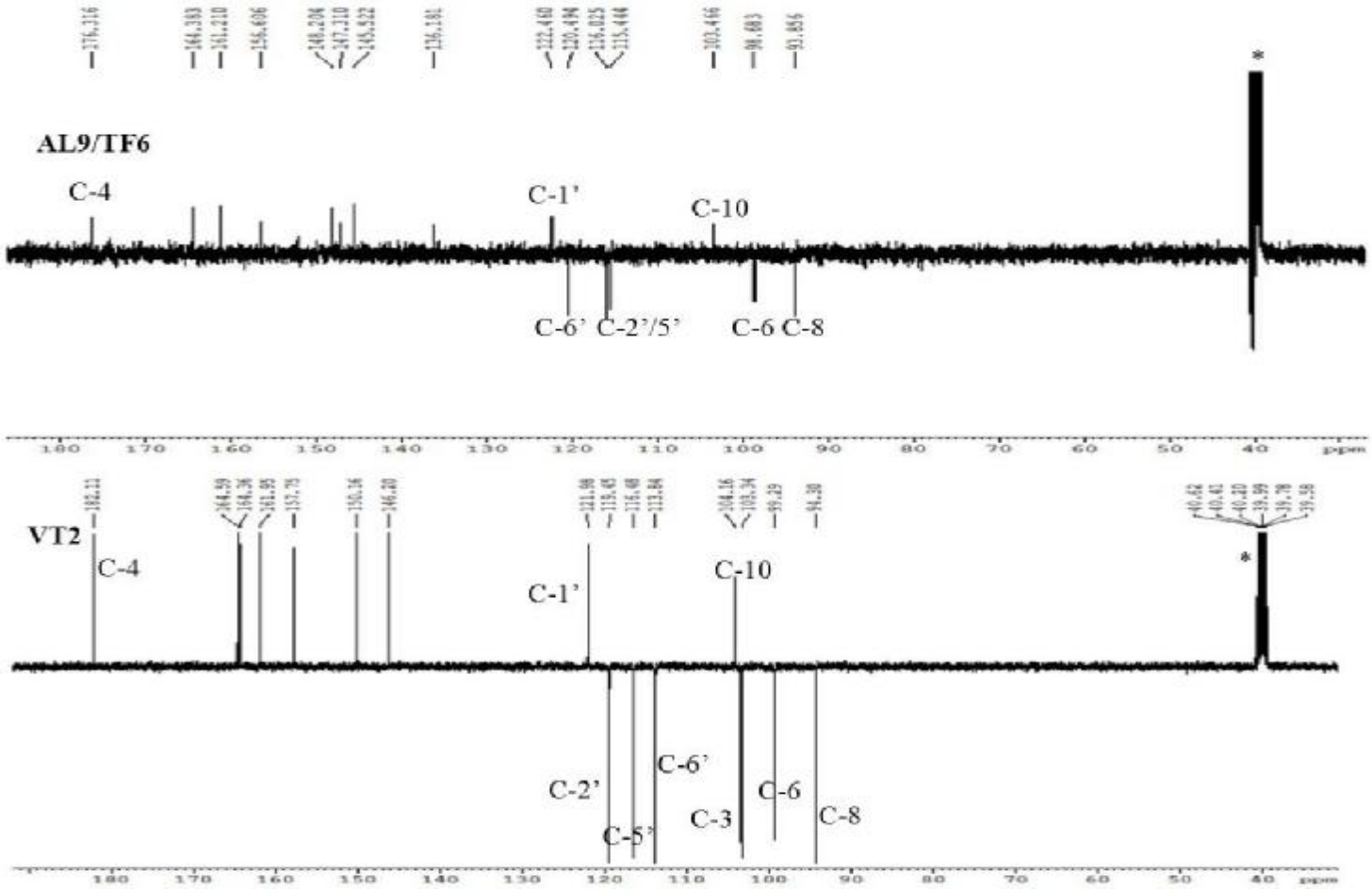

Figure 3.47 DEPTQ 135 ^{13}C NMR spectra (100 MHz) of AL9/TF6 and VT2 in DMSO-d$_6$ (*)

Table 3.11 ^{1}H (400 MHz) and ^{13}C NMR (100 MHz) data of AL8/TF3 and AL10/TF9 in Acetone-d_6

Position	AL8/TF3			AL10/TF9		
	H (δ)	C (δ)	HMBC correlations	H (δ)	C (δ)	HMBC correlations
1	-	-		-	-	
2	-	146.2		-	157.8	
3	-	135.7		-	134.5	
4	-	175.7		-	178.3	
5	12.17 (-OH)	161.5	C-6, C-10, C-5, C-7	12.43 (-OH)	162.1	C-6, C-10, C-5, C-7
6	6.28 (1H, *d*, *J*=2.0 Hz)	98.4	C-8, C-10, C-5, C-7	6.30 (1H, *d*, *J*=2.0 Hz)	98.8	C-8, C-10, C-5, C-7
7	-	164.1		-	164.4	
8	6.54 (1H, *d*, *J*=2.0 Hz)	93.6	C-8, C-6, C-10, C-9, C-7, C-4	6.53 (1H, *d*, *J*=2.0 Hz)	93.8	C-6, C-10, C-9, C-7, C-4
9	-	156.9		-	157.1	
10	-	103.5		-	104.6	
1’	-	122.6		-	121.7	
2’	8.17 (1H, *dd*, *J*=2.1, 8.0 Hz)	129.6	C-3’, C-6’, C-2, C-4’	8.15 (1H, *dd*, *J*=2.1, 8.0 Hz)	131.3	C-3’, C-6’, C-2, C-4’
3’	7.03 (1H, *dd*, *J*=2.1, 8.0 Hz)	115.5	C-5’, C-1’, C-2’, C-4’	6.98 (H, *dd*, *J*=2.1, 8.0 Hz)	115.0	C-5’, C-1’, C-4’
4’	-	159.4		-	160.2	
5’	7.03 (1H, *dd*, *J*=2.1, 8.0 Hz)	115.5	C-3’, C-1’, C-6’, C-4’	6.98 (H, *dd*, *J*=2.1, 8.0 Hz)	115.0	C-3’, C-1’, C-4’
6’	8.17 (1H, *dd*, *J*=2.1, 8.0 Hz)	129.6	C-5’, C-2’, C-2, C-4’	8.15 (1H, *dd*, *J*=2.1, 8.0 Hz)	131.3	C-5’, C-2’, C-2, C-4’
1”				5.26 (1H, *d*, *J*=7.5 Hz)	104.0	C-3
2”				3.45 (1H, *m*)	74.6	C-1”, C-4”
3”				3.29 (1H, *m*)	77.0	C-5”, C-1”, C-4”
4”				3.49 (1H, *m*)	77.2	C-5”, C-2”
5”				3.37 (1H, *m*)	70.4	C-6”, C-3”
6”				3.53 (1H, *m*) /3.66 (1H, *m*)	61.9	

Table 3.12 ^{1}H (400 MHz) and ^{13}C NMR (100 MHz) data of AL9/TF6 and VT2 in DMSO-d_6

Position	AL9/TF6			VT2		
	H (δ)	C (δ)	HMBC correlations	H (δ)	C (δ)	HMBC correlations
1	-	-		-	-	
2	-	147.3		-	164.4	
3	-	136.2		-	103.4	
4	-	176.3		-	182.1	
5	12.48 (-OH)	161.2		12.97 (-OH)	161.9	C-6, C-10, C-5, C-7
6	6.19 (1H, *d*, *J*=2.0 Hz)	98.9	C-8, C-10, C-5, C-7	6.20 (1H, *d*, *J*=2.1 Hz)	99.3	C-8, C-10, C-5, C-7
7	-	164.4		-	164.6	
8	6.40 (1H, *d*, *J*=2.0 Hz)	93.9	C-6, C-10, C-9, C-7	6.45 (1H, *d*, *J*=2.1 Hz)	94.3	C-8, C-6, C-10, C-9, C-7, C-4
9	-	156.6		-	157.8	
10	-	103.5		-	104.2	
1’	-	122.5		-	122.0	
2’	7.67 (1H, *d*, *J*=2.2 Hz)	115.4	C-6’, C-4’, C-3, C-3’	7.43 (1H)	119.5	C-6’, C-4’, C-3
3’	-	145.5		-	146.2	
4’	-	148.2		-	150.2	
5’	6.89 (1H, *d*, *J*=8.5 Hz)	116.0	C-1’, C-3’, C-4’	6.90 (1H, *d*, *J*=8.1 Hz)	116.5	C-1’, C-3’, C-4’, C-6, C-5’
6’	7.54 (1H, *dd*, *J*=2.2, 8.5 Hz)	120.5	C-2’, C-3, C-4’	7.40 (1H)	113.8	C-2’, C-3’, C-4’, C-3, C-1’

3.4 Benzoic acid and hydroxycinnamic acid derivatives

3.4.1 Characterisation of benzoic acid derivatives

3.4.1.1 Characterisation of VT9 as 4-hydroxybenzoic acid

VT9 was isolated from the ethyl acetate extract of *V. thapsus* as a white amorphous solid **(Section 2.4: Protocol 9, 0.0001% yield)**. A dark spot on the TLC plate was detected under short UV light and it turned brown upon treatment with vanillin-sulphuric acid reagent and followed by heating.

The negative ion mode HRESI-MS data showed a quasi-molecular ion $[M-H]^-$ at *m/z* 137.0246, suggesting a molecular fomula of $C_7H_6O_3$ (DBE=5).

The ^{1}H NMR spectrum **(Table 3.13)** displayed two signals, presenting at δ7.87 (2H, *dd*, *J*=2.1, 8.8 Hz) and δ6.83 (2H, *dd*, *J*=2.1, 8.8 Hz), which indicated a 1, 4-*para* disubtituted aromatic ring. In the HMBC spectrum **(Table 3.13)**, the signal at δ7.87 (H-2/6) exhibited ^3J couplings to the carbonyl at δ168.9 (C-7) and the oxygen-bearing quaternary carbon at δ161.9 (C-4). The signal at δ6.83 (H-3/5) revealed correlations to carbons at δ114.6 (^3J, C-5/3), δ121.4 (^3J, C-1) and δ161.9 (^2J, C-4). The above information led to the identification of **VT9** as 4-hydroxybenzoic acid. The NMR results were consistent with the literature data (Yoshioka *et al*., 2004). This compound has already been isolated from *V. phlomoides* and *V. thapsiforme* (Tatli and Akdemir, 2004), but this is the first report of its isolation from *V. thapsus*.

3.4.1.2 Characterisation of VT8 as 4-hydroxy-3-methoxy benzoic acid

VT8 was isolated from the ethyl acetate extract of *V. thapsus* as a brown amorphous solid **(Section 2.4: Protocol 9, 0.0004% yield)**. On TLC plate, it revealed a dark spot under short UV light which turned brown upon spraying with vanillin-sulphuric acid reagent and heating.

The negative ion mode HRESI-MS data revealed a quasi-molecular ion $[M-H]^-$ at m/z 167.0352, suggesting a molecular fomula of $C_8H_8O_4$ (DBE=5).

The ^{1}H NMR spectrum **(Table 3.13)** displayed a singlet at δ3.86 (3H) accounting for a methoxy group. It also exhibited protons of an ABX system at δ6.83 (1H, *d*, *J*=8.3 Hz, H-5), δ7.56 (1H, *dd*, *J*=1.8, 8.3 Hz, H-6) and δ7.49 (1H, *d*, *J*=1.8 Hz, H-2). The ^{13}C NMR spectrum **(Table 3.13)** consisted of eight carbons, including one methoxyl, three aromatic methines, three quaternary carbons and one carbonyl. In the HMBC spectrum **(Table 3.13)**, the methoxyl protons at δ3.86 demonstrated a ^3J coupling to the carbon at δ146.8 (C-3). Protons at δ6.83 (H-5) and δ7.49 (H-2) also ^3J and ^2J correlated to C-3, respectively, indicating that the methoxyl group was attached in C-3. Protons at δ7.56 (H-6) and δ7.49 (H-2) both displayed ^3J couplings to the carbonyl at δ168.9 (C-7) and to the oxygen-bearing carbon at 150.6 (C-4). The identification of C-1 (δ121.9) was confirmed with the ^3J correlation between proton at δ6.83 (H-5) and the carbon signal at δ121.9

The above data identified **VT8** as 4-hydroxy-3-methoxybenzoic acid (vanillic acid). All spectroscopic data were in agreement with the literature data (Yu *et al*., 2006). This compound has previously been isolated from other *V. species* (*V. phlomoides* and *V. thapsiforme*) (Tatli and Akdemir , 2004). This is the first report of its isolation from *V. thapsus.*

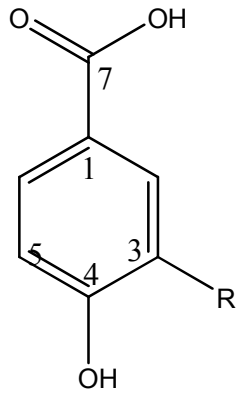

R=H, 4-hydroxybenzoic acid (**VT9**)

R=OCH_3, 4-hydroxy-3-methoxybenzoic acid (**VT8**)

Figure 3.48 Structures of VT9 and VT8

Table 3.13 ^{1}H (400 MHz) and ^{13}C (100 MHz) NMR data of VT9 and VT8 in CD_3OD

Position	VT9			VT8 (CD_3OD*)		
	H (δ)	C (δ)	HMBC correlations	H (δ)	C (δ)	HMBC correlations
1	-	121.4		-	121.9	
2	7.87 (*dd*, *J*=2.1, 8.8 Hz)	131.6	C-6, C-4, C-7	7.49 (1H, *d*, *J*=1.8 Hz)	112.4	C-1, C-6, C-3, C-4, C-7, C-2
3	6.83 (*dd*, *J*=2.1, 8.8 Hz)	114.6	C-5, C-1, C-4	-	146.8	
4	-	161.9		-	150.6	
5	6.83 (*dd*, *J*=2.1, 8.8 Hz)	114.6	C-3, C-1, C-4	6.83 (1H, *d*, *J*=8.3 Hz)	114.3	C-1, C-3, C-4, C-5, C-2, C-7
6	7.87 (*dd*, *J*=2.1, 8.8 Hz)	131.6	C-2, C-4, C-7	7.56 (1H, *dd*, *J*=1.8, 8.3 Hz)	124.3	C-2, C-4, C-7, C-3
7	-	168.9		-	168.9	
8				3.86 (3H, *s*)	55.8	C-8, C-3

* CD_3OD with 1~2 drops of $CDCl_3$

3.4.2 Characterisation of hydroxycinnamic acid derivatives

3.4.2.1 Characterisation of AL7/TF7 as trans-caffeic acid

AL7 and **TF7** were isolated as brown amorphous solids from the methanol extract of *A. lappa* and the ethyl acetate extract of *T. farfara*, respectively **(Section 2.4: Protocol 4 and 6; AL7 0.0018% yield, TF7 0.0001% yield)**. TLC analysis displayed a quenching spot under short UV light which turned brown upon spraying with anisaldehyde-sulphuric acid reagent followed by heating.

The negative ion mode HRESI-MS data for **AL7/TF7** gave a quasi-molecular ion $[M-H]^-$ at *m/z* 179.0355, suggesting a molecular fomula of $C_9H_8O_4$ (DBE=6).

The ^{1}H NMR spectrum **(Table 3.14, Figure 3.50)** displayed two *trans* olefinic protons at δ7.41 (1H, *d*, *J*=15.8 Hz) and δ6.17 (1H, *d*, *J*=15.8 Hz). Three aromatic protons were observed at δ7.02 (1H, d, *J*=2.0 Hz), δ6.95 (1H, *dd*, *J*=8.2, 2.0 Hz) and δ6.76 (1H, *d*, *J*=8.2 Hz). This suggested the structure of a phenylpropanoid derivative. The ^{13}C NMR spectrum **(Table 3.14)** revealed 9 carbons including 5 methines, 3 quaternary carbons and a carbonyl.

In the HMBC spectrum **(Table 3.14)**, the olefinic proton at δ7.41 (H-7) showed a ^2J correlation to one quaternary carbon at δ126.4 (C-1) and ^3J correlations to two carbons at δ115.3 (C-2), δ121.6 (C-6) and the carbonyl at δ168.5 (C-9). The other olefinic proton at δ6.17 (H-8) exhibited a ^2J coupling to the carbonyl and a ^3J coupling to the carbon at δ126.4 (C-1). The protons at δ7.02 (H-2) and δ6.95 (H-6) both ^3J coupled to one oxygen-bearing quaternary carbon at δ148.5 (C-4) and the olefinic carbon at δ144.9 (C-7).

The above data established **AL7/TF7** as *trans*-caffeic acid. The spectroscopic data were in agreement with a previously reported data (Durust *et al*., 2001). Caffeic acid has been reported in the roots, leaves and seeds of *A. lappa* (Bhat *et al*., 2007; Pari and Prasath, 2008) and *T. farfara* flower buds (Wu *et al*., 2010)

3.4.2.2 Characterisation of TF12 as methylcaffeate

TF12 was isolated from the methanol extract of *T. farfara* as a brown powder **(Section 2.4: Protocol 7, 0.0003% yield)**. TLC analysis displayed a dark spot under short UV light which turned brown upon spraying with anisaldehyde-sulphuric acid reagent followed by heating.

The negative ion mode HRESI-MS data for **TF12** revealed a quasi-molecular ion $[M-H]^-$ at *m/z* 179.0509, suggesting a molecular fomula of $C_{10}H_{10}O_4$ (DBE=6).

The ^{1}H NMR spectrum **(Table 3.14, Figure 3.50)** was similar to that of **AL7/TF7**, with *trans* olefinic protons at δ7.55 (1H, *d*, *J*=16.0 Hz) and δ6.29 (1H, *d*, *J*=15.2 Hz), and three aromatic protons at δ7.17 (1H, *d*, *J*=2.0 Hz), δ7.05 (1H, *dd*, *J*=8.2, 2.0 Hz) and δ6.88 (1H, *d*, *J*=8.2 Hz). The only difference was the presence of methoxy group observed at δ3.73 (3H, *s*).

The ^{13}C NMR spectrum **(Table 3.14)** displayed 10 carbons including 5 methines, 3 quaternary carbons, one methoxyl at δ50.6 and a carbonyl at δ167.0. Correlations observed in the HMBC spectrum **(Table 3.14)** were similar to those observed for **AL7/TF7** (caffeic acid), only the methyl at δ3.73 (OMe-10) was found to correlate via a ^3J coupling to the carbonyl at δ167.0 (C-9).

The above data led to the identification of **TF12** as caffeic acid methylester or

methylcaffeate. The spectroscopic data were in agreement with previously reported data (Lee *et al*., 2009; Xiang *et al*., 2011). Methylcaffeate has previously been isolated from *T. farfara* flower buds (Wu *et al*., 2010). .

3.4.2.3 Characterisation of TF4 as *p*-coumaric acid

TF4 was isolated from the ethyl acetate extract of *T. farfara* as a white amorphous solid **(Section 2.4: Protocol 6, 0.0001% yield)**. When analysed on TLC plate, it showed a dark spot under short UV light which turned brown after spraying with anisaldehyde-sulphuric acid reagent followed by heating.

The negative ion mode HRESI-MS data gave a quasi-molecular ion $[M-H]^-$ at *m/z* 179.0403, suggesting a molecular fomula of $C_9H_8O_3$ (DBE=6).

The ^{1}H NMR spectrum **(Table 3.15, Figure 3.50)** displayed two *trans* olefinic protons at δ7.62 (1H, *d*, *J*=16.0 Hz) and δ6.35 (1H, *d*, *J*=16.0 Hz), and a pair of *ortho*, *meta*-coupled signals at δ7.55 (2H, *dd*, *J*=2.0, 8.0 Hz) and δ6.92 (2H, *dd*, *J*=2.0, 8.0 Hz) indicating a 1, 4-*para* disubstituted aromatic ring. The ^{13}C NMR spectrum **(Table 3.15)** demonstrated six methines at δ114.9, δ115.8 (C×2), δ130.0 (C×2) and δ144.6. The assignments of quaternary carbons at δ126.2, δ159.6 and δ167.0 were extracted from the HMBC spectrum.

The above ^{1}H and ^{13}C NMR data suggested the identification of **TF4** as 4-hydroxycinamic acid (*p*-coumaric acid), and the characterisation was further confirmed with the HMBC spectrum **(Table 3.15)**. The NMR data showed agreement with previous reports (Durust *et al*., 2001; Zhou and Li, 2006; Kuddus *et al*., 2010; Ou *et al*., 2011). This compound has previously been isolated from *T. farfara* leaves (Chanaj-kaczmarek *et al*., 2013).

3.4.2.4 Characterisation of VT5 as *trans*-cinnamic acid

VT5 was isolated from the ethyl acetate extract of *Ve. thapsus* as a brown amorphous solid **(Section 2.4: Protocol 9, 0.0033% yield)**. It appeared as a dark spot on the TLC plate under short UV light and it turned brown after spraying with vanillin-sulphuric acid reagent and heating.

In the positive ion mode HRESI-MS, **VT5** gave a quasi-molecular ion $[M+H]^+$ at *m/z* 149.0597, suggesting a molecular fomula of $C_9H_8O_3$ (DBE=6). Data from the negative ion mode HRESI-MS revealed a base peak at *m/z* 295.0977 for $[2M-H]^-$.

In the ^{1}H NMR spectrum **(Table 3.15, Figure 3.50)**, two distinctive *trans* olefinic-proton signals were present at δ7.84 (1H, *d*, *J*=16.0 Hz, H-7) and δ6.49 (1H, *d*, *J*=16.0 Hz, H-8). Two protons were dectected at δ7.59 (*dd*, *J*=2.2, 8.0 Hz) and three protons overlapped at δ7.44 (*m*), which indicated a monosubstituted aromatic ring.

The ^{13}C NMR spectrum **(Table 3.15)** established the presence of 9 carbons, including the methine at δ128.4 (C×2) and another one at δ129.0 (C×2). In the HMBC spectrum **(Table 3.15)**, the olefinic proton at δ7.84 (1H, *d*, *J*=16.0 Hz, H-7) displayed ^3J correlation to one methine at δ128.4, suggesting the assignment of the methine at δ128.4 (C×2) as C-2/6, thus the other at δ129.0 (C×2) assigned to C-3/5. With the aid of the HSQC experiment, the protons at δ7.59 were assigned as H2/6 and the three protons at δ7.44 assigned as H-3/5 and H-4.

On the basis of the above information, **VT5** was identified as *trans*-cinnamic acid. The NMR data were in agreement with previously reported data (Liu *et al*., 2004). Although several hydroxycinnamic acids have previously been isolated from other

Verbascum species (*V. phlomoides* and *V. thapsiforme*) (Tatli and Akdemir, 2004), this is the first report of the isolation of *trans*-cinnamic acid from *V. thapsus*.

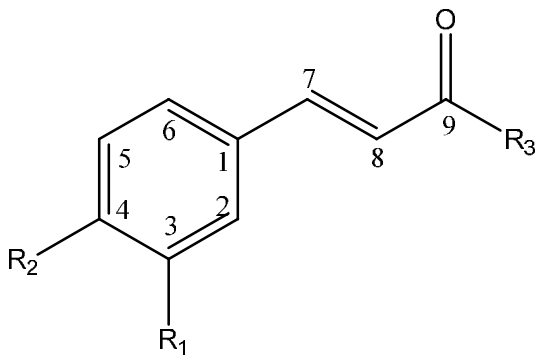

R_1=R_2=R_3=OH Caffeic acid (**AL7/TF7**)

R_1=R_2=OH, R_3=OCH_3 Methylcaffeate (**TF12**)

R_1=H, R_2=R_3=OH *p*-coumaric acid (**TF4**)

R_1= R_2=H, R_3=OH Cinnamic acid (**VT5**)

Figure 3.49 Structures of AL7/TF7, TF12, TF4 and VT5

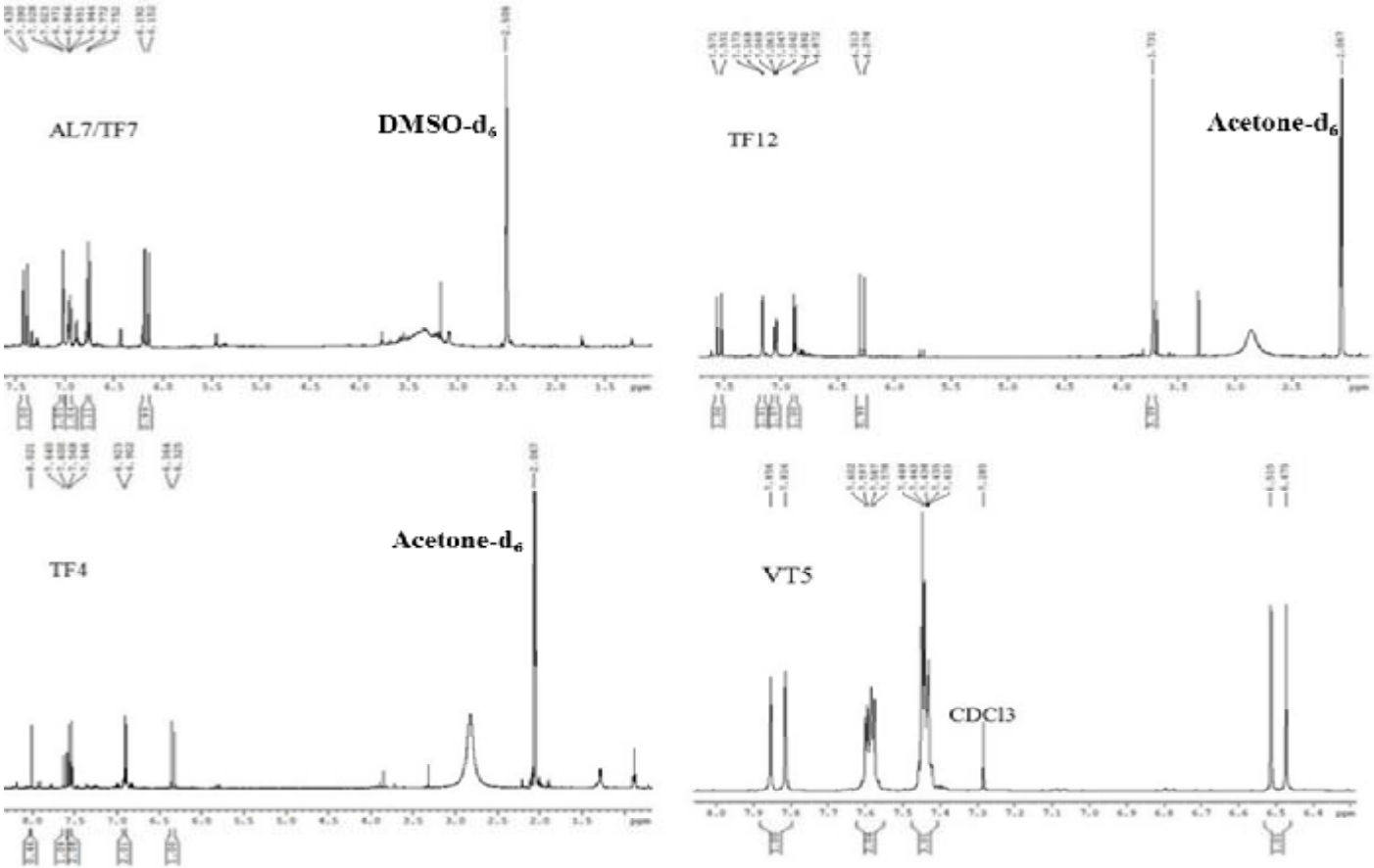

Figure 3.50 ^{1}H NMR spectra (400 MHz) of AL7/TF7, TF12, TF4 and VT5

Table 3.14 ^{1}H (400 MHz) and ^{13}C (100 MHz) NMR data of AL7/TF7 and TF12

Position	AL7 /TF7 (DMSO-d_6)			TF12 (Acetone-d_6)		
	H (δ)	C (δ)	HMBC correlations	H (δ)	C (δ)	HMBC correlations
1	-	126.4		-	126.7	
2	7.02 (1H, *d*, *J*=2.0 Hz)	115.3	C-6, C-7, C-4, C-3	7.17 (1H, *d*, *J*=2.0 Hz)	114.3	C-6, C-7, C-4, C-3
3	-	146.1		-	145.5	
4	-	148.5		-	147.9	
5	6.76 (1H, *d*, *J*=8.2 Hz)	116.2	C-6, C-1, C-3, C-4	6.88 (1H, *d*, *J*=8.2 Hz).	115.5	C-6, C-1, C-3, C-4
6	6.95 (1H, *dd*, *J*=8.2, 2.0 Hz)	121.6	C-2, C-5, C-7, C-4	7.05 (1H, *dd*, *J*=8.2, 2.0 Hz)	121.6	C-2, C-5, C-7, C-4
7	7.41 (1H, *d*, *J*=15.8 Hz)	144.9	C-2, C-6, C-7, C-9	7.55 (1H, *d*, *J*=16.0 Hz)	144.7	C-2, C-6, C-7, C-9
8	6.17 (1H, *d*, *J*=15.8 Hz)	115.8	C-1, C-9	6.29 (1H, *d*, *J*=15.2 Hz)	114.5	C-1, C-9
9	-	168.5		-	167.0	
10				3.73 (3H, *s*)	50.6	C-9

Table 3.15 ^{1}H (400 MHz) and ^{13}C (100 MHz) NMR data of TF4 and VT5

position	TF4 (Acetone-d_6)			VT5 ($CDCl_3$)		
	H (δ)	C (δ)	HMBC correlations	H (δ)	C (δ)	HMBC correlations
1	-	126.2		-	134.0	
2	7.55 (1H, *dd*, *J*=2.0, 8.0 Hz)	130.0	C-6, C-4, C-7	7.59 (*dd*, *J*=2.2, 8.0 Hz)	128.4	C-6, C-4, C-1,C-7
3	6.92 (1H, *dd*, J=2.0, 8.0 Hz)	115.8	C-5, C-1	7.44	129.0	C-5,C-1,C-4
4	-	159.6		7.44	130.8	C-2, C-6, C-3, C-5
5	6.92 (1H, *dd*, *J*=2.0, 8.0 Hz)	115.8	C-3, C-1	7.44	129.0	C-3,C-1,C-4
6	7.55 (1H, *dd*, *J*=2.0, 8.0 Hz)	130.0	C-2, C-4, C-7	7.59 (*dd*, *J*=2.2, 8.0 Hz)	128.4	C-2, C-4, C-1,C-7
7	7.62 (1H, *d*, *J*=16.0 Hz))	144.6	C-2, C-6, C-9	7.84 (1H, *d*, *J*=16.0 Hz)	147.2	C-3/5,C-9, C-1, C-8
8	6.35 (1H, *d*, *J*=16.0 Hz)	114.9	C-1, C-9	6.49 (1H, *d*, *J*=16.0 Hz)	117.3	C-3/5, C-1, C-7, C-9
9	-	167.0		-	172.7	

3.4.2.5 Characterisation of TF5 as a mixture of *p*-coumaric acid (a) and 4-hydroxybenzoic acid (b)

TF5 was isolated from the ethyl acetate extract of *T. farfara* as a brown amorphous solid **(Section 2.4: Protocol 6, 0.0028% yield)**. It appeared a dark spot on the TLC plate under short UV light which turned brown after treatment with anisaldehyde-sulphuric acid reagent and heating.

The negative ion mode HRESI-MS data displayed one quasi-molecular ion $[M-H]^-$ at *m/z* 179.0403, suggesting a molecular fomula of $C_9H_8O_3$ (DBE=6), and one quasi-molecular ion $[M-H]^-$ at *m/z* 137.0246 indicating a molecular fomula of $C_7H_6O_3$ (DBE=5).

The ^{1}H NMR spectrum **(Figure 3.51)** established the presence of two 1, 4-*para* disubstituted aromatic rings with signals at δ7.55 (2H, *dd*, *J*=1.8, 6.9 Hz, H-2a/6a), δ6.91 (2H, *dd*, *J*=2.2, 6.6 Hz, H-3a/5a), δ7.93 (2H, *dd*, *J*=2.0, 8.8 Hz, H-2b/6b), δ6.93 (2H, *dd*, *J*=2.1, 8.6 Hz, H-3b/5b). Two olefinic protons were observed at δ7.62 (1H, d, *J*=16.0 Hz, H-7a) and δ6.34 (1H, d, *J*=16.0 Hz, H-8a). The integration for proton signals at δ7.55 (H-2a/6a) and δ7.93 (H-2b/6b) were in a 4:1 ratio. The ^{13}C NMR spectrum demonstrated 10 methines at δ114.9 (C-8a), δ115.1 (C×2, C-3b/5b), δ115.8 (C×2, C-3a/5a), δ130.0 (C×2, C-2a/6a), δ131.8 (C×2, C-2b/6b) and δ144.7 (C-7a), and six quaternary carbons at δ121.8 (C-1b), δ126.2 (C-1a), δ159.6 (C-4a), δ161.7 (C-4b), δ166.7 (C-7b)and δ167.4 (C-9a).

In the HMBC spectrum, the olefinic protons at δ7.62 (H-7a) and δ6.34 (H-8a) exhibited ^3J and ^2J correlations, respectively, to the carbonyl at δ167.4 (C-9a), and ^2J and ^3J couplings, respectively, to the quaternary carbon at δ126.2 (C-1a). Two protons at δ7.55 (H-2a/6a) displayed ^3J correlations to carbons at δ130.0 (C-6a/2a),

δ159.6 (C-4a) and δ144.7 (C-7a). Another two protons at δ6.91 (H-3a/5a) ^{3}J coupled to carbons at δ126.2 (C-1a) and δ115.8 (C-5a/3a). This established the presence of *p*-coumaric acid.

Additionally, the signal at δ7.93 (H-2b/6b) ^{3}J correlated to the oxygen-bearing carbon at δ161.7 (C-4b) and the carbonyl at δ166.7 (C-7b). The signal at δ6.93 (H-3b/5b) displayed a ^{3}J coupling to the carbon at δ121.8 (C-1b). This established the presence of 4-hydroxybenzoic acid.

On the basis of above data and by comparison with previous reports (Peungvicha *et al*., 1998; Ou *et al*., 2011), **TF5** was identified as a mixture of of *p*-coumaric acid (a) and 4-hydroxybenzoic acid (b) in the ratio of 4:1.

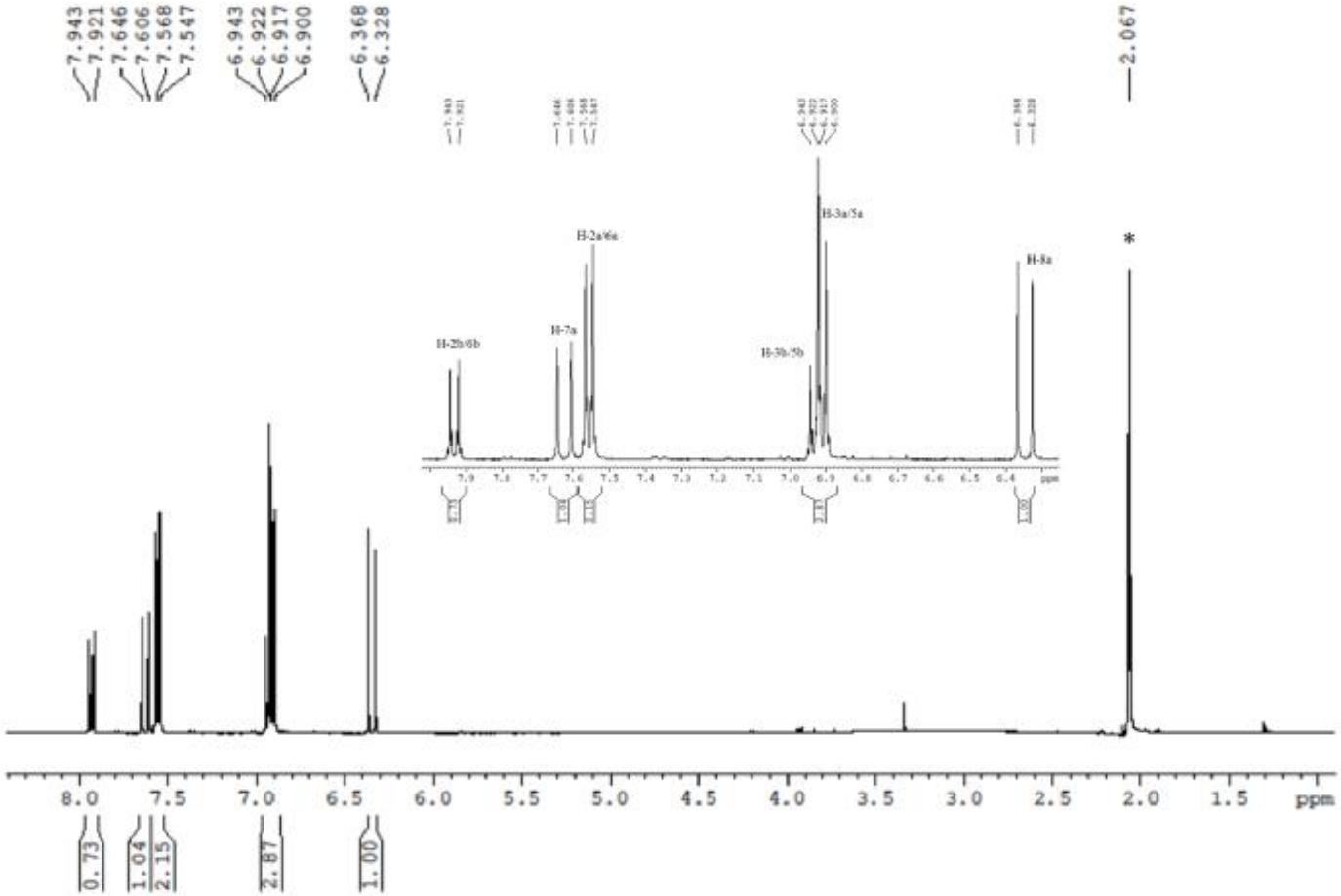

Figure 3.51 ^{1}H NMR spectrum (400 MHz) and selected expansion of TF5 in Acetone-d_6 (*)

3.4.2.6 Characterisation of TF10, TF11, AL12 as dicaffeoylquinic acids

3.4.2.6.1 Common spectroscopic features

TF10 and **TF11** were isolated from the methanol extract of *T. farfara* **(Section 2.4: Protocol 7; TF10 0.0018% yield, TF11 0.0045% yield)**, and **AL12** was isolated from the methanol extract of *A. lappa* **(Section 2.4: Protocol 4, 0.0046% yield)**. All compounds were obtained as brown amorphous solids. TLC analysis revealed a dark spot under short UV light which turned brown after spraying with anisaldehyde-sulphuric acid reagent followed by heating.

The negative ion mode HRESI-MS data for these compounds showed a quasi-molecular ion $[M-H]^-$ at *m/z* 515.1199, suggesting a molecular fomula of $C_{25}H_{24}O_{12}$ (DBE=14). The mass spectra also gave two fragment ions at *m/z* 353 and *m/z* 179.

The ^{1}H NMR spectra **(Table 3.16, Figure 3.53, 3.58 and 3.62)** revealed three oxymethines in the region of δ3.70~6.00 and two methylenes between δ2.00 and δ2.70. They also showed signals for two ABX aromatic spin systems in the region of δ6.70~7.20, and two pairs of *trans*-olefinic methines at around δ6.30 (*J*=15.8 Hz) and δ7.60 (*J*=15.8 Hz).

The ^{13}C NMR spectra **(Table 3.16, Figure 3.54)** estabilished 25 carbons with four oxygenated quaternary carbons in the region of δ145.0~148.5 and three carbonyls including one acidic at δ170.0~181.0 and two esterified positions at δ167.0. The above information suggested the identification of these compounds as dicaffeoylquinic acids. The observation of fragment ions at *m/z* 353 (chlorogenic acid) and at *m/z* 179 (caffeic acid) further supported this hypothesis.

3.4.2.6.2 Characterisation of TF10 as 3, 4-dicaffeoylquinic acid

The ^{1}H NMR spectrum **(Table 3.16, Figure 3.53)** exhibited one quinic acid moiety with three oxymethines at δ5.65 (1H, ddd, *J*= 3.6, 8.2, 11.9 Hz, H-3), δ5.21 (1H, dd, *J*= 2.9, 6.0 Hz, H-4), and δ4.16 (1H, dd, *J*=5.1, 10.7 Hz, H-5), and two methylenes at δ2.21 (1H, m)/δ2.10 (1H, m) and δ2.09 (2H, m). Two caffeoyl groups were established with signals at δ7.60 (H-7'), δ7.53 (H-7''), δ6.32 (H-8'), δ6.26 (H-8''), δ7.08 (H-2'), δ7.04 (H-2''), δ6.95 (H-6'), δ6.90 (H-6''), δ6.79 (H-5') and δ6.76 (H-5''). The COSY spectrum **(Figure 3.55)** revealed a correlation between the signal at δ5.21 and both protons at δ5.65 and δ4.16, indicating that the proton at δ5.21 was H-4. The protons at δ5.65 (H-3) and δ5.21 (H-4) were highly deshielded, suggesting that the hydroxyl groups at position 3 and 4 were substistuted by caffeoyl groups.

The ^{13}C NMR spectrum **(Table 3.16, Figure 3.54)** gave 25 carbons in total. Some distinctive signals from caffeoyl groups included two carbonyls at δ167.0 (C-9') and δ167.1 (C-9''), four olefinic carbons at δ146.0 (C-7'), δ145.8 (C-7''), δ113.7 (C-8'/8'') and six aromatic carbons at δ121.8 (C-6'), δ121.7 (C-6''), δ115.1 (C-5'/5''), δ113.6 (C-2') and δ113.8 (C-2''). Three oxymethines at δ68.6 (C-3), δ73.2 (C-4) and δ66.3 (C-5), two methylenes at δ36.7 (C-2) and δ38.3 (C-6) and one carbonyl at δ180.6 (C-7) were also observed.

In the HMBC spectrum **(Figure 3.56)**, the proton at δ5.21 (H-4) diaplayed ^{2}J and ^{3}J correlations to carbons at δ66.3 (C-5) and δ36.7 (C-2), repectively. Protons at δ5.65 (H-3) and δ4.16 (H-5) both correlated via ^{3}J couplings to the quaternary carbon at δ74.3 (C-1). Two methylenes at δ2.21/δ2.10 (H-2a/b) and δ2.09 (H-6a/b) exhibited ^{3}J correlations to one oxymethine at δ73.2 (C-4) and one carbonyl at δ180.6 (C-7). The olefinic proton at δ7.60 (H-7') showed ^{3}J correlations to two methines at δ113.6

(C-2') and δ121.8 (C-6'), and to the carbonyl at δ167.0 (C-9'). The olefinic proton at δ6.32 (H-8') ^{3}J coupled to the quaternary carbon at δ126.4 (C-1'). Protons at δ6.95 (H-6') and δ7.08 (H-2') both correlated via ^{3}J couplings to the oxygen-bearing carbon at δ148.3 (C-4'). Similarly, the proton at δ7.53 (H-7'') correlated via ^{3}J couplings to carbons at δ113.8 (C-2''), δ121.7 (C-6'') and the carbonyl at δ167.1 (C-9''). Protons at δ6.90 (H-6'') and δ7.04 (H-2'') both showed ^{3}J correlations to the carbon at δ148.1 (C-4''). The proton at δ5.65 (H-3) displayed a ^{3}J coupling to one caffeoyl carbonyl at δ167.1 (C-9'), and the proton at δ5.21 (H-4) correlated via a ^{3}J coupling to the other caffeoyl carbonyl at δ167.0 (C-9''), further establishing that both hydroxyl groups at position 3 and 4 of the quinic acid moiety were esterified with caffeic acid units.

The above information led to the identification of **TF10** as 3, 4-dicaffeoylquinic acid and the NMR data were in agreement with previouly reported data (Wang and Liu, 2007; Wu *et al*., 2007). This compound has previously been isolated from *T. farfara* flower buds (Wu *et al*., 2010).

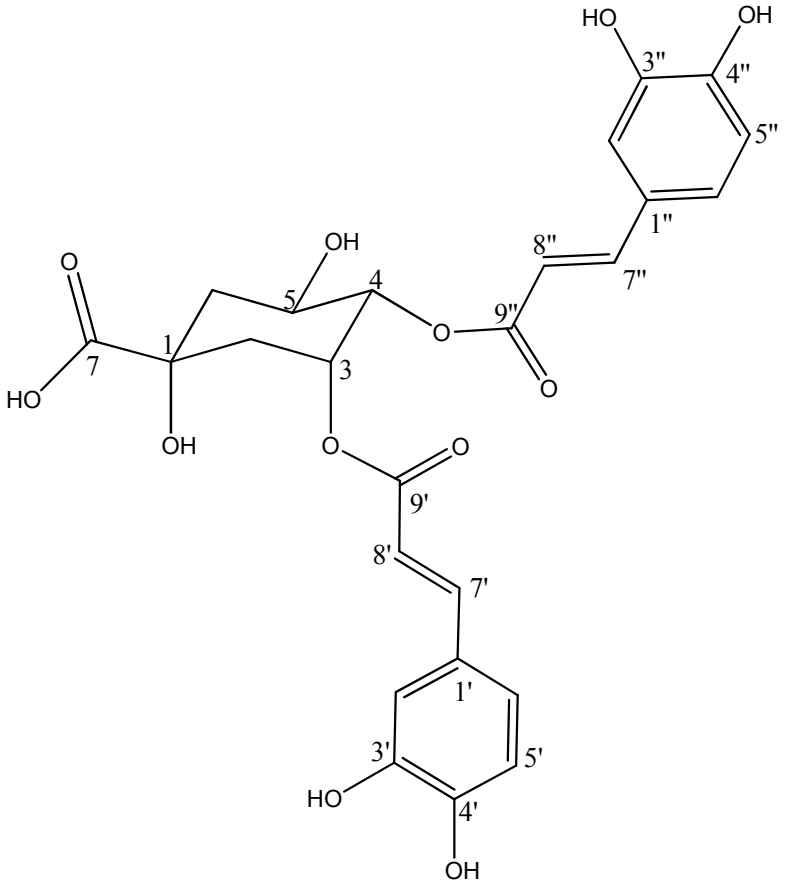

Figure 3.52 Structure of TF10

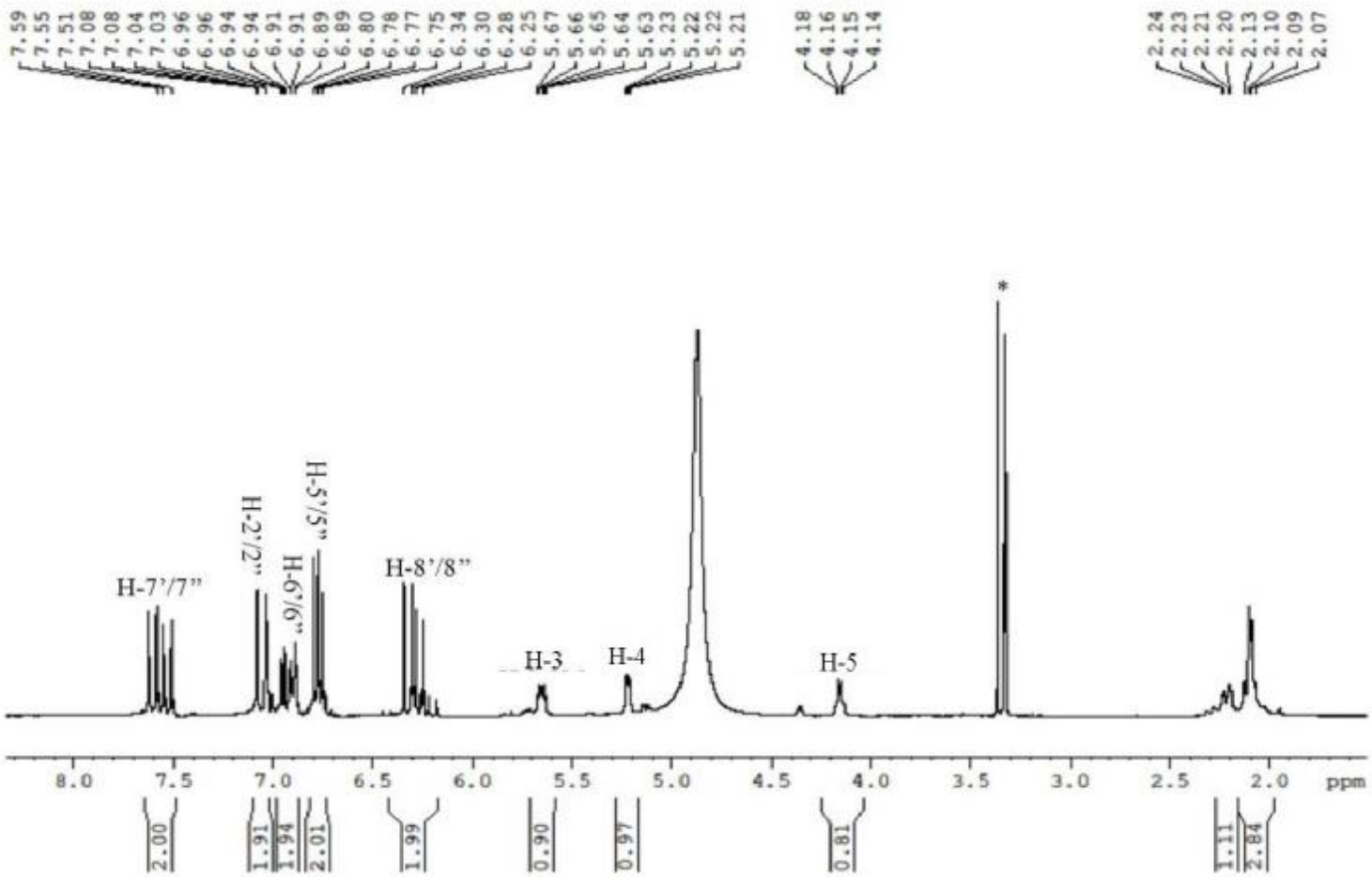

Figure 3.53 ^{1}H NMR spectrum (400 MHz) of TF10 in CD_3OD (*)

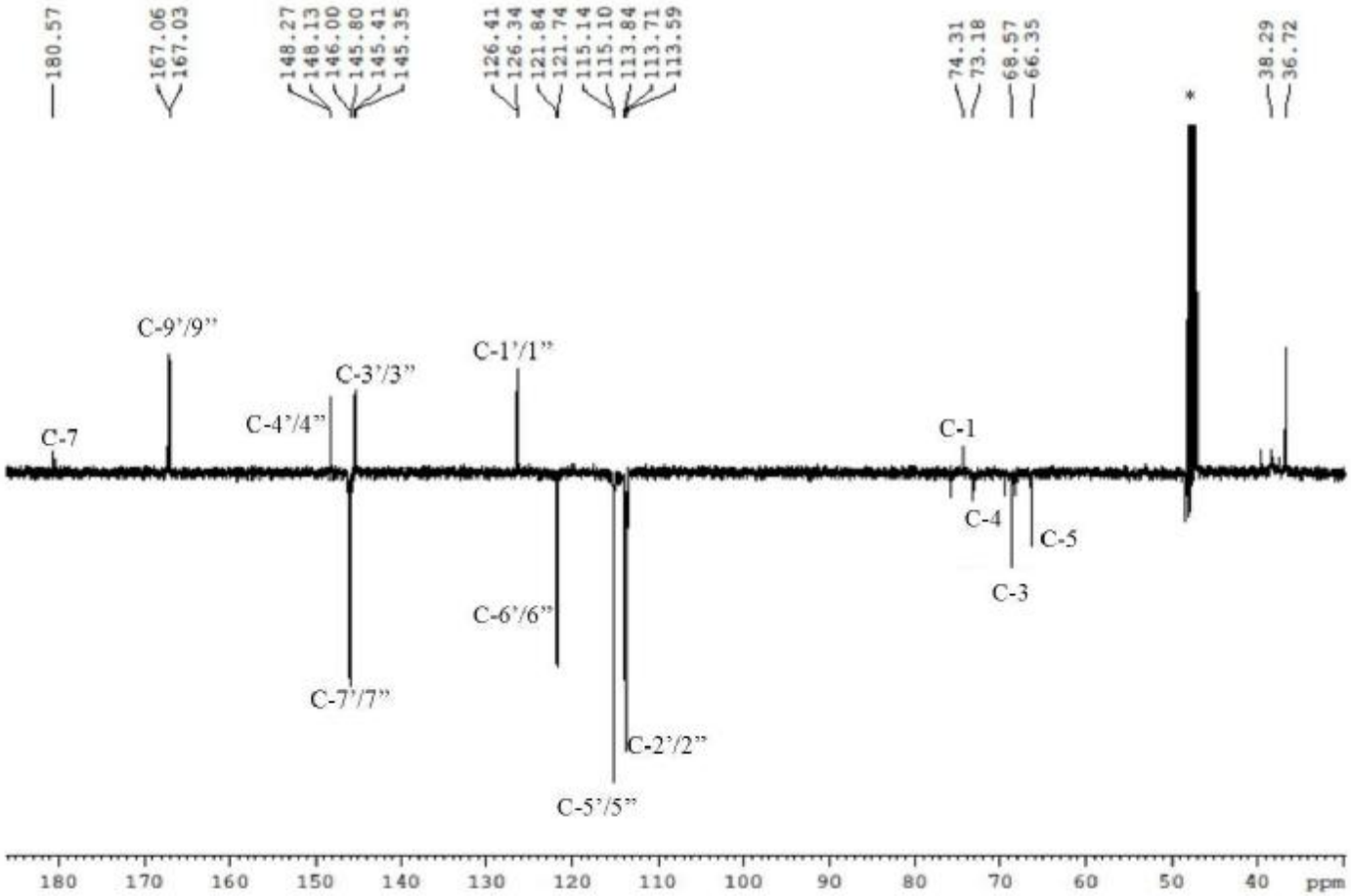

Figure 3.54 DEPTQ 135 ^{13}C NMR spectrum (100 MHz) of TF10 in CD_3OD (*)

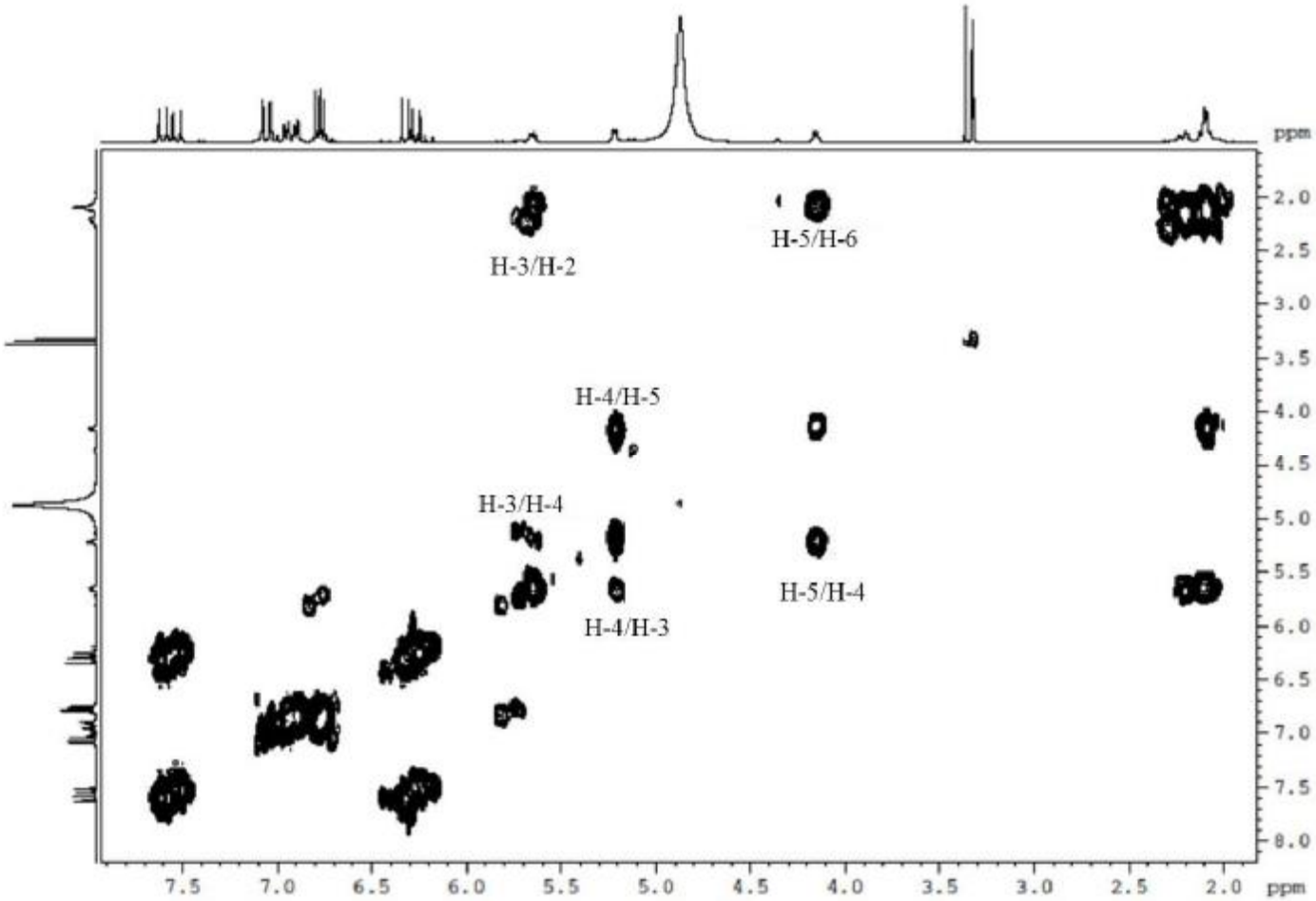

Figure 3.55 COSY spectrum (400 MHz) of TF10 in CD_3OD

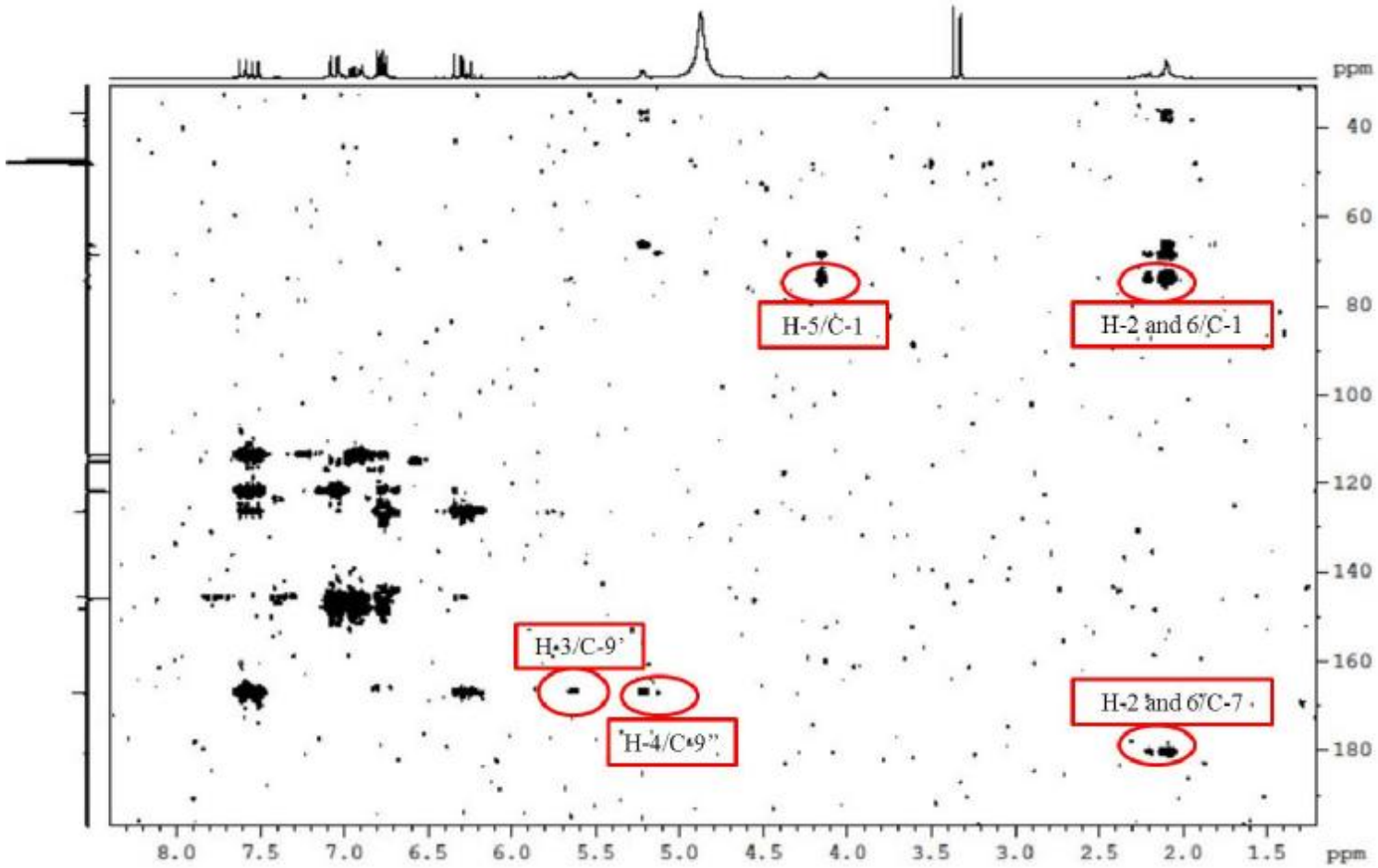

Figure 3.56 HMBC spectrum (400 MHz) of TF10 in CD_3OD

3.4.2.6.3 Characterisation of TF11 as 3, 5-dicaffeoylquinic acid

In the ^{1}H NMR spectrum **(Table 3.16, Figure 3.58)**, the structure of quinic acid was identified with three oxymethines at δ5.53 (H-5), δ5.44 (H-3) and δ3.97 (H-4), and two methylenes at δ2.33/δ2.14 and δ2.19. The presence of two caffeoyl groups was established with signals at 7.63 (H-7'), δ7.59 (, H-7''), δ6.40 (H-8'), δ6.30 (H-8''), δ7.09 (H-2'/H-2''), δ6.96 (H-6'/H-6'') and δ6.80 (H-5'/H-5''). All protons were assigned with the aid of the COSY spectrum **(Figure 3.59)**. The deshielded signals at δ5.53 (H-5) and δ5.44 (H-3) suggested a 3, 5-dicaffeoyl substitution on the quinic acid ring.

The ^{13}C NMR spectrum **(Table 3.16)** indicated the presence of 25 carbons with three carbonyls at δ178.9 (C-7), δ167.9 (C-9') and δ167.6 (C-9'').

In the HMBC spectrum **(Figure 3.60)**, the proton at δ3.97 (H-4) showed ^{3}J correlations to two methylenes at δ38.5 (C-6) and δ35.8 (C-2), and ^{2}J correlations to two oxymethines at δ72.5 (C-3) and δ71.0 (C-5). Four methylene protons at δ2.33/δ2.14 (H-2a/b) and δ2.19 (H-6a/b) displayed ^{2}J and ^{3}J correlations, respectively, to the carbon at δ74.6 (C-1) and to the carbonyl at δ178.9 (C-7). The deshielded protons at δ5.53 (H-5) and δ5.44 (H-3) both correlated via ^{3}J couplings to the quaternary carbon at δ74.6 (C-1). H-5 exhibited a ^{3}J correlation to one caffeoyl carbonyl at δ167.6 (C-9''), and H-3 displayed a ^{3}J coupling to the other caffeoyl carbonyl at δ167.9 (C-9'), confirming the presence of two caffeic acid units in **TF11**. The above information further established a 3, 5-dicaffeoyl substitution on the quinic acid ring.

The NMR data were in good agreement with previous reports for 3, 5-dicaffeoylquinic acid (Kojima and Kondo, 1985; Peng *et al.*, 2000). This

compound has previously been isolated from *T. farfara* flower buds (Liu *et al*., 2007).

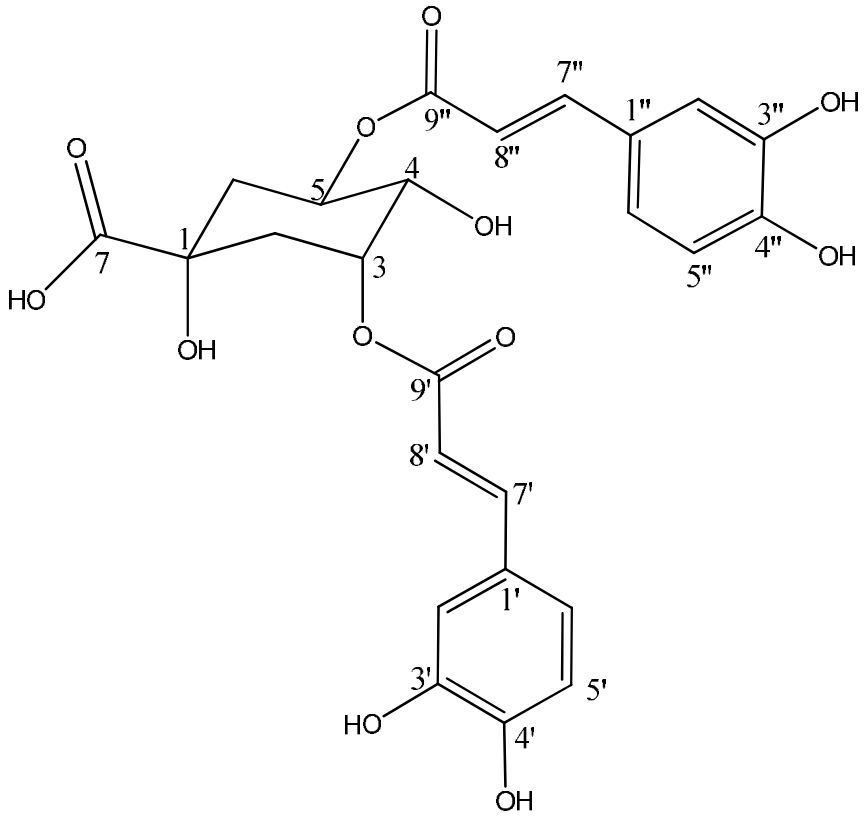

Figure 3.57 Structure of TF11

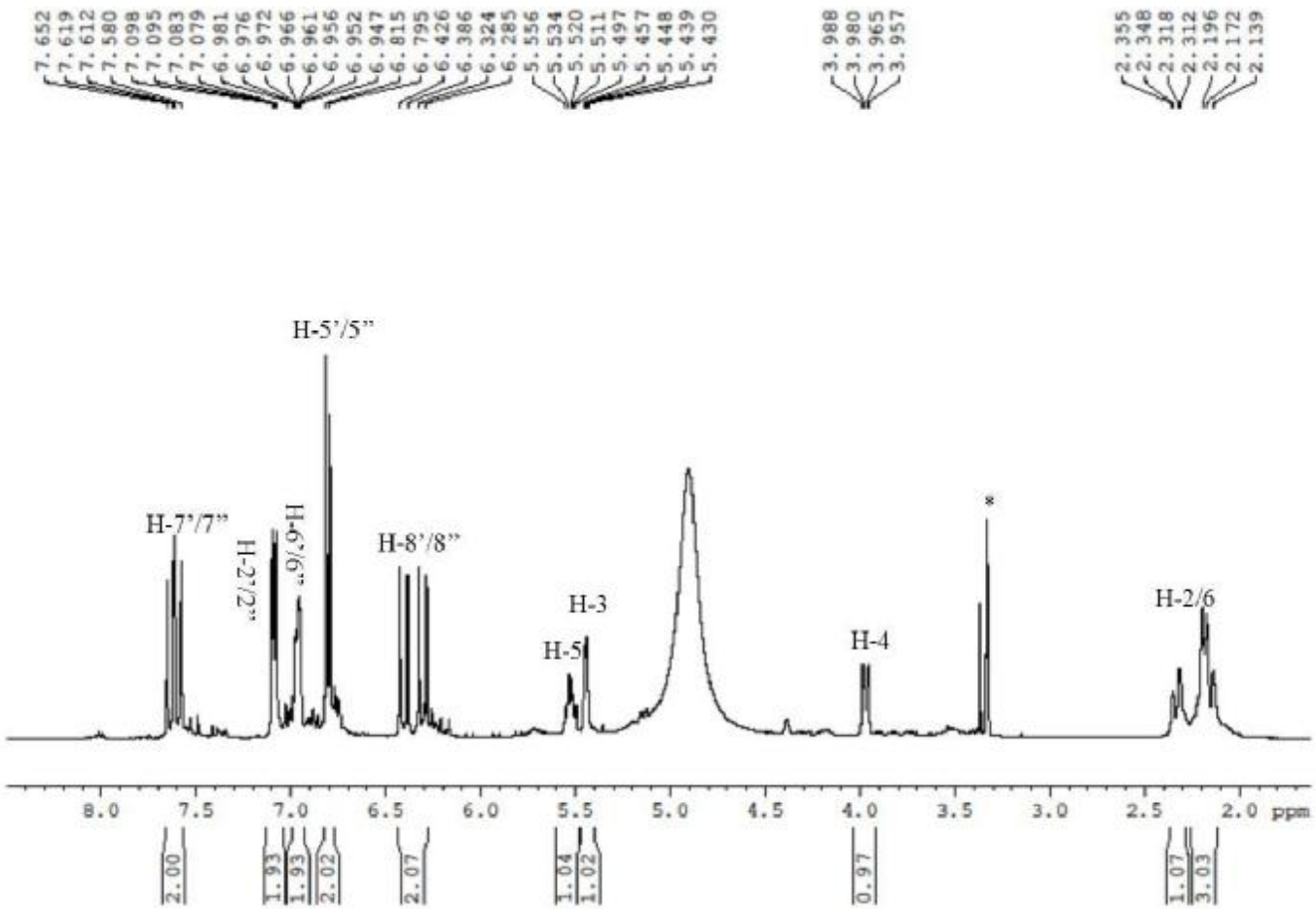

Figure 3.58 ^{1}H NMR spectrum (400 MHz) of TF11 in CD_3OD (*)

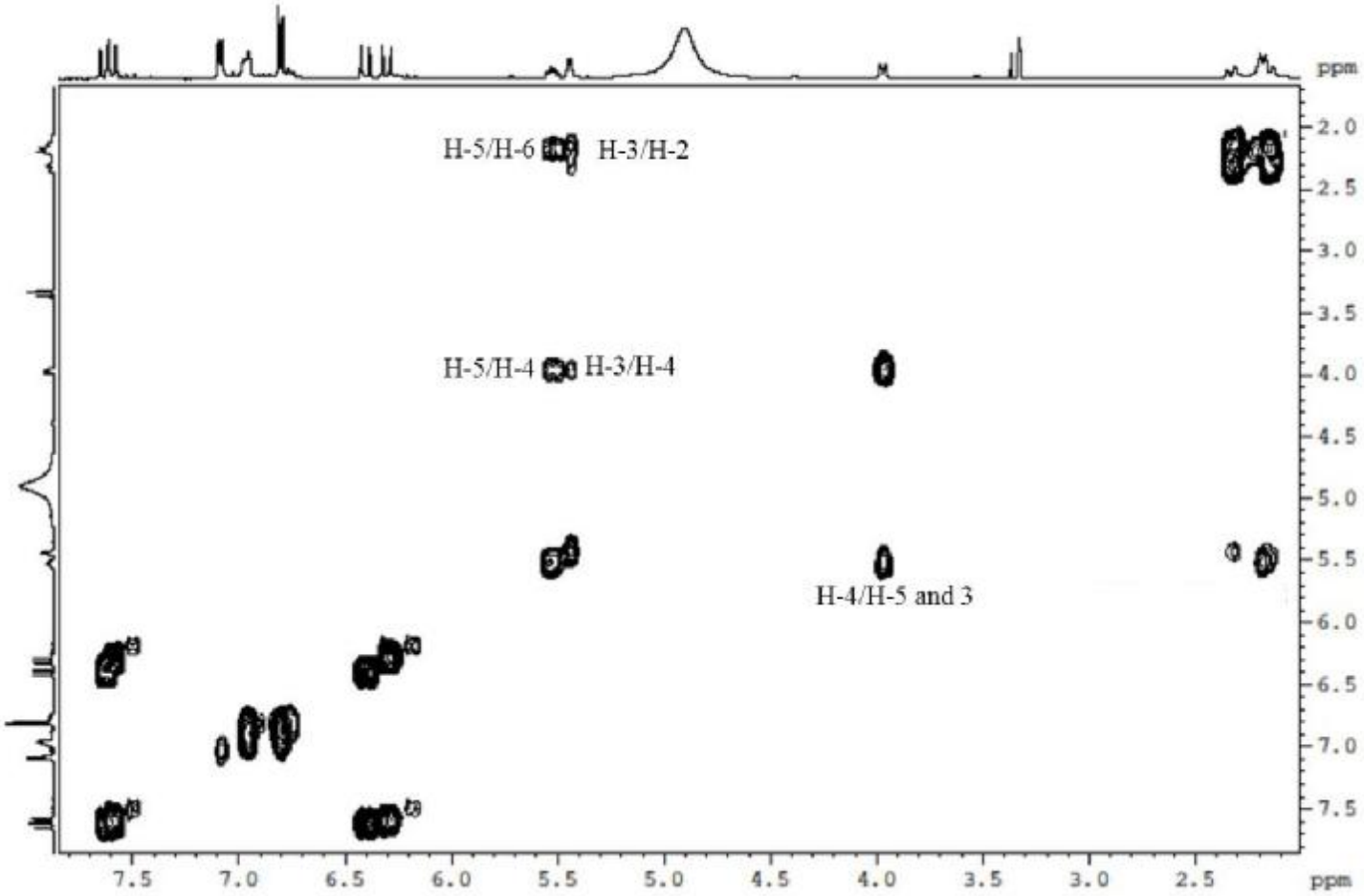

Figure 3.59 COSY spectrum (400 MHz) of TF11 in CD_3OD

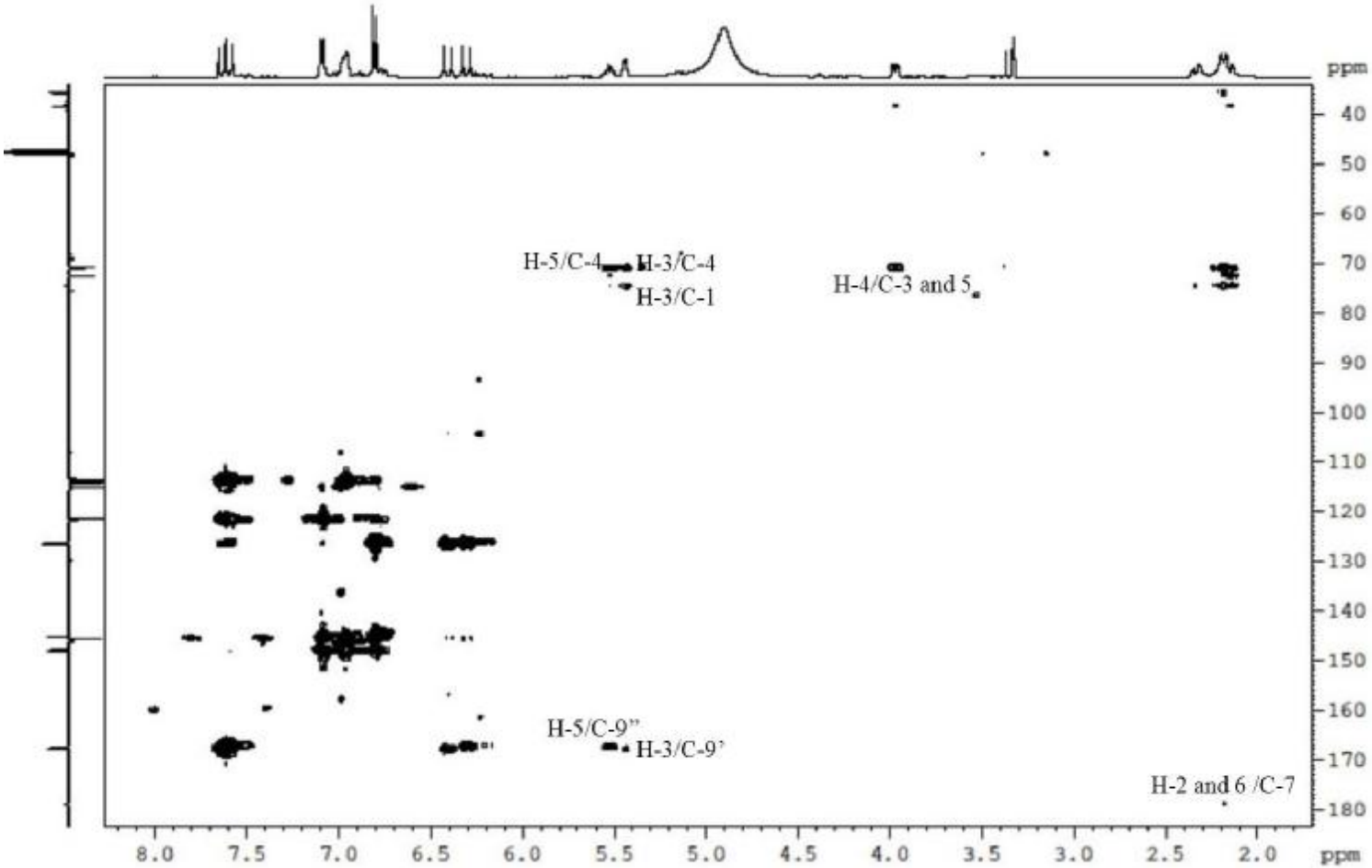

Figure 3.60 HMBC spectrum (400 MHz) of TF11 in CD_3OD

3.4.2.6.4 Characterisation of AL12 as 1, 3-dicaffeoylquinic acid (cynarin)

The ^{1}H NMR spectrum **(Table 3.16, Figure 3.62)** demonstrated typical signals of quinic acid with three oxymethines at δ5.42 (H-3), δ3.79 (H-4) and δ4.30 (H-5) and two methylenes at δ2.07/δ2.62 and δ2.41/δ2.55. The presence of two caffeoyl groups was established with signals at δ7.60 (H-7'/7''), δ6.32 (H-8'), δ6.29 (H-8'') and δ7.08 (H2'/2''), δ6.97 (H-6'/6''), δ6.80 (H-5'/5''). All protons were assigned with the aid of the COSY spectrum **(Figure 3.63)**. The proton at δ5.42 (H-3) was highly deshielded, suggesting that the hydroxyl group at position 3 of quinic acid was substituted by a caffeoyl group.

The ^{13}C NMR spectrum **(Table 3.16)** displayed 25 carbons including two carbonyls, four olefinic metines, six aromatic carbons from caffeoyl groups, three oxymethines, two methylenes and one carbonyl from quinic acid.

In the HMBC spectrum **(Figure 3.64)**, the quinic acid moiety and caffeoyl units revealed similar correlations to those observed for **TF10** and **TF11**. The proton at δ3.79 (H-4) exhibited ^{3}J and ^{2}J correlations, respectively, to one methylene at δ35.9 (C-2) and one oxymethine at δ70.2 (C-3). The proton at δ4.30 (H-5) correlated via ^{3}J couplings to the methine at δ70.2 (C-3) and one quaternary carbon at δ80.4 (C-1). The proton at δ5.42 (H-3) displayed ^{3}J and ^{2}J correlations, respectively, to carbons at δ68.4 (C-5) and δ71.8 (C-4). Four methylene protons at δ2.07/δ2.62 (H-2a/b) and δ2.41/δ2.55 (H-6a/b) correlated via a ^{3}J coupling to the oxymethine at δ71.8 (C-4), and the one at δ2.07 (H-2a) also correlated to one carbonyl at δ173.6 (C-7). The HMBC revealed another important correlation between the deshielded proton at δ5.42 (H-3) and the carbonyl from one caffeoyl group at δ167.4 (C-9''), which established that one caffeic acid unit was attached in C-3 of the quinic acid moiety. No correlation was observed between any other proton on the quinic acid moiety and

the carbonyl on the other caffeoyl group at δ166.7 (C-9'), however the carbon chemical shift of the oxygenated quaternary carbon (C-1) was downfield shifted to δ80.4 compared to that of quinic acid containing a free hydroxyl group at C-1 (e.g. δ74.3 in **TF10** and δ74.6 in **TF11)**, suggesting the second caffeoyl unit was placed at C-1 of the quinic acid moiety (Lee *et al*., 2013).

Based on the above information and by comparision with the data obtained for **TF10** and **TF11**, **AL12** was identified as 1, 3-dicaffeoylquinic acid (cynarin) and the NMR data were in agreement with previously reported data (Wu *et al*., 2007; Danino *et al*., 2009). This compound has been reported from the roots, leaves and seeds of *A. lappa* (Ferracane *et al*., 2010).

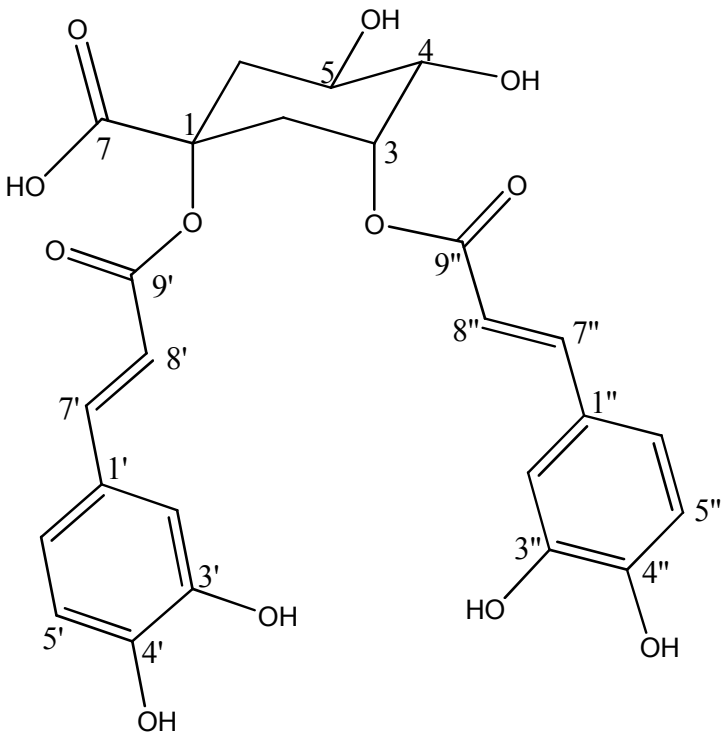

Figure 3.61 Structure of AL12

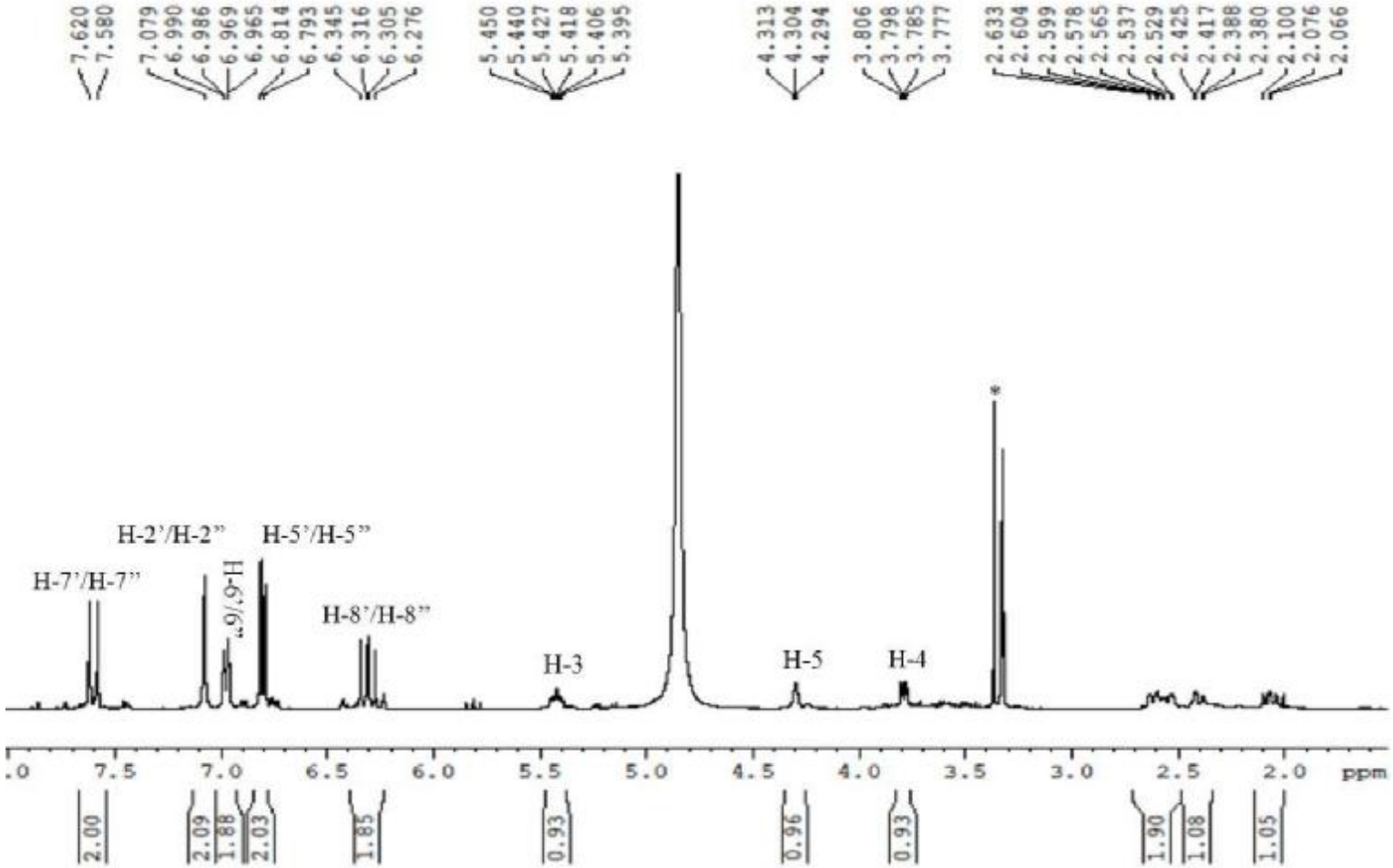

Figure 3.62 ^{1}H NMR spectrum (400 MHz) of AL12 in CD_3OD (*)

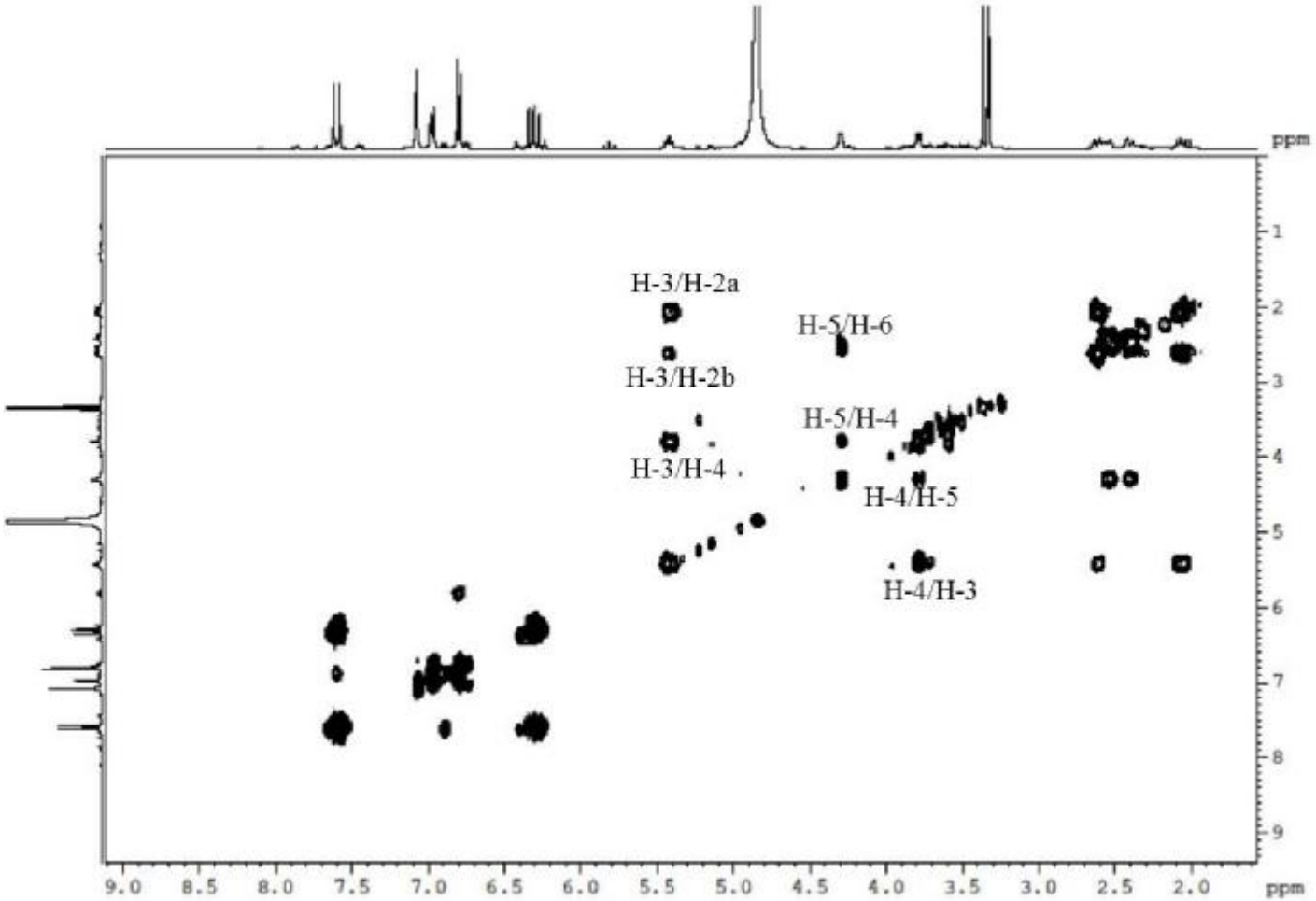

Figure 3.63 COSY spectrum (400 MHz) of AL12 in CD_3OD

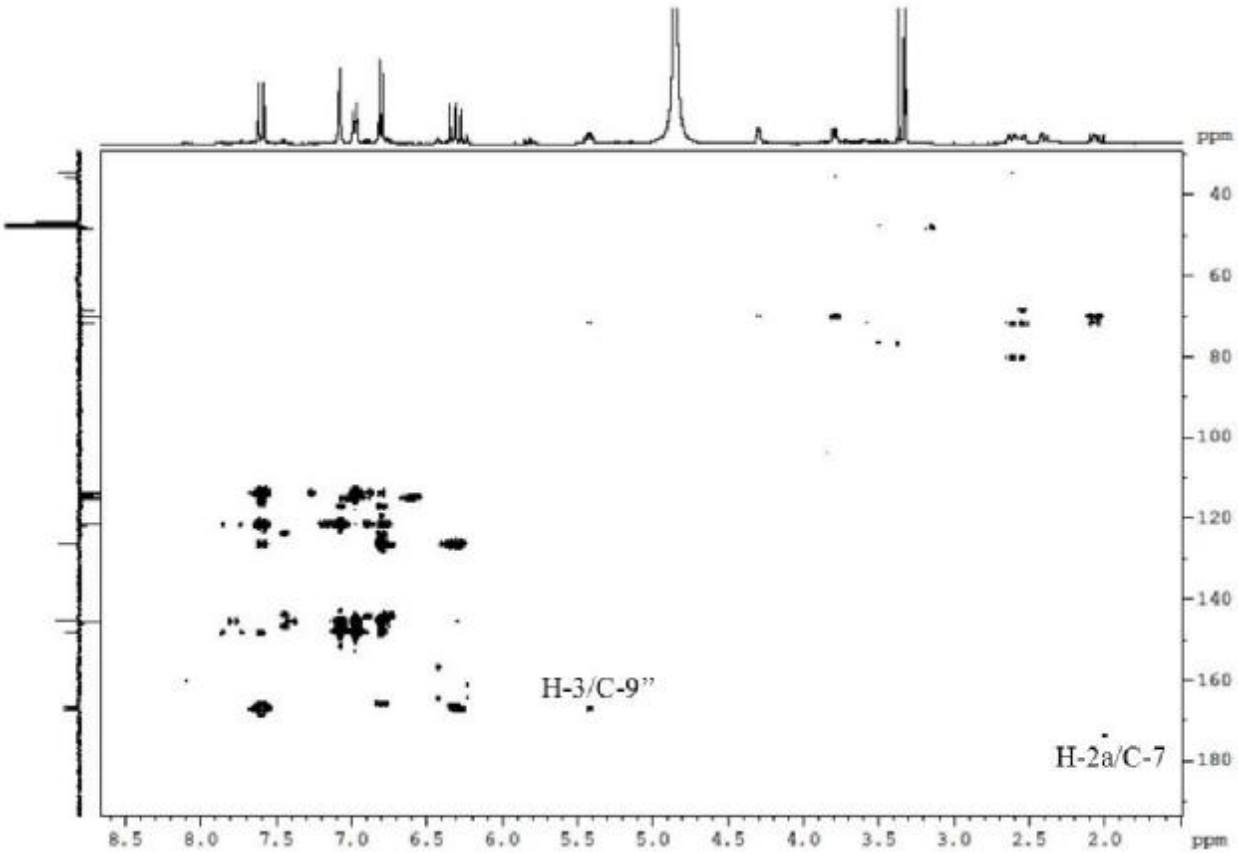

Figure 3.64 HMBC spectrum (400 MHz) of AL12 in CD_3OD

Table 3.16 ^{1}H (400 MHz) and ^{13}C (100 MHz) NMR of TF10, TF11 and AL12 in CD_3OD

Postion	TF10		TF11		AL12	
	H (δ)	C (δ)	H (δ)	C (δ)	H (δ)	C (δ)
1	-	74.3	-	74.6	-	80.4
2	2.21 (1H, *m*)/2.10 (1H, *m*)	36.7	2.33 (1H, *m*)/2.14 (1H, *m*)	35.8	2.07 (1H, *m*)/δ2.62 (1H, *m*)	35.9
3	5.65 (1H, *ddd*, *J*= 3.6, 8.2, 11.9 Hz)	68.6	5.44 (1H, *dd*, *J*= 3.4, 7.2 Hz)	72.5	5.42 (1H, *ddd*, *J*= 4.0, 9.2, 17.8 Hz)	70.2
4	5.21 (1H, *dd*, *J*= 2.9, 6.0 Hz)	73.2	3.97 (1H, *dd*, *J*=3.2, 9.1 Hz)	71.1	3.79 (1H, *dd*, *J*=3.4, 8.4 Hz)	71.8
5	4.16 (1H, *dd*, *J*=5.1, 10.7)	66.3	5.53 (1H, *dd*, *J*= 9.1, 14.4 Hz)	71.0	4.30 (1H, *dd*, *J*=3.8, 8.0 Hz)	68.4
6	2.09 (2H, *m*)	38.3	2.19 (2H, *m*)	38.5	2.41 (1H, *m*)/δ2.55 (1H, *m*)	34.6
7	-	180.9	-	178.9	-	173.6
1’	-	126.4	-	126.7	-	126.4
2’	7.08 (1H, *d*, *J*=2.0 Hz)	113.6	7.09 (H, *d*, *J*=1.5 Hz)	113.9	7.08 (1H, *s*)	113.9
3’	-	145.4	-	145.3	-	145.4
4’	-	148.3	-	148.0	-	148.1
5’	6.79 (1H, *d*, *J*=8.2 Hz)	115.1	6.80 (1H, *d*, *J*=8.1 Hz)	115.1	6.80 (1H, *d*, *J*=8.2 Hz)	115.1
6’	6.95 (1H, *dd*, *J*=2.0, 8.2 Hz)	121.8	6.96 (1H, *dd*, *J*=1.7, 8.1 Hz)	121.7	6.97 (1H, *dd*, *J*=1.7, 8.4 Hz)	121.6
7’	7.60 (1H, *d*, *J*=15.8 Hz)	146.0	7.63 (1H, *d*, *J*=15.8 Hz)	145.6	7.60 (2H, *d*, *J*=15.8 Hz)	145.9
8’	6.32 (1H, *d*, *J*=15.8 Hz)	113.7	6.40 (1H, *d*, *J*=15.9 Hz)	114.5	6.32 (1H, *d*, *J*=15.8 Hz)	114.3
9’	-	167.0	-	167.9	-	166.7
1’’	-	126.3	-	126.5	-	126.5
2’’	7.04 (1H, *d*, *J*=2.0 Hz)	113.8	7.09 (H, *d*, *J*=1.5 Hz)	113.9	7.08 (1H, *s*)	113.9
3’’	-	145.3	-	145.3	-	145.4
4’’	-	148.1	-	148.1	-	148.2
5’’	6.76 (1H, *d*, *J*=8.2 Hz)	115.2	6.80 (1H, *d*, *J*=8.1 Hz)	115.2	6.80 (1H, *d*, *J*=8.2 Hz)	115.1
6’’	6.90 (1H, *dd*, *J*=2.0, 8.2 Hz)	121.7	6.96 (1H, *dd*, *J*=1.7, 8.1 Hz)	121.7	6.97 (1H, *dd*, *J*=1.7, 8.4 Hz)	121.6
7’’	7.53 (1H, *d*, *J*=15.8 Hz)	145.8	7.59 (1H, *d*, *J*=15.8 Hz)	145.7	7.60 (2H, *d*, *J*=15.8 Hz)	145.9
8’’	6.26 (1H, *d*, *J*=15.8 Hz)	113.7	6.30 (1H, *d*, *J*=15.9 Hz)	114.0	6.29 (1H, *d*, *J*=15.8 Hz)	113.8
9’’	-	167.1	-	167.6	-	167.4

3.5 Phenylethanoid glycoside

3.5.1 Characterisation of VT11 as verbascoside

VT11 was isolated from the ethyl acetate extract of *V. thapsus* as a greenish amorphous solid **(Section 2.4: Protocol 9 and 10, 0.0352% yield)**. On the TLC plate, it revealed a quenching spot under short UV light and a light blue fluorescence under long UV. It turned mauve brown after spraying with vanillin-sulphuric acid reagent followed by heating.

The negative ion mode HRESI-MS data gave a quasi-molecular ion $[M-H]^-$ at *m/z* 623.1984, suggesting a molecular formula of $C_{29}H_{36}O_{15}$ (DBE=12).

The ^{1}H NMR spectrum **(Table 3.17, Figure 3.66)** exhibited signals typical of a caffeoyl group with an ABX system at δ7.10 (1H, *brs*, H-2), δ6.97 (1H, *d*, *J*=8.2 Hz, H-6) and δ6.82 (1H, *d*, *J*=8.2 Hz, H-5) and two olefinic protons at δ6.31 (1H, *d*, *J*=15.9 Hz, H-8) and δ7.62 (1H, *d*, *J*=15.9 Hz, H-7). The large *J*-coupling constant (15.9 Hz) revealed the *trans*-configuration of the double bond in the caffeic acid moiety.

The spectrum also displayed another ABX system with aromatic protons at δ6.58 (1H, *d*, *J*=8.0 Hz, H-6'), δ6.71 (1H, *d*, *J*=8.0 Hz, H-5') and δ6.73 (1H, *brs*, H-2'). The HSQC and COSY experiments further revealed one methylene at δ2.80 (2H, *t*, *J*=7.0 Hz, H-7') and an oxymethylene group at δ3.73 (1H, *m*, H-8a')/δ4.05 (1H, *m*, H-8b'). These data suggested the presence of one hydroxytyrosol moiety.

A methyl group at δ1.12 (3H, *d*, *J*=6.1 Hz, H-6''') and an anomeric proton at δ5.22 (1H, *d*, *J*=1.5 Hz, H-1''') accounted for one 6-deoxy sugar unit. Another anomeric

proton at δ4.39 (1H, *d*, *J*=7.9 Hz, H-1''), one oxymethylene and four additional oxymethines were also observed, suggesting the presence of a second sugar unit. With the aid of the COSY and TOCSY experiments **(Figure 3.68)**, the two sugar units were identified as rhamnose and glucose. Protons H-1''' and H-2''' of the rhamnose unit were assigned as equatorial due to the small coupling constant detected for H-1''' (*J*=1.5 Hz). The coupling constant for H-4''' (δ3.33, *t*, *J*=9.1 Hz) indicated a *trans*-diaxial orientation of H-3'''/H-4'''/H-5'''. In contrast, the large coupling constant for H-1'' (δ4.39, *J*=7.9 Hz) indicated that H-1'' and H-2'' were *trans*-diaxial. Proton H-4'' (δ4.96, *t*, *J*=9.1 Hz) also appeared as a triplet with a large coupling constant, thus allowing the assignment of H-3'', H-4'' and H-5'' as *trans*-diaxial. On the basis of the above data one sugar moiety was identified as α-L-rhamnopyranose and the other as β-D-glucopyranoside.

The ^{13}C NMR spectrum **(Table 3.17, Figure 3.67)** established 29 carbons including one carbonyl, one methyl, three methylenes, eighteen methines and six quaternary carbons. Distinctive signals for two anomeric carbons at δ101.7 (C-1''') and δ102.8 (C-1''), one oxymethylene at δ61.0 (C-6'') and the methyl at δ17.2 (C-6''') further confirmed the presence of one glucose and one rhamnose uint.

In the HMBC spectrum **(Table 3.17, Figure 3.69)**, the olefinic proton on the caffeoyl group at δ7.62 (H-7) correlated via ^{3}J couplings to the carbonyl at δ167.1 (C-9) and two aromatic methines at δ122.0 (C-6) and δ114.0 (C-2). The other olefinic proton at δ6.31 (H-8) exhibited a ^{3}J correlation to one quaternary carbon at δ126.4 (C-1). The protons at δ7.10 (H-2) and δ6.97 (H-6) showed ^{3}J and ^{2}J couplings to oxygen-bearing quaternary carbons at δ148.4 (C-4) and δ1465.4 (C-3), respectively. On the hydroxytyrosol moiety, the methylene protons at δ2.80 (H-7') displayed ^{3}J couplings to carbons at δ115.9 (C-2') and δ120.1 (C-6'), and a ^{2}J correlation to the oxymethylene carbon at δ70.9 (C-8'). The oxymethylene signals at δ 3.73 and δ 4.05

(H-8'a/b) correlated via ^{3}J couplings to one anomeric carbon at δ102.8 (C-1''), indicating the hydroxytyrosol was linked to the C-1'' of β-D-glucopyranoside. On the glucose unit, the ^{3}J correlation between the anomeric proton at δ4.39 (H-1'') and the oxymethylene carbon at δ70.9 (C-8') further established the bridge link between β-D-glucopyranoside and hydroxytyrosol. The link between the caffeoyl group and β-D-glucopyranoside was also detected with the ^{3}J coupling between the proton at δ4.96 (H-4'') the carbonyl at δ167.1 (C-9). In addition, the protons at δ3.84 (H-3'') and δ5.22 (H-1''') showed ^{3}J correlations to the carbons at δ101.7 (C-1''') and δ80.5 (C-3''), respectively, suggesting that the glucose and rhamnose units were linked through C-3'' and C-1'''.

The above data led to the identification of **VT11** as verbascoside. The NMR data were in good agreement with a previous publication (Ersoz *et al*., 2002). This compound has previously been isolated from the whole plants of *V. thapsus* (Hussain *et al*., 2009).

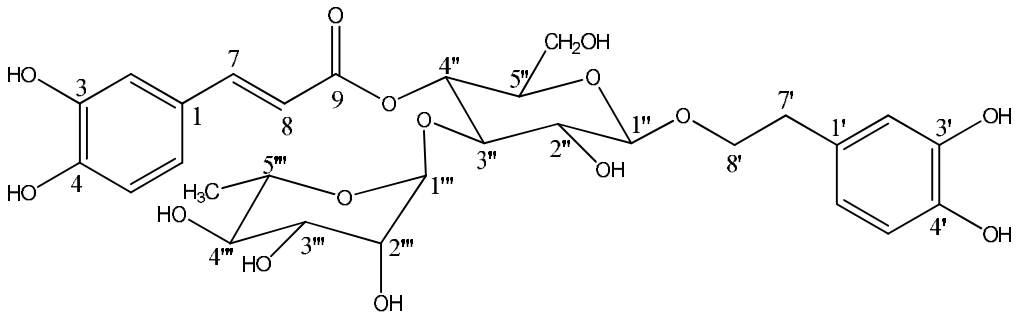

Figure 3.65 Structure of VT11

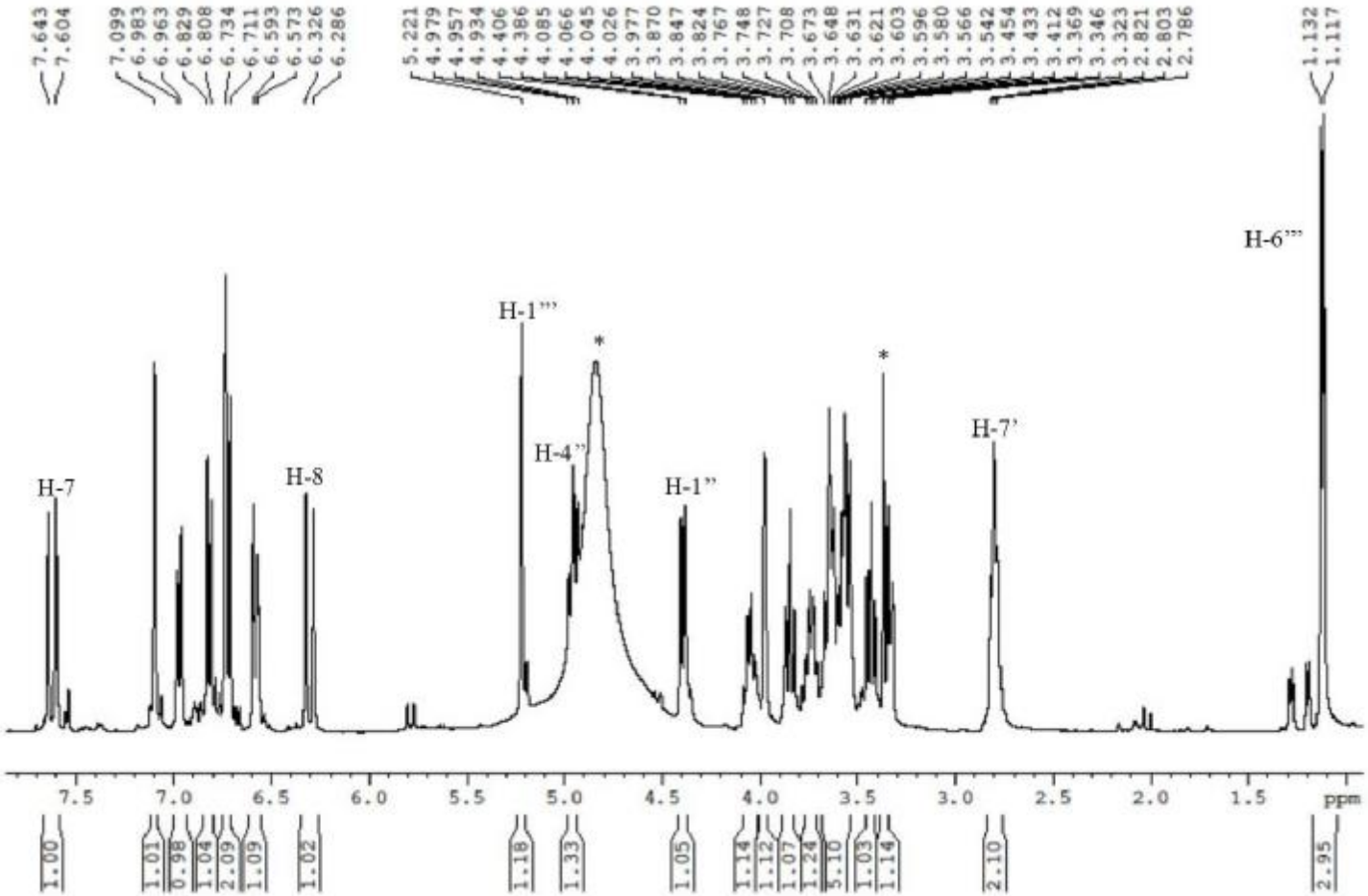

Figure 3.66 ^{1}H NMR spectrum (400 MHz) of VT11 in CD_3OD (*)

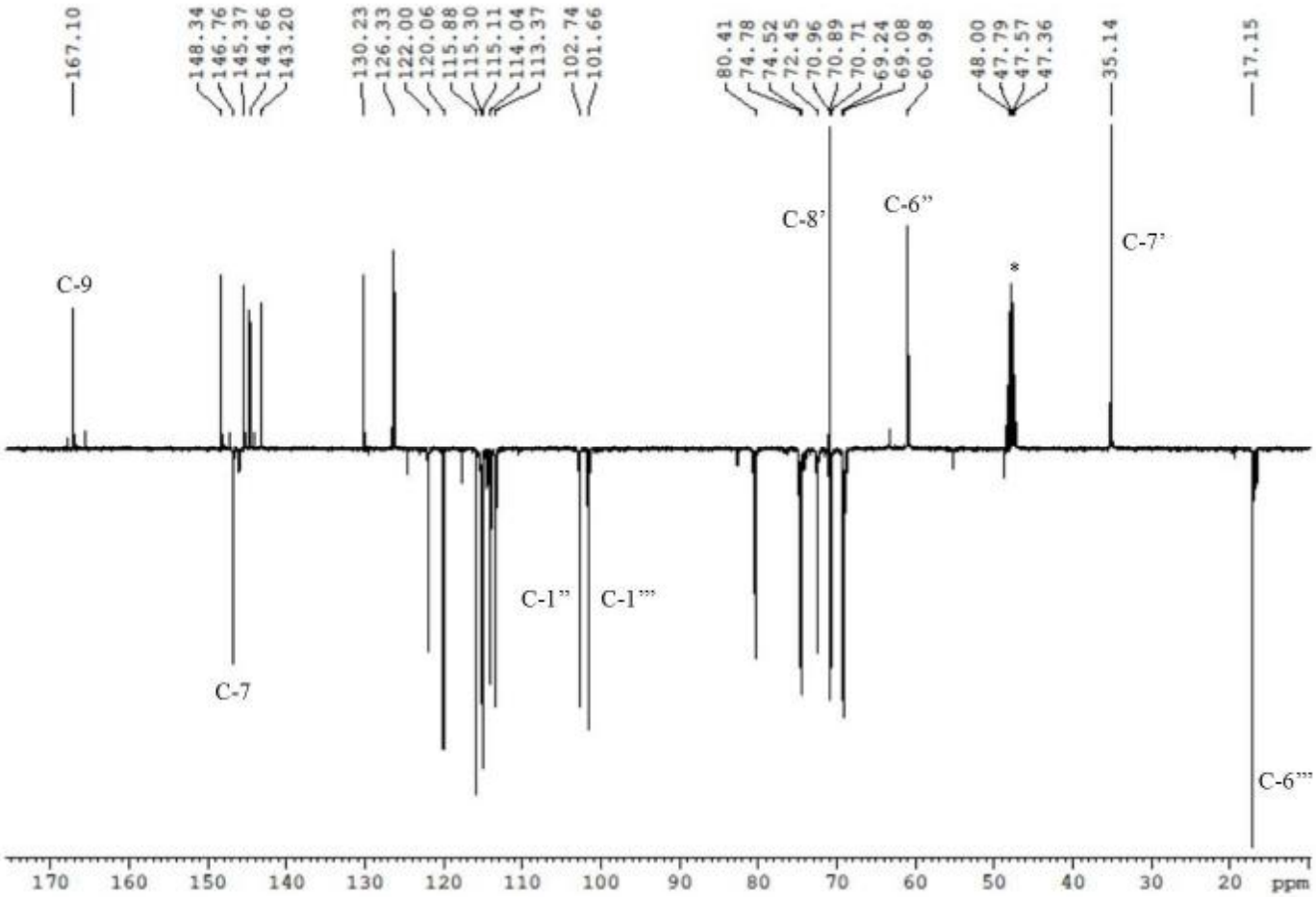

Figure 3.67 DEPTQ 135 ^{13}C NMR spectrum (100 MHz) of VT11 in CD_3OD (*)

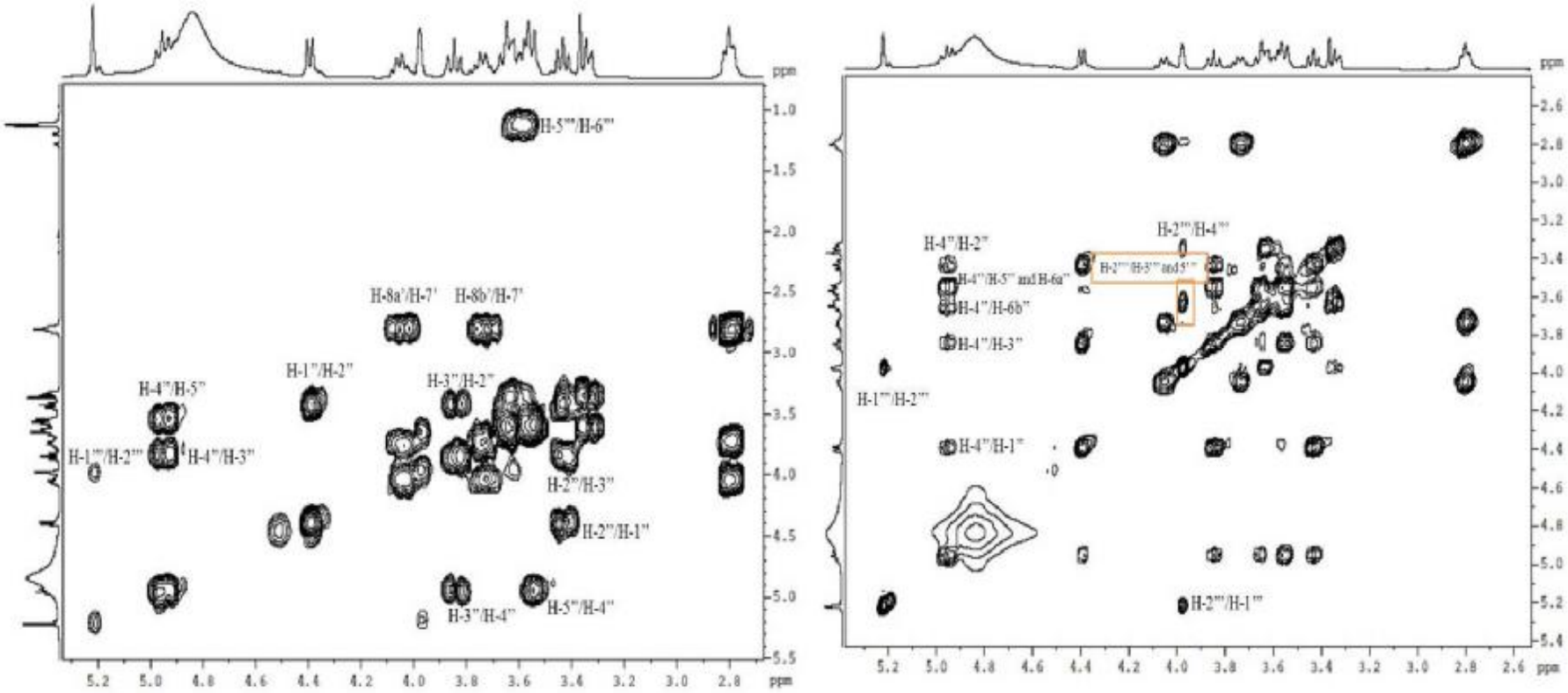

Figure 3.68 COSY (left) and TOCSY (right) NMR spectra (400 MHz) of VT11 in CD_3OD

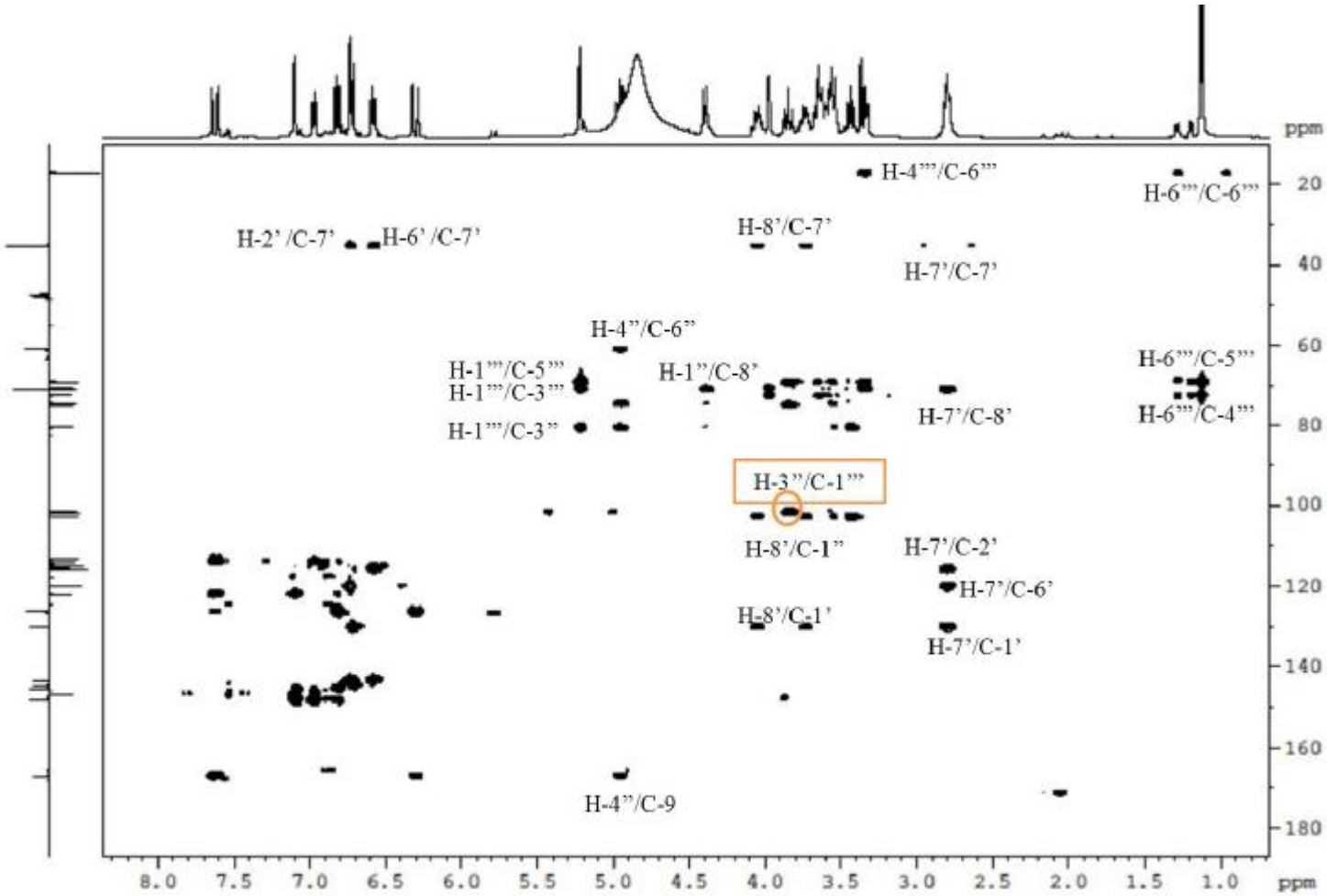

Figure 3.69 HMBC spectrum (400 MHz) of VT11 in CD_3OD

Table 3.17 ^{1}H (400 MHz) and ^{13}C (100 MHz) NMR of VT11 in CD_3OD

Position	H (δ)	C (δ)	Selected HMBC correlations
Caffeoyl moiety			
1	-	126.4	
2	7.10 (1H, *brs*)	114.0	C-6, C-4, C-7, C-3
3	-	145.4	
4	-	148.4	
5	6.82 (1H, *d*, *J*=8.2 Hz)	115.3	C-1, C-3, C-4, C-6
6	6.97 (1H, *d*, *J*=8.2 Hz)	122.0	C-2, C-4, C-7, C-3
7	7.62 (1H, *d*, *J*=15.9 Hz)	146.8	C-9, C-7, C-1, C-6, C-2
8	6.31 (1H, *d*, *J*=15.9 Hz)	113.4	C-1, C-9
9	-	167.1	
Hydroxytyrosol			
1’	-	130.2	
2’	6.73 (1H, *brs*)	115.9	C-6’, C-4’, C-7’
3’	-	144.8	
4’	-	143.2	
5’	6.71 (1H, *d*, *J*=8.0 Hz)	115.1	C-1’, C-3’
6’	6.58 (1H, *d*, *J*=8.0 Hz)	120.1	C-7’, C-2’, C-4’
7’	2.80 (2H, *t*, *J*=6.8, 7.6 Hz)	35.2	C-8’, C-2’, C-6’, C-1’
8’	3.73 (1H, *m*) /4.05 (1H, *m*)	70.9	C-7’, C-1’’, C-1’
Glucose			
1’’	4.39 (1H, *d*, *J*=7.9 Hz)	102.8	C-8’, C-5’’, C-3’’
2’’	3.43 (1H, *t*, *J*=8.4 Hz)	74.8	
3’’	3.84 (1H, *t*, *J*=9.2 Hz)	80.5	C-4’’, C-5’’, C-2’’, C-1’’’
4’’	4.96 (1H, *t*, *J*=9.1 Hz)	69.2	C-9, C-3’’, C-5’’, C-6’’
5’’	3.54 (1H, *m*)	74.5	C-1’’, C-4’’, C-5’’
6’’	3.56 (1H, *m*) /3.65 (1H, *m*)	61.0	C-4’’
Rhamnose			
1’’’	5.22 (1H, *d*, *J*=1.5 Hz)	101.7	C-1’’’, C-3’’, C-3’’’, C-5’’’
2’’’	3.98 (1H, *brs*)	71.0	C-4’’’, C-3’’’
3’’’	3.64 (1H, *m*)	70.7	C-4’’’, C-5’’’
4’’’	3.33 (1H, *t*, *J*=9.1 Hz)	72.5	
5’’’	3.60 (1H, *m*)	69.1	
6’’’	1.12 (3H, *d*, *J*=6.1 Hz)	17.2	

3.6 Miscellaneous compounds

3. 6.1 Characterisation of AL1 as *n*-nonacosane

AL1 was isolated from the *n*-hexane extract of *A. lappa* as a white flaky solid **(Section 2.4: Protocol 1, 0.0159% yield)**. On the TLC plate, **AL1** showed no quenching spot under short UV light and no fluorescence under long UV. It gave a bright pink spot after spraying with anisaldehyde-sulphuric acid reagent and heating.

HREI-MS analysis displayed a molecular ion $[M]^+$ at *m/z* 408 and some fragments at *m/z* 57, 71, 85, 99, 133, 127, indicating a molecular formula of $C_{29}H_{60}$ (DBE=0).

The ^{1}H NMR spectrum revealed a sharp singlet at δ1.24 and a triplet at δ0.87, integrating for 54 and 6 protons, respectively. This indicated that there were two methyl groups and 27 methylenes

The above ^{1}H NMR and HREI-MS data established the identification of **AL1** as *n*-nonacosaneand and the data were in good agreement with the literature data (Chen *et al.*, 2008). This is the first report of the isolation of *n*-nonacosane from *A. lappa*.

3.6.2 Characterisation of VT4 as 1-monoacylglycerol

VT4 was isolated from the ethyl acetate extract of *V. thapsus* as a greenish oil **(Section 2.4: Protocol 9, 0.0219% yield)**. A brown spot was observed on the TLC plate after treatment with vanillin-sulphuric acid reagent and heating.

The positive ion mode HRESI-MS spectrum gave a quasi-molecular ion $[M+H]^+$ at *m/z* 135.0651, suggesting a molecular formula of $C_5H_{10}O_4$ (DBE=1).

The ^{1}H NMR spectrum **(Figure 3.70)** displayed a sharp singlet at δ2.13 (3H) typical of methyl protons of an acetyl group. The spectrum also showed protons signals at δ3.62 (1H, *dd*, *J*=3.9, 11.5 Hz)/δ3.71 (1H, *dd*, *J*=3.9, 11.5 Hz) and δ4.18 (1H, *dd*, *J*=4.7, 11.6 Hz)/δ4.21 (1H, *dd*, *J*=4.7, 11.6 Hz) for a pair of two non-equivalent oxymethylene protons. A multiplet accounting for one proton was observed at δ3.96.

The ^{13}C NMR spectrum exhibited one mthyl at δ20.8, two oxymethylenes at δ63.3 and δ65.3, one oxymethine at δ70.2 and a carbonyl at δ171.5.

In the HMBC spectrum, the signal at δ2.13 (Me-5) correlated to the carbonyl at δ171.5 (C-4), establishing the presence of the acetyl group. The oxymethylene protons at δ4.18/δ4.21 (H-1a/b) revealed ^3J couplings to carbons at δ63.3 (C-3) and δ171.5 (C-4). The other oxymethylene protons at δ3.62/δ3.71 (H-3a/b) displayed ^3J and ^2J correlations to carbons at δ65.3 (C-1) and δ70.2 (C-2), respectively.

This led to the characterisation of **VT4** as 1-monoacylglycerol and the NMR data were in agreement with previously published data (Homma *et al*., 2012). This is the first report of the isolation of 1-monoacylglycerol from *V. thapsus*.

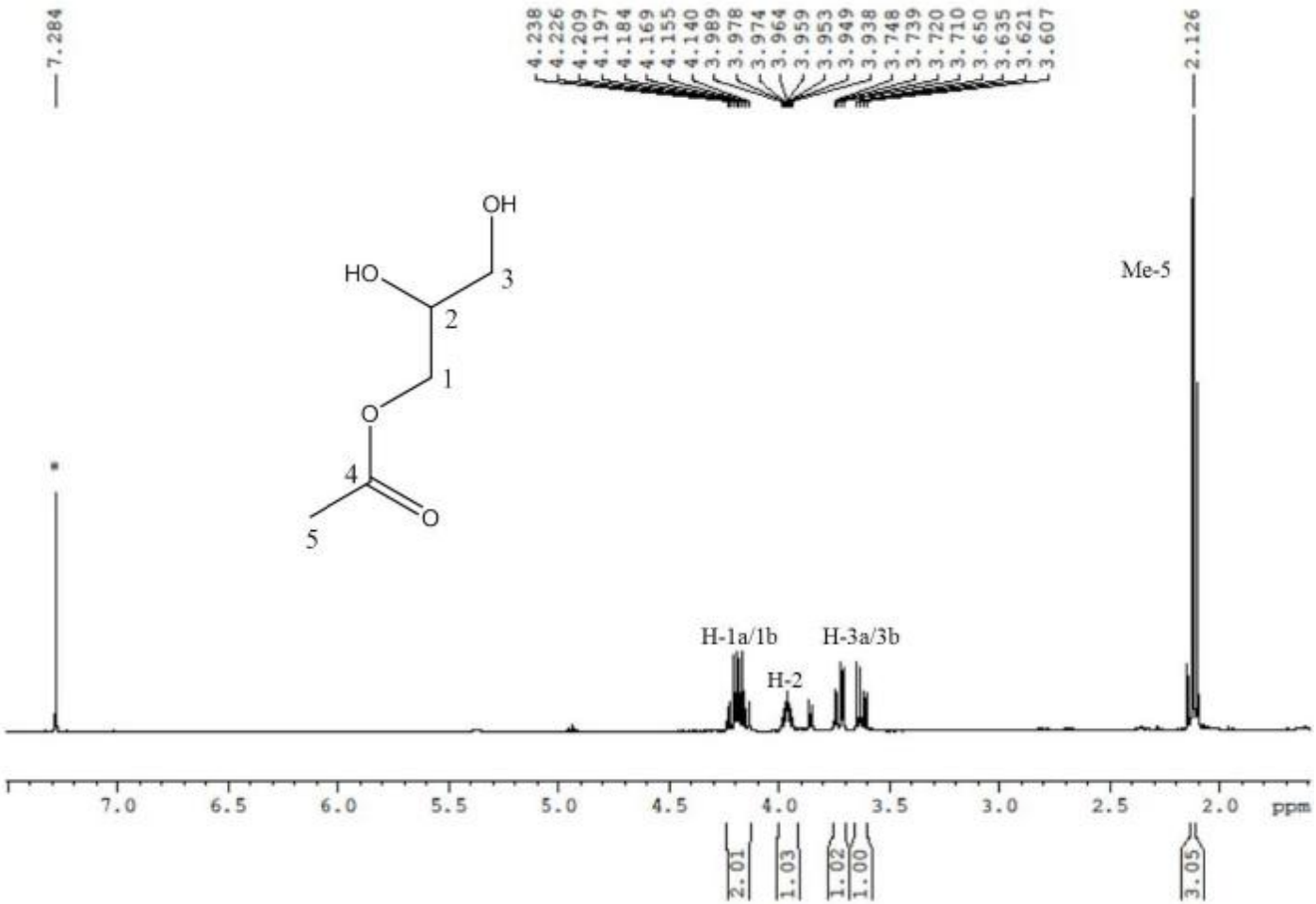

Figure 3.70 ^{1}H NMR spectrum (400 MHz) of VT4 in $CDCl_3$ (*)

Part B Antibacterial studies

3.7 Antitubercular activity of crude extracts and isolated compounds

3.7.1 Results from the SPOTi assay

3.7.1.1 *Arctium lappa* extracts and isolated compounds

Results of the activity of *A. lappa* extracts and selected isolated compounds against *M. tuberculosis* $H_{37}Rv$ in the SPOTi assay are presented in **Table 3.18**. The *n*-hexane extract **(325H)** showed the highest activity with an MIC value of 62.5 µg/mL. The ethyl acetate extract **(325E)** exhibited moderate activity (MIC=125 µg/mL) and the methanol extract **(325M)** was inactive at the highest concentration of 125 µg/mL used in the assay. Subsequent screening of the three phases obtained following liquid-liquid partition of the methanol extract revealed that the dichloromethane phase **(325MD)** was active with an MIC value of 62.5 µg/mL, whereas the *n*-butanol and water phases **(325MB** and **325MW)** were both inactive at the highest concentration (125 µg/mL). The MIC values of isoniazid and rifampicin against *M. tuberculosis* $H_{37}Rv$ used in this assay were consistent with the literature (Guzman *et al*., 2013). This is the first time that the antitubercular acitivity of *A. lappa* is investigated. These results provide in part some scientific basis for the ethnomedicinal use of *A. lappa* as a traditional anti-TB remedy.

Among the screened compounds isolated from the *n*-hexane extract, only the β-sitosterol/stigmasterol mixture **(AL2)** revealed moderate activity (MIC=125 µg/mL). Taraxasterol **(AL3)** and taraxasterol acetate **(AL4)** were both inactive at the concentration (125 µg/mL), and *n*-nonacosane **(AL1)** had no activity at 500 µg/mL.

The activity observed for the crude *n*-hexane extract was stronger than that observed

for the pure isolated compounds, suggesting that the acitivity could either be attributable to other (non-purified) phytochemical(s) or to compounds acting synergistically. Previous studies have reported the activity of β-sitosterol and stigmasterol against *M. tuberculosis* $H_{37}Rv$ using a MABA assay (MICs=32.8 and 64.0 μg/mL, respectively) (Gutierrez-Lugo *et al*., 2005); their mixture also inhibited the growth of *M. tuberculosis* $H_{37}Rv$ in the MABA assay (MIC=128 μg/mL) (Tan *et al*., 2008). Although the MABA assay relies on a different method to the SPOTi assay, our results seemed to correlate well with previous reports.

The anti-TB activity of taraxasterol has been reported previously, and it was active against *M. tuberculosis* $H_{37}Rv$ (ATCC 27294) in the MABA assay with an MIC value of 64.0 μg/mL (Akihisa *et al*., 2005). This is the first report of the anti-TB activity of taraxasterol using the SPOTi aasay. The antitubercular investigation of taraxasterol acetate and *n*-nonacosane is also reported for the first time.

A literature search revealed that daucosterol (**AL6**) has previously reported as active against *M. tuberculosis* $H_{37}Rv$ with an MIC value of 128.0 μg/mL (Woldemichael *et al*., 2004). In this study, daucosterol was isolated from the active ethyl acetate extract of *A. lappa*, suggesting the activity of the ethyl acetate extract may be in part attributable to this comound.

The active dichloromethane phase yielded isololiolide **(AL13)** and melitensin **(AL14)**. Results exhibited that both compounds were inactive at the highest concentration (500 μg/mL) used in the assay, suggesting that the activity of the dichloromethane phase was probably due to other phytochemical(s). Nevertheless, this is the first report of the screening of isololiolide and melitensin for antitubercular activity.

Taraxasterol **(AL3)**, taraxasterol acetate **(AL4)**, isololiolide **(AL13)** and melitensin **(AL14)** belong to the group of terpenes/terpenoids. Numerous terpenes/terpenoids, mainly sesquiterpenes and triterpenes, have been reported with moderate to high activity against *M. tuberculosis*. A study on structure-activity relationships revealed that the α-methylene-γ-lactone moiety seems to be an essential, but not sufficient, structural requirement for significant antitubercular activity of sesquiterpenes, and the presence of a second alkylating site may enhance the activity, whereas some conflicting results observed for various types of triterpenoids makes it difficult to predict structural requirements for antitubercular activity (Cantrell *et al*., 2001).

β-Sitosterol/stigmasterol mixture **(AL2)** and daucosterol **(AL6)** are plant steroids. Steroids are promising antimycobacterial agents; their polar ‘‘head groups’’ and flexible nonpolar ‘‘phytyl tails’’ are involved in mycobacterial cell wall disruption (Rugutt and Rugutt, 2002). It was reported that the antimycobacterial activity of steroids depends on hydrophobicity and the type of substituents on the phytyl moiety (Rugutt and Rugutt, 2002; 2012).

Table 3.18 Activity of *A. lappa* extracts and selected isolated compounds against *M. tuberculosis* $H_{37}Rv$ in SPOTi assay

Sample	MICs µg/mL (µM)
325H	62.5
325E	125
325M	NA[1]
325MD	62.5
325MB	NA[1]
325MW	NA[1]
AL1	NA[2]
AL2	125
AL3	NA[1]
AL4	NA[1]
AL13	NA[2]
AL14	NA[2]
INH	0.01 (0.07)
RIF	0.01 (0.01)

325H: *A. lappa n*-hexane extract; **325E**: *A. lappa* ethyl acetate extract; **325M**: *A. lappa* methanol extract; **325MD**: dichloromethane phase from *A. lappa* methanol extract partitioning; **325MB**: *n*-butanol phase from *A. lappa* methanol extract partitioning; **325MW**: water phase from *A. lappa* methanol extract partitioning; INH: isoniazid; RIF: rifampicin; NA[1]: no activity at 125 µg/mL; NA[2]: no activity at 500 µg/mL

3.7.1.2 *Tussilago farfara* extracts and isolated compounds

Results of the activity of *T. farfara* extracts and selected isolated compounds against *M. tuberculosis* $H_{37}Rv$ in the SPOTi assay are presented in **Table 3.19**. The *n*-hexane and ethyl acetate extracts **(326H** and **326E)** demonstrated good activity both with an MIC value of 62.5 µg/mL. The methanol extract **(326M)** showed moderate activity (MIC=125 µg/mL). The dichloromethane phase **(326MD)** had an MIC value of 500 µg/mL, and the *n*-butanol and water phases **(326MB** and **326MW)** were both inactive at the highest concentration of 500 µg/mL used in the assay. The above results provide for the first time scientific evidence to support the ethnomedicinal use of *T. farfara* as a traditional antitubercular remedy.

β-Sitosterol/stigmasterol mixture **(TF1)** and loliolide **(TF2)**, isolated from the *n*-hexane extract, were active at MICs of 125 and 250 µg/mL (1273.9 µM), respectively. The activity of the *n*-hexane extract may be attributable to these compounds. This is the first report of the anti-TB study of loliolide. Loliolide and isololiolide are isomers, but the latter, from the active dichloromethane phase of *A. lappa*, was not active at the highest concentration (500 µg/mL) used in this study.

Among the compounds isolated from the ethyl acetate extract, *p*-coumaric acid **(TF4)**, the *p*-coumaric acid/4-hydroxybezoic acid mixture **(TF5)**, and caffeic acid **(TF7)**, revealed strong to weak activity with MICs of 31.3 (190.7 µM), 62.5 and 250 µg/mL (1387.6 µM), respectively. Among the flavonoids, quercetin **(TF6)** had an MIC of 500 µg/mL (1654.3 µM), kaempferol **(TF3)** and kaempferol-3-*O*-glucoside **(TF9)** were both inactive at the highest concentration of 500 µg/mL. Thus, the activity of the ethyl acetate extract may be attributable to the combined effect of simple phenolics. A previous report has identified that *p*-coumaric acid had an MIC>128 µg/mL in the MABA assay (Gutierrez-Lugo *et al*., 2005). The

antitubercular activity of the *p*-coumaric acid/4-hydroxybenzoic acid mixture and caffeic acid is reported for the first time in this study. Quercetin has previously been reported as active in the MABA assay at the concentration of 312.5 µg/mL (Boligon *et al*., 2012), and even more active in the BACTEC radiometric assay with an MIC value of 50.0 µg/mL (Yadav *et al*., 2013). Both kaempferol and kaempferol-3-*O*-glucoside have been reported as inactive in the BACTEC radiometric assay (MIC>100 and 128 µg/mL, respectively) (Yadav *et al*., 2013; Woldemichael *et al*., 2004). This is the first report of the screening of all compounds in the SPOTi assay.

Cinnamic acid derivatives are attractive anti-TB drug leads when used along with known antibiotics (De *et al*., 2012b). *p*-Coumaric acid and caffeic acid are hydroxy cinnamic acids, arising from deamination of phenylalanine in plants. The mode of anti-TB action of these small molecules remains unidentified to date (De *et al*., 2012a).

Many flavonoids have been reported with anti-TB activity. One possible mechanism is that flavonoids inhibit the putative dehydratase enzyme involved in *M. tuberculosis* fatty acid synthase II (Brown *et al*., 2007). Structure-activity relationships studies have been carried out to determine the specific structural requirements for flavonoids to be anti-TB active. It was revealed that hydroxyls in C-5 and C-7 did not contribute to the activity, but hydroxyls in C-5, 6, 7 (trihydroxy) or 3', 4' (dihydroxy) were particularly important, and that *O*-methylation or glycosylation at any of the di- or tri-hydroxyl substitutions inactivated the anti-TB potential of the flavonoids (Yadav *et al*., 2013). This correlates well with the results obtained for the three flavonoids in this study.

Table 3.19 Activity of *T. farfara* extracts and selected isolated compounds against *M. tuberculosis* $H_{37}Rv$ in SPOTi assay

Sample	MICs µg/mL (µM)
326H	62.5
326E	62.5
326M	125
326MD	500
326MB	NA
326MW	NA
TF1	125
TF2	250 (1273.9)
TF3	NA
TF4	31.3 (190.7)
TF5	62.5
TF6	500 (1654.3)
TF7	250 (1387.6)
TF9	NA
INH	0.01 (0.07)
RIF	0.01 (0.01)

326H: *T. farfara n*-hexane extract; **326E**: *T. farfara* ethyl acetate extract; **326M**: *T. farfara* methanol extract; **326MD**: dichloromethane phase from *T. farfara* methanol extract partitioning; **326MB**: *n*-butanol phase from *T. farfara* methanol extract partitioning; **326MW**: water phase from *T. farfara* methanol extract partitioning; INH: isoniazid; RIF: rifampicin; NA: no activity at 500 µg/mL

3.7.1.3 *Verbascum thapsus* extracts and isolated compounds

Results of the activity of *V. thapsus* extracts and selected isolated compounds against *M. tuberculosis* $H_{37}Rv$ in the SPOTi assay are presented in **Table 3.20**. The ethyl acetate extract **(605E**) showed weak activity (MIC=250 µg/mL), the methanol extract **(605E**) revealed an MIC value of 500 µg/mL and the *n*-hexane extract **(605H)** had no activity at 500 µg/mL. Among the three phases derived from the methanol extract, the dichloromethane phase **(605MD)** had an MIC of 500 µg/mL, and the other two phases **(605MB** and **605MW)** were inactive at 500 µg/mL. This is the first report of the study of the antitubercular activity of *V. thapsus*.

Ten compounds were isolated from the ethyl acetate extract, including four phenolic derivatives, two pheophorbides and two pheophytins. *Trans*-cinnamic acid **(VT5)** exhibited weak activity with an MIC value of 250 µg/mL (1687.4 µM), 4-hydroxybenzoic acid **(VT9)** and 4-hydroxy-3-methoxybenzoic acid **(VT8)** had MICs of 500 µg/mL (3620.0 and 2973.7 µM, respectively), and verbascoside **(VT11)** had no activity at 500 µg/mL. Pheophorbide A **(VT3)** and its ethyl ester **(VT10)** had MICs of 500 µg/mL (843.6 and 806.1 µM, respectively), and pheophytin A **(VT6)** and pheophytin B **(VT7)** showed no activity at 500 µg/mL. Luteolin **(VT2)** displayed an MIC of 500 µg/mL (1746.8 µM) and 1-monoacylglycerol **(VT4)** was not active at 500 µg/mL. It is not clear whether the activity observed for the ethyl acetate extract is due to a single compound or to synergism between compounds present in the extract.

In a previous study reported by Rastogi *et al*., *trans*-cinnamic acid showed activity in the BACTEC radiometric assay against various *M. tuberculosis* strains with MICs ranging from 50.0 to 200.0 µg/mL, and it also synergistically enhanced the action of drugs (rifampicin, amikacin and clofazimine) against *M. tuberculosis* $H_{37}Rv$ (Rastogi

et al., 1998). The antitubercular activity previously reported for 4-hydroxybenzoic acid and 4-hydroxy-3-methoxybenzoic acid (MICs of 50 and 62.5 µg/mL, respectively) was greater than what was observed in our study (Chen *et al*., 2007). Verbascoside has previously been reported as inactive at the concentration of 100 µg/mL in the XTT reduction menadione assay (XRMA) (Kulkarni *et al*., 2012). The flavonoid luteolin has also previously been tested against *M. tuberculosis* $H_{37}Rv$, with strong activity at MIC of 25 µg/mL (Yadav *et al*., 2013). The activity of pheophytin A has been studied before (Su *et al*., 2009). This is the first report of the screening of 1-monoacylglycerol and pheophytin B, pheophorbide A and its ethyl ester for anti-TB activity and of all compounds for activity using the SPOTi assay.

Table 3.20 Activity of *V. thapsus* extracts and selected isolated compounds against *M. tuberculosis* $H_{37}Rv$ in SPOTi assay

Sample	MICs µg/mL (µM)
605H	NA
605E	250
605M	500
605MD	500
605MB	NA
605MW	NA
VT2	500 (1746.8)
VT3	500 (843.6)
VT4	NA
VT5	250 (1687.4)
VT6	NA
VT7	NA
VT8	500 (2973.7)
VT9	500 (3620.0)
VT10	500 (806.1)
VT11	NA
INH	0.01 (0.07)
RIF	0.01 (0.01)

605H: *V. thapsus n*-hexane extract; **605E**: *V. thapsus* ethyl acetate extract; **605M**: *V. thapsus* methanol extract; **605MD**: dichloromethane phase from *V. thapsus* methanol extract partitioning; **605MB**: *n*-butanol phase from *V. thapsus* methanol extract partitioning; **605MW**: water phase from *V. thapsus* methanol extract partitioning; INH: isoniazid; RIF: rifampicin; NA: no activity at 500 µg/mL

3.7.2 Results from the MABA assay

Results of the activity of crude extracts and selected isolated compounds against *M. tuberculosis* $H_{37}Rv$ in the MABA assay are presented in **Table 3.21**. All extracts and tested compounds were initially screened at the highest concentrations of 25 or 50 µg/mL and identified as inactive at such concentrations. This is the first report of the screening of *A. lappa*, *T. farfara* and *V. thapsus* extracts and of all tested compounds in the MABA assay.

Previous studies have reported the anti-TB activity of kaempferol **(AL8/TF3)**, luteolin **(VT2)** and *trans*-cinnamic acid **(VT5)** in the BACTEC radiometric assay (Rastogi *et al*., 1998; Yadav *et al*., 2013); methylcaffeate **(TF12)** in a standard broth assay (Balachandran *et al*., 2012); 4-hydroxybenzoic acid **(VT9)** and 4-hydroxy-3-methoxybenzoic acid **(VT8)** in a proportion method based assay (Chen *et al*., 2007), and verbascoside **(VT11)** in the XRMA assay (Kulkarni *et al*., 2012). All tested compounds in the present study were first investigated in the MABA assay.

The MABA assay is a microplate-based assay, using Alamar blue reagent for the determination of growth. It is sensitive, rapid, inexpensive, non-radiometric and offers high-throughput screening of compounds against slow-growing mycobacteria (Collins and Franzblau, 1997). It has been used for many years, prefered choice rather than the proportion method and the radiometric BACTEC 460 system. However, its drawback is that as a liquid-based colorimetric method, it is prone to contamination of samples during assay manipulation, and results between different laboratories may vary (Evangelopoulos and Bhakta, 2010). The SPOTi assay is a newly developed solid agar-based method. It is rapid, convenient, and high-throughput for the determination of inhibitory concentration of samples against slow-growing mycobacteria alone or in combination. It principally measures the

growth of the bacilli from generated spots inoculated to the centre of wells containing a range of different concentrations of samples. Compared with other screening methods, this assay can be done with a simple as low as 1 mg in amount, and moreover the sample mixed to the agar media has optimum access to the bacteria and will reflect on their biological property through growth inhibition or killing (Evangelopoulos and Bhakta, 2010).

Table 3.21 Activity of crude extracts and selected isolated compounds against *M. tuberculosis* $H_{37}Rv$ in MABA assay

Sample	MICs µg/mL (µM)	Sample	MICs µg/mL (µM)
325H	NA[1]	**TF11**	NA[2]
325E	NA[2]	**TF12**	NA[2]
325M	NA[2]	**VT1**	NA[1]
326H	NA[1]	**VT2**	NA[2]
326E	NA[2]	**VT3**	NA[2]
326M	NA[2]	**VT4**	NA[2]
605H	NA[1]	**VT5**	NA[2]
605E	NA[2]	**VT6**	NA[2]
605M	NA[2]	**VT7**	NA[2]
AL1	NA[1]	**VT8**	NA[2]
AL4	NA[1]	**VT9**	NA[2]
AL7/TF7	NA[2]	**VT10**	NA[2]
AL12	NA[2]	**VT11**	NA[2]
AL13	NA[2]	RIF	0.06 (0.07)
AL14	NA[2]	INH	0.44 (3.21)
TF2	NA[2]	CAP	1.93 (2.44)
AL8/TF3	NA[2]	SM	0.48 (0.83)
TF10	NA[2]	PA-824	0.86 (2.39)

CAP: capreomycin; SM: streptomycin; PA-824: a nitroimidazopyran-derived experimental antitubercular drug candidate; other notes same as above Tables 3.18, 3.19 and 3.20; NA[1]: no activity at 25 µg/mL; NA[2]: no activity at 50 µg/mL

3.8 Anti-MRSA activity of isolated compounds

Results of the activity of selected isolated compounds against a clinical Methicillin-resistant *S. aureus* isolate (LF78) in the MTT assay are presented in **Table 3.22**. All compounds except 4-hydroxybenzoic acid **(VT9)** were obtained in sufficient yield to allow for antibacterial screening, and 4-hydroxybenzoic acid was purchased from Sigma-Aldrich. Luteolin **(VT2)** showed the best activity with an MIC of 62.5 μg/mL (218.3 μM). α-Spinasterol **(VT1)** had an MIC value of 500 μg/mL (1211.6 μM). No other compound was active at the highest concentration (500 μg/mL) used in this assay.

4-Hydroxybenzoic acid **(VT9)**, 4-hydroxy-3-methoxybenzoic acid **(VT8)**, *trans*-cinnamic acid **(VT5)** and *p*-coumaric acid **(TF4)** belong to the class of simple phenolics. Their anti-MRSA activity has also been studied in a rapid *p*-iodonitrotetrazolium chloride (INT) colorimetric assay, and the results revealed that 4-hydroxy-3-methoxybenzoic and *p*-coumaric acids had MICs of 500 μg/mL and 1000 μg/mL, respectively; 4-hydroxybenzoic and *trans*-cinnamic acids were both inactive at 1000 μg/mL (Alves *et al*., 2013). Although the INT assay relies on a different method to the MTT assay, our results were consistent with previous report. The study further reported that the OH and OCH_3 groups in the *para* and *meta* positions of benzene ring, respectively, play an important role in anti-MRSA activity of simple phenolics; the absence of OCH_3 group in the *meta* position may reduce the activity; only OCH_3 or H in position 5 of the benzene ring also produces anti-MRSA activity (Alves *et al*., 2013). For the other tested phenolic derivatives, verbascoside **(VT11)**, 1, 3-dicaffeoylquinic acid **(AL12)**, 3, 4-dicaffeoylquinic acid **(TF10)**, and 3, 5-dicaffeoylquinic acid **(TF11)** are all investigated for the first time for their anti-MRSA activity in this study.

Luteolin **(VT2)** and kaempferol **(TF3)** belong to the group of flavonoids. Luteolin has been previously reported as active against some clinical MRSA strains (MICs=64 μg/mL) (Qiu *et al*., 2011), our result seemed to correlate well with previous report. The anti-MRSA activity of kaempferol was first invsetigated in this study. Several other flavonoids (e.g. dihydrokaempferol and some kaempferol glycosides) have also been reported with anti-MRSA acitivity (Ibrahim *et al*., 2009; Sasaki *et al*., 2012). A structure-activity study has revealed that the carbonylic group is part of the bioactive region inducing anti-MRSA activity in flavonoids; the presence of OH group in position 5 of flavanones (or flavones) increases activity, whereas the OCH_3 group provides the reverse effect (Alcaraz *et al*., 2000). One possible mechanism is that flavonoids may inhibit β-ketoacyl acyl carrier protein synthase III (KAS III) that initiates fatty acid synthesis in bacteria and is a key target enzyme to overcome the antibiotic resistance problem (Lee *et al*., 2011).

α-Spinasterol **(VT1)**, daucosterol **(AL6)** and taraxasterol **(AL3)** are grouped into the class of steroids and triterpenoids. The screening of α-spinasterol for anti-MRSA activity is reported for the first time in this study, though it has been tested against various strains of *S. aureus* (Salvador *et al*., 2009). Taraxasterol and daucosterol have been previously studied for anti-MRSA activity but reported as inactive (Amer, 2013). The results obtained in this study seemed consistent with previous report. A study has establshed that some triterpenoids can inhibit the activity of MRSA efflux pumps and the activity may correlate to the topological polar surface area of the compounds (Ramalhete *et al*., 2010).

Among the tested pheophorbides and pheophytins, only pheophorbide A **(VT3)** has previously been investigated and reported to potentiate berberine growth inhibition of resistant *S. aureus* (Stermitz *et al*., 2000). The screening of pheophorbide A ethyl

ester **(VT10)**, pheophytin A **(VT6)** and pheophytin B **(VT7)** for anti-MRSA activity is reported for the first time in this study. However, a study reported that metalloporphyrins pheophytins (pheophytin A Ag and the pheophytin A Ag/pheophytin B Ag mixture, synthesized from chlorophylls) had high potent anti-MRSA activity with MICs of 0.2 and 0.0625 µg/mL, respectively (Ghazaryan *et al*., 2008). This is also the first report of the study of anti-MRSA activity of 1-monoacylglycerol **(VT4)**.

Table 3.22 Activity of selected isolated compounds against Methicillin-resistant *S. aureus* isolate (LF78) in MTT assay

Sample	MICs µg/mL (µM)
AL3	NA[1]
AL6	NA[1]
AL12	NA[1]
TF3	NA[1]
TF4	NA[1]
TF10	NA[1]
TF11	NA[1]
VT1	500 (1211.6)
VT2	62.5 (218.3)
VT3	NA[1]
VT4	NA[1]
VT5	NA[1]
VT6	NA[1]
VT7	NA[1]
VT8	NA[1]
VT9	NA[1]
VT10	NA[1]
VT11	NA[1]
Vancomycin	3.125 (2.16)
Oxacillin	NA[2]

NA[1]: no activity at 500 µg/mL; NA[2]: no activity at 200 µg/mL

CHAPTER 4

CONCLUSION AND FUTURE WORK

4 Conclusion and future work

The phytochemical investigation of *A. lappa* led to the isolation of four terpenoids, two phytosterols, three flavonoids and some phenolic derivatives. Although all are known compounds, *n*-nonacosane **(AL1)**, kaempferol-3-*O*-glucoside **(AL10)**, isololiolide **(AL13)** and melitensin **(AL14)** are reported from *A. lappa* for the first time. Antitubercular study revealed that the *n*-hexane extract, ethyl acetate extract and dichloromethane phase were acitive against *M. tuberculosis* $H_{37}Rv$. This important finding provides scientific support for the traditional anti-TB use of *A. lappa*. Subsequent screening of compounds isolated from active extracts found that only β-sitosterol/stigmasterol mixture **(AL2)** was moderately active. It would be necessary to investigate the synergistic action between compounds present in the extracts in the future, especially the combined effect of taraxasterol **(AL3)** and taraxasterol acetate **(AL4)** in different ratio, and the synergistic action between isololiolide **(AL13)** and melitensin **(AL14)** in different ratio.

A total of twelve known compounds were isolated from *T. farfara*. Most of them are simple phenolics/derivatives or flavonoids. The compound loliolide **(TF2)** is first reported from *T. farfara*. The antitubercular investigation revealed that the *n*-hexane, ethyl acetate and methanol extracts showed good to moderate activity. Further study on isolated compounds indicated that β-sitosterol/stigmasterol mixture **(TF1)** and loliolide **(TF2)** might be responsible for the activity of the *n*-hexane extract and that *p*-coumaric acid **(TF4)** could account for the activity of the ethyl acetate extract. Future work should be carried out to investigate the synergism between compounds, for example, the synergistic action between β-sitosterol/stigmasterol mixture **(TF1)** and loliolide **(TF2)**, and the combined effect of *p*-coumaric acid **(TF4)** and other compunds isolated from the ethyl acetate extract. It would be also interesting to work

on *p*-coumaric acid chemical modification to optimize its structural phenotype or to acquire novel structures through structure-activity relationship analysis in the future.

The phytochemical investigation of *V. thapsus* provided eleven known compounds, mainly including some simple phenolics or derivatives and some pheophytins. This is the first report of the isolation of pheophorbide A **(VT3)**, pheophorbide ethyl ester **(VT10)**, pheophytin A **(VT6)**, pheophytin B **(VT7)**, 4-hydroxybenzoic acid **(VT9)**, 4-hydroxy-3-methoxybenzoic acid **(VT8)**, *trans*-cinnamic acid **(VT5)** and 1-monoacylglycerol **(VT4)** from *V. thapsus*. Results of the antitubercular study revealed that only the ethyl acetate extract had weak activity and among the compounds isolated from the extract only *trans*-cinnamic acid **(VT5)** showed weak activity. Future work could be performed to modify the chemical structure of *trans*-cinnamic acid to ameliorate its activity.

Compounds isolated from the three plants in suffient yield were also investigated for their anti-MRSA activity. The result revealed that only luteolin **(VT2)** displayed good activity with an MIC value of 62.5 μg/mL, and α-spinasterol had an MIC of 500 μg/mL. No other compound was active at the concentration of 500 μg/mL.

In conclusion, the present study provided some interesting outcomes in the field of natural products with the isolation of 27 secondary metabolites from three selected medicinal plants. A few of plant extracts and isolated compounds showed anti-TB activity, and one compound had anti-MRSA activity. In the future, toxicity studies need to be preformed on individual compounds to establish their safety, and then some work can be carried out to investigate their other biological activity and to modify their chemical structures for drug discovery.

Appendix I: Summary of Isolated Compounds

Code	Chemical Name	Appearance	TLC Profile	Anti-TB Activity (SPOTi data)	Anti-TB Activity (MABA data)	Anti-MRSA Activity
AL1	*n*-nonacosane	white flaky solid	R_f=0.75 (H:E=8:2)	No activity at 500 µg/mL	No activity at 25 µg/mL	Not tested
AL2/TF1	β-sitosterol/stigmasterol mixture	white solid	R_f=0.17 (H:E=8:2)	MIC=125 µg/mL	Not tested	Not tested
AL3	taraxasterol	white powder	R_f=0.44 (H:E=8:2)	No activity at 125 µg/mL	Not tested	No activity at 500 µg/mL
AL4	taraxasterol acetate	white amorphous solid	R_f=0.56 (H:E=8:2)	No activity at 125 µg/mL	No activity at 25 µg/mL	Not tested
AL6/TF8	daucosterol	white solid	R_f=0.73 (E:M=6:4)	Not tested	Not tested	Not tested
AL7/TF7	*trans*-caffeic acid	brown amorphous solid	R_f=0.62 (E:M=7:3)	MIC=250 µg/mL	No activity at 50 µg/mL	Not tested

Appendix I:

Code	Chemical Name	Appearance	TLC Profile	Anti-TB Activity (SPOTi data)	Anti-TB Activity (MABA data)	Anti-MRSA Activity
AL8/TF3	kaempferol	yellow amorphous solid	R_f=0.62 (H:E=1:9)	No activity at 500 μg/mL	No activity at 50 μg/mL	No activity at 500 μg/mL
AL9/TF6	quercetin	yellow amorphous solid	R_f=0.55 (H:E=1:9)	MIC=500 μg/mL	Not tested	Not tested
AL10/TF9	kaempferol-3-*O*-glucoside	yellow amorphous solid	R_f=0.31 (E:M=7:3)	No activity at 500 μg/mL	Not tested	Not tested
AL12	1, 3-dicaffeoylquinic acid	brown amorphous solid	R_f=0.31 (E:M=7:3)	Not tested	No activity at 50 μg/mL	No activity at 500 μg/mL
AL13	isololiolide	colourless oil	R_f=0.18 (H:E=4:6)	No activity at 500 μg/mL	No activity at 50 μg/mL	Not tested
AL14	melitensin	colourless oil	R_f=0.15 (H:E=4:6)	No activity at 500 μg/mL	No activity at 50 μg/mL	Not tested
TF2	loliolide	colourless oil	R_f=0.53 (H:E=3:7)	MIC=250 μg/mL	No activity at 50 μg/mL	Not tested

Appendix I:

Code	Chemical Name	Appearance	TLC Profile	Anti-TB Activity (SPOTi data)	Anti-TB Activity (MABA data)	Anti-MRSA Activity
TF4	*p*-coumaric acid	white amorphous solid	R_f=0.51 (H:E=2:8)	MIC=31.3 μg/mL	Not tested	No activity at 500 μg/mL
TF5	*p*-coumaric acid/ 4-hydroxybenzoic acid mixture	brown amorphous solid	R_f=0.55 (H:E=2:8)	MIC=62.5 μg/mL	Not tested	Not tested
TF10	3, 4-dicaffeoylquinic acid	brown amorphous solid	R_f=0.51 (E:M=7:3)	Not tested	No activity at 50 μg/mL	No activity at 500 μg/mL
TF11	3, 5-dicaffeoylquinic acid	brown amorphous solid	R_f=0.51 (H:E=3:7)	Not tested	No activity at 50 μg/mL	No activity at 500 μg/mL
TF12	methylcaffeate	brown powder	R_f=0.58 (H:E=3:7)	Not tested	No activity at 50 μg/mL	Not tested
VT1	α-spinasterol	colourless needle	R_f=0.64 (H:E=4:6)	Not tested	No activity at 25 μg/mL	MIC=500 μg/mL
VT2	luteolin	yellow amorphous solid	R_f=0.53 (H:E=0:10)	MIC=500 μg/mL	No activity at 50 μg/mL	MIC=62.5 μg/mL
VT3	pheophorbide A	dark-green solid	R_f=0.36 (H:E=0:10)	MIC=500 μg/mL	No activity at 50 μg/mL	No activity at 500 μg/mL

Appendix I:

Code	Chemical Name	Appearance	TLC Profile	Anti-TB Activity (SPOTi data)	Anti-TB Activity (MABA data)	Anti-MRSA Activity
VT4	1-monoacylglycerol	greenish oil	R_f=0.55 (E:M=7:3)	No activity at 500 μg/mL	No activity at 50 μg/mL	No activity at 500 μg/mL
VT5	*trans*-cinnamic acid	brown amorphous solid	R_f=0.33 (H:E=5:5)	MIC=250 μg/mL	No activity at 50 μg/mL	No activity at 500 μg/mL
VT6	pheophytin A	dark-green solid	R_f=0.64 (H:E=6:4)	No activity at 500 μg/mL	No activity at 50 μg/mL	No activity at 500 μg/mL
VT7	pheophytin B	dark-green solid	R_f=0.56 (H:E=6:4)	No activity at 500 μg/mL	No activity at 50 μg/mL	No activity at 500 μg/mL
VT8	4-hydroxy-3-methoxy benzoic acid	brown amorphous solid	R_f=0.33 (H:E=4:6)	MIC=500 μg/mL	No activity at 50 μg/mL	No activity at 500 μg/mL
VT9	4-hydroxybenzoic acid	white amorphous solid	R_f=0.27 (H:E=4:6)	MIC=500 μg/mL	No activity at 50 μg/mL	No activity at 500 μg/mL
VT10	pheophorbide A ethyl ester	dark-green solid	R_f=0.58 (H:E=4:6)	MIC=500 μg/mL	No activity at 50 μg/mL	No activity at 500 μg/mL
VT11	verbascoside	greenish amorphous solid	R_f=0.58 (E:M=7:3)	No activity at 500 μg/mL	No activity at 50 μg/mL	No activity at 500 μg/mL

H: *n*-hexane; E: ethyl acetate: M: methanol; TLC plates were developed in 10 mL of solvent mixture.

References

Adiguzel, A., Ozer, H., Kilic, H., Cetin, B. (2007) Screening of Antimicrobial Activity of Essential Oil and Methanol Extract of *Satureja hortensis* on Foodborne Bacteria and Fungi. *Czech. J. Food. Sci.,* 25(2):81-89.

Afifi, M.S., Salama, O.M., Gohar, A.A., Marzouk, A.M. (2006) Iridoids with antimicrobial activity from *Plumeria alba* L. *Bull. Pharm. Sci.*, 29:215-223.

Ahmad, M., Rizwani, G.H., Aftab, K., Ahmad, V.U., Gilani, A.H., Ahmad, S.P. (1995) Acteoside: A new antihypertensive drug. *Phytother. Res.*, 9(7):525-527.

Akihisa, T., Franzblau, S.G., Ukiya, M., Okuda, H,, Zhang, F., Yasukawa, K., Suzuki, T., Kimura, Y. (2005) Antitubercular activity of triterpenoids from Asteraceae flowers. *Biol. Pharm. Bull.*, 28(1):158-160.

Akiyama, H., Fujii, K., Yamasaki, O., Oono, T., Iwatsuki, K. (2001) Antibacterial action of several tannins against *Staphylococcus aureus*. *J. Antimicrob. Chemother.*, 48:487-491.

Al-Haj, N.A., Amghalia, E., Shamsudin, N.M., Abdullah, R., Mohamed, R., Sekawi, Z. (2009) Antibacterial Activity of honey against methicillin-resistant *Staphylococcus aureus*. *Res. J. Biol. Sci.*, 4(8):943-947.

Alcaraz, L.E., Blanco, S.E., Puig, O.N., Tomas, F., Ferretti, F.H. (2000) Antibacterial activity of flavonoids against methicillin-resistant *Staphylococcus aureus* strains. *J. Theor. Biol.*, 205(2):231-240.

Ali, N., Shah, S.W.A., Shah, I., Ahmed, G., Ghias, M., Khan, I., Ali, W. (2012) Anthelmintic and relaxant activities of *Verbascum thapsus* Mullein. *CAM*, 12:29-34.

Allen, D.E., Hatfield, G. (2004) Medicinal plants in folk tradition an ethnobotany of Britain & Ireland. Portland: *Timber Press*.

Alves, M.J., Ferreira, I.C., Froufe, H.J., Abreu, R.M., Martins, A., Pintado, M. (2013)

Antimicrobial activity of phenolic compounds identified in wild mushrooms, SAR analysis and docking studies. *J. Appl. Microbiol*., 15(2):346-357.

Amer, Z.B. (2013) Chemical constituents of flora of algeria and chemical constituents of *Pergularia tomentosa*. Ouargla: *University of Kasdi Merbah*.

Bahk, J., Marth, E. (1983) Aflatoxin production is inhibited by selected herbal drugs. *Mycopathologia*., 83(3):129-134.

Baker, R.A., Tatum, J.H., Nemec, J.S. (1989) Antimicrobial activity of naphthoquinones from fusaria. *Mycopathologia.*, 111:9-15.

Balachandran, C,, Duraipandiyan, V,, Al-Dhabi, N.A., Balakrishna, K., Kalia, N.P., Rajput, V.S., Khan, I.A., Ignacimuthu, S. (2012) Antimicrobial and antimycobacterial activities of methyl maffeate isolated from *Solanum torvum* Swartz. fruit. *Indian J. Med. Microbiol.*, 52(4):676-681.

Baratta, M.T., Dorman, H.J.D., Deans, S.G., Figueiredo, A.C., Barroso, J.G., Ruberto, G. (1998) Antimicrobial and antioxidant properties of some commercial essential oils. *Flavour. Frag. J.*, 13:235-244.

Barbosa-Filho, J.M., Costa, M., Gomes, C., Trolin, G. (1993) Isolation of onopordopicrin, the toxic constituent of *Arctium lappa* L. *J. Braz. Chem. Soc.*, 4(3):186-187.

Barbosa, P., Martins, A., Toyama, M., Joazeiro, P., Beriam, L., Fonteles, M., Monteiro, H. (2010) Purification and biological effects of a C-type lectin isolated from *Bothrops moojeni*. *J. Venom. Anim. Toxins.*, 16(3):493-504.

Barnes, J., Anderson, L.A., Philipson, J.D. (2007) Herbal medicines. Third edition. London: *Pharmaceutical Press*, p102-104.

Becconsall, J.K. (2005) Basic one- and two- dimentional NMR spectroscopy. Germany: *Wiley-VCH Verlag GmbH & Co. KGaA*.

Benoit, P., Fong, H., Svoboda, G., Farmsworth, N. (1976) Biological and phytochemical evaluation of plants. XIV. Antiinflammatory evaluation of 163

species of plants. *Lloydia.*, 39(2):160-171.

Bensky, D., Clavey, S., Stoger, E., Gamble, A. (2004) Chinese herbal medicine. Niemeier G, editor. 3rd edition. Seattle: *Eastland Press*.

Berk, S.A. (1996) The naturalist's herb guide. *New York Black Dog & Leventhal Publishers*.

Bhat, S., Azmi, A., Hadi, S. (2007) Prooxidant DNA breakage induced by caffeic acid in human peripheral lymphocytes: involvement of endogenous copper and a putative mechanism for anticancer properties. *Toxicol. Appl. Pharmacol.*, 218(3):249-55

Bloom, B.R. (1994) Tuberculosis: pathogenesis, protection and pontrol.

Boligon, A.A., Agertt, V., Janovik, V., Cruz, R.C., Campos, M.M.A., Guillaume, D., Athayde, M.L., Santos, A.R.S.D. (2012) Antimycobacterial activity of the fractions and compounds from *Scutia buxifolia*. *Rev. bras. farmacogn.*, 22(1):45-52.

Bond, W., Davies, G., Turner, R. (2007) The biology and non-chemical control of coltsfoot (*Tussilago farfara* L.).

Boonsri, S., Karalai, C., Ponglimanont, C., Kanjana-opas, A., Chantrapromma, K. (2006) Antibacterial and cytotoxic xanthones from the roots of *Cratoxylum formosum*. *Phytochemistry.*, 67(7):723-727.

Boucher, H.W., Talbot, G.H., Benjamin, D.K., Bradley, J., Guidos, R.J., Jones, R.N., Murray, B.E., Bonomo, R.A., Gilbert, D. (2013) 10×'20 Progress-development of new drugs active against gram-negative bacilli: an update from the infectious diseases society of America. *Clin. Infect. Dis.*, 56(12):1685-1694.

Boucher, H.W., Talbot, G.H., Bradley, J.S., Edwards, J.E., Gilbert, D., Rice, L.B., Scheld, M., Spellberg, B., Bartlett, J. (2009) Bad bugs, no drugs: no ESKAPE! an update from the infectious diseases society of America. *Clin. Infect. Dis.*,

48(1):1-12.

Braithwaite, A., Smith, F.J. (1996) Chromatographic methods. 5th edition.

Brantner, A., Grein, E. (1994) Antibacterial activity of plant extracts used externally in traditinonal medicine. *J. Ethnopharmacol.*, 44:35-50.

Breitmaier, E. (1993) Structure elucidation by NMR in organic chemistry.

Brown, A.K., Papaemmanouil, A., Bhowruth, V., Bhatt, A., Dover, L.G., Besra, G.S. (2007) Flavonoid inhibitors as novel antimycobacterial agents targeting Rv0636, a putative dehydratase enzyme involved in *Mycobacterium tuberculosis* fatty acid synthase II. *Microbiology.*, 153(Pt 10):3314-3322.

British National Formulary. (2013) Antitubercular drugs. *http://www.medicinescomplete.com/mc/bnf/current/PHP3588-antituberculosis-drugs.htm*.

Can-Aké, R., Erosa-Rejón, G., May-Pat, F., Peña-Rodríguez, L.M., Peraza-Sánchez, S.R. (2004) Bioactive terpenoids from roots and leaves of *Jatropha gaumeri*. *Rev. Soc. Quím. Méx.*, 48:11-14.

Cantrell, C.L., Franzblau, S.G., Fischer, N.H. (2001) Antimycobacterial plant terpenoids. *Planta. Med.*, 67(8):685-694.

Cao, J.F., Li, C.P., Zhang, P.Y., Cao, X., Huang, T.T., Bai, Y.G., Chen, K.S. (2012) Antidiabetic effect of burdock (*Arctium lappa* L.) root ethanolic extract on streptozotocin-induced diabetic rats. *Afr. J. Biotechnol.*, 11(37):9079-9085.

Cardona, M.L., Garcia, B., Pedro, J.R., Sinisterra, J.F. (1989) Sesquiterpene lactones and an elemane derivatives from *Onopordon corymbosum*. *Phytochemistry.*, 28(4):1264-1267.

Chan, Y.S., Cheng, L.N., Wu, J.H., Chan, E., Kwan, Y.W., Lee, S.M., Leung, G.P., Yu, P.H., Chan, S.W. (2011) A review of the pharmacological effects of *Arctium lappa* (burdock). *Inflammopharmacology.*, 19(5):245-254.

Chanaj-kaczmarek, J., Wojcinska, M., Matlawska, I. (2013) Phenolics in the

Tussilago farfara leaves. *Herba. Pol.*, 59(1):35-43.

Chang, I.M. (1997) Antiviral activity of aucubin against hepatitis B virus replication. *Phytother. Res.*, 11(3):189-192.

Chen, F., Wu, A., Chen, C. (2004) The influence of different treatments on the free radical scavenging activity of burdock and variations of its active components. *Food Chem.*, 86:479-484.

Chen, F.Z., Peng, S.L., Ding, L.S., He, Y.H., Wang, M.K. (2001) Chemical constitents from fruits of *Rosa davidii*. *Acta. Bot. Sin.*, 43(1):101-104.

Chen, J.J., Chou, T.H., Peng, C.F., Chen, I.S., Yang, S.Z. (2007) Antitubercular dihydroagarofuranoid sesquiterpenes from the roots of *Microtropis fokienensis*. *J. Nat. Prod.*, 70(2):202-205.

Chen, S.X., Bao, S.Y., Shao, T.L., Chen, K.S. (2011) Chemical constituents of the root of *Arctium lappa* L. *Nat. Prod. Res. Dev.*, 23(6):1055.

Chen, Z., Liu, Y.M., Yang, S., Song, B.A., Xu, G.F., Bhadury, P.S., Jin, L.H., Hu, D.Y., Liu, F., Xue, W., Zhou, X. (2008) Studies on the chemical constituents and anticancer activity of *Saxifraga stolonifera* (L) Meeb. *Bioorg. Med. Chem.*, 16:1337-1344.

Chiang, L,, Chiang, W., Chang, M. (2002) Antiviral activity of *Plantago major* extracts and related compounds in vitro. *Antiviral. Res.*, 55:53-62.

Cho, J., Kim, H.M., Ryu, J.H., Jeong, Y.S., Lee, Y.S., Jin, C. (2005) Neuroprotective and antioxidant effects of the ethyl acetate fraction prepared from *Tussilago farfara* L. *Biol. Pharm. Bull.*, 28(3):455-460.

Church, B. (2008) Medicinal plants, trees & shrubs of sppalachia- a field guide.

Ciocan, I.D., Bara, I.I. (2007) Plant products as antimicrobial agents. *Genetică Si Biologie Moleculară*, 8(1):151-156.

Claridge, T.D.W. (2006) High-resolution NMR techniques in organic chemistry. Netherlands.

Coll, J.C., Bowden, B.F. (1986) The application of vacuum liquid chromatography to the seoaration of terpene mixtures. *J. Nat. Prod.*, 49:934-936.

Collins, L., Franzblau, S.G. (1997) Microplate alamar blue assay versus BACTEC 460 system for high-throughput screening of compounds against *Mycobacterium tuberculosis* and *Mycobacterium avium*. *Antimicrob. Agents Chemother.*, 41(5):1004-1009.

Committee on Herbal Medicinal Products. (2010) Assessment report on *Arctium lappa* L., radix. *European Medicines Agency*.

Costa, M., Gomes, C., Trolin, G. (1993) Isolation of onopordopicrin, the toxic constituent of *Arctium lappa* L. *J. Braz. Chem. Soc.*, 4:186-187.

Costa, R.M.P.B., Vaz, F.M., Oliva, M.L.V., Coelho, L.C.B.B., Correia, M.T.S., Carneiro-da-Cunha, M.G. (2010) A new mistletoe *Phthirusa pyrifolia* leaf lectin with antimicrobial properties. *Process. Biochem.*, 45:526-533.

Cotoras, M., Mendoza, L., Muñoz, A., Yáñez, K., Castro, P., Aguirreemail, M. (2011) Fungitoxicity against *Botrytis cinerea* of a flavonoid isolated from *Pseudognaphalium robustum*. *Molecules.*, 16(5):3885-3895.

Cowan, M. (1999) Plant products as antimicrobial agents. *Clin. Microbiol. Rev.*, 12(4):564-582.

Critchfield, J.W., Butera, S. T., Folks, T.M. (1996) Inhibition of HIV activation in latently infected cells by flavonoid compounds. *AIDS Res. Hum. Retroviruses.*, 12:39.

Culvenor, C. (1976) The occurrence of senkirkine in *Tussilago farfara*. *Aust. J. Chem.*, 29:229-230.

Daisy, P., Mathew, S.S.S, Rayan, N.A. (2008) A novel terpenoid from *Elephantopus scaber*–antibacterial activity on *Staphylococcus Aureus*: a substantiate computational approach. *Int. J. Biomed. Sci.*, 4(3):196-203.

Danino, O,, Gottlieb, H.E., Grossman, S., Bergman, M. (2009) Antioxidant activity

of 1, 3-dicaffeoylquinic acid isolated from *Inula viscosa*. *Food Res. Int.*, 42:1273-1280.

Darwin, T. (1996) The scots herbal the plant lore of Scotland. 1st edition, Wiltshire: *Mercat Press*.

Darwish, R.M., Fares-Re, J.A., Zarga, M.H.A., Nazer, I.K. (2010) Antibacterial effect of Jordanian propolis and isolated flavonoids against human pathogenic bacteria. *Afr. J. Biotechnol* ., 9(36):5966-5974.

Dayisoylu, K.S., Duman, A.D., Alma, M.H., Digrak, M. (2009) Antimicrobial activity of the essential oils of rosin from cones of *Abies cilicica* subsp. cilicica. *Afr. J. Biotechnol* ., 8(19):5021-5024.

De-Almeida, A., Sánchez-Hidalgo, M., Martín ,A., Luiz-Ferreira, A., Trigo, J., Vilegas, W., Dos-Santos, L., Souza-Brito, A,, De-la-Lastra, C. (2013) Anti-inflammatory intestinal activity of *Arctium lappa* L. (Asteraceae) in TNBS colitis model. *J. Ethnopharmacol.*, 146(1):300-310.

De-Pascual-Teresa, J., Diaz, F., Grande, M. (1978a) Components del *Verbascum thapsus* L. *An. Quim.*, 74:311-314.

De-Pascual-Teresa, J., Diaz, F., Grande, M. (1978b) Components del *Verbascum thapsus* L. II. Aceite de las semilas. *An. Quim.*, 78C:107-110.

De-Pascual-Teresa, J., Diaz, F., Grande, M. (1980) Components of *Verbascum thapsus* L. III. Contribution to the study of saponins. *An. Quim. Ser. C.*, 76(2):107-110.

De, P., De, K., Veau, D., Bedos-Belval, F., Chassaing, S., Baltas, M. (2012b) Recent advances in the development of cinnamic-like derivatives as antituberculosis agents. *Expert. Opin. Ther. Pat.*, 22(2):155-168.

De, P., Veau, D., Bedos-Belval, F., Chassaing, S., Baltas, M. (2012a) Cinnamic derivatives in tuberculosis. Cardona, P.J., editor.

Determann, H., Brewer, J.E. (1975) Gel chromatography. Heftmann, E., editor. 3rd

edition.

Dharmaratne, H.R., Sakagami, Y., Piyasena, K.G., Thevanesam, V. (2013) Antibacterial activity of xanthones from *Garcinia mangostana* (L.) and their structure-activity relationship studies. *Nat. Prod. Res.*, 27(10):938-941.

Didry, N. (1982) Components and activity of *Tussilago farfara*. *Ann. Pharm. Fr.*, 40:75-80.

Dong, X.Z., Xu, H.B., Huang, K.X., Liou, Q., Zhou, J. (2002) The preparation and characterization of an antimicrobial polypeptide from the loach, *Misgurnus anguillicaudatus*. *Protein Expres. Purif.*, 26:235-242.

Doss, A., Mubarack, H.M., Dhanabalan, R. (2009) Antibacterial activity of tannins from the leaves of *Solanum trilobatum* Linn. *Indian J. Sci. Technol.*, 2(2):41-43.

Duke, J.A. (2002) Handbook of medicinal herbs. Second edition. Boca Raton: *CRC Press*.

Dulger, B., Gonuz, A. (2004) Antimicrobial activity of certain plants used in Turkish traditional medicine. *Asian J. Plant Sci.*, 3(1):104-107.

Durust, N., Ozden, S., Umur, E., Durust, Y., Kucukislamoglu, M. (2001) The isolation of carboxylic acids from the flowers of *Delphinium formosum*. *Turk. J. Chem.*, 25:93-97.

Eich, E., Pertz, H., Kaloga, M. (1996) (-)-Arctigenin as a lead structure for inhibitors of human immunodeficiency virus type-1 integrase. *J. Med. Chem.*, 39:86-95.

Erosa-Rejón, G., Peña-Rodríguez, L.M., Sterner, O. (2009) Secondary metabolites from *Heliotropium angiospermum*. *J. Mex. Chem. Soc.*, 53(2):44-47.

Ersoz, T., Harput, U.S., Calis, I. (2002) Iridoid, phenylethanoid and monoterpene glycosides from *Phlomis sieheana*. *Turk. J. Chem.*, 26:1-8.

Escobar, F.M., Sabini, M.C., Zanon, S.M., Tonn, C.E., Sabini, L.I. (2012) Antiviral effect and mode of action of methanolic extract of *Verbascum thapsus* L. on

pseudorabies virus (strain RC/79). *Nat. Prod. Res.*, 26(17):1621-1625.

Evangelopoulos, D., Bhakta, S. (2010) Rapid methods for testing inhibitors of mycobacterial growth. Gillespie, S.H., McHugh, T.D., editors: *Humana Press.*

Fang, L.V., Xu, X.J. (2008). Studies on the chemical constituents of *Rabdosia rubescens*. *Chin. Med. Materi. J.*, 31:1340-1343.

Favela-Hernández, J.M., García, A., Garza-González, E., Rivas-Galindo, V.M., Camacho-Corona, M.R. (2012) Antibacterial and antimycobacterial lignans and flavonoids from *Larrea tridentata*. *Phytother. Res.*, 26(12):1957-1960.

Fernandez I, Pedro JR, Vidal R. (1993) Norisoprenoids from *Centaurea aspera* and *C. Salmantica*. *Phytochemistry.*, 34(3):733-736.

Ferracane, R., Graziani, G., Gallo, M., Fogliano, V., Ritieni, A. (2010) Metabolic profile of the bioactive compounds of burdock (*Arctium lappa*) seeds, roots and leaves. *J. Pharm. Biomed. Anal.*, 51(2):399-404.

Freeman, B.C., Beattie, G.A. (2008) An overview of plant defenses against pathogens and herbivores. *The Plant Health Instructor*.

Ganz, T. (2004) Antimicrobial polypeptides. *J. Leukoc. Biol.*, 75:36-38.

Ge, H.M., Huang, B., Tan, S.H., Shi, D.H., Song, Y.C., Tan, R.X. (2006) Bioactive oligostilbenoids from the stem bark of *Hopea exalata*. *J. Nat. Prod.*, 69(12):1800-1802.

Ghazaryan, R.K., Sahakyan, L.A., Tovmasyan, A.G., Movsisyan, L.D., Hambardzumyan, A.D. (2008) Novel antimicrobial agents on the base of natural and synthetic metalloporphyrins. *New Armenian Med. J.*, 2(4):40-48.

Ghoshal, S., Prasad, B.N.K., Lakshmi, V. (1996) Antiamoebic activity of *Piper longum* fruits against *Entamoeba histolytica* in vitro and in vivo. *J. Ethnopharmacol.*, 50:167-170.

González-Lamothe, R., Mitchell, G., Gattuso, M., Diarra, M.S., Malouin, F., Bouarab,

K. (2009) Plant antimicrobial agents and their effects on plant and human pathogens. *Int. J. Mol. Sci.*, 10(8):3400-3419.

Gordien, A.Y., Gray, A.I., Franzblau, S.G., Seidel, V. (2009) Antimycobacterial terpenoids from *Juniperus communis* L. (Cuppressaceae). *J. Ethnopharmacol.*, 126(3):500-505.

Grieve, M. (1981) A modern herbal (Vol II). New York: *Dover Publications*.

Gross, K.L., Werner, P.A. (1978) The biology of Canadian weeds: *Verbascum thapsus* and *Verbascum blattaia*. *Can. J. Plant. Sci.*, 58:401-403.

Güçlü-Ustündağ O, Mazza G. (2007) Saponins: properties, applications and processing. *Crit. Rev. Food Sci. Nutr.*, 47(3):231-258.

Gupta, A., Bhakta, S. (2012) An integrated surrogate model for screening of drugs against *Mycobacterium tuberculosis*. *J. Antimicrob. Chemother.*, 67(6):1380-1391.

Gutierrez-Lugo, M.T., Wang, Y., Franzblau, S.G., Suarez, E., Timmermann, B.N. (2005) Antitubercular sterols from *Thalia multiflora* Horkel ex Koernicke. *Phytother. Res.*, 19(10):876-880.

Guvenalp, Z., Demirezer, L.O. (2005) Flavonol glycosides from *Asperula arvensis* L. *Turk. J. Chem.*, 29:163-169.

Guzman, J.D., Evangelopoulos, D., Gupta, A., Birchall, K., Mwaigwisya, S., Saxty, B., McHugh, T.D., Gibbons, S., Malkinson, J., Bhakta, S. (2013) Antitubercular specific activity of ibuprofen and the other 2-arylpropanoic acids using the HT-SPOTi whole-cell phenotypic assay. *BMJ.*, 3(6):1-13.

Hargus, J.A., Fronczek, F.R., Vicente, M.G., Smith, K.M. (2007) Mono-(L)-aspartylchlorin-e6. *Photochem. Photobiol.*, 83(5):1006-1015.

Hasegawa, H., Matsumiya, S., Uchiyama, M., Kurokawa, T., Inouye, Y., Kasai, R., Ishibashi, S., Yamasaki, K. (1994) Inhibitory effect of some triterpenoid saponins on glucose transport in tumor cells and its application to in vitro

cytotoxic and antiviral activities. *Planta Med.*, 6:240-243.

Haslam, E. (1996) Natural polyphenols (vegetable tannins) as drugs: possible modes of action. *J. Nat. Prod.*, 59:205-215.

Hatano, T., Kusuda, M., Inada, K., Ogawa, T.O., Shiota, S., Tsuchiya, T., Yoshida, T. (2005) Effects of tannins and related polyphenols on methicillin-resistant *Staphylococcus aureus*. *Phytochemistry*, 66(17):2047-2055.

He, J.P., Zhao, Y., Sun, X.H., Wu, Q.H., Pan, Y.J. (2012) Antibacterial effects of burdock (*Arctium Lappa* L.) boncentrate on vibrio parahemolyticus. *Nat. Prod. Res. Dev.*, 24(3):381.

Herna´ndez, N.E., Tereschuk, M.L., Abdala, L.R. (2000) Antimicrobial activity of flavonoids in medicinal plants from Tafi´ del Valle (Tucuma´n, Argentina). *J. Ethnopharmacol.*, 73:317-322.

Hirose, M., Nishikawa, A., Shibutani, M., Imai, T., Shirai, T. (2002) Chemoprevention of heterocyclic amino-induced mammary carcinogenesis in rats. *Environ. Mol. Mutagen.*, 39(271-278).

Homma, R., Yamashita, H., Funaki, J., Ueda, R., Sakura, T., Ishimaru, Y., Abe, K., Asakura, T. (2012) Identifcation of bitterness-masking compounds from cheese. *J. Agric. Food Chem.*, 60:4492-4499.

Huang, D,, Guh, J., Chueh, S., Teng, C. (2004) Modulation of anti-adhesion molecule MUC-1 is associated with arctiin-induced growth inhibition in PC-3 cells. *Prostate.*, 59:260-267.

Hussain, H., Aziz, S., Miana, G.A., Ahmad, V.U., Anwar, S., Ahmed, I. (2009) Minor chemical constituents of *Verbascum thapsus*. *Biochem. Syst. Ecol.*, 37(2):124-126.

Hwang, C.H., Jaki, B.U., Klein, L.L., Lankin, D.C., McAlpine, J., Napolitano, J.G., Franzblau, S.G., Cho, S.H., Stamets, P.E., Pauli, G.F. (2012) Biological and chemical evaluation of anti-TB coumarins from the polypore mushroom,

Fomitopsis officinalis. *Planta Med.*, 78.

Hwang, S.B., Chang, M.N., Garcia, M.L., Han, Q.Q., Huang, L., King, V.F., Kaczorowski, G.J., Winquist, R.J. (1987) L-652, 469-a dual receptor antagonist of platelet activating factor and dihydropyridines from *Tussilago farfara* L. *Eur. J. Pharmacol.*, 141:269-281.

Hwangbo, C., Lee, H.S., Park, J., Choe, J., Lee, J.H. (2009) The anti-inflammatory effect of tussilagone, from *Tussilago farfara*, is mediated by the induction of heme oxygenase-1 in murine macrophages. *Int. Immunopharmacol.*, 9:1578-1584.

Ibrahim, M.A., Mansoor, A.A., Gross, A., Ashfaq, M.K., Jacob, M., Khan, S.I., Hamann, M.T. (2009) Methicillin-resistant *Staphylococcus aureus* (MRSA)-active metabolites from *Platanus occidentalis* (American Sycamore). *J. Nat. Prod.*, 72(12):2141-2144.

Ibrahim, A,K. (2013) New terpenoids from *Mentha pulegium* L. and their antimicrobial activity. *Nat. Prod. Res.: Formerly Nat. Prod. Lett.*, 27(8):691-696.

Ichihara, A., Oda, K., Numata, Y., Sakamura, S. (1976) Lappaol A and B, novel lignans from *Arctium lappa* L. *Tetrahedron Lett.*, 44:3961-3964.

Iida, T., Tamura, T., Matsumoto, T. (1980) Proton nuclear magnetic resonance identification and discrimination of side chain isomers of phytosterols using a lanthanide shift reagent. *J. Lipid Res.*, 21: 326-338.

Ignacimuthu, S., Pavunraj, M., Duraipandiyan, V., Raja, N., Muthu, C. (2009) Antibacterial activity of a novel quinone from the leaves of *Pergularia daemia* (Forsk.), a traditional medicinal plant. *Asian J. Trad. Med.*, 4(1):36-40.

Ishihara, K., Yamagishi, N., Saito, Y. (2006) Arctigenin from *Fructus Arctii* is a novel suppressor of heat shock response in mammalian cells. *Cell Stress*

Chaperones., 11:154-161.

Iwakami, S., Wu, J., Ebizuka, Y., Sankawa, U. (1992) Platelet activating factor (PAF) antagonists contained in medicinal plants: lignans and sesquiterpenes. *Chem. Pharm. Bull.*, 40:1196-1198.

Izadpanah, A., Gallo, R.L. (2005) Antimicrobial peptides. *J. Am. Acad. Dermatol.*, 52:381-390.

Janovska, D., Kubikova, K., Kokoska, L. (2003) Screening for antimicrobial activity of some medicinal plants species of traditional chinese medicine. *Czech. J. Food Sci.*, 21:107-110.

Jeong, S.C., Koyyalamudi, S.R., Hughes, J.M., Khoo, C., Bailey, T., Park, J.P., Song, C.H. (2013) Modulation of cytokine production and complement activity by biopolymers extracted from medicinal plants. *Phytopharmacology.*, 4(1):19-30.

Jeonga, E.Y., Jeona, J.H., Lee, CH, Lee, H.S. (2009) Antimicrobial activity of catechol isolated from *Diospyros kaki* Thunb. roots and its derivatives toward intestinal bacteria. *Food Chem.*, 115(3):1006-1010.

Johann, S., Oliveira, V.L.D., Pizzolatti, M.G., Schripsema, J., Braz-Filho, R., Branco, A., Jr, A.S. (2007) Antimicrobial activity of wax and hexane extracts from *Citrus spp*. peels. *Mem. Inst. Oswaldo Cruz., Rio. de Janeiro.*, 102(6):681-685.

Johari, J., Kianmehr, A., Mustafa, M.R., Abubakar, S., Zandi, K. (2012) Antiviral activity of baicalein and quercetin against the *Japanese Encephalitis* Virus. *Int. J. Mo.l Sci.*, 13(12):16785-16795.

Kačániová, M., Hleba, L., Petrová, J., Felšöciová, S., Pavelková, A., Rovná, K., Bobková, A., Čuboň, J. (2013) Antimicrobial activity of *Tussilago farfara* L. *JMBFS.*, 2:1343-1350.

Kalemba, D., Kunicka, A. (2003) Antibacterial and antifungal properties of essential

oils. *Curr. Med. Chem.*, 10:813-829.

Kamkaen, N., Matsuki, Y., Ichino, C., Kiyohara, H., Yamada, H. (2006) The isolation of the anti-helicobacter pylori compounds in seeds of *Arctium lappa* Linn. *Thai. Pharm. Health Sc.i J.*, 1(2):12-18.

Karou, D., Savadogo, A., Canini, A., Yameogo, S., Montesano, C., Simpore, J., Colizzi, V., Traore, A.S. (2006) Antibacterial activity of alkaloids from *Sida acuta*. *Afr. J. Biotechnol.*, 5(2):195-200.

Kartala, M., Yıldızb, S., Kayaa, S., Topçuc, G. (2003) Antimicrobial activity of propolis samples from two different regions of Anatolia. *J. Ethnopharmacol.*, 86(1):69-73.

Kayser, O., Kolodziej, H. (1997) Antibacterial activity of extracts and constituents of *Pelargonium sidoides* and *Pelargonium reniforme*. *Planta Medica.*, 63:508-510.

Kazmi, M., Malik, A., Hameed, S., Akhtar, N., Ali, S. (1994) An naphthoquinone derivative from *Cassia italica*. *Phytochemistry*, 36:761-763.

Kejela, T., Bacha, K. (2013) Prevalence and antibiotic susceptibility pattern of methicillin-resistant *Staphylococcus aureus* (MRSA) among primary school children and prisoners in Jimma Town, Southwest Ethiopia. *Ann. Clin. Microbiol. Antimicrob.*, 12(1):11.

Kemper, K.J. (1999) Burdock (*Arctium lappa*).

Keyhanfar, M., Nazeri, S., Bayat, M. (2011) Evaluation of antibacterial activities of some medicinal palnts traditionally used in Iran. *Iran. J. Pharm. Sci.*, 8(1):353-358.

Khalilov, L.M., Khalilova, A.Z., Shakurova, E.R., Nuriev, I.F., Kachala, V.V., Shashkov, A.S., Dzhemilev, U.M. (2003) PMR and ^{13}C NMR spectra of biologically active compounds. XII. taraxasterol and its acetate from the aerial parts of *Onpordum acanthium*. *Chem. Nat. Compd.*, 39(3):285-288.

Khuroo, M.A., Qureshi, M.A., Razdan, T.K., Nicholsa, P. (1988) Sterones, iridoids and a sesquiterpene from *Verbascum thapsus*. *Phytochemistry*, 27(11):3541-3544.

Ki-Bong, O., Mar, W., Kim, S., Kim, J.Y., Lee, T.H., Kim, J.G., Shin, D., Sim, C.J., Shin, J. (2006) Antimicrobial activity and cytotoxicity of bis (indole) alkaloids from the *Sponge Spongosorites* sp. *Biol. Pharm. Bull.*, 29(3):570-573.

Kikuchi, M., Suzuki, N. (1992) Studies on the constituents of *Tusssilago farfara* L. II：structures of new sesquiterpenoids isolated from the flower buds. *Chem. Pharm. Bull.*, 40(10):2753.

Kim, B.H., Hong, S.S., Kwon, S.W., Lee, H.Y. (2008) Diarctigenin, a lignan constituent from *Arctium lappa*, down-regulated zymosan-induced transcription of inflammatory genes through suppression of DNA binding ability of nuclear factor-B in macrophages. *J. Pharm. Exp. Ther.*, 327:393-401

Kimura, J., Maki, N. (2002). New loliolide derivatives from the brown alga *Unidaria pinnatifida*. *J. Nat. Prod.*, 65:57-58.

Kimura, Y., Okuda, H., Nishibe, S., Arichi, S. (1987) Effects of caffeoylglycosides on arachidonate metabolism in leukocytes. *Planta Med.*, 53(2):148-153.

Kocacalıskana, I., Talanb, I., Terzic, I. (2006) Antimicrobial activity of catechol and pyrogallol as allelochemicals. *Z. Naturforsch.*, 61c:639-642.

Köck, R., Becker, K., Cookson, B., Gemert-Pijnen, J.E.V., Harbarth, S., Kluytmans, J., Mielke, M., Peters, G., Skov, R.L., Struelens, M.J., Tacconelli, E., Navarro, T,A., Witte, W., Friedrich, A.W. (2010) Methicillin-resistant *Staphylococcus aureus* (MRSA): burden of disease and control challenges in Europe. *Euro. Surveill.* 15(41):19688-19694.

Kojima, M., Kondo, T. (1985) An enzyme in sweet potato root which catalyzes the

conversion of chlorogenic acid, 3-caffeoylquinic acid, to isochlorogenic acid, 3, 5-dicaffeoylquinic acid. *Agric. Biol. Chem.*, 49(8):2467-2469.

Kokoska, L., Polesnya, Z., Radab, V., Nepovimc, A., Vanekc, T. (2002) Screening of some Siberian medicinal plants for antimicrobial activity *J. Ethnopharmacol.*, 82(1):51-53.

Kremmer ,T., Boross, L. (1979) Gel chromatography.

Kuddus, M.R., Rumi, F., Kaisar, M.A., Hasan, C.M. (2010) Sesquiterpenen and phenylpropanoids from *Curcuma longa*. *Bangladesh Phar. J.*, 13(2):31-34.

Kuete, V., Ngameni, B., Simo, C.C., Tankeu, R.K., Ngadjui, B.T., Meyer, J.J., Lall, N., Kuiate, J.R. (2008) Antimicrobial activity of the crude extracts and compounds from *Ficus chlamydocarpa* and *Ficus cordata* (Moraceae). *J. Ethnopharmacol.*, 20(1):17-24.

Kulkarni, R.R., Shurpali, K., Gawde, R.L., Sarkar, D., Puranik, V.G., Joshi, S.P. (2012) Phyllocladane diterpenes from *Anisomeles heyneana*. *J. Asian. Nat. Prod. Res.*, 14(12):1162-1168.

Kumar, P., Singh, A., Sharma, U., Singh, D., Dobhal, M.P., Singh, S. (2013) Anti-mycobacterial activity of plumericin and isoplumericin against MDR *Mycobacterium tuberculosis*. *Pulm. Pharmacol. Ther.*, 26(3):332-335.

Kumarasamy, Y., Cox, P.J., Jaspars, M., Nahar, L., Sarker, S.D. (2002) Screening seeds of Scottish plants for antibacterial activity. *J. Ethnopharmacol.*, 83(1-2):73-77.

Kwon, Y.S., Kobayashi, A., Kajiyama, S.I., Kawazu, K., Kanzaki, H., Kim, C.M. 1997. Antimicrobial constituents of *Angelica dahurica* roots. *Phytochemistry*, 44(5):887-889.

Lai, C.S., Mas, R.H., Nair, N.K., Mansor, S.M., Navaratnam, V. (2010) Chemical constituents and in vitro anticancer activity of *Typhonium flagelliforme* (Araceae). *J. Ethnopharmacol.*, 127(2):486-494.

Lee, D.G., Jung, H.J., Woo, E.R. (2005) Antimicrobial property of (+)-lyoniresinol-3alpha-*O*-beta-D-glucopyranoside isolated from the root bark of *Lycium chinense* Miller against human pathogenic microorganisms. *Arch. Pharm. Res.*, 28(9):1031-1036.

Lee, I.K., Kim, K.H., Choi, S.U., Lee, J.H., Lee, K.R. (2009) Phytochemical constituents of thesium chinense TURCZ and their cytotoxic activities in vitro. *Nat. Prod. Sci.*, 15(4):246-249.

Lee, J.Y., Lee, J., Jeong, K.W., Lee, E., Kim, Y. 2011. Flavonoid inhibitors of β-ketoacyl acyl carrier protein synthase III against Methicillin-Resistant *Staphylococcus aureus*. *Bull. Korean Chem. Soc.*, 32(8):2695-2699.

Lee S, Kim KS, Jang JM, Park Y, Kim YB, Kim BK. (2002) Pytochemical constituents from the herb of *Artemisi apiacea*. *Arch. Pharm. Res.*, 25(3):285-288.

Lee, S.Y., Moon, E., Kim, S.Y., Lee, K.R. (2013) Quinic acid derivatives from Pimpinella brachycarpa exert anti-neuroinflammatory activity in lipopolysaccharide-induced microglia. *Bioorg. Med. Chem. Lett.*, 23(7): 2140-2144.

Leven, M., Berghe, D.V., Mertens, F., Vlietinck, A., Lammens, E. (1979) Screening of higher plants for biological activities. I. Antimicrobial activity. *Planta Med.*, 36(4):311-321.

Li, J., Huang, X., Du, X., Sun, W., Zhang, Y. (2009). Study of chemical composition and antimicrobial activity of leaves and roots of *Scrophularia ningpoensis*. *Nat. Prod. Res.*, 23(8):775-780.

Li, Y.P., Wang, Y.M. (1988) Evaluation of tussilagone: a cardiovascular-respiratory stimulant isolated from chinese herbal medicine. *Gen. Pharmac.*, 19(2):261-263.

Lim, H.J., Lee, H.S., Ryu, J.H. (2008) Suppression of inducible nitric oxide synthase

and cyclooxygenase-2 expression by tussilagone from *Farfarae Flos* in BV-2 microglial cells. *Arch. Pharm. Res.*, 31(5):645-652.

Lin, J., Lu, J., Yang, J., Chuang, S., Ujiie, T. (1996) Anti-inflammatory and radical scavenge effects of *Arctium lappa*. *Am. J. Chin. Med.*, 24:127-137.

Lin, W.Y., Peng, C.F., Tsai, I.L., Chen, J.J., Cheng, M.J., Chen, I.S. (2005) Antitubercular constituents from the roots of *Engelhardia roxburghiana*. *Planta Med.*, 71(2):171-175.

Lin, X., Liu, C., Chen, K. (2004) Extraction and content comparison of chlorogenic acid in *Arctium lappa* L. leaves collected from different terrain and its restraining bacteria test. *Nat. Prod. Res. Dev* .,16:328-330.

Liu, K.Y., Zhang, T.J., Cao, W.Y., Chen, H.X., Zheng, Y.N. (2006) Phytochemical and pharmacological research progress in *Tussilago farfara·*. *China Journal of Chinese Materia Medica*, 31(22):1837-1841.

Liu, M., Katerere, D.R., Gray, A.I., Seidel, V. (2009) Phytochemical and antifungal studies on *Terminalia mollis* and *Terminalia brachystemma*. *Fitoterapia.*, 90(6):369-373.

Liu, R., Li, A., Sun, A. (2004) Preparative isolation and purification of hydroxyanthraquinones and cinnamic acid from the Chinese medicinal herb *Rheum officinale* Baill. by high-speed counter-current chromatography. *J. Chromatogr. A.*, 105(2):217-221.

Liu, S., Chen, K., Schliemann, W., Strack, D. (2005) Isolation and identification of arctiin and arctigenin in leaves of burdock (*Arctium lappa* L.) by polyamide column chromatography in combination with HPLC-ESI/MS. *Phytochem. Anal.*, 16(2):86-89.

Liu, Y.F., Yang, X.W., Wu, B. (2007) Studies on chemical constituents in the buds of *Tussilago farfar*. *China Journal of Chinese Materia Medica*, 32(22):2378-2381.

Livermore, D.M. (2000) Antibiotic resistance in staphylococci. *Int. J. Antimicrob. Agents.*, 16(Suppl 1):3-10.

Luangnarumitchai, S., Lamlertthon, S., Tiyaboonchai, W. (2007) Antimicrobial activity of essential oils against five strains of *Propionibacterium acnes*. *J. Phar. Sci.*, 34(1-4):60-64.

Luethy, J,, Zweifel, U., Schlatter, C. (1980) Pyrrolizidine alkaloids in colts (*Tussilago farfara* L.) of various sources. *Mitt. Geb. Lebenlun. Hyg.*, 71(1):73.

Mabberleg, D. (2003) The Plant Book. 2nd edition. London: *Cambrige University Press*.

Maeda, Y., Loughrey, A., Earle, J.A., Millar, B.C., Rao, J.R., Kearns, A., McConville, O., Goldsmith, C.E., Rooney, P.J., Dooley, J.S., Lowery, C.J., Snelling, W.J., McMahon, A., McDowell, D., Moore, J.E. (2008) Antibacterial activity of honey against community-associated methicillin-resistant *Staphylococcus aureus* (CA-MRSA). *Complement. Ther. Clin. Pract* .,14(2):77-82.

Magiorakos, A.P., Srinivasan, A., Carey, R.B., Carmeli, Y., Falagas, M.E., Giske, C.G., Harbarth, S., Hindler, J.F., Kahlmeter, G., Olsson-Liljequist, B., Paterson, D.L., Rice, L.B., Stelling, J., Struelens, M.J., Vatopoulos, A., Weber, J.T., Monnet, D.L. (2012) Multidrug-resistant, extensively drug-resistant and pandrug-resistant bacteria: an international expert proposal for interim standard definitions for acquired resistance. *Clin. Microbiol. Infec.*, 18(3):268-281.

Mahato, S.B., Kundu, A.P. (1994) ^{13}C NMR spectra of pentacyclic triterpenoids-a compilation and some salient features. *Phytochemistry*, 37(6):1517-1575.

Mann, A., Ibrahim, K., Oyewale, A.O., Amupitan, J.O., Fatope, M.O., Okogun, J.I. (2011) Antimycobacterial friedelane-terpenoid from the root bark of *Terminalia avicennioides*. *Am. J. Chem*, 1(2):52-55.

Marcal, F.J., Cortez, D.A., Ueda-Nakamura, T., Nakamura, C.V., Filho, B.P.D. (2010) Activity of the extracts and neolignans from *Piper regnellii* against methicillin-resistant *Staphylococcus aureus* (MRSA). *Molecules.*, 15(4):2060-2069.

Maruta, Y., Kawabata, J., Niki, R. (1995) Antioxidative caffeoylquinic acid derivatives in the roots of burdock (*Arctium lappa* L.). *J. Agr. Food Chem.*, 43(10):2592-2595.

Mata, R., Morales, I., Pérez, O., Rivero-Cruz, I., Acevedo, L., Enriquez-Mendoza, I., Bye, R., Franzblau, S., Timmermann, B. (2004) Antimycobacterial compounds from *Piper sanctum*. *J. Nat. Prod.*, 67(12):1961-1968.

Mathabe, M.C., Hussein, A.A., Nikolova, R.V., Basson, A.E., Meyer, J.J.M., Lall, N. (2008) Antibacterial activities and cytotoxicity of terpenoids isolated from *Spirostachys africana*. *J. Ethnopharmacol.*, 116:194-197.

Matsumoto, T., Hosono-Nishiyama, K., Yamada, H. (2006) Antiproliferative and apoptotic effects of butyrolactone lignans from *Arctium lappa* on leukemic cells. *Planta Med.*, 72(276-278).

Matsuzaki, Y., Koyama, M., Hitomi, T., Yokota, T. (2008) Arctiin induces cell growth inhibition through the down-regulation of cyclin D1 expression. *Oncol. Rep.*, 19:721-727.

McCutcheon, A.R., Ellis, S.M., Hancock, R.E., Towers, G.H. (1992) Antibiotic screening of medicinal plants of the British Columbian native peoples. *J. Ethnopharmacol.*, 37(3):213-223.

McCutcheon, A.R., Ellis, S.M., Hancock, R.E., Towers, G.H. (1994) Antifungal screening of medicinal plants of British Columbian native peoples. *J. Ethnopharmacol.*, 44(3):157-169.

Meazza, G., Dayan, F.E., Wedge, D.E. (2003) Activity of quinones on colletotrichum species. *J. Agric. Food Chem.*, 51(13):3824-3828.

Medjroubi, K., Bouderdara, N., Benayache, F., Akkal, S., Seguin, E., Tillequin, F. (2003) Sesquiterpene lactones of *Centaurea nicaensis*. *Chem. Nat. Compd.*, 39(5):506-507.

Mehdinezhad, B., Rezaei, A., Mohajeri, D., Ashrafi, A., Asmarian, S., Sohrabi-Haghdost, I., Hokmabad, R.V., Safarmashaei, S. (2011) Comparison of in-*vivo* wound healing activity of *Verbascum thapsus* flower extract with zinc oxide on experimental wound model in rabbits. *Adv. Environ. Biol.*, 1501-1509.

Mehrotra, R., Ahmed, B., Vishwakarma, R.A., Thakur, R.S. (1989) Verbacoside: a new luteoln glycoside from *Verbascum thapsus*. *J. Nat. Prod.*, 52(3):640-643.

Millspaugh, C.F. (1974) American Medicinal Plants. New York: Dover.

Min, B.R., Pinchak, W.E., Merkel, R., Walker, S., Tomita, G., Anderson, R.C. (2008) Comparative antimicrobial activity of tannin extracts from perennial plants on mastitis pathogens. *Sci. Res. Essay.*, 3(2):66-73.

Ming, D.S., Guns, E., Eberding, A., Towers, N. (2004) Isolation and characterization of compounds with anti-prostate cancer activity from *Arctium lappa* L. using bioactivity-guided fractionation. *Phar.l Biol.* (Formerly *Int. J. Pharmacog.*) , 42(1):44-48.

Mizushina, Y., Nakanishi, R., Kuriyama, I. (2006) Beta-sitosterol-3-*O*-beta-D-glucopyranoside: a eukaryotic DNA polymerase lambda inhibitor. *J. Steroid Biochem.*, 99:100-107.

Modaressi, M., Delazar, A., Nazemiyeh, H., Fathi-Azad, F., Smith, E., Rahman, M.M., Gibbons, S., Nahar, L., Sarker, S.D. (2009) Antibacterial iridoid glucosides from *Eremostachys laciniata*. *Phytother. Res.*, 23(1):99-103.

Moellering, R.C. (2008) Current treatment options for community-acquired methicillin-resistant *Staphylococcus aureus* infection. *Clin. Infect. Dis.*, 46(7):1032.

Molinari, G. (2009) Natural products in drug discovery: present status and perspectives. *Adv. Exp. Med. Biol.*, 655: 13-27.

Moore, C.L., Osaki-Kiyan, P., Perri, M., Donabedian, S., Haque, N.Z., Chen, A., Zervos, M.J. (2010) USA600 (ST45) methicillin-resistant *Staphylococcus aureus* bloodstream infections in urban Detroit. *J. Clin. Microbiol.*, 48(6):2307-2310.

Morteza-Semnaniab, K., Saeedibc, M., Akbarzadehd, M. (2012) Chemical composition and antimicrobial activity of the essential oil of *Verbascum thapsus* L. *J. Essen. Oil Bear. Pl.*, 15(3):373-379.

Moskalenko, S. (1986) Preliminary screening of far-eastern ethnomedicinal plants for antibacterial activity. *J. Ethnopharmacol.*,15:231-259.

Mskhiladze, L., Kutchukhidze, J., Chincharadze, D., Delmas, F., Elias, R., Favel, A. (2008) In vitro antifungal and antileishmanial activities of steroidal saponins from *Allium leucanthum* C. Koch-a Caucasian endemic species. *Georgian Med. News.*, (154):39-43.

Gallucci, N., Oliva, M., Carezzano, E., Zygadlo, J., Demo, M. (2010) Terpenes antimicrobial activity against slime producing and non-producing staphylococci. *Mole. Med. Chem.*, 21:132-136.

Nakamura, Y., Murakami, A., Koshimizu, K., Ohigashi, H. (1996) Identification of pheophorbide a and its related compounds as possible anti-tumor promoters in the leaves of *Neptunia oleracea*. *Biosci. Biotechnol. Biochem.*, 60(6):1028-1030.

Namba, T., Morita, O., Huang, S.L., Goshima, K., Hattori, M., Kakiuchi, N. (1988) Studies on cardio-active crude drugs. I. Effect of coumarins on cultured myocardial cells. *Planta Med.*, 54:277-282.

Namita, P., Mukesh, R. (2012). Medicinal plants used as antimicrobial agents: a review. *Int. Res. J. Phar.*, 3(1):31-40.

National Institute for Health and Clinical Excellence. (2011) Tuberculosis: clinical diagnosis and management of tuberculosis, and measures for its prevention and control. NICE clinical guideline 117, *guidance.nice.org.uk/cg117*.

Navarro, V., Delgado, G. (1999) Two antimicrobial alkaloids from *Bocconia arborea*. *J. Ethnopharmacol.*, 66:223-226.

Oliveira, J.H.H.L., Seleghim, M.H.R., Timm, C., Grube, A., Köck, M., Nascimento, G.G.F., Martins, A.C.T., Silva, E.G.O., Souza, A.O.D., Minarini, P.R.R., Galetti, F.C.S., Silva, C.L., Hajdu, E., Berlinck, R.G.S. (2006) Antimicrobial and antimycobacterial activity of cyclostellettamine alkaloids from sponge *Pachychalina sp. Mar. Drugs*. 4:1-8.

Ormerod, L.P. (2005) Multidrug-resistant tuberculosis (MDR-TB): epidemiology, prevention and treatment. *Br. Med. Bull.*, 14(73-74):17-24.

Otto, M. (2012) Methicillin-resistant *Staphylococcus aureus* infection is associated with increased mortality. *Future Microbiol.*, 7(2):189-191.

Ou, C., Pu, X., Li, S., Pan, Q., Hou, N. (2011) Effect of 4-hydroxycinnamic acid on chickens ifected with inectiuos bursal disease virus. *J. Anim. Vet. Adv.*, 10(1):2292-2296.

Pan, X., Bligh, S.W.A., Smith, E. (2013) Quinolone alkaloids from *Fructus euodiae* show activity against methicillin-resistant *Staphylococcus aureus*. *Phytother. Res.*

Panthong, K., Pongcharoen, W., Phongpaichit, S., Taylor, W.C. (2006) Tetraoxygenated xanthones from the fruits of *Garcinia cowa*. *Phytochemistry*, 67(10):999-1004.

Pardo, F., Perich, F., Torres, R., Monache, F.D. (1998) Phytotoxic iridoid glucosides from the roots of *Verbascum thapsus*. *J. Chem. Ecol.*, 24(4):645-653.

Pari, L., Prasath, A. (2008) Efficacy of caffeic acid in preventing nickel induced oxidative damage in liver of rats. *Chem. Biol. Interact.*, 173:77-83.

Park, H.R., Yoo, M.Y., Seo, J.H., Kim, I.S., Kim, N.Y., Kang, J.Y., Cui, L., Lee, C.S., Lee, C.H., Lee, H.S. (2008) Sesquiterpenoids isolated from the flower buds of *Tussilago farfara* L. inhibit diacylglycerol acyltransferase. *J. Agric. Food Chem.*, 56:10493-10497.

Park, S.Y., Hong, S.S., Han, X.H., Hwang, J.S., Lee, D. (2007) Lignans from *Arctium lappa* and their inhibition of LPS-induced nitric oxide production. *Chem. Pharm. Bull.*, 55(1):150-152.

Pasqua, R.D., Feo, V.D., Villani, F., Mauriello, G. (2005) In vitro antimicrobial activity of essential oils from *Mediterranean Apiaceae*, *Verbenaceae* and *Lamiaceae* against foodborne pathogens and spoilage bacteria. *Ann. Microbiol.*, 55(2):139-143.

Peirce, A. (1999) American pharmaceutical association practical guide to natural medicines. New York: *William Morrow and Company*.

Pelegrini, P.B., Sarto, R.P.D., Silva, O.N., Franco, O.L., Grossi-de-Sa, M.F. (2011) Antibacterial peptides from plants: what they are and how they probably work. *Biochem Res Int*.

Pelletier, S.W., Choksi, H.P., Desai, H.K. (1986) Separation of diterpenoid alkaloid mixtures using vacuum liquid chromatography. *J. Nat. Prod.*, 49:892-900.

Peng, L.Y., Mei, S.X., Jiang, B., Zhou, H., Sun, H.D. (2000) Constituents from *Lonicera japonica*. *Fitoterapia.*, 71:713-715.

Peng, S.C., Cheng, C.Y., Sheu, F., Su, C.H. (2008) The antimicrobial activity of heyneanol A extracted from the root of Taiwanese wild grape. *J. Appl. Microbiol.*, 105(2):485-491.

Pennacchio, M., Syah, Y.M., Alexander, E., Ghisalberti, E.L. (1999) Mechanism of action of verbascoside on the isolated rat heart: increases in level of prostacyclin. *Phytother. Res.*, 13(3):254-255.

Pereira, J.V., Bergamo, D.C.B., Pereira, J.O., Franca, S.D.C. (2005) Antimicrobial

activity of *Arctium lappa* constituents against microorganisms commonly found in endodontic infections. *Braz. Dent. J.*, 16(3):192-196

Peungvicha, P., Temsiririrkkul, R., Prasain, J.K., Tezuka, Y., Kadota, S., Thirawarapan, S.S., Watanabe, H. (1998) 4-Hdroxybenic acid: a hypoglycemic constitent of aqueous extract of *Pandanus odorus* root. *J. Ethnopharmacol.*, 62:79-84.

Phongmaykin, J., Kumamoto, T., Ishikawa, T., Suttisri, R., Saifah, E. (2008) A new sesquiterpene and other terpenoid constituents of *Chisocheton penduliflorus*. *Arch. Pharm. Res.*, 31(1):21-27.

Picher, M.T., Seoane, E., Tortajada, A. (1984) Flavones, sesquiterpenen laetones and glycosides isolated from *Centaurea aspera* Var. Stenophylla. *Phytochemistry*, 23(9):1995-1998.

Qiu, J., Li, H., Meng, H., Hu, C., Li, J., Luo, M., Dong, J., Wang, X., Wang, J., Deng, Y., Deng, X. (2011) Impact of luteolin on the production of alpha-toxin by *Staphylococcus aureus*. *Lett. Appl. Microbiol.*, 53(2):238-243.

Ragasa, C.Y., Lim, K. (2005) Sterols from *Cucurbita maxima*. *Philippine J. Sci.*, 134(2):83-87.

Raghukumar, R., Vali, L., Watson, D., Fearnley, J., Seidel, V. (2010) Anti-methicillin resistant *Staphylococcus aureus* (MRSA) activity of "Pacific propolis" and isolated prenylflavanones. *Phytother. Res.*, 24:1181-1187.

Rahman, M.M., Khondkar, P., Gray, A.I. (2005) Terpenoids from *Atylosia scarabaeoides* and their antimicrobial activity. *Dhaka Univ. J. Pharm. Sci.*, 4(2):141-144.

Ramalhete, C., Spengler, G., Martins, A., Martins, M., Viveiros, M., Mulhovo, S., Ferreira, M.J., Amaral, L. (2011) Inhibition of efflux pumps in methicillin-resistant *Staphylococcus aureus* and *Enterococcus faecalis* resistant strains by triterpenoids from *Momordica balsamina*. *Int. J.*

Antimicrob. Agents., 37(1):70-74.

Raman, M.S., Sultana, N., Anwar, M.N. (2004) In vitro antimicrobial activity of holarrifine–24ol isolated from the stem bark of *Holarrhena antidysenterica*. *Int. J. Agri. Biol.*, 6(4):698-700.

Rastogi, N., Goh, K.S., Horgen, L., Barrow, W.W. (1998) Synergistic activities of antituberculous drugs with cerulenin and trans-cinnamic acid against *Mycobacterium tuberculosis*. *FEMS Immunol. Med. Microbiol.*, 21(2):149-157.

Ravindranath, B. (1989) Principles and practice of chromatography. *Ellis Harwood Ltd*.

Raygada, J.L., Levine, D.P. (2009) Managing CA-MRSA infections: current and emerging options. *Infections in Medicine*, 26(2):1-9.

Riera, A.S., Daud, A., Gallo, A., Genta, S., Aybar, M., Sánchez, S. (2003) Antibacterial activity of lactose-binding lectins from *Bufo arenarum* skin. *Biocell.*, 27(1):37-46.

Rijo, P., Simões, M.F., Francisco, A.P., Rojas, R., Gilman, R.H., Vaisberg, A.J., Rodríguez, B., Moiteiro, C. (2010) Antimycobacterial metabolites from *Plectranthus: royleanone* derivatives against *Mycobacterium tuberculosis* strains. *Chem. Biodivers.*, 7(4):922-932.

Ríos, J.L., Recio, M.C. (2005) Medicinal plants and antimicrobial activity. *J. Ethnopharmacol.*, 100(1-2):80-84.

Ritchason, J. (1995) The little herb encyclopedia: the handbook of natures remedies for a healthier life, *Woodland Publishing, Incorporated*, p 40-41

Rivero-Cruz, I., Acevedo, L., Guerrero, J.A., Martínez, S., Bye, R., Pereda-Miranda, R., Franzblau, S., Timmermann, B.N., Mata, R. (2005) Antimycobacterial agents from selected Mexican medicinal plants. *J. Pharm. Pharmacol.*, 57(9):1117-1126.

Roder, E.H., Wiedenfeld, E. (1981) Tussilagine-a new pyrrolizidene alkaloid from *Tussilago farfara*. *Planta Med.*, 43:99.

Rogan, M.P., Geraghty, P., Greene, C.M., O'Neill, S.J., Taggart, C.C., McElvaney, N.G. (2006) Antimicrobial proteins and polypeptides in pulmonary innate defence. *Respir. Res.*, 7:29.

Rothman, R.E., Hsieh, Y.H., Yang, S. (2006) Communicable respiratory threats in the ED: tuberculosis, influenza, SARS, and other aerosolized infections. *Emerg. Med. Clin. N. Am.*, 24:989-1017.

Rugutt, J.K., Rugutt, K.J. (2002) Relationships between molecular properties and antimycobacterial activities of steroids. *Nat. Prod. Lett.*, 16(2):107-113.

Rugutt, J.K., Rugutt, K.J. (2012) Antimycobacterial activity of steroids, long-chain alcohols and lytic peptides. *Nat. Prod. Res.*, 26(11):1004-1011.

Rukachaisirikul, T., Prabpai, S., Kongsaeree, P., Suksamrarn, A. (2004) (+)-Bornyl piperate, a new monoterpene ester from *Piper aff.* pedicellatum roots. *Chem. Pharm. Bull. (Tokyo)*, 52(6):760-761.

Ryu, J.H., Jeong, Y.S., Sohn, D.H. (1999) A new bisabolene epoxide from *Tussilago farfara*, and inhibition of nitric oxide synthesis in LPS-activated macrophages. *J. Nat. Prod.*, 62(10):1437-1438.

Saeidnia, S., Ghari, A., Malmir, M., Moradi-Afrapoli, F., Ajani, Y. (2011) Trytophan and sterols from *Salvia limbata*. *J. Med. Pl.*, 10(37):41-47.

Saeidnia, S., Yassa, N., Rezaeipoor, R., Shafiee, A., Gohari, A.R., Kamalinejad, M., Goodarzy, S. (2009) Immunosuppressive principles from *Achillea talagonica*, an endemic species of Iran. *DARU*, 17(1):37-41.

Saleem, M., Nazir, M., Ali, M.S., Hussain, H., Lee, Y.S., Riaz, N., Jabbar, A. (2010) Antimicrobial natural products: an update on future antibiotic drug candidates. *Nat. Prod. Rep.*, 27(2):238-254.

Saludes, P.J., Garson, M.J., Franzblau, S.G., Aguinaldo, A.M. (2002) Antitubercular

constituents from the hexane fraction of *Morinda citrifolia* Linn. (Rubiaceae). *Phytother. Res.*, 16(7):683-685.

Salvador, M.J., Pereira, P.S., França, S.C., Candido, R.C., Ito, I.Y., Dias, D.A. (2009) Bioactive chemical constituents and comparative antimicrobial activity of callus culture and adult plant extracts from *Alternanthera tenella*. *Z. Naturforsch. C.*, 64(5-6):373-381.

Sasaki, H., Kashiwada, Y., Shibata, H., Takaishi, Y. (2012) Prenylated flavonoids from *Desmodium caudatum* and evaluation of their anti-MRSA activity. *Phytochemistry.*, 82:136-142.

Sathiamoorthy, B., Gupta, P., Kumar, M., Chaturvedi, A.K., Shukla, P.K., Maurya, R. (2007) New antifungal flavonoid glycoside from *Vitex negundo*. *Bioorg. Med. Chem. Lett.*, 17(1):239-242.

Sato, Y., Suzaki, S., Nishikawa, T., Kihara, M., Shibata, H., Higuti, T. (2000) Phytochemical flavones isolated from *Scutellaria barbata* and antibacterial activity against methicillin-resistant *Staphylococcus aureus*. *J. Ethnopharmacol.*, 72:483-488.

Saxena, V.K., Albert, S. (2005) β-sitosterol-3-*O*-β-D-xylopyranoside from the flowers of *Tridax procumbens* Linn. *J. Chem. Sci.*, 117(3):263-266.

Schapoval, E.E., Vargas, M.R., Chaves, C.G., Bridi, R., Zuanazzi, J.A., Henriques, A.T. (1998) Antiinflammatory and antinociceptive activities of extracts and isolated compounds from *Stachytarpheta cayennensis*. *J. Ethnopharmacol.*, 60(1):53-59.

Schroder, H., Merz, H., Steffen, R. (1990) Differential in vitro anti-HIV activity of natural lignans. *Z. Naturforsch.*, 45:1215-1221.

Seidel, V., Peyfoon, E., Watson, D.G., Fearnley, J. (2008) Comparative study of the antibacterial activity of propolis from different geographical and climatic zones. *Phytother. Res.*, 22:1256-1263.

Seifert, K., Schmidt, J., Lien, N.T., Johne, S. (1985) Iridoids from Verbascum species. *Planta Med.*, (5):409-411.

Shakeel-u-Rehman, Khan, R., Bhat, K.A., Raja, A.F., Shawl, A.S., Alam, M.S. (2010) Isolation, characterisation and antibacterial activity studies of coumarins from *Rhododendron lepidotum* Wall. ex G. Don, Ericaceae. *Braz. J. Pharmacog.*, 4210-4214.

Shen, C.C., Syu, W.J., Li, S.Y., Lin, C.H., Lee, G.H., Sun, C.M. (2002) Antimicrobial activities of naphthazarins from *Arnebia euchroma*. *J. Nat. Prod.*, 65(12):1857-1862.

Sher, A. (2009) Antimicrobial activity of natural products from medicinal plants. *Gomal. J. Med. Sci.*, 7:72-78.

Sherma, J., Fried, F. (2006) Handbook of thin layer chromatography. 2nd Edition. New Yeak.

Shi, L. (2009) A novel fructan possessing DB value from roots of *Arctium lappa* L. *Open Glycosci.*, 2:25-27.

Shimizu, M., Shiota, S., Mizushima, T., Ito, H., Hatano, T., Yoshida, T., Tsuchiya, T. (2001) Marked potentiation of activity of beta-lactams against methicillin-resistant *Staphylococcus aureus* by corilagin. *Antimicrob. Agents. Chemother.*, 45(11):3198-3201.

Shin, D.Y., Kim, H.S., Min, K.H., Hyun, S.S., Kim, S.A., Huh, H., Choi, E.C., Choi, Y.H., Kim, J., Choi, S.H., Kim, W.B., Suh, Y.G. (2000) Isolation of a potent anti-MRSA sesquiterpenoid quinone from *Ulmus davidiana* var. japonica. *Chem. Pharm. Bull. (Tokyo)*, 48(11):1805-1806.

Shiota, S., Shimizu, M., Sugiyama, J., Morita, Y., Mizushima, T., Tsuchiya, T. (2004) Mechanisms of action of corilagin and tellimagrandin I that remarkably potentiate the activity of beta-lactams against methicillin-resistant *Staphylococcus aureus*. *Microbiol. Immunol.*, 48(1):67-73.

Singh, B., Singh, S.. (2003) Antimicrobial activity of terpenoids from *Trichodesma amplexicaule* Roth. *Phytother. Res.*, 17:814-816.

Skwarek, T. (1979) Effects of herbal preparations on the propagation of influenza viruses. *Acta. Polon. Pharm.*, 36(2):19791984.

Solis, C., Becerra, J., Flores, C., Robledo, J., Silva, M. (2004) Antibacterial and antifungal terpenes from *Pilgerodendron uviferum* (D. Don) florin. *J. Chil. Chem. Soc.*, 49(2):157-161.

Souzaa, S.M.D., Monache, F.D., Jr, A.S.N. (2005) Antibacterial activity of coumarins. *Z. Naturforsch.*, 60c:693-700.

Stein, A.C., lvarez, S.A., Avancini, C.S., Zacchino, S., Poser, G.V. (2006) Antifungal activity of some coumarins obtained from species of *Pterocaulon* (Asteraceae). *J. Ethnopharmacol.*, 107:95-98.

Stermitz, F.R., Tawara-Matsuda, J., Lorenz, P., Mueller, P., Zenewicz, L., Lewis, K. (2000) 5'-Methoxyhydnocarpin-D and pheophorbide A: berberis species components that potentiate berberine growth inhibition of resistant *Staphylococcus aureus*. *J. Nat. Prod.*, 63(8):1146-1149.

Stern, J.L., Hagerman, A.E., Steinberg, P.D., Mason, P.K. (1996) Phlorotannin-protein interactions. *J. Chem. Ecol.*, 22:1887-1899.

Stjepan, P., Ivan, K. (2003) Antimicrobial activity of propolis and galangin (3, 5, 7-trihydroxyflavone) against MRSA, multiple-resistant *Enterococcus spp.* and *Pseudomonas aeruginosa*. *Croatian Microbiological Society*, 36.

Strange, R. (1977) A history of herbal plants. New York: *Arco Publishing Company*.

Su, T.J., Chang, H.S., Peng, C.F., Lee, S.J., Chen, I.S. 2009. Antitubercular resorcinols and cytotoxic alkyl benzoquinones from *Ardisia kusukusensis*. *Taiwan Phar. J.*, 61(4):89-105.

Suksamrarn, S., Suwannapoch, N., Phakhodee, W., Thanuhiranlert, J., Ratananukul, P., Chimnoi, N., Suksamrarn, A. (2003) Antimycobacterial activity of

prenylated xanthones from the fruits of *Garcinia mangostana*. *Chem. Pharm. Bull. (Tokyo)*, 51(7):857-859.

Sun, W.J., Sha, Z.F., Gao, H. (1992) Determination of arctiin and arctigenin in *Fructus Arctii* by reverse-phase HPLC. *Acta. Phar. Sin.*, 27:549-551.

Sureram, S., Senadeera, S.P., Hongmanee, P., Mahidol, C., Ruchirawat, S., Kittakoop, P. (2012) Antimycobacterial activity of bisbenzylisoquinoline alkaloids from *Tiliacora triandra* against multidrug-resistant isolates of *Mycobacterium tuberculosis*. *Bioorg. Med. Chem. Lett.*, 22(8):2902-2905.

Takaoka, D., Hiroi, M. (1976) Two acyclic monoterpene diols from *Cinnamomum camphora*. *Phytochemistry.*, 15(2):330.

Takasugi, M., Kawashima, S., Katsui, N. (1987) Studies on stress metabolites. 5. 2 polyacetylenic phytoalexins from *Arctium lappa*. *Phytochemistry*, (26):2957-2958.

Tan, M.A., Takayama, H., Aimi, N., Kitajima, M., Franzblau, S.G., Nonato, M.G. (2008) Antitubercular triterpenes and phytosterols from *Pandanus tectorius* Soland. var. laevis. *J. Nat. Med.*, 62(2):232-235.

Tanaka, J.C.A., Silva, C.C., Oliveira, A.J.B., Nakamura, C.V., Filho, B.P.D. (2006) Antibacterial activity of indole alkaloids from *Aspidosperma ramiflorum*. *Braz. J. Med. Biol. Res.*, 39:387-391.

Tatli, I.I., Akdemir, Z.S. (2004) Chemical constituents of *Verbascum* L. Species. FABAD *J. Pharm. Sci.*, 29:93-107.

Tiwari, N., Thakur, J., Saikia, D., Gupta, M.M. (2013) Antitubercular diterpenoids from *Vitex trifolia*. *Phytomedicine.*, 20(7):605-610.

Trombetta, D., Castelli, F., Bisignano, G. (2005) Mechanisms of antibacterial action of three monoterpenes. *Antimicrob. Agents. Chemother.*, 49(6):2474-2478.

Tsai, W.J., Chang, C.T., Wang, G.J., Lee, T.H., Chang, S.F., Lu, S.C., Kuo, Y.C. (2011) Arctigenin from *Arctium lappa* inhibits interleukin-2 and interferon gene

expression in primary human T lymphocytes. *Chin. Med.*, 6(1):12.

Tsao, R., Coats, J.R. (1995) Starting from nature to make better insecticides. *Chemtech.*, 25:23-28.

Tsuneki, H., Ma, E., Kobayashi, S. (2005) Antiangiogenic activity of beta-eudesmol in vitro and in vivo. *Eur. J. Pharmacol.*, 512:105-115.

Tundis, R., Loizzo, M.R., Menichini, F., Statti, G.A., Menichini, F. (2008) Biological and pharmacological activities of iridoids: recent developments. *Mini. Rev. Med. Chem.*, 8(4):399-420.

Turker, A.U., Camper, N.D. (2002) Biological activity of common mullein, a medicinal plant. *J. Ethnopharmacol.*, 82(2-3):117-125.

Turker, A.U., Gurel, E. (2005) Common mullein (*Verbascum thapsus* L.): recent advances in research. *Phytother. Res.*, 19:733-739.

Turker, A.U., Usta, C. (2008) Biological screening of some Turkish medicinal plant extracts for antimicrobial and toxicity activities. *Nat. Prod. Res.*, 22(2):136-146.

Tyler, V.E. (1993) The honest herbal. New York: *Pharmarceutical Products Press*.

Tyler, V.E. (1994) Herbs of choice: the therapeutic use of phytomedicinals. New York: *Pharmarceutic Products Press*.

Vachalkova, A., Ovesna, Z., Horvathova, K. (2004) Taraxasterol and β-sitosterol: new naturally compounds with chemoprotective/chemopreventive effects. *Neoplasma.*, 51:407-414.

Valdes III, L.J. (1986) Loliolide from *Salvia divinorum*. *J. Nat. Prod.*, 49(1): 171.

Vogt, V., Cravero, C., Tonn, C., Sabini, L., Rosas, S. (2010) *Verbascum thapsus*: antifungal and phytotoxic properties. *Mole. Med. Chem.*, 20:105-108.

Wandji, J., Tillequin, F., Mulholland, D.A., Wansi, J.D., Fomum, T.Z., Fuendjiep, V., Libot, F., Tsabang, N. (2002) Fatty acid esters of triterpenoids and steroid glycosides from *Gambeya africana*. *Planta Med.*, 68(9):822-826.

Wang, H.Y., Yang, J.S. (1993) Studies on the chemical constituents of *Arctium lappa* L. *Acta. Phar. Sin.*, 28(12):911-917.

Wang, Y., Liu, B. (2007) Preparative isolation and purification of dicaffoeylquinic acid from *Ainsliaea fragrans* Champ by high-speed counter-current chromatography. *Phytochem. Anal.*, 18:436-440.

Warashina, T., Miyase, T., Ueno, A. (1991) Iridoid glycosides from *Verbascum thapsus* L. *Chem. Pharm. Bull.*, 39(12):3261-3264.

Warashina, T., Miyase, T., Ueno, A. (1992) Phenylethanoid and lignan glycosides from *Verbascum thapsus*. *Phytochemistry*, 31(3):961-965.

Wei, F., Ma, S.C., Ma, L.Y., But, P.P.H., Lin, R.C., Khan, I.A. (2004) Antiviral flavonoids from the seeds of *Aesculus chinensis*. *J. Nat. Prod.*, 67(4):650-653.

WHO. (2012a) Global report for research on infectious diseases of poverty.

WHO. (2012b) Global tuberculosis report 2012.

WHO. (2013a) World Health Statistics.

WHO. (2013b) Multidrug-resistant tuberculosis (MDR-TB) 2013 Update.

Widelski, J., Popova, M., Graikou, K., Glowniak, K., Chinou, I. (2009) Coumarins from *Angelica lucida* L. - antibacterial activities. *Molecules*., 14:2729-2734.

Widmer, T.L., Laurent, N. (2006) Plant extracts containing caffeic acid and rosmarinic acid inhibit zoospore germination of *Phytophthora spp.* pathogenic to theobroma cacao. *Eur. J. Pl. Pathol.*, 115:377-388.

Williams, D.H., Fleming, I. (2008) Spectroscopic methods in organic chemistry. 6th edition: *The MCGraw-Hill Companies*.

Williams, L., Wilkins. (1999) Quick access patient information on conditions, herbs & supplements, 1st edition, integrative medicine communications, facts and comparisons.

Woldemichael, G.M., Franzblau, S.G., Zhang, F., Wang, Y., Timmermann, B.N. (2003)

Inhibitory effect of sterols from *Ruprechtia triflora* and diterpenes from *Calceolaria pinnifolia* on the growth of *Mycobacterium tuberculosis*. *Planta Med.*, 69(7):628-631.

Woldemichael, G.M., Gutierrez-Lugo, M.T., Franzblau, S.G., Wang, Y., Suarez, E., Timmermann, B.N. (2004) *Mycobacterium tuberculosis* growth inhibition by constituents of sapium haematospermum. *J. Nat. Prod.*, 67(4):598-603.

Wongsinkongman, P., Brossi, A., Wang, H.K., Bastow, K.F., Lee, K.H. 2002. Antitumor agents. Part 209: pheophorbide A perivatives as photo-independent cytotoxic cgents. *Bioorg. Med. Chem.*, 10:583-591.

Wright, J.L.C., Mcinnes, A.G., Shimizu, S., Smith, D.G., Walter, J.A. (1978) Identification of C-24 alkyl epimers of marine sterols by ^{13}C nuclear magnetic resonance spectroscopy. *Can. J. Chem.*, 56:1898.

Wu, C., Chen, F., Wang, X., Wu, Y., Dong, M., He, G., Galyean, R.D., He, L., Huang, G. (2007) Identification of antioxidant phenolic compounds in feverfew (*Tanacetum parthenium*) by HPLC-ESI/MS and NMR. *Phytochem. Anal.*, 18:401-410.

Wu, D,. Zhang, C.F., Zhang, M., Zhang, J.W., Wang, Z.T. (2008) Study on chemical constituents of the flower buds of *Tussilago farfara*. *Chinese Pharmaceutical Journal*, 43(4).

Wu, D., Zhang, M., Zhang, C., Wang, Z. (2010) Flavonoids and phenolic acid derivatives from flos farfarae. *China Journal of Chinese Materia Medica*, 35(9):1142-1144.

Xiang, M., Su, H., Hu, J., Yan, Y. (2011) Isolation, identification and determination of methyl caffeate, ethyl caffeate and other phenolic compounds from *Polygonum amplexicaule* var. sinense. *J. Med. Pl. Res.*, 5(9):1685-1691.

Xiao, Z.P., Wu, H.K., Wu, T., Shi, H., Hang, B., Aisa, H.A. (2006) Kaempferol and quercetin flavonoids from *Rosa rugosa*. *Chem. Nat. Compd.*, 42(6):736-737.

Xiong, Q., Hase, K., Tezuka, Y., Namba, T., Kadota, S. (1999) Acteoside inhibits apoptosis in D-galactosamine and lipopolysaccharide-induced liver injury. *Life Sci.*, 65(4):421-430.

Xu, H.X., Zeng, F.Q., Wan, M., Sim, K.Y. (1996) Anti-HIV triterpene acids from *Geum japonicum*. *J. Nat. Prod.*, 59:643-645.

Yadav, A.K., Thakur, J., Prakash, O., Khan, F., Saikia, D., Gupta, M.M. (2013) Screening of flavonoids for antitubercular activity and their structure-activity relationships. *Med. Chem. Res.*, 22(6):2706-2716.

Yaoita, Y., Masao, K. (1998) Triterpenoids from flower buds of *Tussilago farara* L. *Natr. Med.*, 52(3):273.

Yaoita, Y., Suzuki, N., Kikuchii, M. (1999) Structures of new oplopanetype sesquiterpenoids from the flowers of *Tussilago farfara* L. *Chem. Pharm. Bull.*, 47(5):705.

Yaoita, Y., Suzuki, N., Kikuchii, M. (2001) Structures of new sesquiterpenoids from *Farfarae Flos*. *Chem. Pharm. Bull.*, 49(5):645-648.

Yoshioka, T., Inokuchi, T., Fujioka, S., Kimura, Y. (2004) Phenolic compounds and flavonoids as plant growth regulators from fruit and leaf of *Vitex rotundifolia*. *Z. Naturforsch. C.*, 59(7-8):509-514.

Yu, Y., Gao, H., Tang, Z., Song, X., Wu, L. (2006) Several phenolic acids from the fruit of *Capparis spinosa*. *Asian J. Trad. Med.*, 1(3-4):1-4.

Zhang, Y., Lewis, K. (1997) Fabatins: new antimicrobial plant peptides. *FEMS Microbiol. Lett.*, 149:59-64.

Zhang, Y., Li, H.Z., Zhang, Y.J., Jacob, M.R., Khan, S.I., Li, X.C., Yang, C.R. (2006) Atropurosides A-G, new steroidal saponins from *Smilacina atropurpurea*. *Steroids.*, 71(8):712-719.

Zhao, Y.L., Wang, S.F., Li, Y., He, Q.X., Liu, K.C., Yang, Y.P., Li, X.L. (2011) Isolation of chemical constituents from the aerial parts of *Verbascum thapsus*

and their antiangiogenic and antiproliferative activities. *Arch. Pharm. Res.*, 34(5):703-707.

Zhao, Z.Y., Yin, Z.X., Xu, X.P., Weng, S.P., Rao, X.Y., Dai, Z.X., Luo, Y.W., Yang, G., Li, Z.S., Guan, H.J., Li, S.D., Chan, S.M., Yu, X.Q., He, J.G. 2009. A Novel C-Type lectin from the shrimp litopenaeus vannamei possesses anti-white spot syndrome virus activity. *J. Virol.*, 83:347-356.

Zhou, H.Y., Li, S.M. (2006) Study on constituents from leaves of *Phyllostachys pubescens*. *Chinese Pharm. J.*, 41:662-663.

Zuo, G.Y., Meng, F.Y., Hao, X.Y., Zhang, Y.L., Wang, G.C., Xu, G.L. (2008) Antibacterial alkaloids from *Chelidonium majus* Linn (Papaveraceae) against clinical isolates of methicillin-resistant *Staphylococcus aureus*. *J. Pharm. Pharmaceut. Sci.*, 11(4):90-94.

Zuo, W.J., Dai, H.F., Chen, J., Chen, H.Q., Zhao, Y.X., Mei, W.L., Li, X., Wang, J.H. (2011) Triterpenes and triterpenoid saponins from the leaves of *Ilex kudincha*. *Planta Med.*, 77(16):1835-1840.